UNIVERSITÀ
DEGLI STUDI
DI PADOVA

Head Office: Università degli Studi di Padova

Department of Biology

Ph.D. COURSE IN: Biosciences
CURRICULUM: Genetics Genomics and Bioinformatics
SERIES 34°

Combining omics approaches with flux balance analysis for unraveling population dynamics in anaerobic microbiomes

Coordinator: Prof. Ildikò Szabò
Supervisor: Prof. Giorgio Valle

Ph.D. student :
Arianna Basile

Abstract

Microbial methanogenic metabolism is one of the oldest bioactivities on Earth. This process is one of the main determinants of the fluxes in the global carbon cycle. In fact, in natural ecosystems, around one billion tons of methane is formed through microbial activity. Methanogenic process, mediated by complex microbial communities in anaerobic and microaerophilic environments, has raised great attention due to its energy generation potential. Constraint-based genome-scale metabolic modelling and metabolic flux balance analysis are pioneeristic tools for the investigation of large-scale relationships between genotype, phenotype and environment. Metabolic flux balance allows the integration of genomic data in the individual species-level metabolic models, feedstock information in the form of import flux bounds, and abundance data derived from metagenomic shotgun sequencing. The research reported in this PhD thesis focused on the establishment of a robust pipeline of flux balance analysis to unravel dynamics behind microbial communities involved in anaerobic digestion through two different cases of study: the investigation of a bioengineering process and the analysis of health-related microbial dynamics. The first case of study has been the analysis of the global microbial community behind the Anaerobic Digestion process in engineered systems. Anaerobic Digestion is the process leading to the generation of energy from biogas. Deciphering the anaerobic digestion "black box" is essential to optimise the biogas production and can allow the development of strategies to improve the process efficiency. The microbial community responsible for biogas generation is extremely complex and modifications of the environmental and operational parameters of the reactors deeply influence the abundance of the community members. This investigation helped decipher the correlation existing between species abundance and operational parameters of the biogas reactors. Understanding the required conditions for natural enhancement of desired endogenous consortia under anaerobic conditions paved the way to improve the yield of methane produced. The use of reactors enables a fine tuning of the anaerobic digestion, a dissection and a magnification of each step and component of the process. Therefore, the second case of study involved the application of the anaerobic digestion system as an ecosystem in a vessel for the analysis of metagenomic data from Crohn's disease patients. In this model an additional complexity was considered: the integration of microbial and host metabolisms. Crohn's disease is an inflammatory bowel disease affecting the digestive tract, it can lead to abdominal pain, severe diarrhea, weight loss and malnutrition. The inflammation often spreads deep into layers of affected bowel tissues and can be both painful and debilitating, and sometimes may lead to life-threatening complications. Although there is not widespread agreement on the aetiology of Crohn's disease, microorganisms are recognized as the leading cause of the characteristic severe inflammatory response. The second case of study aimed to analyze metagenomic data of a Crohn's disease patient with flux balance analysis to inspect the major modifications occurring in his gut microbiota during each stage of the disease development. The core of the project was the integration of longitudinal metagenomic data with flux balance analysis. In particular the development of the gut microbiome during acute and relapsing phases was studied to inspect the main microbe-microbe and microbe-host interplays responsible for the inflammation. The analysis shed light on the most altered metabolites during the disease onset.

Acronyms

AD - Anaerobic Digestion
ATP - Adenosine Triphosphate
BQH - Black Queen Hypothesis
CD - Crohn's disease
CH_4 - Methane
CO_2 - Carbon dioxide
COBRA - Constraint-based Reconstruction and Analysis
EPS - Exopolysaccharidic matrix
FBA - Flux Balance Analysis
GSMM - Genome-Scale Metabolic Model
H_2 - Hydrogen
H_2S - Hydrogen sulfide
HMP - Human Microbiome Project
HMR - Human Metabolic Reaction
KEGG - Kyoto Encyclopedia of Genes and Genomes
MAGs - Metagenome Assembled Genomes
NAFLD - non-alcoholic fatty liver disease
NH_4 - Ammonium
P2G - Power-To-Gas
RQH - Red Queen Hypothesis
rRNA - Ribosomal RNA
SAO - Syntrophic Acetate Oxidation
SAOB - Syntrophic Acetate Oxidisers Bacteria
VFA - Volatile Fatty Acids
WBM - Whole-Body Model
WL - Wood-Ljungdahl

Introduction

The importance of the microbial community in an environment

Everything humans need for survival has an intimate connection with microbial activity, from drinkable water to the food we generally consume, from drugs we take in case of illnesses to the soil we rely on for farming (Brüssow, 2015). The microbiome (from the Greek micro meaning "small" and bíos meaning "life") is the basis of the biosphere and pivotal for all of life (Silbergeld, 2017). The microbiome accounts both for *Prokaryotes* (i.e. *Bacteria* and *Archaea*) but also for *Eukaryotes* (i.e. *Protozoa*, *Fungi*, and *Algae*) (Kodio *et al*., 2020). Microbes are so all-pervading that they are present in every environmental niche and in every nook of the human body (Berg *et al*., 2020). The scale of life in the microbial world is such that it should be described with numbers so complex to lose any meaning. Even numbers used in the field of astronomy are dwarfed in comparison with numbers used for describing microbial life ("Microbiology by numbers," 2011). As an example, in the ocean there are 100 million times as many bacteria as there are stars in the known universe. Their importance, though, is not dependent solely by their numerousness. Microbial species produce key compounds that are not synthesizable by other living organisms, provide nutrients to the soil, and help maintain the balance in the gut of different animals (including humans) (Rowland *et al*., 2018; Thursby and Juge, 2017). Furthermore, their peculiar metabolic capabilities are biotechnologically exploited for the synthesis of metabolites of interest like drugs and food products, e.g., kefir (Bengoa *et al*., 2019), cocoa (De Vuyst and Weckx, 2016), and even coffee (Zhang *et al*., 2019).

Microbial interactions

As for eukaryotes, it is very rare for prokaryotes to live, in nature, on their own (Abisado *et al*., 2018). Microbial species don't live in isolation but form complex relationships. The main driving forces of evolution in any population are mutation, natural selection, genetic drift and gene flow, which together allow adaptation to different ecosystems (Lenski, 2017). The complex network of interactions defines the structure and the spatial and temporal persistence of a community (Faust and Raes, 2012). Different types of interactions have been defined based on the benefit for an organism. Indeed, interactions can give a benefit or a disadvantage to the partner (Canon *et al*., 2020). The third option is that the interplay does not affect either positively or negatively the fitness of the partner, in this case we talk of neutral interactions (Grosskopf and Soyer, 2014). Microbial interactions are never one-to-one because all species influence the growth rate of many others in some way, be it the production of some toxic compound or the absorption of key metabolites. However, the description of microbial interactions would be impossible without simplifying the interactions in a dual system. Considering one-to-one cross-feedings, six patterns of interplay can be defined, namely: competition, amensalism, parasitism, neutralism, commensalism, mutualism (Heinken and Thiele, 2015). In particular competition, amensalism, parasitism are called "negative interactions" because at least one partner is harmed by the interplay (Mendes-Soares *et al*.,

2016). The negative outcome can be driven mainly by two different mechanisms. A possibility is that one or both partners produce some compounds which are toxic for the other species. For example, *Lactococcus lactis* can produce antibacterial compounds such as Nisin to exert a selection over Gram-positive bacteria (Azhar *et al*., 2017). The other possibility is that both partners compete for a limited source like a molecule crucial for the metabolism of the partners. A model case is represented by two autotrophic species competing for oxygen, in this case the limited source is the oxygen. Therefore, there is a spatial competition for the attachment to the surface (Geets *et al*., 2006). Neutralism, commensalism and mutualism are termed "positive interactions" because neither of the partners are negatively affected. In commensalism and mutualism the driving force of the interaction is the production by one microbial species of a compound needed by the other species (Geets *et al*., 2006). Another mechanism behind commensalism and mutualism is when one species absorbs a compound toxic for the other. The most studied case of mutualism is syntrophy. Syntrophies (from Greek *syn* meaning together, *trophe* meaning nourishment) have been defined by Stams and colleagues (Stams and Plugge, 2009) as a "nutritional situation in which two or more organisms combine their metabolic capabilities to catabolise a substrate that cannot be metabolised by either one of them alone", their role in the community of the Anaerobic Digestion will be widely discussed in the paragraph "Synthrophies in Anaerobic Digestion". This ultrasemplification of the topic could deceive the reader to think that microbial interactions are linear and straightforward. In reality, the definition of interactions in complex communities is much more complex and the whole is more than the sum of the parts. Interactions are not dependent only on metabolic capabilities of the members of the community (Larsen *et al*., 2012; Zengler and Zaramela, 2018). Accordingly, they are prone to change over time due to modifications in parameters of physiological and physical nature such as nutrients availability. In addition, spatial organization of members of the community is a limiting factor at the cross-feeding as well (Cao *et al*., 2019). Due to the high complexity of the topic, the description of cross-feedings other than dual is impossible without exploring the two main theories of ecological evolution namely: the Red Queen hypothesis (RQH) and the Black Queen hypothesis (BQH).

Red Queen hypothesis and Black Queen hypothesis

"It takes all the running you can do, to keep in the same place" is a sentence from the book by Lewis Carrol "*Through the Looking glass*", which was pronounced by the (red) Queen of Hearts. From the sentence which inspired the name we can easily guess that the RQH is proper for highly competitive communities. The RQH was postulated in 1973 by the American evolutionary biologist Leigh Van Valen (Liow *et al*., 2011). The theory postulates that adaptation and evolution of species are aimed not only for reproduction but also for survival since competing organisms are evolving as well. The BQH was postulated only 40 years later. According to this hypothesis, evolution is driven by gene loss which culminates in commensalistic behaviour among organisms in order to support the growth (Morris *et al*., 2012). When applied to microbial communities, two different and opposite behaviours are observed. In the gut microbiome, for example, there are many species with overlapping nutritional requirements. These species are characterised by big genomes and very complex metabolic demands. Contrariwise, in the communities of the soil, microbial species have

smaller genomes and their growth and survival is dependent from multiple auxotrophies. In the community there are many cooperative species which take over the community collaborating (Machado *et al*., 2021). The pioneeristic study of Leigh Van Valen has paved the way to many other laws of coevolution with names resembling the RQH. Eventually, Leigh Van Valen can be really said to have had the capability of looking through the Looking Glass.

From classical to modern microbiology

Microbiology as a field of study was initiated in 1674 when a dutch scientist named Antonie Van Leeuwenhoek created the first microscope (Robertson, 2015). From 1674 to the twenty-first century, many scientific revolutions have followed. More accurate microscopic, genetic, molecular and genomic investigations have enabled a far deeper understanding of what Antonie Van Leeuwenhoek could describe just as "animalcules" (small animals) (Lane, 2015). There are some important differences among different "animalcules", now known as bacteria, and biotechnological advances revealed that it is possible to exploit their metabolism for the production of antibiotics, vaccines and other drugs. Culturing, isolation and description of microorganisms have been essential to decipher the features of the different microbial species (Bilen *et al*., 2018). However, a crucial leap was needed since not all microbes are susceptible to cultivation. In the last two decades, new methods aiming to study the microbiome more than the single microbial species were developed (Almeida *et al*., 2019). High-throughput metagenomic sequencing and analysis involving binning of de-novo assembled contigs into clusters called Metagenome Assembled Genomes (MAGs) is a ground-breaking approach (Cani, 2018; Koren *et al*., 2018). More specifically, MAGs are obtained by grouping together assembled contigs with similar sequence composition and coverage depth across different related samples. This process is called "binning" (Albertsen *et al*., 2013; Mande *et al*., 2012; Nielsen *et al*., 2014). Binning enables the extraction of genomes starting from metagenomic data. Even if closed genomes have been obtained with binning metagenomic data, MAGs are by nature incomplete and contaminated by contigs from other strains or species due to challenges in discriminating among similar community members both during the assembly and the binning processes (Kunin *et al*., 2008; Pérez-Cobas *et al*., 2020). Metagenomics enables the description of microbial species in an environment and is now beginning the main method to study the microbiomes in natural and selected ecosystems (Garza and Dutilh, 2015; Quince *et al*., 2017). Amplicon sequencing, which targets the 16S ribosomal RNA (rRNA) gene, enables the description of bacterial and archaeal compositions and is able to detect variations in the structure of microbial communities (Poretsky *et al*., 2014). However, crucial biological differences occur even among taxonomically close strains of the same species and strain differences are very unlikely to be distinguished by amplicon sequencing (Ong *et al*., 2013). On the other hand, shotgun metagenomic sequencing enables the assessment of the entire genomic repertoire of any microbiome and accomplishes precise taxonomic and functional attribution of most of the microbial species (Almeida *et al*., 2021). Nowadays, the drop in costs of sequencing, made possible thanks to Next-Generation Sequencing technology, was far greater than predicted by Moore's law (Lundstrom, 2003). As a consequence, approaches to shotgun metagenomics are becoming more and more important in the microbiological field. Furthermore, newer and promising techniques, such as long sequencing and the pioneeristic single-molecule real-time sequencing are becoming crucial in enriching the knowledge of diverse microbiomes (van Dijk *et al*., 2018). These approaches, adopted by Oxford Nanopore Technologies and Pacific Biosciences respectively, are collectively termed "third-generation sequencing" and are suitable for long reads sequencing which can lead to the assembly of closed genomes without needing isolation and culturing (Schadt *et al*., 2010). In the last ten years second-generation and third-generation sequencing have been applied to the analysis of

a variety of environments ranging from soil to seawater, from human gut to bioreactors (Ji *et al*., 2019). These new approaches can pave the way to the analysis of the uncultured species, the so-called "microbial dark matter", which nowadays still covers a strikingly proportion of more than 90% of *Bacteria* and 40% of *Archaea* (Dance, 2020; Zamkovaya *et al*., 2021). However, the use of MAGs requires careful considerations as biases in binning contigs can affect subsequent taxonomical and functional analysis (Chen *et al*., 2020).

Anaerobic Digestion

Anaerobic Digestion (AD) is a complex and biological mediated process which occurs in anaerobic environments (Angelidaki *et al*., 2003). This process can occur in wetlands, landfills, as well as inside the rumen of animals (Vasco-Correa *et al*., 2018). However, this process has great biotechnological potential and can be exploited as a renewable energy source. The metabolic steps performed by the microbial community in the AD process lead to the conversion of complex molecules (e.g. polysaccharides, lipids and proteins) into simpler compounds (e.g. acetate, CO_2, H_2 and finally CH_4) (Campanaro *et al*., 2016). For this reason the AD has been described as a "funnel" and a "food chain". Each species in the funnel has a different bio-convertive role and takes part in a complex network of metabolic interplays. The four main steps of the AD process are: hydrolysis, acidogenesis, acetogenesis and methanogenesis (Li *et al*., 2018). The final result is the conversion of organic matter into biogas and other effluents of interest. Biogas resulting from AD is a mixture composed by different percentages of methane (CH_4) (50-75%) and carbon dioxide (CO_2) (25-50%), with minor amounts of contaminants, such as hydrogen sulfide (H_2S) and ammonia (NH_4) (Angelidaki *et al*., 2018). AD has been biotechnological employed for several decades aiming to waste stabilization and bioenergy production, in structured bioreactors. According to the temperature of the reactor, the process can be thermophilic, if carried out at 50°-60° C, or mesophilic, when the temperature is in the range between 30°-40° C (Kim *et al*., 2002).

Biogas upgrading

As mentioned above, biogas is not exclusively composed of CH_4 but CO_2 and minor amounts of contaminants such as H_2S and NH_4 are present, as well. The other gasses are unintended, because their presence lowers the calorific value and therefore the energy content of the biogas itself. Moreover, NH_4 and H_2S are toxic and corrosive compounds. In order to raise the calorific value of biogas through the conversion of CO_2 into CH_4 the approach called "Biogas upgrading" can be adopted (Fu *et al*., 2021). The final goal is to reach almost natural gas purity with a yield of CH_4 close to 95%. At this purity the biogas can be injected directly in the natural gas grid. Biogas upgrading can go through chemical or physico-chemical processes as well (Kapoor *et al*., 2019). The biological upgrading can be performed at mild operational conditions, e.g., at atmospheric pressure. The biological biogas upgrading involves the injection of hydrogen (H_2) into the reactor. The H_2 can be obtained from water hydrolysis using energy surplus of windmills or solar panels (Adnan *et al*., 2019). Renewable sources of

electricity can suffer from overproduction, and this can cause grid instability. One solution is to store the surplus energy into batteries. However, this option is not eco-friendly since batteries can contain heavy metals. The use of energy exceedings for water hydrolysis can overcome the issues derived from fluctuating electricity profile. The H_2 produced by hydrolysis is very difficult to store. However, it can be pumped in the reactor in order to use CH_4 as an energy carrier (Bušić *et al*., 2018). The process of energy conversion which enables the coupling of renewable energy and CH_4 generation is named Power-To-Gas (P2G) (Geppert *et al*., 2016; Nguyen *et al*., 2021). One of the main technical aspects, which need to be tackled since limiting the possibility of biogas upgrading, is the low H_2 gas-liquid mass transfer rate. Although not fully developed, this technology is nevertheless proving its validity well over the laboratory-scale. Biogas upgrading opens new horizons to the integration of different forms of renewable energy and is gaining a central role in the circular economy and in the environmental policy debate (Wulf *et al*., 2018).

Microbial communities in Anaerobic Digestion

The AD process involves several biochemical steps, performed by a highly diversified community including *Bacteria* and *Archaea* species (Campanaro *et al*., 2020). Microbial composition is variable between thermophilic and mesophilic reactors because temperature exerts a strong selective pressure on the community (Campanaro *et al*., 2018). As already stated, the process can be divided into four main steps namely: hydrolysis, acidogenesis, acetogenesis and methanogenesis (**Figure 1**). The microbial populations include many functional guilds performing one or more steps of the process. When microbial species perform one step of the process, they are named “specialists”, “generalists” otherwise (Campanaro *et al*., 2020). Hydrolytic bacteria secrete various enzymes of the cellulases, xylanases and proteases families. The vast majority of the microbiota carries out the first steps of the biochemical conversions. During acidogenesis, fermentative bacteria utilise simple sugars and amino acids to produce either organic acids such as volatile fatty acids (VFA) (i.e. propionate, butyrate and acetate) (Lukitawesa *et al*., 2020; Wainaina *et al*., 2019) or alcohols, depending on the substrate used. The acetogenesis, conversely, is performed mainly by secondary fermenter and syntrophic bacteria (Nobu *et al*., 2015). The main products of this step are H_2, CO_2 and acetate. The acidogenesis is achieved thanks to functionally distinct and specialised bacterial families: long-chain fatty acid oxidisers (e.g. *Syntrophomonas* bacteria), homoacetogens (e.g. *Moorella*, *Sporomusa* and *Acetobacterium* bacteria) (Pan *et al*., 2021), and syntrophic fatty-acid oxidisers (Dubé and Guiot, 2015) (**Figure 1**). The latter groups comprise syntrophic species which will be further discussed in the paragraph “Synthrophies in Anaerobic Digestion”. The diversity of syntrophic bacteria is much lower in comparison to the fermenters and results in the funnel concept aforementioned where there is a progressive specialisation of the AD community (Campanaro *et al*., 2018). The final step, which is the methanogenesis, is performed by archaeal species alone. conversion of simple compounds to methane is mediated only by highly specialised methanogenic archaea. According to the compounds they use as methanogenic substrate, three different types of methanogenesis can be identified (Costa and Leigh, 2014; Lyu *et al*., 2018). Hydrogenotrophic methanogenesis is the most frequent, methanogenic species can use H_2 and CO_2, acetoclastic methanogens utilise

acetate. The third group is made by methylotrophic methanogens which use methylated compounds, preferably methylamines or methanol. AD communities are abundant in many uncharacterized and uncultivated organisms, named 'microbial dark matter', with yet-to-be identified relationships among the three trophic groups. The main features of these relationships will be investigated in the next paragraph, entitled "Synthrophies in Anaerobic Digestion".

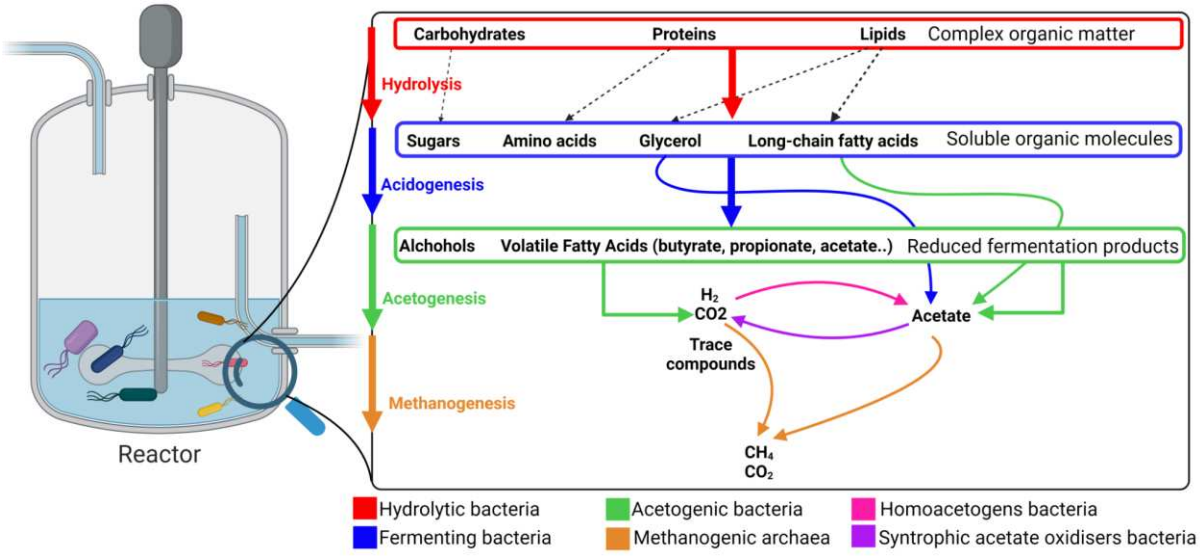

Figure 1: Schematic representation of the four subsequent biochemical steps of AD. Arrow color is related to the functional guild performing the conversion between different compounds, as indicated in the legend under the figure.

Synthrophies in Anaerobic Digestion

The AD community targeting methane production is driven by cooperative behaviours of different species in the food chain. In particular, in the latter steps of AD as in the biogas upgrading, syntrophic relations have a crucial role in keeping the concentration of key metabolites in the bioreactors stable. In recent years many mutualistic relationships have been hypothesized (Tan *et al*., 2016). Fontana and colleagues (Fontana *et al*., 2018) proposed, a putative syntrophic association between *Coprothermobacter proteolyticus* UC0011 and *Methanothermobacter wolfeii* UC0008 in the second phase of a two-stage reactor with acidogenic and methanogenic guilds divided. In another publication (Zhu *et al*., 2020), a glucose mutualistic mineralization model with no acetate intermediate was proposed between *Clostridiaceae* sp. and *Methanoculleus thermophilus*. Among all, Syntrophic Acetate Oxidation (SAO) is the most studied type of interplay. The complex net of relationships among archaea, homoacetogens bacteria and Syntrophic Acetate Oxidisers Bacteria (SAOB) will be discussed in the next paragraph. However, the stable activity of the microbial community is based on many other interrelationships which are inter-guilds and intra-guilds.

Syntrophic Acetate Oxidisers Bacteria and homoacetogens

Both SAOB and homoacetogens are involved in the AD process and drive the transformation or the generation of acetate, respectively. The homoacetogens reduce two moles of CO_2 with

H_2 to one mole of acetate (Diekert and Wohlfarth, 1994). This process is mediated by the Wood-Ljungdahl (WL) pathway (Borrel *et al*., 2016). In the WL pathway H_2 and CO_2, serves as donor and acceptor of electrons, respectively, to produce acetate, and ATP is formed in this pathway as well. On the other hand, SAOB convert acetate into H_2 and CO_2. Since the oxidation of acetate to H_2 and CO_2 is not thermodynamically favourable ($\Delta G0' = +104.6$ kJ mol^{-1}) (Pan *et al*., 2021), in order to keep the reaction on the edge of the thermodynamic feasibility, H_2 must be constantly removed. For this reason, SAO involves H_2 transfer between SAOB and hydrogenotrophic methanogens. By using H_2 as a methanation substrate, they maintain the hydrogen partial pressure (pH_2) below the value of 10^{-4} atm. Additionally, formate can be served as interspecies electron carriers as well (Costa *et al*., 2013). The interaction between SAOB and hydrogenotrophic methanogens also plays a significant role when acetoclastic methanogens are suppressed e.g., in anaerobic digester inhibited by high concentrations of VFA and high temperature (Wang *et al*., 2020). SAO often happens in biofilm communities (Tolker-Nielsen and Molin, 2000), which are complex structures constituted by prokaryotes but also fungi, yeasts and protozoa (Wimpenny *et al*., 2000). These species secrete an exopolysaccharidic matrix (EPS) which creates a protected growth environment (Limoli *et al*., 2015). The EPS is a gelatinous matrix made up of polysaccharides, proteins and lipids. Furthermore, the EPS confers to the biofilm its main features, i.e., mechanical stability and bacterial adhesion to the surface (Flemming *et al*., 2016).

From their side, homoacetogens outcompete with hydrogenotrophic methanogens for H_2 in an acidic environment (Stams and Plugge, 2009). However, homoacetogens and hydrogenotrophic methanogens work optimally at very different pH_2 thresholds (Wang *et al*., 2020). At high pH_2 (>500 Pa), homoacetogenesis is favoured, while, at low pH_2 and in mesophilic conditions, hydrogenotrophic archaea outcompete the bacterial antagonist. Homoacetogens compete with hydrogenotrophic methanogens for H_2, SAOB are mutualistic with hydrogenotrophic methanogens while competing with acetoclastic methanogens for acetate (Dyksma *et al*., 2020). The coexistence of these three mechanisms in the community of AD is possible only because the abundance and roles of the microbial species is strongly influenced by experimental parameters, e.g., ammonia concentration, temperature etc. This framework is even more complex because SAOB and homoacetogens species are very difficult to isolate and belong to the so-called “microbial dark matter” (Campanaro *et al*., 2018). As an example, to date, only six pure cultures of SAOB have been isolated: AOR (Lee and Zinder, 1988), *Clostridium ultunense* (Schnurer *et al*., 1996), *Thermoacetogenium phaeum* (Hattori *et al*., 2000), *Pseudothermotoga lettingae* (Balk *et al*., 2002), *Syntrophaceticus schinkii* (Westerholm *et al*., 2010) and *Tepidanaerobacter acetatoxydans* (Westerholm *et al*., 2011). Therefore, the use of approaches alternative to classical microbiology, such as flux balance analysis can help to have insights into SAOB behaviour in anaerobic conditions.

Gut microbiome

The human gut microbiome has important implications in health (Schmidt *et al*., 2018). Many diseases, named multifactorial, depend on a wide range of mechanisms (Stolk *et al*., 2008). This group includes a wide range of human diseases spanning from eating disorders and neurodegenerative to immune and metabolic disorders. The incidence of many multifactorial human diseases has substantially increased in the industrial revolution spanning the last two centuries (Cresci and Bawden, 2015). This short period ecompasses only a small number of human generations, therefore it is unlikely to explain these disorders with genetic factors alone. Contrariwise, they seem to be associated with changes in lifestyle. Lifestyle is an umbrella term which includes diet, exposure to xenobiotics (i.e., drugs and food additives), as well as the possibility of altering temperature and light conditions with domestic heating, air conditioning and artificial lightning (Trovato, 2012). In the investigation aimed at better figuring out the causes of these diseases, a recent link with a gene pool other than the human one has been drawn to inspect the impact of the environmental factors mentioned above on human health (Liang *et al*., 2018). The additional gene repertoire is named metagenome and is referred to as the global gene repertoire of the microbiome (Wang *et al*., 2015). With regard to the composition, the microbiome is represented by *Bacteria*, *Archaea* and *Viruses* but also *Fungi* and *Protozoa* (El-Sayed *et al*., 2021).

In recent years, anomalies in the gut microbial community composition, named dysbiosis, have been linked with such diseases (Carding *et al*., 2015). The dysbiosis affects the taxonomic composition of the community and the functional core of the metagenome, as well. Most of the microbial functions are tightly interconnected with the metabolites produced in the gut and, therefore, with human physiology (Brun, 2019). The importance of the gut microbiome spans from the fermentation of indigestible food components to the catabolism of vitamins and the strengthening of the intestinal barrier. As a consequence, for humans it was not necessary to develop these traits autonomously. Furthermore, products of microbial fermentation, such as short-chain fatty acids and VFA, are important for T-cell differentiation, which production in turn can modify the gut microbiome composition (den Besten *et al*., 2013). Microbiome and the eukaryotic genome coevolve. However, the microbiome is capable of evolutionary changes on a timescale much shorter than human one (Gordo, 2019). It is suggested that lifestyle alterations modify the metagenome faster than the host genome. The mutations accumulated in the microbiome can determine changes having effects already visible in a lifespan period (Rinninella *et al*., 2019). The first effort aimed at the enhancement of knowledge about human-associated microbial diversity is the Human Microbiome Project (HMP) (Integrative HMP (iHMP) Research Network Consortium, 2019; NIH HMP Working Group *et al*., 2009). During this pioneeristic project, the first collection including bacterial species without sequenced representatives were obtained. This collection included a few hundreds of genomes of uncultured species. In the last few years, big efforts have been made to expand the repertoire of species of the human gut with new cultured and uncultured genomes (Almeida *et al*., 2021). Two independent studies aimed to culture, isolate and sequence, in total, over 1000 human-gut-associated bacteria (Browne *et al*., 2016; Lagier *et al*., 2016). On the uncultured side, three independent projects recovered between 60,000 and 150,000 MAGs from human microbiome data previously deposited in public databases (Almeida *et al*., 2019; Pasolli *et al*., 2019).

Subsequently, redundant genomes have been clustered in single species thus establishing a unified dataset (Almeida *et al*., 2021). As already mentioned, many different diseases (e.g. Alzehimer disease, colorectal cancer, obesity) are linked to specific signatures in the gut microbiome (Rinninella *et al*., 2019). The comment of each of them is out of the scope of the present thesis, only the main features of the gut microbiota of Crohn's disease (CD) patients will be discussed in the paragraph entitled "Gut microbiota in Crohn's Disease"

Analogies between anaerobic digestion and gut

The gut microbiome is structured in a similar way to the AD community. In both cases the metabolic capabilities of the community lead to the conversion of complex organic molecules to simpler ones in an anoxic environment. As a consequence, in both communities the anabolism of complex molecules follows a funnel-like structure. One very big difference is that in the gut, the microbial community is not alone in performing the different digestive steps but is teamed with human secretions and mechanical activity. Saliva and biliar acids together with mastication and peristaltic movements provide fundamental help to the microbial community (Pedersen *et al*., 2002). However, in both communities an imbalance in the concentration of some key compounds results in an alteration of the process itself. For example, in dysbiosis the production of butyrate is lower than in healthy individuals (DeGruttola *et al*., 2016). In the case of the AD, the concentration of VFA produced by the microbial community is measured in order to monitor the proper functioning of the reactor (Lukitawesa *et al*., 2020). CH_4 is the final product of AD in industrial biogas production, while in the gut microbiome it represents only a byproduct of the microbial activity. However, an imbalance in the production of CH_4 can lead to unpleasant symptoms such as bloating events (Iovino *et al*., 2014). Bloating events and other symptoms related to an imbalance of methane production are frequently present among the CD symptoms.

Gut microbiota in Crohn's Disease

Crohn's Disease (CD) is a multifactorial disease and one of the inflammatory bowel diseases, together with Ulcerative Colitis (Gajendran *et al*., 2018). CD has a prevalence of 0.3% in Western countries affecting several million people worldwide. In developing countries, the incidence is lower. CD incidence seems to be highly correlated with a diet rich in polyunsaturated fatty acids, omega-6 fatty acids and animal fats (M'Koma, 2013). Another hypothesis for its high prevalence is "the hygiene hypothesis". This hypothesis postulates that a continuous and gradual exposure to helminthic and microbial pathogens during infancy and childhood boosts the immune system (Koloski *et al*., 2008). In westernised countries, where hygiene levels have strongly increased in the last two centuries, children are less exposed to microbial stimulation. The gut microbiota of CD patients is characterised by pathological alterations which activate a mucosal immune response and, as a consequence, provoke the development of chronic intestinal inflammation (Khan *et al*., 2019). Therefore, it can be stated that the unbalance in the eubiotic status of the intestine is a cause rather than a consequence of chronic inflammation (Khan *et al*., 2019; Lazar *et al*., 2018). More than genetic factors, environmental factors such as diet and use of antibiotics cause a decrease in bacterial diversity (Rinninella *et al*., 2019). Alterations in the gut microbiota trigger the dysbiosis. According to literature (Henson and Phalak, 2017), the triggering factor is an alteration of intestinal permeability and leaky gut caused by inflammation and physical stressors. The leaking gut causes dysbiosis, characterised by a lack in protective anaerobic commensal bacteria and in particular of butyrate producing bacteria such as *Faecalibacterium prausnitzii* (Leylabadlo *et al*., 2020) and *Roseburia hominis* (Patterson *et al*., 2017). At the same time an increase of facultative anaerobes belonging to the *Enterobacteriaceae* including adherent-invasive *Escherichia coli* and *Shigella* is correlated with CD onset (Baldelli *et al*., 2021). This hypothesis is called "the oxygen hypothesis" (Henson and Phalak, 2017). Furthermore, some studies reported that the severity of the symptoms are dependent on the O_2 gut leakage and the *Enterobacteriaceae* invasion in the gut (Caruso *et al*., 2020; Hosseinkhani *et al*., 2021).

Genome-scale metabolic modelling

Genome-scale metabolic models (GSMMs) are made by a whole set of stoichiometry-based and stoichiometric-balanced reactions describing together the gene-protein-reaction associations for the entire metabolic repertoire of an organism (O'Brien *et al*., 2015). GSMMs are based on the genomic annotation and experimentally obtained information (Thiele and Palsson, 2010). Furthermore, GSMMs can also be used as a platform to integrate and intersect various types of data such as omics and kinetic data (Zampieri *et al*., 2019). GSMMs can be used to predict metabolic potential for various system-level metabolic studies. *Haemophilus influenzae* was the first species serving as template for the generation of a GSMM in 1999 (Edwards and Palsson, 1999). Since that model, advances have been made to develop and simulate GSMMs for an increasing number of organisms belonging not only to *Bacteria* but also to *Archaea* and to *Eukarya*. Since 1999 lots of effort has been addressed to obtain more complete and curated GSMMs. GSMM reconstruction has been established as one of the most successful approaches for system-level modelling (Gu *et al*., 2019). The most common application for GSMMs is the prediction of metabolic flux values using optimisation techniques such as Flux Balance Analysis (FBA), which uses different approaches of linear programming (Orth *et al*., 2010). As genome sequencing techniques and omics analyses continue to expand, the quality and application scope of GSMMs have evolved accordingly. The integration of different approaches has permitted to understand in a more detailed way the metabolic capabilities of various organisms by generating model-driven hypotheses and implementing various context-specific simulations (Blais *et al*., 2013). GSMMs of various monocellular, but also multicellular organisms, have been reconstructed. Furthermore, many different collections of metabolic reconstructions have been developed, as well as numerous tools for large-scale generation of metabolic models.

Large-scale collections of metabolic reconstructions

During the years, different databases aimed to collect GSMMs have been developed. One of the main sources is the online VMH database (Noronha *et al*., 2019). The VMH database was selected for the storage of the AGORA collection (Magnúsdóttir *et al*., 2017) (which will be soon updated in AGORA2 (Heinken *et al*., 2020)). The reconstructions were made with a comparative metabolic method which enables propagation of refinement performed on one metabolic model to the others. Furthermore, all the reconstructions were curated based on literature-derived experimental data and the results of comparative genomics analyses. With this mixed approach a collection of 773 gut microbes including 205 different genera and 605 species was developed. Since the human gut is an anoxic environment (Heinken and Thiele, 2015), for all the GSMMs the anaerobic growth was enabled. Additionally, another centralised repository for GSMMs is the BiGG Models database (King *et al*., 2016). The BiGG database contains less GSMMs than the VMH, even if the name would suggest otherwise. All the GSMMs in BiGG are manually curated and to be loaded must pass strict quality checks. In total, to date, BiGG accounts for 108 different GSMMs (Norsigian *et al*., 2020b). All models have passed an internal testing suite accounting for 54 different tests to check model consistency and spot-check bugs and the presence of blocked reactions.

Homo sapiens reconstructions

One of the most challenging and ground breaking metabolic reconstructions created is the model of *Homo sapiens*. The availability of a model covering the metabolic potential of *Homo sapiens* has contributed to understanding the biological mechanisms behind various diseases (Angione, 2019). The first human reconstruction released was Recon 1 in 2007 (Duarte *et al*., 2007). Since the release of Recon 1, the Recon series has gone through several updates, accounting for the incorporation of additional biological information. In the version Recon2M.2 (Ryu *et al*., 2017), a framework for gene-transcript-protein-reaction association, named GeTPRA was developed in order to generate metabolic reconstructions which account also for the alternative splicing of metabolic genes. The latest version is Recon3D (Brunk *et al*., 2018) which contains information also on structural information of metabolites and enzymes. Recon3D can be used as a resource for many biomedical applications including also the analysis of disease-associated mutations and the metabolic responses to drugs. The Human Metabolic Reaction (HMR) is another collection of human reconstructions. HMR contains information on subcellular localisation and tissue-specific gene expression extracted from the Human Protein Atlas database (Pornputtapong *et al*., 2015). The HMR series contains comprehensive information on the fatty acid metabolism which has been manually curated (Gu *et al*., 2019). The HMR series has been used to generate cell-type-specific GSMMs such as iAdipocytes1809 (Mardinoglu *et al*., 2013), *i*Hepatocytes2322 (Mardinoglu *et al*., 2014), and *i*Myocyte2419 (Väremo *et al*., 2016). The aim of tissue-specific reconstructions was the study of obesity, non-alcoholic fatty liver disease (NAFLD), and diabetes, respectively. However, their application was not limited to that. Indeed in 2020, two new reconstructions of the human metabolism were published: Harvey and Harvetta (Thiele *et al*., 2020). Harvey and Harvetta are two sex-specific whole-body metabolic reconstructions integrating molecular and physiological data. They cover the metabolism of 26 different organs (e.g., liver, brain, pancreas) and six blood cell types (e.g., red blood cells, natural killer cells). Each whole-body model (WBM) accounts for more than 80,000 biochemical reactions in an anatomically and physiologically coherent framework. Harvey and Harvetta are based on Recon3D and integrate biological information retrieved from *i*Adipocytes1809 and the other tissue-specific reconstructions as well. The WBMs are parameterised with physiological, dietary and metabolomic data retrieved from literature. The biggest novelty of Harvey and Harvetta, however, is the ability to recapitulate inter-organ metabolic cycles like the gut-liver (Tripathi *et al*., 2018) and the gut-brain axes (Clapp *et al*., 2017). Finally, the integration of microbiome data with models can enable the inspection of host-microbiome co-metabolism.

Tools for genome-scale reconstructions and gap-filling

Building a genome-scale model is a process which starts either from data obtained from literature, previous knowledge stored in databases or functional annotation (Baart and Martens, 2012). The final aim is the representation of the biochemical network resembling the metabolic capabilities in the organism of interest. The recent years have seen the establishment of many GSMMs generator tools such as ModelSeed (Seaver *et al*., 2021), CarveMe (Machado *et al*., 2018) and gapseq (Zimmermann *et al*., 2021). The main characteristic of CarveMe in comparison to ModelSeed is the peculiar “top-down” approach opposite to the traditional

"bottom-up". In the top-down approach, a universal model is generated according to the group they were assigned to (e.g. gram positive/negative, Archaea). The model is used as a template to carve through homology or orthology predictions to generate an organism-specific model (Gu *et al*., 2019). However, automatic reconstructions are very prone to incorporate errors. Errors can manifest as missing reactions, gaps in the biochemical network, generation of futile cycles, etc. (Yizhak *et al*., 2010). Importantly, these errors are not due to missing enzymes caused by gene loss, gene disruption or auxotrophies, which result in biological gaps. In general, in a draft model, some reactions cannot carry fluxes, we refer to them as blocked reactions (Ponce-de-León *et al*., 2013). In other cases, metabolic models can produce metabolites which are neither incorporated in the biomass for the growth of the cell itself nor transported outside of the cell. In this case, the metabolic models accumulate the so-called dead-end metabolites (Mackie *et al*., 2013). This possibility is in contrast with one of the postulates of flux balance analysis, the steady-state behaviour (Raman and Chandra, 2009) which will be further discussed in the paragraph named "Flux Balance Analysis". Inaccuracies in the models can cause inconsistencies in the subsequent simulations. The bloom of semi-automated GSMM reconstruction tools of the last years, made the need for manual checking of the reactions included crucial (Norsigian *et al*., 2020a). In order to prevent those errors, the so-called gap-filling approach is frequently coupled with the metabolic model reconstruction process (Karp *et al*., 2018). Different strategies of gap-filling are used, for example, in some cases the gap-filling problem is formulated using a graph-based approach. Tools like Meneco, for example, query a minimal set of reactions which can restore the production of some target metabolites starting from the compounds given in the growth medium (Prigent *et al*., 2017). Other approaches are based on "subsystems of functional roles". If the draft reconstruction of an organism does not include a particular reaction present in other microbial species with the same functioning, the information is used as an indication of a missing pathway to be filled (Heinken *et al*., 2021b; Ong *et al*., 2020). The limitation of this comparison to closely-related organisms can lead to results more significant from a biological point of view. Furthermore, it can enable gene cluster comparison to inquire about alternative pathways or enzyme usage. A lot of tools and methods rely on databases of reactions, like the Kyoto Encyclopedia of Genes and Genomes (KEGG) (Kanehisa and Goto, 2000) or MetaCyc (Caspi *et al*., 2020; Karp *et al*., 2002), in order to detect the best candidates for gap-filling addition to the models. The gap-filling step has two important applications. They can discover unannotated or mis-annotated genes, but they can also identify new activities of existing enzymes to bypass some pathways of interest. Furthermore, they can also identify bridge molecules between pathways previously reputed not connected (Pan and Reed, 2018).

Flux Balance Analysis

GSMMs can be used in combination with simulations of fluxes in order to generate the so-called fluxomic data. Fluxomic can be used as an additional "-omic" layer and be complemented with the other "omics" (Zampieri *et al*., 2019). The fluxomic can permit the complete evaluation of the metabolic state of a set of cells, particularly when metabolic profiling using analytical techniques such as mass spectrometry is infeasible (Cortassa *et al*., 2015). GSMMs are not intended to be directly used for simulation purposes, the reconstruction needs to be converted in context-specific metabolic models. To do this, the genome-scale reconstructions can be converted into stoichiometric matrices (S) (Orth *et al*., 2010). S includes information on metabolites consumed and produced by every reaction and can be interrogated through established approaches such as FBA (Orth *et al*., 2010). FBA can give more reliable results by integrating in the matrix constraints from experimental data, e.g. metabolomics (Cortassa *et al*., 2015) and transcriptomic (Machado and Herrgård, 2014), or environmental information, e.g. nutrient uptake, or even physicochemical knowledge, e.g. mass-charge balance (Shaw and Cheung, 2019). In order to constrain the model a vector of fluxes (v) is defined, and S is multiplied by v. The aim is to reduce the flow of metabolites in the network and, therefore, obtain a solution space of possible flux distributions (Orth *et al*., 2010). The subsequent definition of a biological target, also known as objective function, lies at the heart of FBA (García Sánchez and Torres Sáez, 2014). The most commonly used biological target is the biomass reaction, which represents all the metabolites consumed for the generation of a new cell. Another possibility is to use as the objective function the production of a metabolite of interest. Subsequently, the objective function is minimised or maximised in order to compute the optimal solution by integrating in the reconstruction the condition-specific constraints. Kinetic parameters are not integrated in the standard computation of the optimal solution as in FBA it is assumed that the cells are in a steady-state growth phase where there is no net metabolites accumulation (Diener *et al*., 2020). FBA is implemented in different computational approaches, one of the most used in the modelling community is the Constraint-based Reconstruction and Analysis (COBRA) implemented in different programming languages (e.g. MATLAB, Python) (Ebrahim *et al*., 2013; Heirendt *et al*., 2019).

Flux Balance Analysis applied to communities

The FBA approach, underlying genome-scale metabolic networks, enables the modelling of microbial communities and mechanistic predictions of metabolic fluxes. To this aim the biological framework of the microbial species under examination such as metabolites availability and interspecies boundaries can be taken into account. In particular, FBA can target the inspection of microbial cross-feeding in communities and the analysis of evolutionary trajectory of microbial communities (Thommes *et al*., 2019). During the last twenty years, different pipelines of FBA to analyse the behaviour of different species together have been developed. At the beginning the aim was the inspection of pairwise interactions (Heinken and Thiele, 2015). Some pipelines, such as Mminte (Mendes-Soares *et al*., 2016), were developed for this aim. The interspecies behaviour is inspected creating a two-reconstructions community and performing selective knockout of one species. The pattern of interaction is assigned

according to the influence of each microbial species on the growth rate of the partner, considering the threshold of ±10% to justify a difference in the growth rate (Magnúsdóttir *et al*., 2017). Furthermore, lots of efforts have been addressed to the development of tools which enable the in-silico communication of different reconstructions. The most used approach is the implementation of a compartmentalised approach (Thiele *et al*., 2013). The individual genome-scale reconstructions are joined together creating a shared compartment which represents the environment and consist of all the common exchange reactions. This approach is implemented in different pipelines such as mgPipe (Baldini *et al*., 2019), optCom (Zomorrodi and Maranas, 2012), SteadyCom (Chan *et al*., 2017) and MICOM (Diener *et al*., 2020). The major advantages are that it relies on the formulation of the "community biomass" reaction which encapsulates the growth of all organisms joined. This approach is particularly valuable since the abundances of each reconstruction in the community can be integrated to provide more reliable results of the simulation. The abundances can be retrieved from 16S rRNA or metagenomic sequencing and their incorporation makes the contextualisation of the reconstructions in the community possible. FBA has been used to inspect the behaviour of a wide range of microbial communities. The main application is the study of multifactorial diseases such as Colorectal Cancer (Hertel *et al*., 2021), Crohn's disease (Heinken *et al*., 2019, 2021a), Type 2 Diabetes (Diener *et al*., 2020; Rosario *et al*., 2018) and so on. Furthermore, from animal microbiome (Ankrah *et al*., 2020, 2017; Blow *et al*., 2020), to plant symbiosis (diCenzo *et al*., 2020), from bioremediation (Xu *et al*., 2019) to synthetic communities (Harcombe *et al*., 2014; McNally and Borenstein, 2018), all types of microbial communities have been inspected with FBA. Here, the author will focus on applications of FBA to the AD community and for the analysis of the co-aetiology of the gut microbiota in the onset of CD.

Anaerobic digestion and Flux Balance Analysis

The population wise analysis of AD through flux balance was one of the main novelties brought by the present thesis to the scientific community. However, previous works exist which focus on the synthrophies between the bacterial and archaeal guilds (**Figure 2**).

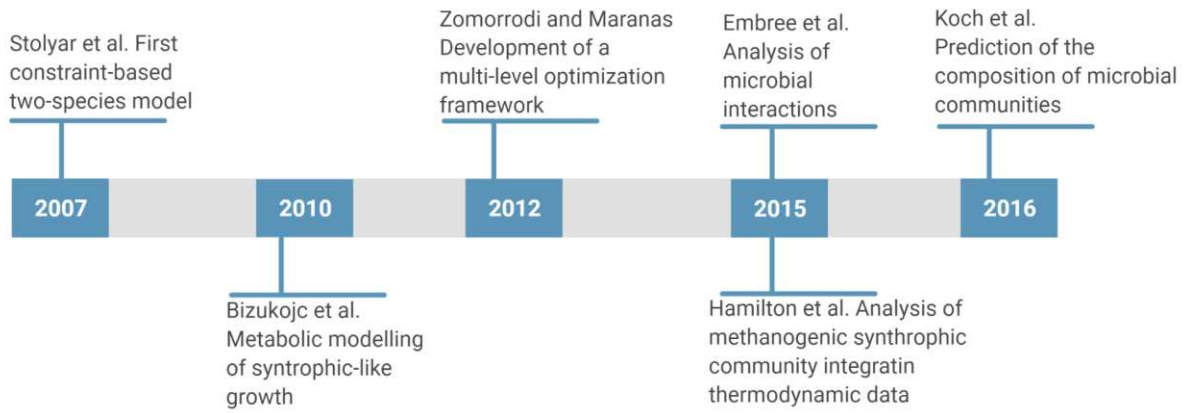

Figure 2: Timeline of the main studies exploring possible applications of flux balance analysis to the anaerobic digestion community

To this aim the first pioneeristic work was published in 2007 by Stolyar and colleagues. In particular they analysed the syntrophic association between *Desulfovibrio vulgaris* and *Methanococcus maripaludis* (Stolyar *et al*., 2007). The metabolic networks for both species were de novo reconstructed and the effect of sulphate removal on the couple was tested. Sulphate is a typical electron acceptor for *D. vulgaris* (Keller and Wall, 2011), while the archaea plays the role of hydrogen scavenger. The hydrogen inhibits the growth of the bacterium and its removal enables the growth of *D. vulgaris* by fermenting lactate or other carbon sources (Voordouw, 2002). The simulations detected formate interspecies electron shuttle as facultative, while hydrogen as mandatory for syntrophic growth. In another publication, the syntrophic-like growth of *Clostridium butyricum* and *Methanosarcina mazei* was inspected (Bizukojc *et al*., 2010). The two systems have some important differences due to the dissimilar metabolisms of the four species. Even if both *M. mazei* and *M. maripaludis* are two methanogenic archaea, they use different substrates for methane synthesis. *M. maripaludis*, is hydrogenotrophic, while *Methanosarcina* species such as *M. mazei*, contrariwise, are generalists, and therefore can use at least four different carbon sources as methanogenesis substrates, i.e. CO_2, formate, methanol and acetate (Assis das Graças *et al*., 2013). Therefore, the model included all the reactions as well as the balance of reduced hydrogen carriers and is able to predict shifts in the metabolism of *Methanosarcina* sp. caused by competing substrates. Furthermore, *C. butyricum* can convert glycerol in 1,3-propanediol, a source of acetate, butyrate and formate as inhibiting by-products (Zhou *et al*., 2020). The interplay between the bacterium and the archaea was inspected in ten different scenarios to understand how the combination of the metabolism of the two species can be exploited in order to convert inconvenient by-products in CH_4. It was observed that the introduction in the medium of methanol enhanced the methane conversion of 130%. Furthermore, according to the prediction, *M. mazei* was able to scavenge over 70% of the acetate produced by *C. butyricum*. In another study (Hamilton *et al*., 2015) the conditions where H_2 and formate produced by *Syntrophobacter fumaroxidans* are completely metabolised by *Methanospirillum hungatei* were identified using a coculture of two metabolic reconstructions named *i*Sfu648 and *i*Mhu428. The models were combined with thermodynamics information and the main drivers of their interaction were identified in the concurring exchange of H_2 and formate. The couple *D. vulgaris* and *M. maripaludis* was further investigated taking into account also the interaction with a third player, *Methanosarcina barkeri* (Koch *et al*., 2016). The two archaea can both behave as hydrogenotrophic since *M. maripaludis* is a pure hydrogenotrophic species while *M. barkeri* is a generalist (Lambie *et al*., 2015), as a consequence they compete for CO_2 and H_2. The main metabolic differences are as follows: *M. barkeri* uses the oxidative branch of the tricarboxylic acid cycle while *M. maripaludis* the reductive branch; additionally, *M. barkeri* possesses a ribulose monophosphate pathway (Kato *et al*., 2006). The simulations included three different scenarios including a competition scenario with both methanogens using the hydrogenotrophic methanogenesis. The second scenario assumes that *M. barkeri* can use only the acetoclastic pathway for methane production. The third scenario assumes that *M. barkeri* has both hydrogenotrophic and acetotrophic pathways. The maximum theoretical CH_4 yield is obtained in the second scenario when all the acetate is consumed. The interplay between *D. vulgaris* and *M. maripaludis* was further inspected also as a case of study during the development of OptCom (Zomorrodi and Maranas, 2012). The results obtained with OptCom

are similar to Stolyar's multi-compartment approach. Hydrogen was predicted to be able to support the syntrophy independently from formate. Furthermore, it was shown that in absence of H_2, *D. vulgaris* is unable to produce sufficient formate to enable the minimum electron transfer necessary for redox balance maintenance. Embree and colleagues (Embree *et al*., 2015) analysed the interaction network among five different species: *Smithella* sp. ME-1, *Syntrophomonas wolfei*, *Desulfovibrio magneticus*, *Methanoculleus marisnigri*, *Methanosaeta concilii*, *Methanocorpusculum labreanum*, and *Melioribacter roseus*. The species were binned from metagenomic experiments. Species-specific gene expression profiles were recovered mapping the sequences of the MAGs on transcriptomic datasets from metatranscriptomic experiments aiming to inspect the hexadecane degradation process. It was underlined that amino acid auxotrophies reinforce interdependence and collaboration within the community, though vulnerability to competing species. Another crucial point to the competition of the species relies on the production of the bacteriocin receptor colicin V. *D. magneticus* encodes the full set of genes which allow for this toxin to enter the cell with a Ton or Tol system, making this species sensitive to the bacteriocin (Lloubès *et al*., 2012). As a consequence its abundance is very low despite the high growth rate. Together with metabolic interdepencies, the presence of mutations inactivating bacteriocin uptake promotes competition among species (Hibbing *et al*., 2010).

Crohn's disease and Flux Balance Analysis

FBA was used to inspect different cases of studies in the framework of CD. An interesting study tested the oxygen hypothesis mentioned above analysing the outcompetition of *E. coli* over *Bacteroides thetaiotaomicron* and *F. prausnitzii* with increasing concentrations of O_2 (Henson and Phalak, 2017). Furthermore, in several manuscripts the modelling of the CD gut microbiome using either 16 rRNA or metagenomic sequencing was charted. For example, personalised microbiome models were built for three different cohorts including pediatric patients of CD, age-matched controls and healthy human adults (Heinken *et al*., 2019). In each sample the potential ability of primary bile acids deconjugation to secondary bile acids was inspected (Gérard, 2013). The potential to synthesise secondary bile acids is significantly lower in CD microbiomes compared to controls. Furthermore, it was found that the deconjugation of primary bile acids into secondary ones is more likely to happen with a shared reaction-pool. It means that in the gut this activity is possible thanks to the synergy between microbial species. A follow-up study with the same controls and patient cohorts revealed a significant difference in the secretion ability of some metabolites between patients and controls. In particular, an increase in the biosynthesis of some amino acids in dysbiotic CD microbiomes was caused by the metabolism of Proteobacteria strains (Heinken and Thiele, 2019). Another effort targeted the identification of individual-specific dietary addictions which can enhance the production of VFA in patients with dysbiotic microbiome. In particular, to this aim pectin resulted to be a valuable food addiction (Bauer and Thiele, 2018). Furthermore, it was found that a diet based on plant fibers and glycans can stimulate *Bacteroides* and *Clostridium* species. These studies highlighted the importance of FBA for the inspection of dysbiosis like CD. However, analysis

reflecting the evolution of the microbial community along longitudinal data is still missing and it is one of the main aspects charted by the present thesis.

Overview on the selected manuscripts and conclusions

For the current PhD thesis, I selected four publications which can shed light on this three years project and evidence the novelty brought from this thesis to the scientific community. I decided to deal in parallel with AD and gut microbiome underlining analogies and contrasts.

Paper I and *Paper II* are focused on the application of FBA to the AD engineering system. *Paper I* aimed to unveil the metabolic mechanisms of interactions through the analysis of pairwise interactivity and the associated metabolite exchanges. To my knowledge, genome-scale metabolic models were built starting from metagenome assembled genomes retrieved from genome-centric metagenomics for the first time. To characterize completely the community under evaluation, a novel collection of 836 GSMMs was established. In the manuscript, the role of glucogenic amino acids was commented as one of the most important compounds exchanged among auxotrophic species. Finally, the effect of hydrogen injection on the microbial dynamics was inspected to simulate the biogas upgrading. External hydrogen positively influences the stability of the community promoting commensalism over amensalistic interplays. The application of FBA suggested strategies to increasing the biogas production efficiency.

Paper II was based on the inspection of ammonia adaptation on microbial communities in reactors fed with simple substrates. In this paper, which I co-authored, FBA was used as a side tool in order to inspect the reliability of hypothesis of interactions based on other bioinformatic analysis. Some of the suggested interplays were confirmed. In particular, *Pelotomaculum* sp. DTU813 and *Methanothermobacter* sp. DTU779, hypothesized to be mutualistic species, were identified as commensalistic partners with *Pelotomaculum* sp. DTU813 being favoured by the coexistence and *Methanothermobacter* sp. DTU779 not being negatively influenced from the coexistence, thus explaining its high abundance in the microbial community.

Paper III and *Paper IV* are focused on application of FBA on gut microbiome. These projects were supported by an EMBO short-term fellowship. *Paper III* is a review aiming to describe the main areas of application of FBA and COBRA modelling with a focus on previous works about IBD and other multifactorial diseases. *Paper III* served as a preliminary work for *Paper IV*.

Paper IV charted for the first time to identify variations in one individual across multiple timepoints rather than between individuals. The different time points cover inflamed and relapsing stages of the gut microbiome of a patient affected by CD. The analysis was focused on the main causes of the bloating and inflammatory events experienced during the disease. An increase in the production of methane and LPS was identified and targeted as typical of the inflamed stages of the disease. A key role was identified for species belonging to the *Dialister* genus and their behavior in the different stages was explored. Indeed, during the inflamed stages they produce L-serine and formate which trigger a cascade of events culminating in a positive interplay with Archaea and an increase of LPS production. Finally, the integration of the human whole-body model was used to track the effect of the dysbiosis on different body

sites, organs and tissues. The analysis evidenced an imbalance in the metabolism of prostaglandin E2 in the pancreas during the inflammatory stages.

As conclusive remarks it can be stated that the four different studies reported in the current research shed light on the main analogies between the AD engineering system and the gut microbiome both in terms of guilds composition and metabolite production. These analogies have been inspected in different case studies through FBA based on shotgun metagenomic analysis. The results reported in this paper collection served this aim and underlined the different yet crucial role of methane and VFA in the two systems. Furthermore, the identification of interactions between functional guilds underlined the importance of cooperation between microbial species to produce beneficial or toxic compounds for either biogas production or human health.

Cited literature

Abisado, R.G., Benomar, S., Klaus, J.R., Dandekar, A.A., Chandler, J.R., 2018. Bacterial Quorum Sensing and Microbial Community Interactions. mBio 9, e02331-17. https://doi.org/10.1128/mBio.02331-17

Adnan, A.I., Ong, M.Y., Nomanbhay, S., Chew, K.W., Show, P.L., 2019. Technologies for Biogas Upgrading to Biomethane: A Review. Bioengineering (Basel) 6, E92. https://doi.org/10.3390/bioengineering6040092

Albertsen, M., Hugenholtz, P., Skarshewski, A., Nielsen, K.L., Tyson, G.W., Nielsen, P.H., 2013. Genome sequences of rare, uncultured bacteria obtained by differential coverage binning of multiple metagenomes. Nat Biotechnol 31, 533–538. https://doi.org/10.1038/nbt.2579

Almeida, A., Mitchell, A.L., Boland, M., Forster, S.C., Gloor, G.B., Tarkowska, A., Lawley, T.D., Finn, R.D., 2019. A new genomic blueprint of the human gut microbiota. Nature 568, 499–504. https://doi.org/10.1038/s41586-019-0965-1

Almeida, A., Nayfach, S., Boland, M., Strozzi, F., Beracochea, M., Shi, Z.J., Pollard, K.S., Sakharova, E., Parks, D.H., Hugenholtz, P., Segata, N., Kyrpides, N.C., Finn, R.D., 2021. A unified catalog of 204,938 reference genomes from the human gut microbiome. Nat Biotechnol 39, 105–114. https://doi.org/10.1038/s41587-020-0603-3

Angelidaki, I., Ellegaard, L., Ahring, B.K., 2003. Applications of the anaerobic digestion process. Adv Biochem Eng Biotechnol 82, 1–33. https://doi.org/10.1007/3-540-45838-7_1

Angelidaki, I., Treu, L., Tsapekos, P., Luo, G., Campanaro, S., Wenzel, H., Kougias, P.G., 2018. Biogas upgrading and utilization: Current status and perspectives. Biotechnology Advances 36, 452–466. https://doi.org/10.1016/j.biotechadv.2018.01.011

Angione, C., 2019. Human Systems Biology and Metabolic Modelling: A Review-From Disease Metabolism to Precision Medicine. Biomed Res Int 2019, 8304260. https://doi.org/10.1155/2019/8304260

Ankrah, N.Y.D., Luan, J., Douglas, A.E., 2017. Cooperative Metabolism in a Three-Partner Insect-Bacterial Symbiosis Revealed by Metabolic Modeling. J Bacteriol 199, e00872-16. https://doi.org/10.1128/JB.00872-16

Ankrah, N.Y.D., Wilkes, R.A., Zhang, F.Q., Aristilde, L., Douglas, A.E., 2020. The Metabolome of Associations between Xylem-Feeding Insects and their Bacterial Symbionts. J Chem Ecol 46, 735–744. https://doi.org/10.1007/s10886-019-01136-7

Assis das Graças, D., Thiago Jucá Ramos, R., Vieira Araújo, A.C., Zahlouth, R., Ribeiro Carneiro, A., Souza Lopes, T., Azevedo Baraúna, R., Azevedo, V., Cruz Schneider, M.P., Pellizari, V.H., Silva, A., 2013. Complete Genome of a Methanosarcina mazei Strain Isolated from Sediment Samples from an Amazonian Flooded Area. Genome Announc 1, e00271-13. https://doi.org/10.1128/genomeA.00271-13

Azhar, N.S., Md Zin, N.H., Hamid, T.H.T.A., 2017. Lactococcus Lactis Strain A5 Producing Nisin-like Bacteriocin Active against Gram Positive and Negative Bacteria. Trop Life Sci Res 28, 107–118. https://doi.org/10.21315/tlsr2017.28.2.8

Baart, G.J.E., Martens, D.E., 2012. Genome-scale metabolic models: reconstruction and analysis. Methods Mol Biol 799, 107–126. https://doi.org/10.1007/978-1-61779-346-2_7

Baldelli, V., Scaldaferri, F., Putignani, L., Del Chierico, F., 2021. The Role of Enterobacteriaceae in Gut Microbiota Dysbiosis in Inflammatory Bowel Diseases. Microorganisms 9, 697. https://doi.org/10.3390/microorganisms9040697

Baldini, F., Heinken, A., Heirendt, L., Magnusdottir, S., Fleming, R.M.T., Thiele, I., 2019. The Microbiome Modeling Toolbox: from microbial interactions to personalized microbial

communities. Bioinformatics 35, 2332–2334. https://doi.org/10.1093/bioinformatics/bty941
Balk, M., Weijma, J., Stams, A.J.M., 2002. Thermotoga lettingae sp. nov., a novel thermophilic, methanol-degrading bacterium isolated from a thermophilic anaerobic reactor. Int J Syst Evol Microbiol 52, 1361–1368. https://doi.org/10.1099/00207713-52-4-1361
Bauer, E., Thiele, I., 2018. From metagenomic data to personalized *in silico* microbiotas: predicting dietary supplements for Crohn's disease. NPJ Syst Biol Appl 4, 27. https://doi.org/10.1038/s41540-018-0063-2
Bengoa, A.A., Iraporda, C., Garrote, G.L., Abraham, A.G., 2019. Kefir micro-organisms: their role in grain assembly and health properties of fermented milk. J Appl Microbiol 126, 686–700. https://doi.org/10.1111/jam.14107
Berg, G., Rybakova, D., Fischer, D., Cernava, T., Vergès, M.-C.C., Charles, T., Chen, X., Cocolin, L., Eversole, K., Corral, G.H., Kazou, M., Kinkel, L., Lange, L., Lima, N., Loy, A., Macklin, J.A., Maguin, E., Mauchline, T., McClure, R., Mitter, B., Ryan, M., Sarand, I., Smidt, H., Schelkle, B., Roume, H., Kiran, G.S., Selvin, J., Souza, R.S.C. de, van Overbeek, L., Singh, B.K., Wagner, M., Walsh, A., Sessitsch, A., Schloter, M., 2020. Microbiome definition re-visited: old concepts and new challenges. Microbiome 8, 103. https://doi.org/10.1186/s40168-020-00875-0
Bilen, M., Dufour, J.-C., Lagier, J.-C., Cadoret, F., Daoud, Z., Dubourg, G., Raoult, D., 2018. The contribution of culturomics to the repertoire of isolated human bacterial and archaeal species. Microbiome 6, 94. https://doi.org/10.1186/s40168-018-0485-5
Bizukojc, M., Dietz, D., Sun, J., Zeng, A.-P., 2010. Metabolic modelling of syntrophic-like growth of a 1,3-propanediol producer, Clostridium butyricum, and a methanogenic archeon, Methanosarcina mazei, under anaerobic conditions. Bioprocess Biosyst Eng 33, 507–523. https://doi.org/10.1007/s00449-009-0359-0
Blais, E.M., Chavali, A.K., Papin, J.A., 2013. Linking genome-scale metabolic modeling and genome annotation. Methods Mol Biol 985, 61–83. https://doi.org/10.1007/978-1-62703-299-5_4
Blow, F., Ankrah, N.Y.D., Clark, N., Koo, I., Allman, E.L., Liu, Q., Anitha, M., Patterson, A.D., Douglas, A.E., 2020. Impact of Facultative Bacteria on the Metabolic Function of an Obligate Insect-Bacterial Symbiosis. mBio 11, e00402-20. https://doi.org/10.1128/mBio.00402-20
Borrel, G., Adam, P.S., Gribaldo, S., 2016. Methanogenesis and the Wood-Ljungdahl Pathway: An Ancient, Versatile, and Fragile Association. Genome Biol Evol 8, 1706–1711. https://doi.org/10.1093/gbe/evw114
Browne, H.P., Forster, S.C., Anonye, B.O., Kumar, N., Neville, B.A., Stares, M.D., Goulding, D., Lawley, T.D., 2016. Culturing of "unculturable" human microbiota reveals novel taxa and extensive sporulation. Nature 533, 543–546. https://doi.org/10.1038/nature17645
Brun, P., 2019. The profiles of dysbiotic microbial communities. AIMS Microbiol 5, 87–101. https://doi.org/10.3934/microbiol.2019.1.87
Brunk, E., Sahoo, S., Zielinski, D.C., Altunkaya, A., Dräger, A., Mih, N., Gatto, F., Nilsson, A., Preciat Gonzalez, G.A., Aurich, M.K., Prlić, A., Sastry, A., Danielsdottir, A.D., Heinken, A., Noronha, A., Rose, P.W., Burley, S.K., Fleming, R.M.T., Nielsen, J., Thiele, I., Palsson, B.O., 2018. Recon3D enables a three-dimensional view of gene variation in human metabolism. Nat. Biotechnol. 36, 272–281. https://doi.org/10.1038/nbt.4072
Brüssow, H., 2015. Microbiota and the human nature: know thyself. Environ Microbiol 17, 10–15. https://doi.org/10.1111/1462-2920.12693
Bušić, A., Kundas, S., Morzak, G., Belskaya, H., Marđetko, N., Ivančić Šantek, M., Komes, D., Novak, S., Šantek, B., 2018. Recent Trends in Biodiesel and Biogas Production. Food Technol Biotechnol 56, 152–173. https://doi.org/10.17113/ftb.56.02.18.5547
Campanaro, S., Treu, L., Kougias, P.G., De Francisci, D., Valle, G., Angelidaki, I., 2016.

Metagenomic analysis and functional characterization of the biogas microbiome using high throughput shotgun sequencing and a novel binning strategy. Biotechnol Biofuels 9, 26. https://doi.org/10.1186/s13068-016-0441-1

Campanaro, S., Treu, L., Kougias, P.G., Luo, G., Angelidaki, I., 2018. Metagenomic binning reveals the functional roles of core abundant microorganisms in twelve full-scale biogas plants. Water Res 140, 123–134. https://doi.org/10.1016/j.watres.2018.04.043

Campanaro, S., Treu, L., Rodriguez-R, L.M., Kovalovszki, A., Ziels, R.M., Maus, I., Zhu, X., Kougias, P.G., Basile, A., Luo, G., Schlüter, A., Konstantinidis, K.T., Angelidaki, I., 2020. New insights from the biogas microbiome by comprehensive genome-resolved metagenomics of nearly 1600 species originating from multiple anaerobic digesters. Biotechnol Biofuels 13, 25. https://doi.org/10.1186/s13068-020-01679-y

Cani, P.D., 2018. Human gut microbiome: hopes, threats and promises. Gut 67, 1716–1725. https://doi.org/10.1136/gutjnl-2018-316723

Canon, F., Nidelet, T., Guédon, E., Thierry, A., Gagnaire, V., 2020. Understanding the Mechanisms of Positive Microbial Interactions That Benefit Lactic Acid Bacteria Co-cultures. Front Microbiol 11, 2088. https://doi.org/10.3389/fmicb.2020.02088

Cao, X., Hamilton, J.J., Venturelli, O.S., 2019. Understanding and Engineering Distributed Biochemical Pathways in Microbial Communities. Biochemistry 58, 94–107. https://doi.org/10.1021/acs.biochem.8b01006

Carding, S., Verbeke, K., Vipond, D.T., Corfe, B.M., Owen, L.J., 2015. Dysbiosis of the gut microbiota in disease. Microb Ecol Health Dis 26, 26191. https://doi.org/10.3402/mehd.v26.26191

Caruso, R., Lo, B.C., Núñez, G., 2020. Host-microbiota interactions in inflammatory bowel disease. Nat Rev Immunol 20, 411–426. https://doi.org/10.1038/s41577-019-0268-7

Caspi, R., Billington, R., Keseler, I.M., Kothari, A., Krummenacker, M., Midford, P.E., Ong, W.K., Paley, S., Subhraveti, P., Karp, P.D., 2020. The MetaCyc database of metabolic pathways and enzymes - a 2019 update. Nucleic Acids Res 48, D445–D453. https://doi.org/10.1093/nar/gkz862

Chan, S.H.J., Simons, M.N., Maranas, C.D., 2017. SteadyCom: Predicting microbial abundances while ensuring community stability. PLoS Comput Biol 13, e1005539. https://doi.org/10.1371/journal.pcbi.1005539

Chen, L.-X., Anantharaman, K., Shaiber, A., Eren, A.M., Banfield, J.F., 2020. Accurate and complete genomes from metagenomes. Genome Res 30, 315–333. https://doi.org/10.1101/gr.258640.119

Clapp, M., Aurora, N., Herrera, L., Bhatia, M., Wilen, E., Wakefield, S., 2017. Gut microbiota's effect on mental health: The gut-brain axis. Clin Pract 7, 987. https://doi.org/10.4081/cp.2017.987

Cortassa, S., Caceres, V., Bell, L.N., O'Rourke, B., Paolocci, N., Aon, M.A., 2015. From metabolomics to fluxomics: a computational procedure to translate metabolite profiles into metabolic fluxes. Biophys J 108, 163–172. https://doi.org/10.1016/j.bpj.2014.11.1857

Costa, K.C., Leigh, J.A., 2014. Metabolic versatility in methanogens. Curr Opin Biotechnol 29, 70–75. https://doi.org/10.1016/j.copbio.2014.02.012

Costa, K.C., Yoon, S.H., Pan, M., Burn, J.A., Baliga, N.S., Leigh, J.A., 2013. Effects of H2 and formate on growth yield and regulation of methanogenesis in Methanococcus maripaludis. J Bacteriol 195, 1456–1462. https://doi.org/10.1128/JB.02141-12

Cresci, G.A., Bawden, E., 2015. Gut Microbiome: What We Do and Don't Know. Nutr Clin Pract 30, 734–746. https://doi.org/10.1177/0884533615609899

Dance, A., 2020. The search for microbial dark matter. Nature 582, 301–303.

https://doi.org/10.1038/d41586-020-01684-z
De Vuyst, L., Weckx, S., 2016. The cocoa bean fermentation process: from ecosystem analysis to starter culture development. J Appl Microbiol 121, 5–17. https://doi.org/10.1111/jam.13045
DeGruttola, A.K., Low, D., Mizoguchi, A., Mizoguchi, E., 2016. Current Understanding of Dysbiosis in Disease in Human and Animal Models. Inflamm Bowel Dis 22, 1137–1150. https://doi.org/10.1097/MIB.0000000000000750
den Besten, G., van Eunen, K., Groen, A.K., Venema, K., Reijngoud, D.-J., Bakker, B.M., 2013. The role of short-chain fatty acids in the interplay between diet, gut microbiota, and host energy metabolism. J Lipid Res 54, 2325–2340. https://doi.org/10.1194/jlr.R036012
diCenzo, G.C., Tesi, M., Pfau, T., Mengoni, A., Fondi, M., 2020. Genome-scale metabolic reconstruction of the symbiosis between a leguminous plant and a nitrogen-fixing bacterium. Nat Commun 11, 2574. https://doi.org/10.1038/s41467-020-16484-2
Diekert, G., Wohlfarth, G., 1994. Metabolism of homocetogens. Antonie Van Leeuwenhoek 66, 209–221. https://doi.org/10.1007/BF00871640
Diener, C., Gibbons, S.M., Resendis-Antonio, O., 2020. MICOM: Metagenome-Scale Modeling To Infer Metabolic Interactions in the Gut Microbiota. mSystems 5, e00606-19. https://doi.org/10.1128/mSystems.00606-19
Duarte, N.C., Becker, S.A., Jamshidi, N., Thiele, I., Mo, M.L., Vo, T.D., Srivas, R., Palsson, B.Ø., 2007. Global reconstruction of the human metabolic network based on genomic and bibliomic data. Proc Natl Acad Sci U S A 104, 1777–1782. https://doi.org/10.1073/pnas.0610772104
Dubé, C.-D., Guiot, S.R., 2015. Direct Interspecies Electron Transfer in Anaerobic Digestion: A Review. Adv Biochem Eng Biotechnol 151, 101–115. https://doi.org/10.1007/978-3-319-21993-6_4
Dyksma, S., Jansen, L., Gallert, C., 2020. Syntrophic acetate oxidation replaces acetoclastic methanogenesis during thermophilic digestion of biowaste. Microbiome 8. https://doi.org/10.1186/s40168-020-00862-5
Ebrahim, A., Lerman, J.A., Palsson, B.O., Hyduke, D.R., 2013. COBRApy: COnstraints-Based Reconstruction and Analysis for Python. BMC Syst Biol 7, 74. https://doi.org/10.1186/1752-0509-7-74
Edwards, J.S., Palsson, B.O., 1999. Systems properties of the Haemophilus influenzae Rd metabolic genotype. J Biol Chem 274, 17410–17416. https://doi.org/10.1074/jbc.274.25.17410
El-Sayed, A., Aleya, L., Kamel, M., 2021. The link among microbiota, epigenetics, and disease development. Environ Sci Pollut Res Int 28, 28926–28964. https://doi.org/10.1007/s11356-021-13862-1
Embree, M., Liu, J.K., Al-Bassam, M.M., Zengler, K., 2015. Networks of energetic and metabolic interactions define dynamics in microbial communities. Proc Natl Acad Sci U S A 112, 15450–15455. https://doi.org/10.1073/pnas.1506034112
Faust, K., Raes, J., 2012. Microbial interactions: from networks to models. Nat Rev Microbiol 10, 538–550. https://doi.org/10.1038/nrmicro2832
Flemming, H.-C., Wingender, J., Szewzyk, U., Steinberg, P., Rice, S.A., Kjelleberg, S., 2016. Biofilms: an emergent form of bacterial life. Nat Rev Microbiol 14, 563–575. https://doi.org/10.1038/nrmicro.2016.94
Fontana, A., Kougias, P.G., Treu, L., Kovalovszki, A., Valle, G., Cappa, F., Morelli, L., Angelidaki, I., Campanaro, S., 2018. Microbial activity response to hydrogen injection in thermophilic anaerobic digesters revealed by genome-centric metatranscriptomics. Microbiome 6, 194. https://doi.org/10.1186/s40168-018-0583-4
Fu, S., Angelidaki, I., Zhang, Y., 2021. In situ Biogas Upgrading by CO2-to-CH4 Bioconversion. Trends Biotechnol 39, 336–347. https://doi.org/10.1016/j.tibtech.2020.08.006

Gajendran, M., Loganathan, P., Catinella, A.P., Hashash, J.G., 2018. A comprehensive review and update on Crohn's disease. Dis Mon 64, 20–57. https://doi.org/10.1016/j.disamonth.2017.07.001

García Sánchez, C.E., Torres Sáez, R.G., 2014. Comparison and analysis of objective functions in flux balance analysis. Biotechnol Prog 30, 985–991. https://doi.org/10.1002/btpr.1949

Garza, D.R., Dutilh, B.E., 2015. From cultured to uncultured genome sequences: metagenomics and modeling microbial ecosystems. Cell Mol Life Sci 72, 4287–4308. https://doi.org/10.1007/s00018-015-2004-1

Geets, J., Boon, N., Verstraete, W., 2006. Strategies of aerobic ammonia-oxidizing bacteria for coping with nutrient and oxygen fluctuations. FEMS Microbiol Ecol 58, 1–13. https://doi.org/10.1111/j.1574-6941.2006.00170.x

Geppert, F., Liu, D., van Eerten-Jansen, M., Weidner, E., Buisman, C., Ter Heijne, A., 2016. Bioelectrochemical Power-to-Gas: State of the Art and Future Perspectives. Trends Biotechnol 34, 879–894. https://doi.org/10.1016/j.tibtech.2016.08.010

Gérard, P., 2013. Metabolism of cholesterol and bile acids by the gut microbiota. Pathogens 3, 14–24. https://doi.org/10.3390/pathogens3010014

Gordo, I., 2019. Evolutionary change in the human gut microbiome: From a static to a dynamic view. PLoS Biol 17, e3000126. https://doi.org/10.1371/journal.pbio.3000126

Grosskopf, T., Soyer, O.S., 2014. Synthetic microbial communities. Curr Opin Microbiol 18, 72–77. https://doi.org/10.1016/j.mib.2014.02.002

Gu, C., Kim, G.B., Kim, W.J., Kim, H.U., Lee, S.Y., 2019. Current status and applications of genome-scale metabolic models. Genome Biol 20, 121. https://doi.org/10.1186/s13059-019-1730-3

Hamilton, J.J., Calixto Contreras, M., Reed, J.L., 2015. Thermodynamics and H2 Transfer in a Methanogenic, Syntrophic Community. PLoS Comput Biol 11, e1004364. https://doi.org/10.1371/journal.pcbi.1004364

Harcombe, W.R., Riehl, W.J., Dukovski, I., Granger, B.R., Betts, A., Lang, A.H., Bonilla, G., Kar, A., Leiby, N., Mehta, P., Marx, C.J., Segrè, D., 2014. Metabolic resource allocation in individual microbes determines ecosystem interactions and spatial dynamics. Cell Rep 7, 1104–1115. https://doi.org/10.1016/j.celrep.2014.03.070

Hattori, S., Kamagata, Y., Hanada, S., Shoun, H., 2000. Thermacetogenium phaeum gen. nov., sp. nov., a strictly anaerobic, thermophilic, syntrophic acetate-oxidizing bacterium. Int J Syst Evol Microbiol 50 Pt 4, 1601–1609. https://doi.org/10.1099/00207713-50-4-1601

Heinken, A., Acharya, G., Ravcheev, D.A., Hertel, J., Nyga, M., Okpala, O.E., Hogan, M., Magnúsdóttir, S., Martinelli, F., Preciat, G., Edirisinghe, J.N., Henry, C.S., Fleming, R.M.T., Thiele, I., 2020. AGORA2: Large scale reconstruction of the microbiome highlights wide-spread drug-metabolising capacities. bioRxiv 2020.11.09.375451. https://doi.org/10.1101/2020.11.09.375451

Heinken, A., Hertel, J., Thiele, I., 2021a. Metabolic modelling reveals broad changes in gut microbial metabolism in inflammatory bowel disease patients with dysbiosis. NPJ Syst Biol Appl 7, 19. https://doi.org/10.1038/s41540-021-00178-6

Heinken, A., Magnúsdóttir, S., Fleming, R.M.T., Thiele, I., 2021b. DEMETER: efficient simultaneous curation of genome-scale reconstructions guided by experimental data and refined gene annotations. Bioinformatics. https://doi.org/10.1093/bioinformatics/btab622

Heinken, A., Ravcheev, D.A., Baldini, F., Heirendt, L., Fleming, R.M.T., Thiele, I., 2019. Systematic assessment of secondary bile acid metabolism in gut microbes reveals distinct metabolic capabilities in inflammatory bowel disease. Microbiome 7, 75. https://doi.org/10.1186/s40168-019-0689-3

Heinken, A., Thiele, I., 2019. Systematic interrogation of the distinct metabolic potential in gut microbiomes of inflammatory bowel disease patients with dysbiosis. bioRxiv 640649. https://doi.org/10.1101/640649

Heinken, A., Thiele, I., 2015. Anoxic Conditions Promote Species-Specific Mutualism between Gut Microbes *In silico*. Appl Environ Microbiol 81, 4049–4061. https://doi.org/10.1128/AEM.00101-15

Heirendt, L., Arreckx, S., Pfau, T., Mendoza, S.N., Richelle, A., Heinken, A., Haraldsdóttir, H.S., Wachowiak, J., Keating, S.M., Vlasov, V., Magnusdóttir, S., Ng, C.Y., Preciat, G., Žagare, A., Chan, S.H.J., Aurich, M.K., Clancy, C.M., Modamio, J., Sauls, J.T., Noronha, A., Bordbar, A., Cousins, B., El Assal, D.C., Valcarcel, L.V., Apaolaza, I., Ghaderi, S., Ahookhosh, M., Ben Guebila, M., Kostromins, A., Sompairac, N., Le, H.M., Ma, D., Sun, Y., Wang, L., Yurkovich, J.T., Oliveira, M.A.P., Vuong, P.T., El Assal, L.P., Kuperstein, I., Zinovyev, A., Hinton, H.S., Bryant, W.A., Aragón Artacho, F.J., Planes, F.J., Stalidzans, E., Maass, A., Vempala, S., Hucka, M., Saunders, M.A., Maranas, C.D., Lewis, N.E., Sauter, T., Palsson, B.Ø., Thiele, I., Fleming, R.M.T., 2019. Creation and analysis of biochemical constraint-based models using the COBRA Toolbox v.3.0. Nat Protoc 14, 639–702. https://doi.org/10.1038/s41596-018-0098-2

Henson, M.A., Phalak, P., 2017. Microbiota dysbiosis in inflammatory bowel diseases: *in silico* investigation of the oxygen hypothesis. BMC Syst Biol 11, 145. https://doi.org/10.1186/s12918-017-0522-1

Hertel, J., Heinken, A., Martinelli, F., Thiele, I., 2021. Integration of constraint-based modeling with fecal metabolomics reveals large deleterious effects of Fusobacterium spp. on community butyrate production. Gut Microbes 13, 1–23. https://doi.org/10.1080/19490976.2021.1915673

Hibbing, M.E., Fuqua, C., Parsek, M.R., Peterson, S.B., 2010. Bacterial competition: surviving and thriving in the microbial jungle. Nat Rev Microbiol 8, 15–25. https://doi.org/10.1038/nrmicro2259

Hosseinkhani, F., Heinken, A., Thiele, I., Lindenburg, P.W., Harms, A.C., Hankemeier, T., 2021. The contribution of gut bacterial metabolites in the human immune signaling pathway of non-communicable diseases. Gut Microbes 13, 1–22. https://doi.org/10.1080/19490976.2021.1882927

Integrative HMP (iHMP) Research Network Consortium, 2019. The Integrative Human Microbiome Project. Nature 569, 641–648. https://doi.org/10.1038/s41586-019-1238-8

Iovino, P., Bucci, C., Tremolaterra, F., Santonicola, A., Chiarioni, G., 2014. Bloating and functional gastro-intestinal disorders: where are we and where are we going? World J Gastroenterol 20, 14407–14419. https://doi.org/10.3748/wjg.v20.i39.14407

Ji, B., Zhang, X., Zhang, S., Song, H., Kong, Z., 2019. Insights into the bacterial species and communities of a full-scale anaerobic/anoxic/oxic wastewater treatment plant by using third-generation sequencing. J Biosci Bioeng 128, 744–750. https://doi.org/10.1016/j.jbiosc.2019.06.007

Kanehisa, M., Goto, S., 2000. KEGG: kyoto encyclopedia of genes and genomes. Nucleic Acids Res 28, 27–30. https://doi.org/10.1093/nar/28.1.27

Kapoor, R., Ghosh, P., Kumar, M., Vijay, V.K., 2019. Evaluation of biogas upgrading technologies and future perspectives: a review. Environ Sci Pollut Res Int 26, 11631–11661. https://doi.org/10.1007/s11356-019-04767-1

Karp, P.D., Riley, M., Paley, S.M., Pellegrini-Toole, A., 2002. The MetaCyc Database. Nucleic Acids Res 30, 59–61. https://doi.org/10.1093/nar/30.1.59

Karp, P.D., Weaver, D., Latendresse, M., 2018. How accurate is automated gap filling of metabolic models? BMC Syst Biol 12, 73. https://doi.org/10.1186/s12918-018-0593-7

Kato, N., Yurimoto, H., Thauer, R.K., 2006. The physiological role of the ribulose monophosphate pathway in bacteria and archaea. Biosci Biotechnol Biochem 70, 10–21. https://doi.org/10.1271/bbb.70.10

Keller, K.L., Wall, J.D., 2011. Genetics and molecular biology of the electron flow for sulfate respiration in desulfovibrio. Front Microbiol 2, 135. https://doi.org/10.3389/fmicb.2011.00135

Khan, I., Ullah, N., Zha, L., Bai, Y., Khan, A., Zhao, T., Che, T., Zhang, C., 2019. Alteration of Gut Microbiota in Inflammatory Bowel Disease (IBD): Cause or Consequence? IBD Treatment Targeting the Gut Microbiome. Pathogens 8, E126. https://doi.org/10.3390/pathogens8030126

Kim, M., Ahn, Y.-H., Speece, R.E., 2002. Comparative process stability and efficiency of anaerobic digestion; mesophilic vs. thermophilic. Water Res 36, 4369–4385. https://doi.org/10.1016/s0043-1354(02)00147-1

King, Z.A., Lu, J., Dräger, A., Miller, P., Federowicz, S., Lerman, J.A., Ebrahim, A., Palsson, B.O., Lewis, N.E., 2016. BiGG Models: A platform for integrating, standardizing and sharing genome-scale models. Nucleic Acids Res 44, D515-522. https://doi.org/10.1093/nar/gkv1049

Koch, S., Benndorf, D., Fronk, K., Reichl, U., Klamt, S., 2016. Predicting compositions of microbial communities from stoichiometric models with applications for the biogas process. Biotechnol Biofuels 9, 17. https://doi.org/10.1186/s13068-016-0429-x

Kodio, A., Menu, E., Ranque, S., 2020. Eukaryotic and Prokaryotic Microbiota Interactions. Microorganisms 8, E2018. https://doi.org/10.3390/microorganisms8122018

Koloski, N.-A., Bret, L., Radford-Smith, G., 2008. Hygiene hypothesis in inflammatory bowel disease: a critical review of the literature. World J Gastroenterol 14, 165–173. https://doi.org/10.3748/wjg.14.165

Koren, S., Rhie, A., Walenz, B.P., Dilthey, A.T., Bickhart, D.M., Kingan, S.B., Hiendleder, S., Williams, J.L., Smith, T.P.L., Phillippy, A.M., 2018. De novo assembly of haplotype-resolved genomes with trio binning. Nat Biotechnol. https://doi.org/10.1038/nbt.4277

Kunin, V., Copeland, A., Lapidus, A., Mavromatis, K., Hugenholtz, P., 2008. A bioinformatician's guide to metagenomics. Microbiol Mol Biol Rev 72, 557–578, Table of Contents. https://doi.org/10.1128/MMBR.00009-08

Lagier, J.-C., Khelaifia, S., Alou, M.T., Ndongo, S., Dione, N., Hugon, P., Caputo, A., Cadoret, F., Traore, S.I., Seck, E.H., Dubourg, G., Durand, G., Mourembou, G., Guilhot, E., Togo, A., Bellali, S., Bachar, D., Cassir, N., Bittar, F., Delerce, J., Mailhe, M., Ricaboni, D., Bilen, M., Dangui Nieko, N.P.M., Dia Badiane, N.M., Valles, C., Mouelhi, D., Diop, K., Million, M., Musso, D., Abrahão, J., Azhar, E.I., Bibi, F., Yasir, M., Diallo, A., Sokhna, C., Djossou, F., Vitton, V., Robert, C., Rolain, J.M., La Scola, B., Fournier, P.-E., Levasseur, A., Raoult, D., 2016. Culture of previously uncultured members of the human gut microbiota by culturomics. Nat Microbiol 1, 16203. https://doi.org/10.1038/nmicrobiol.2016.203

Lambie, S.C., Kelly, W.J., Leahy, S.C., Li, D., Reilly, K., McAllister, T.A., Valle, E.R., Attwood, G.T., Altermann, E., 2015. The complete genome sequence of the rumen methanogen Methanosarcina barkeri CM1. Stand Genomic Sci 10, 57. https://doi.org/10.1186/s40793-015-0038-5

Lane, N., 2015. The unseen world: reflections on Leeuwenhoek (1677) "Concerning little animals." Philos Trans R Soc Lond B Biol Sci 370, 20140344. https://doi.org/10.1098/rstb.2014.0344

Larsen, P.E., Gibbons, S.M., Gilbert, J.A., 2012. Modeling microbial community structure and functional diversity across time and space. FEMS Microbiol Lett 332, 91–98. https://doi.org/10.1111/j.1574-6968.2012.02588.x

Lazar, V., Ditu, L.-M., Pircalabioru, G.G., Gheorghe, I., Curutiu, C., Holban, A.M., Picu, A., Petcu,

L., Chifiriuc, M.C., 2018. Aspects of Gut Microbiota and Immune System Interactions in Infectious Diseases, Immunopathology, and Cancer. Front Immunol 9, 1830. https://doi.org/10.3389/fimmu.2018.01830

Lee, M.J., Zinder, S.H., 1988. Isolation and Characterization of a Thermophilic Bacterium Which Oxidizes Acetate in Syntrophic Association with a Methanogen and Which Grows Acetogenically on H2-CO2. Applied and Environmental Microbiology 54, 124–129. https://doi.org/10.1128/aem.54.1.124-129.1988

Lenski, R.E., 2017. Experimental evolution and the dynamics of adaptation and genome evolution in microbial populations. ISME J 11, 2181–2194. https://doi.org/10.1038/ismej.2017.69

Leylabadlo, H.E., Ghotaslou, R., Feizabadi, M.M., Farajnia, S., Moaddab, S.Y., Ganbarov, K., Khodadadi, E., Tanomand, A., Sheykhsaran, E., Yousefi, B., Kafil, H.S., 2020. The critical role of Faecalibacterium prausnitzii in human health: An overview. Microb Pathog 149, 104344. https://doi.org/10.1016/j.micpath.2020.104344

Li, L., Peng, X., Wang, X., Wu, D., 2018. Anaerobic digestion of food waste: A review focusing on process stability. Bioresour Technol 248, 20–28. https://doi.org/10.1016/j.biortech.2017.07.012

Liang, D., Leung, R.K.-K., Guan, W., Au, W.W., 2018. Involvement of gut microbiome in human health and disease: brief overview, knowledge gaps and research opportunities. Gut Pathog 10, 3. https://doi.org/10.1186/s13099-018-0230-4

Limoli, D.H., Jones, C.J., Wozniak, D.J., 2015. Bacterial Extracellular Polysaccharides in Biofilm Formation and Function. Microbiol Spectr 3. https://doi.org/10.1128/microbiolspec.MB-0011-2014

Liow, L.H., Van Valen, L., Stenseth, N.Chr., 2011. Red Queen: from populations to taxa and communities. Trends in Ecology & Evolution 26, 349–358. https://doi.org/10.1016/j.tree.2011.03.016

Lloubès, R., Goemaere, E., Zhang, X., Cascales, E., Duché, D., 2012. Energetics of colicin import revealed by genetic cross-complementation between the Tol and Ton systems. Biochem Soc Trans 40, 1480–1485. https://doi.org/10.1042/BST20120181

Lukitawesa, null, Patinvoh, R.J., Millati, R., Sárvári-Horváth, I., Taherzadeh, M.J., 2020. Factors influencing volatile fatty acids production from food wastes via anaerobic digestion. Bioengineered 11, 39–52. https://doi.org/10.1080/21655979.2019.1703544

Lundstrom, M., 2003. Applied physics. Moore's law forever? Science 299, 210–211. https://doi.org/10.1126/science.1079567

Lyu, Z., Shao, N., Akinyemi, T., Whitman, W.B., 2018. Methanogenesis. Curr Biol 28, R727–R732. https://doi.org/10.1016/j.cub.2018.05.021

Machado, D., Andrejev, S., Tramontano, M., Patil, K.R., 2018. Fast automated reconstruction of genome-scale metabolic models for microbial species and communities. Nucleic Acids Res 46, 7542–7553. https://doi.org/10.1093/nar/gky537

Machado, D., Herrgård, M., 2014. Systematic evaluation of methods for integration of transcriptomic data into constraint-based models of metabolism. PLoS Comput Biol 10, e1003580. https://doi.org/10.1371/journal.pcbi.1003580

Machado, D., Maistrenko, O.M., Andrejev, S., Kim, Y., Bork, P., Patil, Kaustubh R., Patil, Kiran R., 2021. Polarization of microbial communities between competitive and cooperative metabolism. Nat Ecol Evol 5, 195–203. https://doi.org/10.1038/s41559-020-01353-4

Mackie, A., Keseler, I.M., Nolan, L., Karp, P.D., Paulsen, I.T., 2013. Dead end metabolites--defining the known unknowns of the E. coli metabolic network. PLoS One 8, e75210. https://doi.org/10.1371/journal.pone.0075210

Magnúsdóttir, S., Heinken, A., Kutt, L., Ravcheev, D.A., Bauer, E., Noronha, A., Greenhalgh, K.,

Jäger, C., Baginska, J., Wilmes, P., Fleming, R.M.T., Thiele, I., 2017. Generation of genome-scale metabolic reconstructions for 773 members of the human gut microbiota. Nat Biotechnol 35, 81–89. https://doi.org/10.1038/nbt.3703

Mande, S.S., Mohammed, M.H., Ghosh, T.S., 2012. Classification of metagenomic sequences: methods and challenges. Brief Bioinform 13, 669–681. https://doi.org/10.1093/bib/bbs054

Mardinoglu, A., Agren, R., Kampf, C., Asplund, A., Nookaew, I., Jacobson, P., Walley, A.J., Froguel, P., Carlsson, L.M., Uhlen, M., Nielsen, J., 2013. Integration of clinical data with a genome-scale metabolic model of the human adipocyte. Mol Syst Biol 9, 649. https://doi.org/10.1038/msb.2013.5

Mardinoglu, A., Agren, R., Kampf, C., Asplund, A., Uhlen, M., Nielsen, J., 2014. Genome-scale metabolic modelling of hepatocytes reveals serine deficiency in patients with non-alcoholic fatty liver disease. Nat Commun 5, 3083. https://doi.org/10.1038/ncomms4083

McNally, C.P., Borenstein, E., 2018. Metabolic model-based analysis of the emergence of bacterial cross-feeding via extensive gene loss. BMC Syst Biol 12, 69. https://doi.org/10.1186/s12918-018-0588-4

Mendes-Soares, H., Mundy, M., Soares, L.M., Chia, N., 2016. MMinte: an application for predicting metabolic interactions among the microbial species in a community. BMC Bioinformatics 17, 343. https://doi.org/10.1186/s12859-016-1230-3

Microbiology by numbers, 2011. . Nat Rev Microbiol 9, 628. https://doi.org/10.1038/nrmicro2644

M'Koma, A.E., 2013. Inflammatory bowel disease: an expanding global health problem. Clin Med Insights Gastroenterol 6, 33–47. https://doi.org/10.4137/CGast.S12731

Morris, J.J., Lenski, R.E., Zinser, E.R., 2012. The Black Queen Hypothesis: evolution of dependencies through adaptive gene loss. mBio 3, e00036-12. https://doi.org/10.1128/mBio.00036-12

Nguyen, L.N., Kumar, J., Vu, M.T., Mohammed, J.A.H., Pathak, N., Commault, A.S., Sutherland, D., Zdarta, J., Tyagi, V.K., Nghiem, L.D., 2021. Biomethane production from anaerobic co-digestion at wastewater treatment plants: A critical review on development and innovations in biogas upgrading techniques. Sci Total Environ 765, 142753. https://doi.org/10.1016/j.scitotenv.2020.142753

Nielsen, H.B., Almeida, M., Juncker, A.S., Rasmussen, S., Li, J., Sunagawa, S., Plichta, D.R., Gautier, L., Pedersen, A.G., Le Chatelier, E., Pelletier, E., Bonde, I., Nielsen, T., Manichanh, C., Arumugam, M., Batto, J.-M., Quintanilha Dos Santos, M.B., Blom, N., Borruel, N., Burgdorf, K.S., Boumezbeur, F., Casellas, F., Doré, J., Dworzynski, P., Guarner, F., Hansen, T., Hildebrand, F., Kaas, R.S., Kennedy, S., Kristiansen, K., Kultima, J.R., Léonard, P., Levenez, F., Lund, O., Moumen, B., Le Paslier, D., Pons, N., Pedersen, O., Prifti, E., Qin, J., Raes, J., Sørensen, S., Tap, J., Tims, S., Ussery, D.W., Yamada, T., MetaHIT Consortium, Renault, P., Sicheritz-Ponten, T., Bork, P., Wang, J., Brunak, S., Ehrlich, S.D., MetaHIT Consortium, 2014. Identification and assembly of genomes and genetic elements in complex metagenomic samples without using reference genomes. Nat Biotechnol 32, 822–828. https://doi.org/10.1038/nbt.2939

NIH HMP Working Group, Peterson, J., Garges, S., Giovanni, M., McInnes, P., Wang, L., Schloss, J.A., Bonazzi, V., McEwen, J.E., Wetterstrand, K.A., Deal, C., Baker, C.C., Di Francesco, V., Howcroft, T.K., Karp, R.W., Lunsford, R.D., Wellington, C.R., Belachew, T., Wright, M., Giblin, C., David, H., Mills, M., Salomon, R., Mullins, C., Akolkar, B., Begg, L., Davis, C., Grandison, L., Humble, M., Khalsa, J., Little, A.R., Peavy, H., Pontzer, C., Portnoy, M., Sayre, M.H., Starke-Reed, P., Zakhari, S., Read, J., Watson, B., Guyer, M., 2009. The NIH Human Microbiome Project. Genome Res 19, 2317–2323. https://doi.org/10.1101/gr.096651.109

Nobu, M.K., Narihiro, T., Rinke, C., Kamagata, Y., Tringe, S.G., Woyke, T., Liu, W.-T., 2015. Microbial dark matter ecogenomics reveals complex synergistic networks in a methanogenic bioreactor. ISME J 9, 1710–1722. https://doi.org/10.1038/ismej.2014.256

Noronha, A., Modamio, J., Jarosz, Y., Guerard, E., Sompairac, N., Preciat, G., Daníelsdóttir, A.D., Krecke, M., Merten, D., Haraldsdóttir, H.S., Heinken, A., Heirendt, L., Magnúsdóttir, S., Ravcheev, D.A., Sahoo, S., Gawron, P., Friscioni, L., Garcia, B., Prendergast, M., Puente, A., Rodrigues, M., Roy, A., Rouquaya, M., Wiltgen, L., Žagare, A., John, E., Krueger, M., Kuperstein, I., Zinovyev, A., Schneider, R., Fleming, R.M.T., Thiele, I., 2019. The Virtual Metabolic Human database: integrating human and gut microbiome metabolism with nutrition and disease. Nucleic Acids Res 47, D614–D624. https://doi.org/10.1093/nar/gky992

Norsigian, C.J., Fang, X., Seif, Y., Monk, J.M., Palsson, B.O., 2020a. A workflow for generating multi-strain genome-scale metabolic models of prokaryotes. Nat Protoc 15, 1–14. https://doi.org/10.1038/s41596-019-0254-3

Norsigian, C.J., Pusarla, N., McConn, J.L., Yurkovich, J.T., Dräger, A., Palsson, B.O., King, Z., 2020b. BiGG Models 2020: multi-strain genome-scale models and expansion across the phylogenetic tree. Nucleic Acids Res 48, D402–D406. https://doi.org/10.1093/nar/gkz1054

O'Brien, E.J., Monk, J.M., Palsson, B.O., 2015. Using Genome-scale Models to Predict Biological Capabilities. Cell 161, 971–987. https://doi.org/10.1016/j.cell.2015.05.019

Ong, S.H., Kukkillaya, V.U., Wilm, A., Lay, C., Ho, E.X.P., Low, L., Hibberd, M.L., Nagarajan, N., 2013. Species identification and profiling of complex microbial communities using shotgun Illumina sequencing of 16S rRNA amplicon sequences. PLoS One 8, e60811. https://doi.org/10.1371/journal.pone.0060811

Ong, W.K., Midford, P.E., Karp, P.D., 2020. Taxonomic weighting improves the accuracy of a gap-filling algorithm for metabolic models. Bioinformatics 36, 1823–1830. https://doi.org/10.1093/bioinformatics/btz813

Orth, J.D., Thiele, I., Palsson, B.Ø., 2010. What is flux balance analysis? Nat Biotechnol 28, 245–248. https://doi.org/10.1038/nbt.1614

Pan, S., Reed, J.L., 2018. Advances in gap-filling genome-scale metabolic models and model-driven experiments lead to novel metabolic discoveries. Curr Opin Biotechnol 51, 103–108. https://doi.org/10.1016/j.copbio.2017.12.012

Pan, X., Zhao, L., Li, C., Angelidaki, I., Lv, N., Ning, J., Cai, G., Zhu, G., 2021. Deep insights into the network of acetate metabolism in anaerobic digestion: focusing on syntrophic acetate oxidation and homoacetogenesis. Water Res 190, 116774. https://doi.org/10.1016/j.watres.2020.116774

Pasolli, E., Asnicar, F., Manara, S., Zolfo, M., Karcher, N., Armanini, F., Beghini, F., Manghi, P., Tett, A., Ghensi, P., Collado, M.C., Rice, B.L., DuLong, C., Morgan, X.C., Golden, C.D., Quince, C., Huttenhower, C., Segata, N., 2019. Extensive Unexplored Human Microbiome Diversity Revealed by Over 150,000 Genomes from Metagenomes Spanning Age, Geography, and Lifestyle. Cell 176, 649-662.e20. https://doi.org/10.1016/j.cell.2019.01.001

Patterson, A.M., Mulder, I.E., Travis, A.J., Lan, A., Cerf-Bensussan, N., Gaboriau-Routhiau, V., Garden, K., Logan, E., Delday, M.I., Coutts, A.G.P., Monnais, E., Ferraria, V.C., Inoue, R., Grant, G., Aminov, R.I., 2017. Human Gut Symbiont Roseburia hominis Promotes and Regulates Innate Immunity. Front Immunol 8, 1166. https://doi.org/10.3389/fimmu.2017.01166

Pedersen, A.M., Bardow, A., Jensen, S.B., Nauntofte, B., 2002. Saliva and gastrointestinal functions of taste, mastication, swallowing and digestion. Oral Dis 8, 117–129. https://doi.org/10.1034/j.1601-0825.2002.02851.x

Pérez-Cobas, A.E., Gomez-Valero, L., Buchrieser, C., 2020. Metagenomic approaches in microbial

ecology: an update on whole-genome and marker gene sequencing analyses. Microb Genom 6. https://doi.org/10.1099/mgen.0.000409

Ponce-de-León, M., Montero, F., Peretó, J., 2013. Solving gap metabolites and blocked reactions in genome-scale models: application to the metabolic network of Blattabacterium cuenoti. BMC Syst Biol 7, 114. https://doi.org/10.1186/1752-0509-7-114

Poretsky, R., Rodriguez-R, L.M., Luo, C., Tsementzi, D., Konstantinidis, K.T., 2014. Strengths and limitations of 16S rRNA gene amplicon sequencing in revealing temporal microbial community dynamics. PLoS One 9, e93827. https://doi.org/10.1371/journal.pone.0093827

Pornputtapong, N., Nookaew, I., Nielsen, J., 2015. Human metabolic atlas: an online resource for human metabolism. Database (Oxford) 2015, bav068. https://doi.org/10.1093/database/bav068

Prigent, S., Frioux, C., Dittami, S.M., Thiele, S., Larhlimi, A., Collet, G., Gutknecht, F., Got, J., Eveillard, D., Bourdon, J., Plewniak, F., Tonon, T., Siegel, A., 2017. Meneco, a Topology-Based Gap-Filling Tool Applicable to Degraded Genome-Wide Metabolic Networks. PLoS Comput Biol 13, e1005276. https://doi.org/10.1371/journal.pcbi.1005276

Quince, C., Walker, A.W., Simpson, J.T., Loman, N.J., Segata, N., 2017. Shotgun metagenomics, from sampling to analysis. Nat Biotechnol 35, 833–844. https://doi.org/10.1038/nbt.3935

Raman, K., Chandra, N., 2009. Flux balance analysis of biological systems: applications and challenges. Brief Bioinform 10, 435–449. https://doi.org/10.1093/bib/bbp011

Rinninella, E., Raoul, P., Cintoni, M., Franceschi, F., Miggiano, G.A.D., Gasbarrini, A., Mele, M.C., 2019. What is the Healthy Gut Microbiota Composition? A Changing Ecosystem across Age, Environment, Diet, and Diseases. Microorganisms 7, E14. https://doi.org/10.3390/microorganisms7010014

Robertson, L.A., 2015. van Leeuwenhoek microscopes-where are they now? FEMS Microbiol Lett 362, fnv056. https://doi.org/10.1093/femsle/fnv056

Rosario, D., Benfeitas, R., Bidkhori, G., Zhang, C., Uhlen, M., Shoaie, S., Mardinoglu, A., 2018. Understanding the Representative Gut Microbiota Dysbiosis in Metformin-Treated Type 2 Diabetes Patients Using Genome-Scale Metabolic Modeling. Front Physiol 9, 775. https://doi.org/10.3389/fphys.2018.00775

Rowland, I., Gibson, G., Heinken, A., Scott, K., Swann, J., Thiele, I., Tuohy, K., 2018. Gut microbiota functions: metabolism of nutrients and other food components. Eur J Nutr 57, 1–24. https://doi.org/10.1007/s00394-017-1445-8

Ryu, J.Y., Kim, H.U., Lee, S.Y., 2017. Framework and resource for more than 11,000 gene-transcript-protein-reaction associations in human metabolism. Proc Natl Acad Sci U S A 114, E9740–E9749. https://doi.org/10.1073/pnas.1713050114

Schadt, E.E., Turner, S., Kasarskis, A., 2010. A window into third-generation sequencing. Hum Mol Genet 19, R227-240. https://doi.org/10.1093/hmg/ddq416

Schmidt, T.S.B., Raes, J., Bork, P., 2018. The Human Gut Microbiome: From Association to Modulation. Cell 172, 1198–1215. https://doi.org/10.1016/j.cell.2018.02.044

Schnurer, A., Schink, B., Svensson, B.H., 1996. Clostridium ultunense sp. nov., a mesophilic bacterium oxidizing acetate in syntrophic association with a hydrogenotrophic methanogenic bacterium. Int J Syst Bacteriol 46, 1145–1152. https://doi.org/10.1099/00207713-46-4-1145

Seaver, S.M.D., Liu, F., Zhang, Q., Jeffryes, J., Faria, J.P., Edirisinghe, J.N., Mundy, M., Chia, N., Noor, E., Beber, M.E., Best, A.A., DeJongh, M., Kimbrel, J.A., D'haeseleer, P., McCorkle, S.R., Bolton, J.R., Pearson, E., Canon, S., Wood-Charlson, E.M., Cottingham, R.W., Arkin, A.P., Henry, C.S., 2021. The ModelSEED Biochemistry Database for the integration of metabolic annotations and the reconstruction, comparison and analysis of metabolic models for plants, fungi and microbes. Nucleic Acids Res 49, D575–D588.

https://doi.org/10.1093/nar/gkaa746
Shaw, R., Cheung, C.Y.M., 2019. A mass and charge balanced metabolic model of Setaria viridis revealed mechanisms of proton balancing in C4 plants. BMC Bioinformatics 20, 357. https://doi.org/10.1186/s12859-019-2941-z
Silbergeld, E.K., 2017. The Microbiome. Toxicol Pathol 45, 190–194. https://doi.org/10.1177/0192623316672073
Stams, A.J.M., Plugge, C.M., 2009. Electron transfer in syntrophic communities of anaerobic bacteria and archaea. Nat Rev Microbiol 7, 568–577. https://doi.org/10.1038/nrmicro2166
Stolk, R.P., Rosmalen, J.G.M., Postma, D.S., de Boer, R.A., Navis, G., Slaets, J.P.J., Ormel, J., Wolffenbuttel, B.H.R., 2008. Universal risk factors for multifactorial diseases: LifeLines: a three-generation population-based study. Eur J Epidemiol 23, 67–74. https://doi.org/10.1007/s10654-007-9204-4
Stolyar, S., Van Dien, S., Hillesland, K.L., Pinel, N., Lie, T.J., Leigh, J.A., Stahl, D.A., 2007. Metabolic modeling of a mutualistic microbial community. Mol Syst Biol 3, 92. https://doi.org/10.1038/msb4100131
Tan, G.-Y.A., Lee, P.-H., Shih, K., 2016. One for all, and all for one: Exploiting microbial mutualism for a new renaissance in anaerobic digestion. Waste Manag 53, 1–2. https://doi.org/10.1016/j.wasman.2016.05.029
Thiele, I., Heinken, A., Fleming, R.M.T., 2013. A systems biology approach to studying the role of microbes in human health. Curr Opin Biotechnol 24, 4–12. https://doi.org/10.1016/j.copbio.2012.10.001
Thiele, I., Palsson, B.Ø., 2010. A protocol for generating a high-quality genome-scale metabolic reconstruction. Nat Protoc 5, 93–121. https://doi.org/10.1038/nprot.2009.203
Thiele, I., Sahoo, S., Heinken, A., Hertel, J., Heirendt, L., Aurich, M.K., Fleming, R.M., 2020. Personalized whole-body models integrate metabolism, physiology, and the gut microbiome. Mol Syst Biol 16, e8982. https://doi.org/10.15252/msb.20198982
Thommes, M., Wang, T., Zhao, Q., Paschalidis, I.C., Segrè, D., 2019. Designing Metabolic Division of Labor in Microbial Communities. mSystems 4, e00263-18. https://doi.org/10.1128/mSystems.00263-18
Thursby, E., Juge, N., 2017. Introduction to the human gut microbiota. Biochem J 474, 1823–1836. https://doi.org/10.1042/BCJ20160510
Spatial Organization of Microbial Biofilm Communities. Microb Ecol 40, 75–84. https://doi.org/10.1007/s002480000057
Tripathi, A., Debelius, J., Brenner, D.A., Karin, M., Loomba, R., Schnabl, B., Knight, R., 2018. The gut-liver axis and the intersection with the microbiome. Nat Rev Gastroenterol Hepatol 15, 397–411. https://doi.org/10.1038/s41575-018-0011-z
Trovato, G.M., 2012. Behavior, nutrition and lifestyle in a comprehensive health and disease paradigm: skills and knowledge for a predictive, preventive and personalized medicine. EPMA J 3, 8. https://doi.org/10.1007/s13167-012-0141-2
van Dijk, E.L., Jaszczyszyn, Y., Naquin, D., Thermes, C., 2018. The Third Revolution in Sequencing Technology. Trends Genet 34, 666–681. https://doi.org/10.1016/j.tig.2018.05.008
Väremo, L., Scheele, C., Broholm, C., Mardinoglu, A., Kampf, C., Asplund, A., Nookaew, I., Uhlén, M., Pedersen, B.K., Nielsen, J., 2016. Proteome- and Transcriptome-Driven Reconstruction of the Human Myocyte Metabolic Network and Its Use for Identification of Markers for Diabetes. Cell Rep 14, 1567. https://doi.org/10.1016/j.celrep.2016.01.054
Vasco-Correa, J., Khanal, S., Manandhar, A., Shah, A., 2018. Anaerobic digestion for bioenergy production: Global status, environmental and techno-economic implications, and government policies. Bioresour Technol 247, 1015–1026. https://doi.org/10.1016/j.biortech.2017.09.004

Voordouw, G., 2002. Carbon monoxide cycling by Desulfovibrio vulgaris Hildenborough. J Bacteriol 184, 5903–5911. https://doi.org/10.1128/JB.184.21.5903-5911.2002

Wainaina, S., Lukitawesa, null, Kumar Awasthi, M., Taherzadeh, M.J., 2019. Bioengineering of anaerobic digestion for volatile fatty acids, hydrogen or methane production: A critical review. Bioengineered 10, 437–458. https://doi.org/10.1080/21655979.2019.1673937

Wang, H.-Z., Li, J., Yi, Y., Nobu, M.K., Narihiro, T., Tang, Y.-Q., 2020. Response to inhibitory conditions of acetate-degrading methanogenic microbial community. J Biosci Bioeng 129, 476–485. https://doi.org/10.1016/j.jbiosc.2019.10.006

Wang, W.-L., Xu, S.-Y., Ren, Z.-G., Tao, L., Jiang, J.-W., Zheng, S.-S., 2015. Application of metagenomics in the human gut microbiome. World J Gastroenterol 21, 803–814. https://doi.org/10.3748/wjg.v21.i3.803

Westerholm, M., Roos, S., Schnürer, A., 2011. Tepidanaerobacter acetatoxydans sp. nov., an anaerobic, syntrophic acetate-oxidizing bacterium isolated from two ammonium-enriched mesophilic methanogenic processes. Systematic and Applied Microbiology 34, 260–266. https://doi.org/10.1016/j.syapm.2010.11.018

Westerholm, M., Roos, S., Schnürer, A., 2010. Syntrophaceticus schinkii gen. nov., sp. nov., an anaerobic, syntrophic acetate-oxidizing bacterium isolated from a mesophilic anaerobic filter. FEMS Microbiol. Lett. 309, 100–104. https://doi.org/10.1111/j.1574-6968.2010.02023.x

Wimpenny, J., Manz, W., Szewzyk, U., 2000. Heterogeneity in biofilms. FEMS Microbiol Rev 24, 661–671. https://doi.org/10.1111/j.1574-6976.2000.tb00565.x

Wulf, C., Linßen, J., Zapp, P., 2018. Review of Power-to-Gas Projects in Europe. Energy Procedia, 12th International Renewable Energy Storage Conference, IRES 2018, 13-15 March 2018, Düsseldorf, Germany 155, 367–378. https://doi.org/10.1016/j.egypro.2018.11.041

Xu, X., Zarecki, R., Medina, S., Ofaim, S., Liu, X., Chen, C., Hu, S., Brom, D., Gat, D., Porob, S., Eizenberg, H., Ronen, Z., Jiang, J., Freilich, S., 2019. Modeling microbial communities from atrazine contaminated soils promotes the development of biostimulation solutions. ISME J 13, 494–508. https://doi.org/10.1038/s41396-018-0288-5

Yizhak, K., Benyamini, T., Liebermeister, W., Ruppin, E., Shlomi, T., 2010. Integrating quantitative proteomics and metabolomics with a genome-scale metabolic network model. Bioinformatics 26, i255-260. https://doi.org/10.1093/bioinformatics/btq183

Zamkovaya, T., Foster, J.S., de Crécy-Lagard, V., Conesa, A., 2021. A network approach to elucidate and prioritize microbial dark matter in microbial communities. ISME J 15, 228–244. https://doi.org/10.1038/s41396-020-00777-x

Zampieri, G., Vijayakumar, S., Yaneske, E., Angione, C., 2019. Machine and deep learning meet genome-scale metabolic modeling. PLoS Comput Biol 15, e1007084. https://doi.org/10.1371/journal.pcbi.1007084

Zengler, K., Zaramela, L.S., 2018. The social network of microorganisms - how auxotrophies shape complex communities. Nat Rev Microbiol 16, 383–390. https://doi.org/10.1038/s41579-018-0004-5

Zhang, S.J., De Bruyn, F., Pothakos, V., Torres, J., Falconi, C., Moccand, C., Weckx, S., De Vuyst, L., 2019. Following Coffee Production from Cherries to Cup: Microbiological and Metabolomic Analysis of Wet Processing of Coffea arabica. Appl Environ Microbiol 85, e02635-18. https://doi.org/10.1128/AEM.02635-18

Zhou, J.-J., Shen, J.-T., Wang, X.-L., Sun, Y.-Q., Xiu, Z.-L., 2020. Metabolism, morphology and transcriptome analysis of oscillatory behavior of Clostridium butyricum during long-term continuous fermentation for 1,3-propanediol production. Biotechnol Biofuels 13, 191. https://doi.org/10.1186/s13068-020-01831-8

Zhu, X., Campanaro, S., Treu, L., Seshadri, R., Ivanova, N., Kougias, P.G., Kyrpides, N., Angelidaki,

I., 2020. Metabolic dependencies govern microbial syntrophies during methanogenesis in an anaerobic digestion ecosystem. Microbiome 8, 22. https://doi.org/10.1186/s40168-019-0780-9
Zimmermann, J., Kaleta, C., Waschina, S., 2021. gapseq: informed prediction of bacterial metabolic pathways and reconstruction of accurate metabolic models. Genome Biol 22, 81. https://doi.org/10.1186/s13059-021-02295-1
Zomorrodi, A.R., Maranas, C.D., 2012. OptCom: a multi-level optimization framework for the metabolic modeling and analysis of microbial communities. PLoS Comput Biol 8, e1002363. https://doi.org/10.1371/journal.pcbi.1002363

Publications

I **Arianna Basile**, Stefano Campanaro, Adam Kovalovszki, Guido Zampieri, Alessandro Rossi, Irini Angelidaki, Giorgio Valle, Laura Treu (2020). Revealing metabolic mechanisms of interaction in the anaerobic digestion microbiome by flux balance analysis. Metabolic Engineering, 62, 138-149.

II Miao Yan, Laura Treu, Xinyu Zhu, Hailin Tian, **Arianna Basile**, Ioannis A. Fotidis, Stefano Campanaro, and Irini Angelidaki (2020). Insights into Ammonia Adaptation and Methanogenic Precursor Oxidation by Genome-Centric Analysis. Environmental Science and Technology, 54, 12568–12582.

III Almut Heinken, **Arianna Basile**, Johannes Hertel, Cyrille Thinnes, Ines Thiele (2020). Genome-Scale Metabolic Modeling of the Human Microbiome in the Era of Personalized Medicine. Annual Review of Microbiology, 75.

IV **Arianna Basile**, Almut Heinken, Johannes Hertel, Larry Smarr, Laura Treu, Giorgio Valle, Stefano Campanaro, Ines Thiele (2020). Longitudinal flux balance analyses of a patient with Crohn's disease. Manuscript under preparation.

Chapter 1

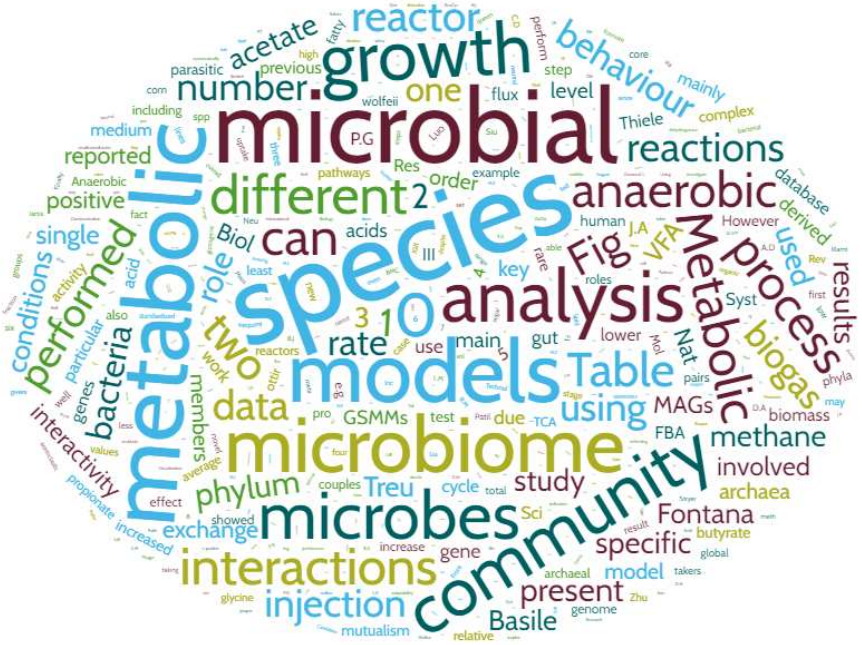

Revealing metabolic mechanisms of interaction in the anaerobic digestion microbiome by flux balance analysis

Arianna Basile[1], Stefano Campanaro[1,2,*], Adam Kovalovszki[3], Guido Zampieri[1,4], Alessandro Rossi[1], Irini Angelidaki[3], Giorgio Valle[1,ψ], Laura Treu[1,ψ]

Metabolic Engineering, Volume 62, November 2020, Pages 138-149
https://doi.org/10.1016/j.ymben.2020.08.013

[1] Department of Biology, University of Padova, Via U. Bassi 58/b, 35121, Padua, Italy
[2] CRIBI Biotechnology Center, University of Padova, 35131, Padua, Italy
[3] Department of Environmental Engineering, Technical University of Denmark, 2800, Kgs. Lyngby, Denmark
[4] Department of Computer Science and Information Systems, Teesside University, Middlesbrough, United Kingdom

*Corresponding author
[ψ]Equal contribution

Metabolic Engineering 62 (2020) 138–149

Contents lists available at ScienceDirect

Metabolic Engineering

journal homepage: www.elsevier.com/locate/meteng

Original Research Article

Revealing metabolic mechanisms of interaction in the anaerobic digestion microbiome by flux balance analysis

Arianna Basile [a], Stefano Campanaro [a,b,*], Adam Kovalovszki [c], Guido Zampieri [a,d], Alessandro Rossi [a], Irini Angelidaki [c], Giorgio Valle [a,1], Laura Treu [a,1]

[a] Department of Biology, University of Padova, Via U. Bassi 58/b, 35121, Padua, Italy
[b] CRIBI Biotechnology Center, University of Padova, 35131, Padua, Italy
[c] Department of Environmental Engineering, Technical University of Denmark, 2800, Kgs. Lyngby, Denmark
[d] Department of Computer Science and Information Systems, Teesside University, Middlesbrough, United Kingdom

ARTICLE INFO

Keywords:
Anaerobic digestion/flux balance analysis/genome-scale metabolic models/microbial interactions/renewable energy

ABSTRACT

Anaerobic digestion is a key biological process for renewable energy, yet the mechanistic knowledge on its hidden microbial dynamics is still limited. The present work charted the interaction network in the anaerobic digestion microbiome via the full characterization of pairwise interactions and the associated metabolite exchanges. To this goal, a novel collection of 836 genome-scale metabolic models was built to represent the functional capabilities of bacteria and archaea species derived from genome-centric metagenomics. Dominant microbes were shown to prefer mutualistic, parasitic and commensalistic interactions over neutralism, amensalism and competition, and are more likely to behave as metabolite importers and profiteers of the coexistence. Additionally, external hydrogen injection positively influences microbiome dynamics by promoting commensalism over amensalism. Finally, exchanges of glucogenic amino acids were shown to overcome auxotrophies caused by an incomplete tricarboxylic acid cycle. Our novel strategy predicted the most favourable growth conditions for the microbes, overall suggesting strategies to increasing the biogas production efficiency. In principle, this approach could also be applied to microbial populations of biomedical importance, such as the gut microbiome, to allow a broad inspection of the microbial interplays.

1. Introduction

Microorganisms play an important role in all fields of biological relevance, ranging from human health (Clemente et al., 2012) to biotechnology (Lebuhn et al., 2015). In particular, diverse microbiomes may have various responsibilities, from causing diseases to influencing applied processes (e.g. biogas production) (Zhu et al., 2020) or the synthesis of polymeric substances (Chow et al., 2008). Microbial networks, however, are still poorly understood due to difficulties in isolating most of the microbial species and to the heterogeneous nature of their interactions (Muller et al., 2018). While the inspection of a core microbiome might reveal which species are the key players for a specific process (Faith, 2015), the role of rare members still remains to be clarified (Jousset et al., 2017). Microbial cooperation is extremely important for environmental niche colonization and completing complex activities (Stolyar et al., 2007), which single species could not perform independently (Hay et al., 2004). This is the case in anaerobic digestion (AD), which is a biotechnological process that produces a potent renewable energy carrier called biogas (Yentekakis and Goula, 2017). During biogas production, when acetoclastic methanogenic archaea are inhibited, a pivotal role is played by hydrogenotrophic methanogenic archaea and syntrophic acetate oxidizing bacteria (Mosbæk et al., 2016) (SAOB). An example is the mutualism between the hydrogen-utilizing methanogen *Methanoculleus bourgensis* and the SAOB *Syntrophaceticus schinkii*, *[Clostridium] ultunense*, and *Tepidanaerobacter acetatoxydans* (Westerholm et al., 2019). SAOB oxidise acetate to formate or to H_2 and carbon dioxide (CO_2). The bacteria rely on archaeal activity, because acetate oxidation rapidly becomes endergonic when H_2 accumulates (Stams and Plugge, 2009). Indeed, subsequently H_2-utilizing methanogens convert these substrates to methane (CH_4) (Treu et al., 2018).

Although direct microbial cultivation and phenotyping experiments

* Corresponding author.
E-mail address: stefano.campanaro@unipd.it (S. Campanaro).
[1] equal contribution.

https://doi.org/10.1016/j.ymben.2020.08.013
Received 5 March 2020; Received in revised form 3 August 2020; Accepted 24 August 2020
Available online 6 September 2020

are essential to investigate metabolite exchanges and species interplays, this is not always possible. In fact, several microbes responsible for important biotechnological processes cannot be isolated and investigated using classical microbiological approaches because their specific growth demands are unknown, or because they cannot grow without the simultaneous existence of synergistic partners (Shlomi et al., 2007). In order to access the vast fraction of uncultivable microbes, genome centric metagenomics has given new possibilities to the scientific community (Parks et al., 2017). The extraction of genomes from complex assemblies allows the inference of metabolic pathways present in Metagenome Assembled Genomes (MAGs) (Nayfach et al., 2019), using the Kyoto Encyclopedia of Genes and Genomes database (KEGG) (Kanehisa et al., 2016) and/or EcoCyc (Keseler et al., 2017). Unfortunately, the use of gene annotation alone cannot fully describe the role of each microbial species in the global metabolic network mainly because many of the functions and reactions are still unknown (Zacher et al., 2014). Thus, a novel approach is needed for deciphering functional roles, microbial interactions and the exchange of molecules. Flux balance analysis (FBA) of *in silico* metabolic networks has recently emerged as one of the most effective methods to unveil microbial interplays (Magnúsdóttir et al., 2017). In fact, such metabolic models account for known intracellular processes (Budinich et al., 2017), as well as for metabolite uptake and secretion. This approach offers a reliable representation of the cross feeding occurring between community members (Khandelwal et al., 2013), and is able to predict how species gather in large consortia (Machado et al., 2020). However, previous studies relied on microbial consortia derived by 16 S-based metagenomes to recover either the closest genomes or models publicly available in database. This assumption may limit the accuracy of the analysis as the correspondence between 16 S-derived information and public data may be imprecise. Furthermore, microbial species can activate different pathways according to the growth medium and the relationship among different members of the same consortia. Metatranscriptomic results can be integrated to constrain the metabolic models and confirm previously flux balance analysis results. The ability to predict the structure and functioning of complex microbiomes is crucial for the study of organic matter degradation (Boon et al., 2014). The AD community is able to produce methane through a biologically mediated process, which is one of the oldest bioactivities on Earth (Sorokin et al., 2017). Anaerobic organic matter degradation naturally occurs in many ecological niches including, for example, the digestive tract of animals and anaerobic sediments (Liebetrau et al., 2019). Moreover, the biotechnological relevance is clear, as it can be exploited for biogas production. From an anthropocentric point of view, the AD microbiome organization can be visualized as a funnel (Campanaro et al., 2020) with methane as the final product. The funnel concept represents the progressive functional specialization, where the microbial players can be classified into four groups: hydrolytic, acidogenic and acetogenic bacteria, and methanogenic archaea (Campanaro et al., 2016). In the last few years, biotechnological applications in renewable energy and CO_2 sequestration fields have been under active development due to the increasing environmental awareness, which is leading to a lower fossil fuel dependency and to a more intelligent management of natural resources (Hall and Scrase, 1998). During biogas production, the reactor efficiency can be increased through an accurate monitoring of process parameters, including temperature, mixing, reactor characteristics, feedstock composition (Angelidaki et al., 2018). All these factors can have a direct effect on the microbial community (Zhu et al., 2019). However, despite the microbiome's pivotal role in organic matter conversion into methane, there is still a lack of knowledge regarding the microbial influence on the process (Koch et al., 2019).

In order to unravel the microbial network and to clarify how process parameters can affect the microbiome structure, a FBA-based approach is proposed to explore metabolic exchanges in the AD community. Specifically, the objectives of the study were: a) to apply and develop a flux balance-based method for analysing coexistence dynamics in microbial consortia; b) to set-up a pipeline for the inspection of both microbial pairwise interactions and metabolites exchanges considering also the implementation of metatranscriptomic data to constrain the solution space; c) to investigate the interdependencies among multiple species, d) to define a comprehensive metabolic model of the AD microbiome. Additionally, bioinformatics approaches were used to understand how cross-feeding varies according to the different experimental conditions and simultaneous metabolite exchange among multiple species were investigated by analysing the flux network (Chaffron et al., 2010).

2. Results

The microbial species selected to be included as case study account for both archaea and bacteria and constitute the biggest known database of AD microbiome derived from metagenomic data (Campanaro et al., 2020). Of the reconstructed MAGs, only 836 have been considered for genome-scale metabolic model (GSMMs) reconstruction, which were identified as "high quality" regarding their genome completeness and contamination according to MIMAG guidelines (Bowers et al., 2017). These MAGs were taxonomically associated to 30 phyla involved in the AD process (Supplementary Table I) and represented the initial step of the investigation into interphylum and inter-kingdom interactions occurring in the anaerobic microbiome. The large-scale assessment of microbial relationships was performed in two stages, considering a feedstock rich in sugar and proteins in the former and the influence of external H_2 injection in the latter (Treu et al., 2019). Subsequently, four different populations of the microbiome were used to analyse the occurring metabolic mechanisms and to determine the microbial interactivity. In this case, only the MAGs having a relative abundance higher than 0.001% were considered, based on the results of a previous experiment (Fontana et al., 2018) and using a feedstock rich in sugar and proteins. The first two populations were methanogenic, responsible for methane production before and after H_2 injection, while the other two were acidogenic and governed the production of acetate and other volatile fatty acids (VFA).

Upon reconstruction, each model underwent a battery of quality control tests to verify biological and formal soundness. All models have full correspondence between reactions and genes, have demand reactions with fluxes in backward direction and pass the single gene deletion tests. The "leak tests" reports a score higher than 0.99 in all GSMMs (both with and without demand reactions) (Supplementary Table II). Moreover, we benchmarked our models against those from a previous large-scale collection of human gut microbiome GSMMs based on the MEMOTE tool (Lieven et al., 2020). This comparison highlighted a few systematic differences between the GSMM collections, probably due to the use of different model reconstruction software, some of which were already observed by Lieven and colleagues (Lieven et al., 2020) (Appendix and Figshare 10.6084/m9. figshare.12,582,746. v2). In particular, MEMOTE results revealed that AGORA models have a more complete GPR annotation and a lower number of mass-unbalanced reactions. However, models generated with CarveMe have a lower number of blocked reactions and so-called "orphan metabolites".

In total, 4132 unique metabolic reactions, involving 1580 different compounds, were identified. Each GSMM included on average 1391 ± 245 reactions, 1012 ± 152 metabolites and 571 ± 159 genes (Fig. 1 and Supplementary Table II). 112 metabolites (7%) (e.g. L-Tryptophan, L-Valine, L-Tyrosine, Glycine, L-Methionine) and many cofactors (e.g. FAD, FADH, NMN, $NADP^+$, $NADPH_2$) were predicted in all models and were identified as "microbiome metabolite core", while 36 compounds were specific to individual models and were defined as "microbiome metabolite cloud". The presence and completeness of pathways responsible for carbohydrate and lipid metabolism have been tested in the metabolic models by tracking the corresponding reactions. Regarding carbohydrate metabolism, *Actinomycetales* sp. GSMM1485, *Clostridiaceae* sp. GSMM0156, *Clostridiales* spp. GSMM0297,

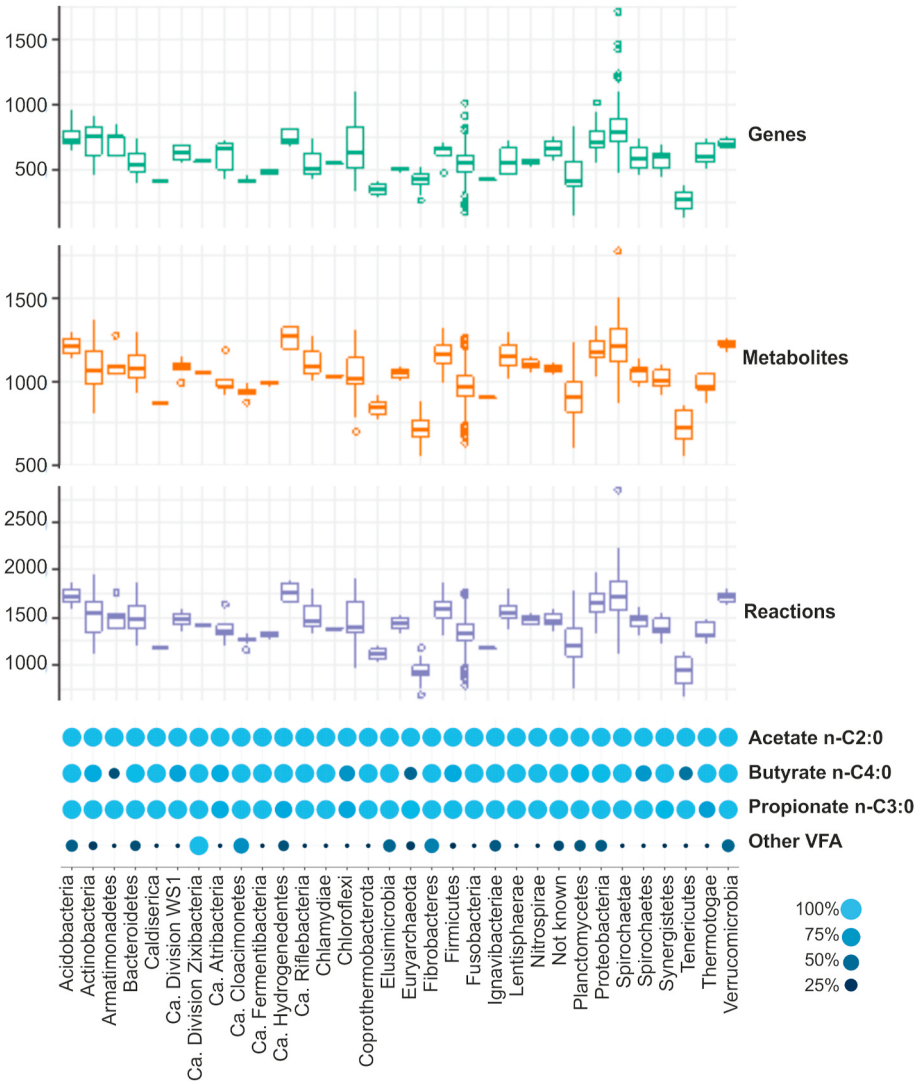

Fig. 1. General information of the metabolic models at phylum level.

GSMM0760, GSMM1021, *Firmicutes* spp. GSMM0866, GSMM0213, *Tepidanaerobacter syntrophicus* GSMM0017 were shown to have the complete anabolic and catabolic pathways. Regarding lipids metabolism, "beta-Oxidation, acyl-CoA synthesis" and "Phosphatidylethanolamine (PE) biosynthesis, PA => PS => PE" are complete in 18 GSMMs obtained from species belonging to the phylum Proteobacteria (Supplementary Table II).

When considering the taxonomic assignment of MAGs at phylum level, some phyla had an average smaller number of genes, metabolites and reactions (Fig. 1), with the microbial species assigned to the *Synergistetes* phylum showing the lowest number of genes recorded. On the other hand, *Proteobacteria* had the highest number of genes, followed by *Acidobacteria*, *Actinobacteria* and *Armatimonadetes*. This result shows consistency with microbes belonging to *Proteobacteria* being considered "generalist", as they can simultaneously perform multiple steps in the AD process, such as fatty acid degradation, butanoate metabolism, propionate metabolism, sulphate reduction and denitrification. This is in agreement with a previously reported study (Kitano, 2007).

A complete description of the metabolic potential present in the microbiome and the identification of new biochemical and physiological traits (both expected and non-intuitive) were accomplished by evaluating the 4132 biochemical reactions represented in the models. Only 33 "core reactions" were ubiquitously identified in all the microbes, which could be classified in three main categories: "transporters of simple molecules", "kinases" and "transferases". Moreover, methane biosynthesis was found in all the 29 archaeal species belonging to the *Euryarchaeota* phylum. A verification performed on the models by taking into account a set of 14 reactions revealed that *Methanosarcina* spp. (e.g. GSMM0042, GSMM0744, GSMM0883) can perform all the three methanogenic processes (acetoclastic, hydrogenotrophic and methylotrophic) as expected, while *Euryarchaeota* sp. GSMM0884, *Thermoplasmatales* Incertae Sedis sp. GSMM1074 and *Euryarchaeota* sp. GSMM0778 have a complete set of enzymes only for the methylotrophic methanogenesis (Supplementary Table II). Among the others, *Methanothermobacter* spp. (e.g. GSMM0047 and GSMM0396) and *Methanoculleus* spp. (GSMM0046, GSMM0045) have been confirmed as hydrogenotrophs. *Methanothrix soehngenii* GSMM0064 and *Methanosaeta* sp. GSMM0125 have the complete acetoclastic pathway consistently with previous findings.

Conversely, 101 species-specific processes were defined as "shell reactions". For instance, the model of *Clostridia* sp. GSMM1577 was the only one predicting the use of coproporphyrinogen as an intermediate for heme biosynthesis (Dailey et al., 2015). Similarly, only Candidatus *Riflebacteria* sp. GSMM0304 could import and metabolize L-gulonate and D-tagatose (Raspor and Goranovič, 2008). These monosaccharides are epimers and precursors of glucose-6-phosphate and precursors respectively of dihydroxyacetone phosphate and pyruvate (Heinken and Thiele, 2015). The unique characteristics of Candidatus *Riflebacteria* sp.

GSMM0304 were related to CO utilization as a carbon source. In fact, this MAG was only present in a single experiment (Jing et al., 2017), suggesting its extreme specialization and possibly reflecting a low adaptability to survive in commonly utilised AD feedstocks. VFA, in particular acetate, propionate and butyrate are crucial intermediate compounds for the production of methane (Molina et al., 2009), as well as indicators of process stability (Jacobi et al., 2009) and agents for process diagnosis (Ahring et al., 1995). It is therefore extremely important to have a balance in the concentration of VFA, avoiding excessive accumulation of these intermediates in anaerobic reactors. The fundamental role of VFA in the AD system means that the possibility to estimate the intermediate compounds production and exchange in the AD microbiome is of great interest to tackle determinants of process instability (Liao et al., 2016). For this reason, the presence of genes involved in VFA production and utilization has been investigated in all the models (Fig. 1). While some VFA, such as hexanoic, isovaleric and valeric acid were absent in the models, acetate was noticeably abundant, evidencing its association with the core microbial metabolism. According to the gene presence, the bacterial Wood–Ljungdahl pathway was identified as complete in nearly 40 species (Supplementary Table II). Regarding other VFA, propionate was reported in 821 GSMMs, while butyrate in 693 (mainly in models of *Bacteroidetes* and *Synergistetes* species), which were respectively 98 and 82% of all GSMMs considered. In particular, propionate was involved in the biosynthesis of different key compounds belonging to the glycolytic pathway, including succinate, fumarate and oxaloacetate (Stryer, 1995). Assuming that the importance of different VFA in the cross-feeding process can be determined by the fraction of microbes which are able to exchange them, butyrate was probably one of the most relevant, since it was exchanged by 635 species. Propionate was exported by a lower number of microbes, suggesting a lower potential in cross-feedings. Among all VFA, isobutyrate was the rarest, being present in 61 models (or 7% of all GSMM) only. These results suggest that the cross-feeding of butyrate is common, consequently redundant in the microbiome, while the role of the few species involved in propionate exchange is crucial. Accordingly, an alteration in the abundance of the propionate producers might trigger a cascade effect, resulting in the loss of species utilizing this VFA to produce other important intermediate metabolic compounds, such as fumarate and oxaloacetate.

Distribution of the number of genes, reactions and metabolites composing the reconstructed genome-scale metabolic models and presence of specific volatile fatty acids, divided by phylum. Whiskers show the minimum and maximum values. Values below "Q1 - 1.5 × IQR" and above "Q3 + 1.5 × IQR" are plotted as outliers (Q1: first quartile, Q3: third quartile, IQR: interquartile range). Colour and diameter of the circles depend on the fraction of microbes predicted to synthesize specific VFA.

2.1. Global landscape of pairwise interactions

The potential of 349,030 microbial couples being involved in positive or negative relationships was systematically investigated. In order to perform this investigation, PAirwise INteractivity analysis (PA.IN.), a computational framework for the prediction of interspecies behaviour was developed. Using the framework, different conditions (including hydrogen concentration) were investigated, obtaining in total 698,060 pairs. In the present work it was found impractical to perform simulations for interactions with order higher than two on 836 models due to computational and time effort, despite this type of analysis was previously applied (Machado et al., 2020).

Results revealed a variety of trade-offs within the microbe pairs depending on both the metabolic potential and the imposed environmental conditions. A comparative inspection of the relationships occurring between the 836 microbes, including those obtained for species belonging to the "rare biosphere", was carried out to estimate the reciprocal potential impact of each species on the growth rate. This analysis was performed considering a diet designed *"ad hoc"* to simulate reactors' feedstock rich in sugar and proteins (the exact medium composition is reported in subsection 4.2). Not all the GSMM groups could grow individually on this specific feedstock; however, all the models showed non-zero growth in at least one of the possible couples. The feedstock components description was obtained integrating data from the VMH database (Noronha et al., 2019) with measurements conducted on the "real" feeding substrate (Fontana et al., 2018). Additionally, results on the microbial community composition were obtained for the same feedstock, but for two different growth conditions, one specifically characterized by external H_2 injection. Hydrogen was supplemented to enhance the hydrogenotrophic methanogenesis and, consequently, to increase the methane content in the biogas, promoting the most important step of the process (Nugent et al., 2013). Due to the relevant role of H_2, both the shift in the functional activity of single microbes after injection and its influence on the microbial cross-talks were inspected.

Based on the modifications in the growth rate of a species occurring while engaging with another member of the microbiome, six different patterns were determined: parasitism (±), commensalism (+/0), neutralism (0/0), amensalism (-/0), competition (−/−) and mutualism (+/+) (where: + is positive, - is negative and 0 is no effect on each other between organisms) (Heinken and Thiele, 2015). When the coexistence negatively influences one of the two partners (growth rate decreases equal to or larger than 10%), the interplay is classified as negative, otherwise as positive. Neutralism is considered as a non-interaction, since the change in the growth rate derived from the microbial coexistence in the pair was included between −10% and +10%.

In the community, commensalism was identified in 33% of the pairs, indicating a general positive reciprocal influence occurring between microbes (Fig. 2). This behaviour, frequently detected in biodegradation processes (Campanaro et al., 2020), is mediated by cross-feeding which is indeed favouring synergies. Furthermore, among negative interactions, competition is the rarest, found only in 1.6% of the pairs (Appendix, Table S1). Similar results were obtained, considering the microbial species analysed before using the cooperative tradeoff algorithm (Diener et al., 2020). This analysis confirmed that positive interactions are more frequent than negative ones (Supplementary Table III). Interestingly, the interactivity pattern identified is markedly different than that identified in other microbial communities where negative cross-talks are dominant. In fact, Heinken and coll (Heinken and Thiele, 2015). found that parasitism is the most frequent meta-communication in human gut microbiome, while mutualism is the rarest. Notably, vessels in AD are strictly anaerobic while the gut is mainly microaerophilic, indicating that anoxicity promotes positive interspecies communication. An additional analysis was performed considering different thresholds for defining interactions: ±1%, ±5%, ±15% and ±20%. The higher the threshold, the higher the number of neutralisms identified (Supplementary Table III). However, it can be concluded that the threshold was not influencing the detection of the specific behaviour characterizing the community. Despite setting the thresholds at 15% and 20% resulted in a higher number of neutral interplays in comparison to the commensalisms, negative interactions remain always lower in number than the positive ones (even without considering neutralism as positive). Relevant trends underlying the general organization of the community were identified at phylum level. All phyla were involved in the six types of co-occurrences (except *Caldiserica* and *Chlamydia* which include very few species) (Supplementary Table III); however, some preferential kinds of interaction were identified via a statistical analysis (p-value < e−16, chi-square test). In particular, some taxa are characterized by a specific pattern of interactivity (validated by Pearson's residuals): *Bacteroidetes,* for example, are frequently involved in neutralism and rarely in parasitism and amensalism (Supplementary Table IV). The opposite happens for *Proteobacteria*, whose species are more involved in parasitic associations than in neutralistic. *Spirochaetes*, *Verrucomicrobia* and *Ignavibacteria*

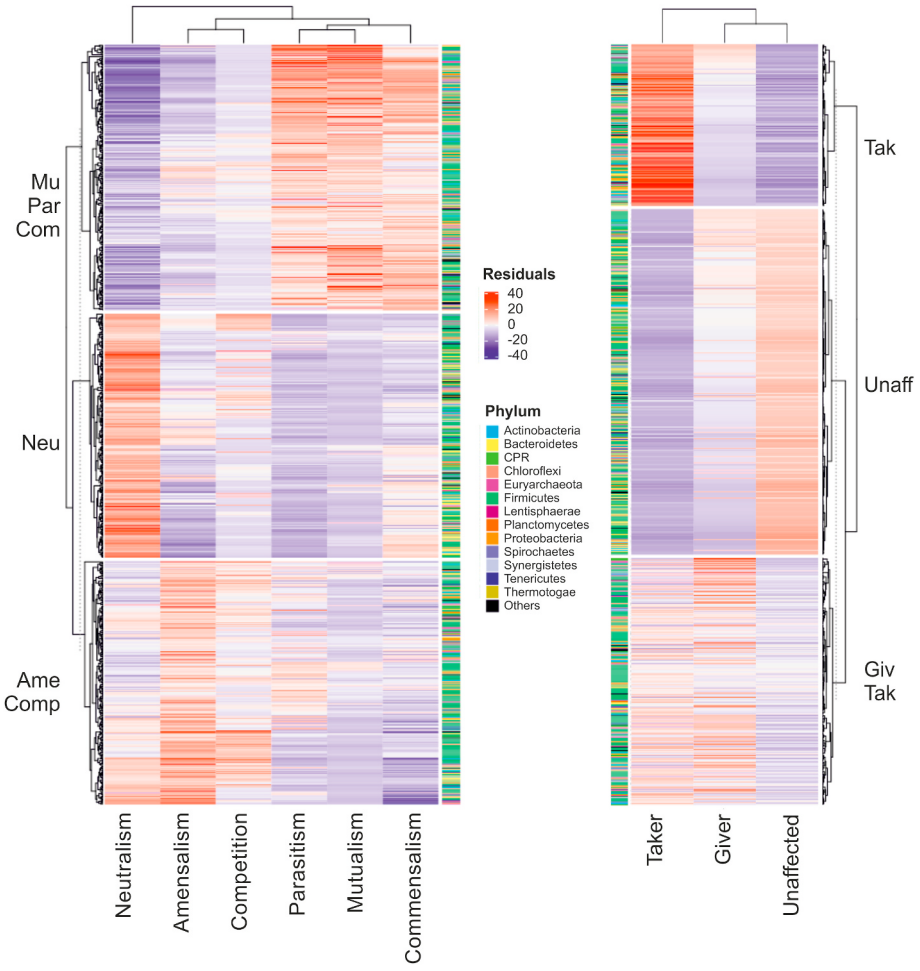

Fig. 2. Hierarchical clustering of the Pearson residual values.

among others, are the species interacting the most through mutualistic association, while *Caldiserica* and *Tenericutes* are frequently amensalistic (Supplementary Table IV).

Clustering has been performed both on interactivity and roles preferences profiles. The first highlights three main groups of species having different interactivity profiles. "Neu" includes species characterized mostly by neutralism and competition; "AmeComp" comprises those being predominantly amensalistic or competitive; "MuParCom" containing those that are primarily mutualistic, parasitic and commensalistic. Clustering of the residual values performed on interactivity roles was performed in order to evidence species behaving as "givers" or "takers". Three main groups of species were identified: "Unaff" includes those correlated neither with "giver", nor with "taker" behaviour (Neutral); "GivTak" consists of those with a heterogeneous behaviour in the interactions; "Tak" involving those behaving mainly as takers.

General preferences at species level were defined by hierarchical clustering identifying three main behavioural clusters (Fig. 2): Neu, for microbes with preference for neutralism, AmeComp, for microbes with preference for amensalism and competition, MuParCom, for microbes with preference for mutualism, parasitism and commensalism. *Euryarchaeota* are mostly associated with Neu and MuParCom, with *Methanosaeta* and *Methanomassiliicoccus* species belonging to Neu and *Methanothermobacter* and *Methanosarcina* species belonging to MuParCom (Fig. 2). This finding indicates that some archaeal species are more likely to express syntrophic behaviour. Among others, *Coprothermobacterota* were also mainly found in MuParCom, which could explain why *Methanothermobacter wolfeii* GSMM0047, *Methanothermobacter* sp. GSMM0492 and *Methanosarcina thermophila* GSMM0009 outcompete other archaea in the establishment of the community (Fontana et al., 2018). However, this behaviour was not limited to archaeal species, as the two dominant bacteria *Coprothermobacter proteolyticus* GSMM0002 and *Defluviitoga tunisiensis* GSMM0021 (up to 68% of combined relative abundance) adopted this behaviour too. Indeed, previous research performed on the metabolic pathways and the distribution of *D. tunisiensis* in the AD environment suggested that it can be involved in syntrophic associations and metabolic exchanges with hydrogenotrophic methanogens (Maus et al., 2016). Nevertheless, *D. tunisiensis* is able to grow in pure culture, suggesting that syntrophies are not obligatory, albeit fruitful (Campanaro et al., 2018).

Another example for the importance of positive syntrophies was given by the PA. IN. inspection of *Bifidobacterium crudilactis* GSMM0001. This microbe presented a neutral behaviour in only 16% of the pairs, while on average other microbes remained unaffected in 51% of the pairs. This result could explain its great abundance, reaching 85% in the acidogenic community. A random sampling-based permutation test (see subsection 4.4 for additional details) revealed that highly abundant species like *B. crudilactis* GSMM0001 tend to show an overall positive behaviour, while low abundant species prefer amensalism. In general, most *Bacteroidetes* fell into the AmeComp cluster, and they were mainly unaffected by the interactions (growth rate variations were between −10% and 10%), indicating that these taxa use the same compounds as others, but without being outcompeted. The dominant biosphere is represented by a cooperative community conforming to the black queen hypothesis (Mas et al., 2016), while the rare microbes have overlapping nutritional requirements resulting in a more competitive community

shaped as in the red queen hypothesis (Bonachela et al., 2017).

2.2. Microbial classification based on individual interaction role

Following the evaluation of microbial couples' behaviour during interactivity, it was possible to isolate and inspect the individual role of each microbe in the community by focusing on growth rate variations of the single species within each couple. In particular, the single microbes could benefit from the coexistence (takers) or were being negatively affected (givers). Species not influenced were defined as "unaffected". The significance of preferences for a specific role (givers or takers) was determined by chi-square statistics. Cluster analysis performed on residuals divided the species in three main clusters according to their behaviour (Fig. 2). Most abundant species were "takers" and included in the "Tak" cluster. This trend shows two relevant exceptions, i.e. the abundant species *D. tunisiensis* GSMM0021 and *Epulopiscium* sp. GSMM0167, both belonging to "GivTak". The rare biosphere was mainly included in cluster "Unaff", characterized by species with an unaffected behaviour (Neutral).

Interspecies interactions could involve members of different phyla (interphyla) or could occur within the same phylum (intraphylum) (Fig. 3). Bacteria exclusively involved in interphyla relationships mainly belonged to *Planctomycetes*, *Actinobacteria*, *Chloroflexi* and *Thermotogae*, while other phyla showed either "intra" or "interphyla" interactivity. Notably, intraphylum mutualism was very rare, representing less than 0.001% of the total number of cross-feedings identified for a specific phylum (Fig. 3A). Possibly, this surprising feature is due to the similarities in the metabolic properties of species belonging to the same phylum, which tend to be involved in the same "trophic level" of the AD microbiome. This can result in species of the same phylum having a higher level of competition and a lower number of mutualistic cross-talks, which in turn were more frequent between microbes participating in different functional steps. On the contrary, amensalism can occur intraphylum, revealing a competitive behaviour between microbes of the same level contending for resources (Fig. 3B). The most prominent amensalistic tendency was observed between *Firmicutes* and *Caldiserica*, whilst *Firmicutes* and *Fusobacteria* had the strongest mutualistic relationships.

(A) and (B) depict mutualistic and amensalistic interplays, respectively. Circumference arc length is proportional to the number of species in the corresponding phylum. Phyla represented by a low number of species were merged and named as "Others". Red (mutualistic) and blue (amensalistic) edge thickness represents the number of interplays normalized per phylum by number of species and having relative frequency higher than 0.001%.

2.3. Influence of externally supplied hydrogen on microbial interplay

Hydrogen injection resulted in an increased number of mutualistic and commensalistic cross-talks as well as in fewer negative and neutral influences (Fig. 4, Supplementary Table III), even though this effect was not widespread in the microbiome. In fact, despite the central role of hydrogen in many metabolic processes (it was present in 823 models and predicted to be exported by 509 species), its exogenous addition impacted only 4.33% of the interacting microbial couples. The cooperative tradeoff algorithm confirmed that hydrogen injection affects less than 5% of the couples and drives the community to a more cooperative behaviour (Supplementary Table III). Analyses performed in a methanogenic reactor supplemented with the feedstock simulated in the present study, revealed that relative abundances of *Leuconostoc* sp. GSMM0134 and *Pseudomonas lactis* GSMM0003 were markedly increased after H_2 injection (Fontana et al., 2018). Interestingly, PA. IN. results revealed that both microbes switched from negative to positive interactivity after H_2 addition. For instance, the growth of *Leuconostoc* sp. GSMM0134 before H_2 injection was negatively affected by 15 different members of the methanogenic community (of 22 in total), which were probably competing for substrates (e.g. lactose, serine) or taking advantage of by-products derived from substrate metabolism (e.g. L-Alanine, L-Arabinose, Diacetyl, Succinate) (Supplementary Table V). External hydrogen addition shifted this metabolic equilibrium, reducing the existing negative interactions to six and enhancing the average growth rate of *Leuconostoc* sp. GSMM0134 from 0.08 to 0.11 1/h. On the contrary, *P. lactis* GSMM0003 initially had a more diverse range of interaction types that changed significantly upon hydrogen addition. Its average growth rate increased slightly from 28.24 to 28.66 1/h and eight of its parasitic relationships became mutualistic or commensalistic, with other five commensalistic relationships shifting to parasitic (Supplementary Table III). Although externally supplied H_2 influenced few selected couples, this finding suggests that changes induced remarkable improvements in the syntrophies between bacteria and, consequently, resulted in an increased methane production.

2.4. From a global inspection to a detailed view of the interactions

In order to substantiate and identify the interaction relations of the AD microcosms a second case study was investigated. It represents the AD microbiome, including metagenomic and metatranscriptomic data derived from the digestion of a simple substrate composed by sugars and proteins in a two stage system (Fontana et al., 2018). Microbial communities inhabiting one methanogenic and one acidogenic reactor were chosen in order to evaluate the compounds exchanged among species. In particular, this experiment is taken as a case of study since it holds a combination of features (i.e. small communities, high quality microbial genomes, simple feedstock) that make it ideal for flux balance

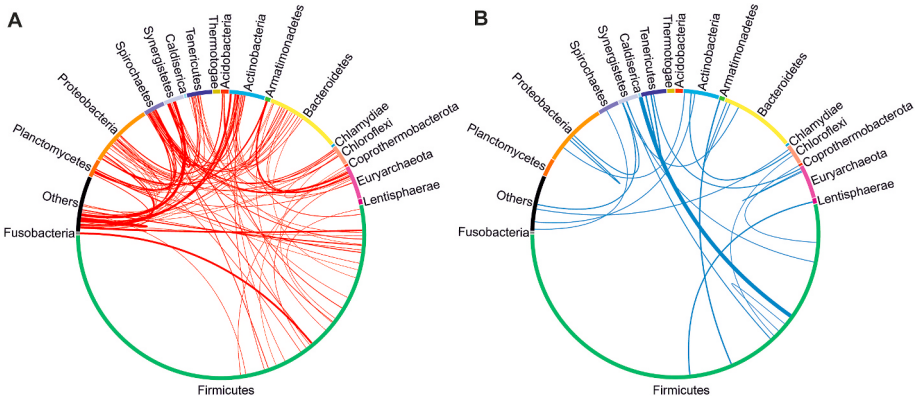

Fig. 3. Representation of interactions at phylum level.

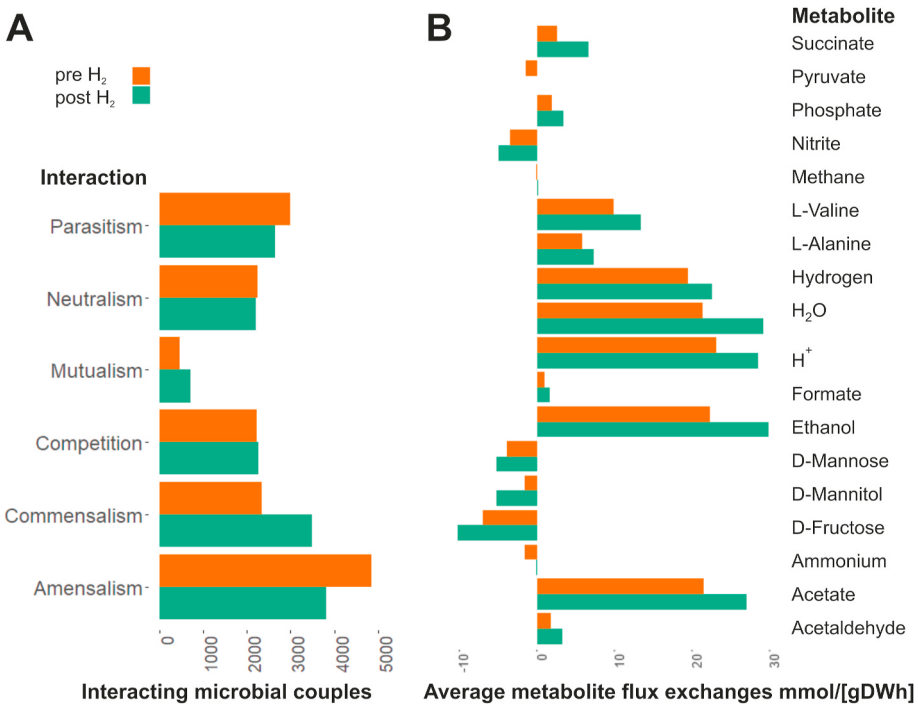

Fig. 4. Histograms representing the effect of H_2 injection on the community.(A), (B) effect on the microbiome interactivity profile and on average metabolite production/consumption respectively. In panel A, shown interactions are only those that change between the two conditions.

simulations. All microbes having relative abundance greater than 0.01% in at least one of the two conditions were considered, representing 69 and 10 species in methanogenic and acidogenic communities respectively. The archaeal repertoire includes five species, one *Methanosarcina* (having the most versatile metabolism), two *Methanothermobacter* and two *Methanoculleus* (pure hydrogenotrophs). The rest of the microbiome includes bacteria of *Actinobacteria*, *Bacteroidetes*, *Coprothermobacterota*, *Firmicutes*, *Proteobacteria*, *Synergistetes* and *Thermotogae*. Consistently with the experimental results, metabolite exchange simulations indicated 10% increase in butyrate and methane, and 5% in acetate production in the single-stage setup (methanogenic reactor). In the microbiome of acidogenic reactor (two-stage system), the repertoire includes only bacteria of the *Firmicutes*, *Proteobacteria* and *Actinobacteria* phyla and no archaea, due to the low pH (i.e. 3.9 ± 0.1) inhibiting the methanogenic process and hampering their growth. Here, the simulations showed an increase in butyrate and acetate production and a global increase of VFA, confirming previous findings about their importance. Furthermore, the computational approach also estimated differences in the production of several other compounds, which were not considered in the original study. In the methanogenic reactor, for example, a decrease in the production of acetaldehyde, (S)-propane-1,2-diol, pyruvate and ethanol was suggested by the simulations, following hydrogen injection. Conversely, the uptake of L-aspartate, glycine, D-alanine and L-glutamate was positively influenced subsequent to hydrogen injection (Supplementary Table V).

A-C. Circles represent the single microbes, the diameter is proportional to the species abundance and the colour denotes the phylum. The medium is represented by the purple circle in the middle. Results for selected glucogenic amino acids such as glycine (A), and valine (B) are reported. In panel (C), key compounds related to the AD process, such as acetate (dashed lines), acetaldehyde (solid lines), formate (parallel lines) and hydrogen (vertical slashed lines), are shown. Arrows thickness is proportional to the fluxes between species. Exchanges occurring in the methanogenic (A-B) and in the acidogenic (C) reactors, respectively, are reported.

In order to verify a putative causal relationship between metabolic compound exchange and results obtained from microbial coexistence, a comparative analysis was performed. In the methanogenic reactor, out of 196 compounds exported by at least one of the microbes, only 58 (29.6%) could be imported by other species and were predicted as "cross feedings". Among those, 18 metabolites were related to amino acid metabolism, to which a similar prediction was evidenced in other complex microbial communities by Parks and colleagues (Parks et al., 2017). Amino acid interdependence is strictly linked with the lack of TCA cycle intermediates (Thommes et al., 2019). However, this imbalance, causing auxotrophies, can be compensated by compounds exchanges between members of the community. Metabolic exchange (ME) analysis (see subsection 4.3 for additional details) underlined the relevant role of glucogenic amino acids such as glycine, valine, and glutamate in the AD microbiome (Fig. 5). These compounds can be converted into intermediates of the TCA cycle, like glycine, the precursor of pyruvate, which is then converted into acetyl-CoA. Other compounds, such as valine and glutamate, are respectively precursors of succinyl-CoA and alpha-ketoglutarate.

According to the FBA carried out on the microbial community growing in the methanogenic reactor, *Defluviitoga tunisiensis* GSMM0021 was the most efficient producer of glycine and valine (Fig. 5A and B and Supplementary Table V), as well as the most abundant species. *Tepidanaerobacter acetatoxydans* GSMM0006 was predicted as the main uptaker of the two metabolites and the second most abundant microbe. Additionally, *P. lundensis* GSMM0004 produced L-proline, which was imported by *B. crudilactis* GSMM0001 and converted into alpha-ketoglutarate. Another potential syntrophy was found between *Lactobacillus paracasei* subsp. *paracasei* GSMM0008 that produced L-Valine, and *Leuconostoc* sp. That imported and converted it to succinyl-CoA (Fig. 6). Both alpha-ketoglutarate and succinyl-CoA are TCA cycle intermediates and can be transformed into adenosine triphosphate (ATP), carbon dioxide and the reducing agent NADH (Moat et al., 2002). This finding hints the presence of a meta-communication, which is relevant also in the acidogenic reactor.

Another interesting result obtained from ME revealed that a simultaneous exchange of acetaldehyde and acetate was occurring in the acidogenic reactor (Fig. 5C). *Serratia liquefaciens* GSMM0007, *P. lactis* GSMM0003 and *Clostridiales* sp. GSMM1607 were the major up-takers of

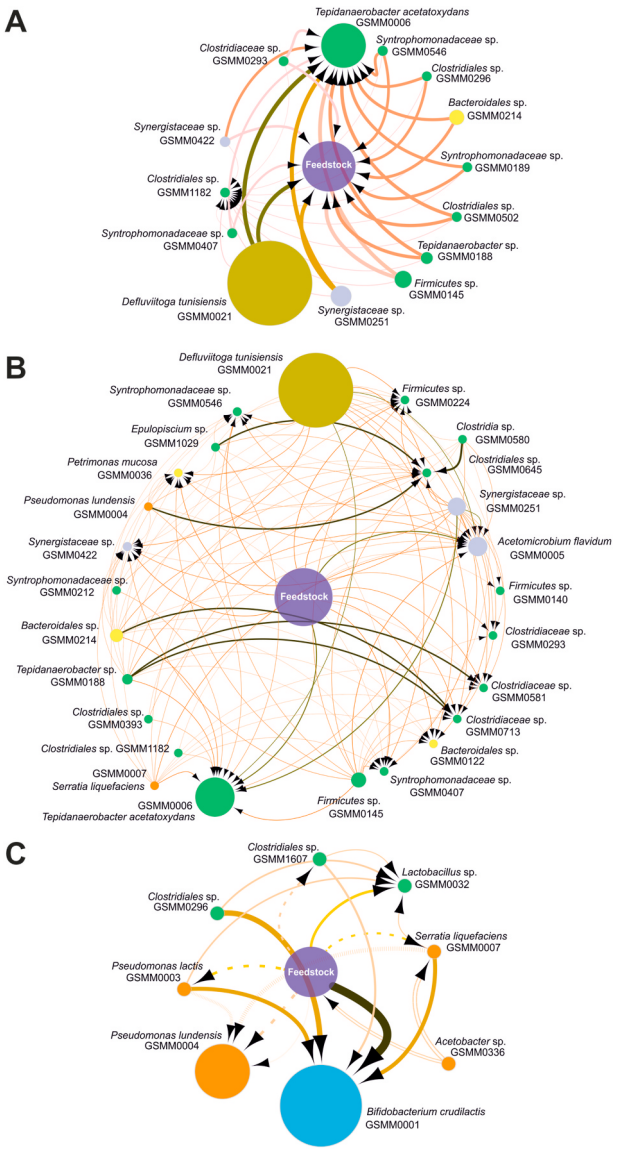

Fig. 5. Visualization of metabolic exchanges occurring between microbes present in the reactor and/or with the medium.

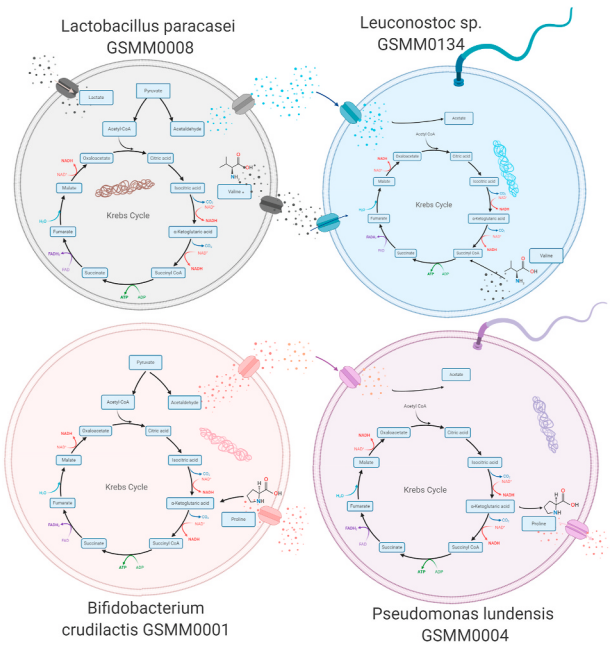

Fig. 6. Schematic representation of the TCA cycle in the four dominant species present in the acidogenic reactor.

acetaldehyde and the main producers of acetate, implying that the latter compound is generated by the activity of acetaldehyde dehydrogenase in specific bacteria. *B. crudilactis* GSMM0001 was the most abundant microbe overall, absorbing the vast majority of acetaldehyde and hydrogen, and concurrently stressing the key role of these compounds for the proper functioning of the acidogenic reactor.

A putative syntrophic association between *Coprothermobacter proteolyticus* GSMM0002 and *Methanothermobacter wolfeii* GSMM0047 was previously proposed (Fontana et al., 2018). Considering the relevance of this syntrophy in the methanogenic process, it was chosen for a detailed analysis, using the new methodology developed and supported by RNA-seq data integration. Previous studies mentioned a cooperative coexistence between proteolytic anaerobic bacteria and hydrogen-converting methanogens, evidencing that this syntrophy can lead to an increased cell growth and a better degradation efficiency (Stams, 1994). The present analysis showed that the two species could indeed reciprocally influence the growth rate of one another, with *C. proteolyticus* GSMM0002 benefiting from this relationship in both conditions analysed and *M. wolfeii* GSMM0047 remaining almost unaffected. Furthermore, ME showed that *C. proteolyticus* GSMM0002 produced H_2 and iron (Fe^{2+}), which were subsequently used by *M. wolfeii* GSMM0047, partially in agreement with FBA integrating simulation of population steady-state metabolism (Supplementary Table III). However, a comparative evaluation performed with ME and starting from the results obtained with PA. IN. revealed a more complex situation. Both *C. proteolyticus* GSMM0002 and *M. wolfeii* GSMM0047 benefited from the presence of several other *Clostridiales* species in commensalistic interactions. *M. wolfeii* GSMM0047 obtained H_2 and formate from *Clostridiales* species, while *C. proteolyticus* GSMM0002 absorbed tryptophan, L-proline and L-isoleucine, which are precursors of alpha-ketoglutarate: a compound with a key role in the TCA cycle (Niehaus et al., 2019). Above result was supported by previous work asserting that SAOB interplays are not simply dualistic as previously thought but are based on multiple cross-feeding effects (Westerholm et al., 2019). Finally, the original study reported an increase in methane production after H_2 injection, and proposed an archaeal species potentially responsible for the biogas upgrading process (Fontana et al., 2018). In support of this proposal, ME estimated that *Methanoculleus thermophilus* GSMM0046 was the microbe that profited the most from injecting H_2 in the reactors, establishing it as the main microbe responsible for the increased methane yield and purity. These results were confirmed by simulations implementing gene expression values used to constrain the solution space (Supplementary Table V). For example, the flux for methane production shifts from 111.73 to 396.35 mmol/[gDWh], indicating an increase subsequent to H2 addition. However, based on the simulations integrating steady-state metabolism, *M. thermophilus* GSMM0046 showed strong profiteer behaviour, further emphasised after additional hydrogen injection (Supplementary Table III). In particular, parasitic relationships may be due to an enhanced uptake of several key metabolites and co-factors (Appendix, Table S2) by the archaeon. These compounds, thus, resulted less available in the medium for the other members of the community.

Since there is not a universally accepted method to perform MFB community simulations and due to potential biases of the different approaches, some discrepancies are expected; however the key patterns obtained are in agreement and support the findings both at coarse and fine grain level related to main behaviour of the AD microbiome.

Results were integrated with the predicted amino acids exchanges influencing the TCA cycle. The enzymatic structure represents the acetaldehyde dehydrogenase performing the conversion of

acetaldehyde into acetate.

3. Conclusions

The major novelty of the current study is the combination of metabolic reconstruction and modelling across hundreds of species for the detection of molecular mechanisms behind their interactions at an unprecedented level of detail. To our knowledge, this is the first attempt to massively generate models from high-quality MAGs, and to use flux balance analysis for the inspection of a complex biologically mediated biogas production system. The generation of metabolic models derived from known species, and identified in the environment by means of 16 S rRNA similarity search, leaves unresolved questions due to the presence of uncultivated microbes. On the contrary, the approach proposed here paves the way to the use of FBA in the functional investigation of the microbiome and allows a deeper understanding of all the species present. The investigation of pairwise influence provided a comprehensive overview of the microbial community involved in the anaerobic digestion process. From the present investigation it emerges that reciprocal influence in the microbial growth rate can be calculated in-silico and largely depends on competition/sharing for/of metabolites. The used approach was successful in picking out strong differences in interactivity roles between species that became prevailing in the community evidencing how in this ecosystem two kinds of complementary communities coexist. The consortium in the AD subsystem is stabilized by syntrophies and auxotrophies. The accuracy of model creation and medium characterization enabled the identification of key metabolites fluctuations between two experimental conditions characterized by H_2 injection. This resulted in differences in microbial growth correlated with specific feedstock compositions. This analysis suggests that investigation of pairwise interactivity can help in providing fundamental insights into complex microbial populations (Weinrich et al., 2019). This approach is shedding light on the network occurring in the AD "black-box" and paves the way to a functional prediction of the AD microbiome based on FBA. In perspective this newly developed procedure can target biogas production improvement through the design of "*ad hoc*" microbial consortia or by predicting substrate effects on the microbiome dynamics.

4. Material and methods

4.1. Description of the experiments

For carrying out the modelling work and validating the metabolic models used in the present study, MAGs were obtained from the comparative analysis recently published by Campanaro (Campanaro et al., 2020). The comparative analysis of more than 130 publicly available experiments from a range of Anaerobic Digestion engineered systems enabled the reconstruction of 5400 MAGs clustered into 1′600 different species with 837 of them identified as high quality according to MIMAG guidelines. This repertoire is available in the database http://microbial-genomes.org/projects/biogasmicrobiome. From this dataset only 836 MAGs, identified as "high quality" regarding their genome completeness and contamination according to MIMAG guidelines (Bowers et al., 2017), have been considered for genome-scale metabolic model (GSMMs) reconstruction.

A comparison of single and two-stage AD setups was used from an earlier publication (Fontana et al., 2018) included in the dataset mentioned above. The single stage reactor characterizes a complete AD process fed with a mixed substrate of cheese whey and residues from cheese processing. On the other hand, the second system was composed of two reactors: the first reactor was fed as in the single-stage setup and used for the acidogenic step of AD, while its effluent was fed to the second reactor where methanogenesis took place. Both reactor systems had an operating temperature of 55±1 °C and were run without and with H_2 injection (period I and II, respectively), in order to evaluate whether the injection of H_2 modified the methane yield. For the present analysis, only the microbial communities from the methanogenic step of the single reactor and from the acidogenic step of the two-stage reactor setup were considered. The communities taken into account consisted of species having relative abundances higher than 0.01% in at least one of the four conditions analysed (acidogenic of the two stage and methanogenic steps of the single stage setup, with and without H_2 injection), following (Fontana et al., 2018).

4.2. Genome-scale metabolic reconstruction and modelling of the anaerobic digestion community

A tutorial was realized specifically for the replication of the analysis described in the present study (https://github.com/arianccbasile/ADinteractions).

Starting from quality-filtered MAGs, the genome scale metabolic models (GSMMs) for the corresponding species were created with CarveMe v. 1.2.1 (Machado et al., 2018) using for each microbe the most appropriate universe (grampos, gramneg or archaea) according to its taxonomy and the default gene matching parameters. The typical top-down reconstruction approach implemented in CarveMe generated models with standardized molecular weight of the biomass product. This is crucial, because without proper normalization, hidden biases in biomass molecular weight can generate significant simulation discrepancies (Siu H.J. Chan et al., 2017).

The solver used for GSMM reconstruction is Cplex (v. 12.8.0.0) (IBM, 2019). Sanity checks were performed on all the metabolic models, testing twelve basic properties through the COBRA toolbox (Brunk et al., 2018; Heirendt et al., 2019). Moreover, the consistency of all models was systematically assessed through the standardized MEMOTE test suite (Lieven et al., 2020). Since AGORA (assembly of gut organisms through reconstruction and analysis) models represent a golden standard in the field of large-scale metabolic reconstructions, the analysis has been performed both on our models and on AGORA models (Magnúsdóttir et al., 2017) to inspect the main differences. To test the soundness of the models, the presence and completeness of their pathways associated to carbohydrate and lipid metabolism have been verified by considering the cross references in the microbial models and tracking the presence of specific reactions. Completeness of the KEGG modules was assessed for those belonging to carbohydrate and lipid metabolism. For the inspection of methanogenesis and the Wood–Ljungdahl pathway (syntrophic acetate oxidation and/or acetogenesis), a manual validation of all the reactions was performed, taking into account relevant information derived from literature for the known species. Composition of the media has been obtained from the nutrition resource of the Virtual Metabolic Human database considering the following food entries: "Whey, acid, fluid", "Whey, acid, dried", "Whey, sweet, fluid", "Whey, sweet, dried". The corresponding exchange reactions have been refined through a manual work based on the experimental data previously reported (Fontana et al., 2018). The media composition is thoroughly described in the dedicated github. The medium composition was integrated in the model as nutrient constraints modifying accordingly the upper and lower bounds of export reactions through an in-house developed function ("apply_diet" in the github).

4.3. Modelling of biological and metabolic interactions

The analysis of the interactions among the different microbes was inferred using FBA. For the current analysis Python and the COBRApy library (v. 0.17.1) (Ebrahim et al., 2013) were used. In order to use the metabolic models generated with CarveMe (v. 1.2.1), and to use the code with multiple processors the original MMinte (v. 1.0.3) (Mendes-Soares et al., 2016) code was adapted and reported in github as PA. IN. The generation of the communities follows the approach used in MMinte for the creation of multi-species stoichiometric models. This approach introduces a fictitious compartment that represents the

extracellular environment shared by both species, and adds reactions allowing metabolites that are imported or secreted by each individual species to be transformed into community metabolites. Singular growth outcomes were computed by maximizing for total biomass production, setting the maximal community growth as the objective function assuming that even for parasitic or competitive microbes the best outcome is the maximal growth of the couple. The growth rates for each species under defined nutrient conditions is estimated in isolation and in the presence of another species, by running FBA in COBRApy. The algorithm simultaneously maximizes for the biomass objective function of both GSMMs for the estimation of the growth rate of each species when coexisting with the other. The algorithm then knocks out all reactions of one species whilst maximizing the biomass objective function of the other to simulate the growth rate of each species individually. In this step the solver used is Glpk (Oki, 2012). A difference in the growth rate of ±10% or more for at least a pair member, compared with the growth rate of the microbes grown separately, was considered significant to define the presence of an interaction. By comparing the growth rate of each microbe when coupled with another, it was possible to distinguish six different types of interaction: parasitism, commensalism, neutralism, amensalism, competition and mutualism. If at least one of the two species was negatively affected by the interaction, the interplay was classified as negative, otherwise as positive. In some of these scenarios (namely Parasitism, Commensalism and Amensalism) each of the two species was classified either as a "giver" or a "taker", depending on the impact of the pairing on their growth.

Interactions among the dominant members of the biosphere were verified using the cooperative tradeoff algorithm of Micom (v.0.10.1) (Diener et al., 2020), an approach mimicking the strategy implemented in OptCom (Zomorrodi and Maranas, 2012). By using this algorithm the individual growth is simultaneously at its maximum rate without diminishing the growth rate of other individuals (thus the term "cooperative"). Analysis of the metabolic exchanges among the different microbes has also been performed using MICOM integrating in the community model the microbial abundance as well and modifying the boundaries of the models according to the medium with an in-house developed script ("apply_diet" in the dedicated github). For each microbial pair, metabolite exchange rates were estimated through parsimonious FBA (Lewis et al., 2010) by setting the community biomass accumulation as objective. In this step, the solver used was Gurobi (v. 8) (Inc, 2014). Results were converted in tabular format and used to generate inputs file for Cytoscape software (3.2.1) (Demchak et al., 2014). Graphical representation of metabolic exchanges was performed with Cytoscape to simplify the interpretation of MICOM results.

Metatranscriptomic data of twelve samples obtained from Fontana et al. (2018) were added to the simulation. Details of RNA extraction and standard raw RNA-seq data processing have been previously reported (Fontana et al., 2018). Gene expression analysis was performed using as reference the MAGs previously identified (Campanaro et al., 2020). Gene finding was performed using Prodigal (v2.6.2) (Hyatt et al., 2010) and reported in a previous study (Campanaro et al., 2020). RNA-seq reads were aligned on reference metagenome assembly using bowtie 2 (v2.2.4) (Langmead and Salzberg, 2012) and the number of reads mapped per each gene was determined from the "bam" file using SeqMonk (v1.45.4) (Anders et al., 2015) using the options "opposing strand specific" and "apply transcript length correction". The metatranscriptomic data were implemented in the metabolic models as constraints readapting the code of METRADE (Angione and Lió, 2015) to the multispecies pairwise communities. Metabolic exchanges obtained starting from models with inner constraints derived from metatranscriptomic data were analysed as before. Metabolic models were deposited in the public repository figshare (10.6084/m9. figshare.12, 661,496. v1).

Finally, we compared our results on metabolic exchanges obtained by Micom with those obtained through SteadyCom, a different approach for metabolic community modelling (Siu Hung Joshua Chan et al., 2017). In the SteadyCom simulations, the medium was integrated as microaerophilic, setting the aggregate oxygen uptake bound to 0.1 mmol/h, upon finding that a completely anaerobic environment prevents most species from growing in isolation.

4.4. Statistical analyses

All the statistical analyses were carried out with R software v.3.5.2 (Breuer, 2017). The χ^2 test of Independence to characterise bacterial interactions across species was accomplished with chisq. test in the package stats. Pearson's residuals were obtained from the same function. Hierarchical clustering was applied via the ComplexHeatmap package (Gu et al., 2016), employing a squared Euclidean distance of the values between the 10th and the 90th percentile, thereby eliminating the influence of the outliers (Appendix, Supplementary Methods, robust_dist). To verify the different interactivity profile of abundant and rare community members, a permutation test was carried out through the R base "sample" function, generating 2000 random permutations (Appendix, Supplementary Methods, casual_campioning).

Declaration of competing interest

The authors declare that they have no known competing financial interests or personal relationships that could have appeared to influence the work reported in this paper.

Acknowledgements

This work was financially supported by the "Budget Integrato della Ricerca Dipartimentale" (BIRD198423) PRID 2019 of the Department of Biology of the University of Padua, entitled "SyMMoBio: inspection of Syntrophies with Metabolic Modelling to optimize Biogas Production". The PhD fellowship of AB is supported by "Progetto di Eccellenza DiBio" of University of Padua. Authors want to thank Emiliano Ciuffa for his significant contribution on linguistic revision of the manuscript and Daniel Machado for the important suggestions provided during the revision process. A final acknowledge to the Italian Consortium for Biotechnologies (CIB) for the support.

Appendix A. Supplementary data

Supplementary data to this article can be found online at https://doi.org/10.1016/j.ymben.2020.08.013.

References

Ahring, B.K., Sandberg, M., Angelidaki, I., 1995. Volatile fatty acids as indicators of process imbalance in anaerobic digestors. Appl. Microbiol. Biotechnol. 43, 559–565. https://doi.org/10.1007/BF00218466.

Anders, S., Pyl, P.T., Huber, W., 2015. HTSeq-A Python framework to work with high-throughput sequencing data. Bioinformatics 31, 166–169. https://doi.org/10.1093/bioinformatics/btu638.

Angelidaki, I., Treu, L., Tsapekos, P., Luo, G., Campanaro, S., Wenzel, H., Kougias, P.G., 2018. Biogas upgrading and utilization: current status and perspectives. Biotechnol. Adv. 36 (2), 452–466. https://doi.org/10.1016/j.biotechadv.2018.01.011.

Angione, C., Lió, P., 2015. Predictive analytics of environmental adaptability in multi-omic network models. Sci. Rep. 5 https://doi.org/10.1038/srep15147.

Bonachela, J.A., Wortel, M.T., Stenseth, N.C., 2017. Eco-evolutionary Red Queen dynamics regulate biodiversity in a metabolite-driven microbial system. Sci. Rep. 7 https://doi.org/10.1038/s41598-017-17774-4.

Boon, E., Meehan, C.J., Whidden, C., Wong, D.H.J., Langille, M.G.I., Beiko, R.G., 2014. Interactions in the microbiome: communities of organisms and communities of genes. FEMS Microbiol. Rev. 38 (1), 90–118. https://doi.org/10.1111/1574-6976.12035.

Bowers, R.M., Kyrpides, N.C., Stepanauskas, R., Harmon-Smith, M., Doud, D., Reddy, T. B.K., Schulz, F., Jarett, J., Rivers, A.R., Eloe-Fadrosh, E.A., Tringe, S.G., Ivanova, N. N., Copeland, A., Clum, A., Becraft, E.D., Malmstrom, R.R., Birren, B., Podar, M., Bork, P., Weinstock, G.M., Garrity, G.M., Dodsworth, J.A., Yooseph, S., Sutton, G., Glöckner, F.O., Gilbert, J.A., Nelson, W.C., Hallam, S.J., Jungbluth, S.P., Ettema, T.J. G., Tighe, S., Konstantinidis, K.T., Liu, W.T., Baker, B.J., Rattei, T., Eisen, J.A., Hedlund, B., McMahon, K.D., Fierer, N., Knight, R., Finn, R., Cochrane, G., Karsch-Mizrachi, I., Tyson, G.W., Rinke, C., Lapidus, A., Meyer, F., Yilmaz, P., Parks, D.H.,

Eren, A.M., Schriml, L., Banfield, J.F., Hugenholtz, P., Woyke, T., 2017. Minimum information about a single amplified genome (MISAG) and a metagenome-assembled genome (MIMAG) of bacteria and archaea. Nat. Biotechnol. 35 (8), 725–731. https://doi.org/10.1038/nbt.3893.

Breuer, J., 2017. R (software). The International Encyclopedia of Communication Research Methods, pp. 1–2. https://doi.org/10.1002/9781118901731.iecrm0201.

Brunk, E., Sahoo, S., Zielinski, D.C., Altunkaya, A., Dräger, A., Mih, N., Gatto, F., Nilsson, A., Preciat Gonzalez, G.A., Aurich, M.K., Prlic, A., Sastry, A., Danielsdottir, A.D., Heinken, A., Noronha, A., Rose, P.W., Burley, S.K., Fleming, R.M. T., Nielsen, J., Thiele, I., Palsson, B.O., 2018. Recon3D enables a three-dimensional view of gene variation in human metabolism. Nat. Biotechnol. 36, 272–281. https://doi.org/10.1038/nbt.4072.

Budinich, M., Bourdon, J., Larhlimi, A., Eveillard, D., 2017. A multi-objective constraint-based approach for modeling genome-scale microbial ecosystems. PloS One 12. https://doi.org/10.1371/journal.pone.0171744.

Campanaro, S., Treu, L., Kougias, P.G., De Francisci, D., Valle, G., Angelidaki, I., 2016. Metagenomic analysis and functional characterization of the biogas microbiome using high throughput shotgun sequencing and a novel binning strategy. Biotechnol. Biofuels 9. https://doi.org/10.1186/s13068-016-0441-1.

Campanaro, S., Treu, L., Kougias, P.G., Luo, G., Angelidaki, I., 2018. Metagenomic binning reveals the functional roles of core abundant microorganisms in twelve full-scale biogas plants. Water Res. 140, 123–134. https://doi.org/10.1016/j.watres.2018.04.043.

Campanaro, S., Treu, L., Rodriguez-R, L.M., Kovalovszki, A., Ziels, R.M., Maus, I., Zhu, X., Kougias, P.G., Basile, A., Luo, G., Schlüter, A., Konstantinidis, K.T., Angelidaki, I., 2020. New insights from the biogas microbiome by comprehensive genome-resolved metagenomics of nearly 1600 species originating from multiple anaerobic digesters. Biotechnol. Biofuels 13 (1). https://doi.org/10.1186/s13068-020-01679-y.

Chaffron, S., Rehrauer, H., Pernthaler, J., Von Mering, C., 2010. A global network of coexisting microbes from environmental and whole-genome sequence data. Genome Res. 20, 947–959. https://doi.org/10.1101/gr.104521.109.

Chan, Siu H.J., Cai, J., Wang, L., Simons-Senftle, M.N., Maranas, C.D., 2017. Standardizing biomass reactions and ensuring complete mass balance in genome-scale metabolic models. Bioinformatics 33, 3603–3609. https://doi.org/10.1093/bioinformatics/btx453.

Chan, Siu Hung Joshua, Simons, M.N., Maranas, C.D., 2017. SteadyCom: predicting microbial abundances while ensuring community stability. PLoS Comput. Biol. 13 https://doi.org/10.1371/journal.pcbi.1005539.

Chow, D., Nunalee, M.L., Lim, D.W., Simnick, A.J., Chilkoti, A., 2008. Peptide-based biopolymers in biomedicine and biotechnology. Mater. Sci. Eng. R Rep. 62 (4), 125–155. https://doi.org/10.1016/j.mser.2008.04.004.

Clemente, J.C., Ursell, L.K., Parfrey, L.W., Knight, R., 2012. The Impact of the Gut Microbiota on Human Health: an Integrative View. Cell. https://doi.org/10.1016/j.cell.2012.01.035.

Dailey, H.A., Gerdes, S., Dailey, T.A., Burch, J.S., Phillips, J.D., 2015. Noncanonical coproporphyrin-dependent bacterial heme biosynthesis pathway that does not use protoporphyrin. Proc. Natl. Acad. Sci. U.S.A. 112, 2210–2215. https://doi.org/10.1073/pnas.1416285112.

Demchak, B., Hull, T., Reich, M., Liefeld, T., Smoot, M., Ideker, T., Mesirov, J.P., 2014. Cytoscape: the Network Visualization Tool for GenomeSpace Workflows, vol. 3. https://doi.org/10.12688/f1000research.4492.1. F1000Research.

Diener, C., Gibbons, S.M., Resendis-Antonio, O., 2020. MICOM: Metagenome-Scale Modeling to Infer Metabolic Interactions in the Gut Microbiota. mSystems vol. 5. https://doi.org/10.1128/msystems.00606-19.

Ebrahim, A., Lerman, J.A., Palsson, B.O., Hyduke, D.R., 2013. COBRApy: COnstraints-based reconstruction and analysis for Python. BMC Syst. Biol. 7 https://doi.org/10.1186/1752-0509-7-74.

Faith, J.J., 2015. Bridging the knowledge gap: from microbiome composition to function. Mol. Syst. Biol. 11, 793. https://doi.org/10.15252/msb.20156045.

Fontana, A., Kougias, P.G., Treu, L., Kovalovszki, A., Valle, G., Cappa, F., Morelli, L., Angelidaki, I., Campanaro, S., 2018. Microbial activity response to hydrogen injection in thermophilic anaerobic digesters revealed by genome-centric metatranscriptomics. Microbiome 6. https://doi.org/10.1186/s40168-018-0583-4.

Gu, Z., Eils, R., Schlesner, M., 2016. Complex heatmaps reveal patterns and correlations in multidimensional genomic data. Bioinformatics 32, 2847–2849. https://doi.org/10.1093/bioinformatics/btw313.

Hall, D.O., Scrase, J.I., 1998. Will biomass be the environmentally friendly fuel of the future? Biomass and Bioenergy, pp. 357–367. https://doi.org/10.1016/S0961-9534(98)00030-0.

Hay, M.E., Parker, J.D., Burkepile, D.E., Caudill, C.C., Wilson, A.E., Hallinan, Z.P., Chequer, A.D., 2004. Mutualisms and aquatic community structure: the enemy of my enemy is my friend. Annu. Rev. Ecol. Evol. Syst. 35, 175–197. https://doi.org/10.1146/annurev.ecolsys.34.011802.132357.

Heinken, A., Thiele, I., 2015. Anoxic conditions promote species-specific mutualism between gut microbes in Silico. Appl. Environ. Microbiol. 81, 4049–4061. https://doi.org/10.1128/AEM.00101-15.

Heirendt, L., Arreckx, S., Pfau, T., Mendoza, S.N., Richelle, A., Heinken, A., Haraldsdóttir, H.S., Wachowiak, J., Keating, S.M., Vlasov, V., Magnusdóttir, S., Ng, C.Y., Preciat, G., Žagare, A., Chan, S.H.J., Aurich, M.K., Clancy, C.M., Modamio, J., Sauls, J.T., Noronha, A., Bordbar, A., Cousins, B., El Assal, D.C., Valcarcel, L.V., Apaolaza, I., Ghaderi, S., Ahookhosh, M., Ben Guebila, M., Kostromins, A., Sompairac, N., Le, H.M., Ma, D., Sun, Y., Wang, L., Yurkovich, J.T., Oliveira, M.A.P., Vuong, P.T., El Assal, L.P., Kuperstein, I., Zinovyev, A., Hinton, H. S., Bryant, W.A., Aragón Artacho, F.J., Planes, F.J., Stalidzans, E., Maass, A., Vempala, S., Hucka, M., Saunders, M.A., Maranas, C.D., Lewis, N.E., Sauter, T., Palsson, B., Thiele, I., Fleming, R.M.T., 2019. Creation and analysis of biochemical constraint-based models using the COBRA Toolbox v.3.0. Nat. Protoc. 14 (3), 639–702. https://doi.org/10.1038/s41596-018-0098-2.

Hyatt, D., Chen, G.L., LoCascio, P.F., Land, M.L., Larimer, F.W., Hauser, L.J., 2010. Prodigal: prokaryotic gene recognition and translation initiation site identification. BMC Bioinf. 11 https://doi.org/10.1186/1471-2105-11-119.

IBM, 2019. CPLEX optimizer [WWW document]. Ibm. URL. https://www.ibm.com/dk-da/analytics/cplex-optimizer.

Inc, G.O., 2014. Gurobi Optimizer Reference Manual, vol. 6, p. 572. Www.Gurobi.com.

Jacobi, H.F., Moschner, C.R., Hartung, E., 2009. Use of near infrared spectroscopy in monitoring of volatile fatty acids in anaerobic digestion. Water Sci. Technol. 60, 339–346. https://doi.org/10.2166/wst.2009.345.

Jing, Y., Campanaro, S., Kougias, P., Treu, L., Angelidaki, I., Zhang, S., Luo, G., 2017. Anaerobic granular sludge for simultaneous biomethanation of synthetic wastewater and CO with focus on the identification of CO-converting microorganisms. Water Res. 126, 19–28. https://doi.org/10.1016/j.watres.2017.09.018.

Jousset, A., Bienhold, C., Chatzinotas, A., Gallien, L., Gobet, A., Kurm, V., Küsel, K., Rillig, M.C., Rivett, D.W., Salles, J.F., Van Der Heijden, M.G.A., Youssef, N.H., Zhang, X., Wei, Z., Hol, G.W.H., 2017. Where less may be more: how the rare biosphere pulls ecosystems strings. ISME J. 11 (4), 853–862. https://doi.org/10.1038/ismej.2016.174.

Kanehisa, M., Sato, Y., Kawashima, M., Furumichi, M., Tanabe, M., 2016. KEGG as a reference resource for gene and protein annotation. Nucleic Acids Res. 44, D457–D462. https://doi.org/10.1093/nar/gkv1070.

Keseler, I.M., Mackie, A., Santos-Zavaleta, A., Billington, R., Bonavides-Martínez, C., Caspi, R., Fulcher, C., Gama-Castro, S., Kothari, A., Krummenacker, M., Latendresse, M., Muñiz-Rascado, L., Ong, Q., Paley, S., Peralta-Gil, M., Subhraveti, P., Velázquez-Ramírez, D.A., Weaver, D., Collado-Vides, J., Paulsen, I., Karp, P.D., 2017. The EcoCyc database: reflecting new knowledge about Escherichia coli K-12. Nucleic Acids Res. 45, D543–D550. https://doi.org/10.1093/nar/gkw1003.

Khandelwal, R.A., Olivier, B.G., Röling, W.F.M., Teusink, B., Bruggeman, F.J., 2013. Community flux balance analysis for microbial consortia at balanced growth. PloS One 8 (5). https://doi.org/10.1371/journal.pone.0064567.

Kitano, H., 2007. Towards a theory of biological robustness. Mol. Syst. Biol. 3 https://doi.org/10.1038/msb4100179.

Koch, S., Kohrs, F., Lahmann, P., Bissinger, T., Wendschuh, S., Benndorf, D., Reichl, U., Klamt, S., 2019. Redcom: a strategy for reduced metabolic modeling of complex microbial communities and its application for analyzing experimental datasets from anaerobic digestion. PLoS Comput. Biol. 15 https://doi.org/10.1371/journal.pcbi.1006759.

Langmead, B., Salzberg, S.L., 2012. Fast gapped-read alignment with Bowtie 2. Nat. Methods 9, 357–359. https://doi.org/10.1038/nmeth.1923.

Lebuhn, M., Weiß, S., Munk, B., Guebitz, G.M., 2015. Microbiology and molecular biology tools for biogas process analysis, diagnosis and control. Adv. Biochem. Eng. Biotechnol. 151 https://doi.org/10.1007/978-3-319-21993-6_1.

Lewis, N.E., Hixson, K.K., Conrad, T.M., Lerman, J.A., Charusanti, P., Polpitiya, A.D., Adkins, J.N., Schramm, G., Purvine, S.O., Lopez-Ferrer, D., Weitz, K.K., Eils, R., König, R., Smith, R.D., Palsson, B., 2010. Omic data from evolved E. coli are consistent with computed optimal growth from genome-scale models. Mol. Syst. Biol. 6 https://doi.org/10.1038/msb.2010.47.

Liao, J.C., Mi, L., Pontrelli, S., Luo, S., 2016. Fuelling the future: microbial engineering for the production of sustainable biofuels. Nat. Rev. Microbiol. 14 (5), 288–304. https://doi.org/10.1038/nrmicro.2016.32.

Liebetrau, J., Sträuber, H., Kretzschmar, J., Denysenko, V., Nelles, M., 2019. Anaerobic digestion. Advances in Biochemical Engineering/Biotechnology, pp. 281–299. https://doi.org/10.1007/10_2016_67.

Lieven, C., Beber, M.E., Olivier, B.G., Bergmann, F.T., Ataman, M., Babaei, P., Bartell, J. A., Blank, L.M., Chauhan, S., Correia, K., Diener, C., Dräger, A., Ebert, B.E., Edirisinghe, J.N., Faria, J.P., Feist, A.M., Fengos, G., Fleming, R.M.T., García-Jiménez, B., Hatzimanikatis, V., van Helvoirt, W., Henry, C.S., Hermjakob, H., Herrgård, M.J., Kaafarani, A., Kim, H.U., King, Z., Klamt, S., Klipp, E., Koehorst, J.J., König, M., Lakshmanan, M., Lee, D.Y., Lee, S.Y., Lee, S., Lewis, N.E., Liu, F., Ma, H., Machado, D., Mahadevan, R., Maia, P., Mardinoglu, A., Medlock, G.L., Monk, J.M., Nielsen, J., Nielsen, L.K., Nogales, J., Nookaew, I., Palsson, B.O., Papin, J.A., Patil, K. R., Poolman, M., Price, N.D., Resendis-Antonio, O., Richelle, A., Rocha, I., Sánchez, B.J., Schaap, P.J., Malik Sheriff, R.S., Shoaie, S., Sonnenschein, N., Teusink, B., Vilaça, P., Vik, J.O., Wodke, J.A.H., Xavier, J.C., Yuan, Q., Zakhartsev, M., Zhang, C., 2020. MEMOTE for standardized genome-scale metabolic model testing. Nat. Biotechnol. 38, 272–276. https://doi.org/10.1038/s41587-020-0446-y.

Machado, D., Andrejev, S., Tramontano, M., Patil, K.R., 2018. Fast automated reconstruction of genome-scale metabolic models for microbial species and communities. Nucleic Acids Res. 46, 7542–7553. https://doi.org/10.1093/nar/gky537.

Machado, D., Maistrenko, O.M., Andrejev, S., Kim, Y., Bork, P., Patil, Kaustubh R., Patil, Kiran R., 2020. Polarization of Microbial Communities between Competitive and Cooperative Metabolism. bioRxiv. https://doi.org/10.1101/2020.01.28.922583, 2020 01.28.922583.

Magnúsdóttir, S., Heinken, A., Kutt, L., Ravcheev, D.A., Bauer, E., Noronha, A., Greenhalgh, K., Jäger, C., Baginska, J., Wilmes, P., Fleming, R.M.T., Thiele, I., 2017. Generation of genome-scale metabolic reconstructions for 773 members of the human gut microbiota. Nat. Biotechnol. 35, 81–89. https://doi.org/10.1038/nbt.3703.

Mas, A., Jamshidi, S., Lagadeuc, Y., Eveillard, D., Vandenkoornhuyse, P., 2016. Beyond the black queen hypothesis. ISME J. 10 (9), 2085–2091. https://doi.org/10.1038/ismej.2016.22.

Maus, I., Cibis, K.G., Bremges, A., Stolze, Y., Wibberg, D., Tomazetto, G., Blom, J., Sczyrba, A., König, H., Pühler, A., Schlüter, A., 2016. Genomic characterization of Defluviitoga tunisiensis L3, a key hydrolytic bacterium in a thermophilic biogas plant and its abundance as determined by metagenome fragment recruitment. J. Biotechnol. 232, 50–60. https://doi.org/10.1016/j.jbiotec.2016.05.001.

Mendes-Soares, H., Mundy, M., Soares, L.M., Chia, N., 2016. MMinte: an application for predicting metabolic interactions among the microbial species in a community. BMC Bioinf. 17 https://doi.org/10.1186/s12859-016-1230-3.

Moat, A.G., Foster, J.W., Spector, M.P., 2002. Microbial physiology, microbial physiology. https://doi.org/10.1002/0471223867.

Molina, F., Ruiz-Filippi, G., Garcia, C., Lema, J.M., Roca, E., 2009. Pilot-scale validation of a new sensor for on-line analysis of volatile fatty acids and alkalinity in anaerobic wastewater treatment plants. Environ. Eng. Sci. 26, 641–649. https://doi.org/10.1089/ees.2007.0308.

Mosbæk, F., Kjeldal, H., Mulat, D.G., Albertsen, M., Ward, A.J., Feilberg, A., Nielsen, J.L., 2016. Identification of syntrophic acetate-oxidizing bacteria in anaerobic digesters by combined protein-based stable isotope probing and metagenomics. ISME J. 10, 2405–2418. https://doi.org/10.1038/ismej.2016.39.

Muller, E.E.L., Faust, K., Widder, S., Herold, M., Martínez Arbas, S., Wilmes, P., 2018. Using metabolic networks to resolve ecological properties of microbiomes. Curr. Opin. Struct. Biol. 8, 73–80. https://doi.org/10.1016/j.coisb.2017.12.004.

Nayfach, S., Shi, Z.J., Seshadri, R., Pollard, K.S., Kyrpides, N.C., 2019. New insights from uncultivated genomes of the global human gut microbiome. Nature 568, 505–510. https://doi.org/10.1038/s41586-019-1058-x.

Niehaus, L., Boland, I., Liu, M., Chen, K., Fu, D., Henckel, C., Chaung, K., Miranda, S.E., Dyckman, S., Crum, M., Dedrick, S., Shou, W., Momeni, B., 2019. Microbial coexistence through chemical-mediated interactions. Nat. Commun. 10 https://doi.org/10.1038/s41467-019-10062-x.

Noronha, A., Modamio, J., Jarosz, Y., Guerard, E., Sompairac, N., Preciat, G., Daníelsdóttir, A.D., Krecke, M., Merten, D., Haraldsdóttir, H.S., Heinken, A., Heirendt, L., Magnúsdóttir, S., Ravcheev, D.A., Sahoo, S., Gawron, P., Friscioni, L., Garcia, B., Prendergast, M., Puente, A., Rodrigues, M., Roy, A., Rouquaya, M., Wiltgen, L., Žagare, A., John, E., Krueger, M., Kuperstein, I., Zinovyev, A., Schneider, R., Fleming, R.M.T., Thiele, I., 2019. The Virtual Metabolic Human database: integrating human and gut microbiome metabolism with nutrition and disease. Nucleic Acids Res. 47, D614–D624. https://doi.org/10.1093/nar/gky992.

Nugent, P., Giannopoulou, E.G., Burd, S.D., Elemento, O., Giannopoulou, E.G., Forrest, K., Pham, T., Ma, S., Space, B., Wojtas, L., Eddaoudi, M., Zaworotko, M.J., 2013. Porous materials with optimal adsorption thermodynamics and kinetics for co2 separation. Nature 495, 80–84. https://doi.org/10.1038/nature11893.

Oki, E., 2012. GLPK (GNU linear programming kit). Linear Programming and Algorithms for Communication Networks, pp. 25–29. https://doi.org/10.1201/b12733-4.

Parks, D.H., Rinke, C., Chuvochina, M., Chaumeil, P.A., Woodcroft, B.J., Evans, P.N., Hugenholtz, P., Tyson, G.W., 2017. Recovery of nearly 8,000 metagenome-assembled genomes substantially expands the tree of life. Nat. Microbiol. 2, 1533–1542. https://doi.org/10.1038/s41564-017-0012-7.

Raspor, P., Goranovič, D., 2008. Biotechnological applications of acetic acid bacteria. Crit. Rev. Biotechnol. 28 (2), 101–124. https://doi.org/10.1080/07388550802046749.

Shlomi, T., Eisenberg, Y., Sharan, R., Ruppin, E., 2007. A genome-scale computational study of the interplay between transcriptional regulation and metabolism. Mol. Syst. Biol. 3 https://doi.org/10.1038/msb4100141.

Sorokin, DiY., Makarova, K.S., Abbas, B., Ferrer, M., Golyshin, P.N., Galinski, E.A., Ciordia, S., Mena, M.C., Merkel, A.Y., Wolf, Y.I., Van Loosdrecht, M.C.M., Koonin, E. V., 2017. Discovery of extremely halophilic, methyl-reducing euryarchaea provides insights into the evolutionary origin of methanogenesis. Nat. Microbiol. 2 https://doi.org/10.1038/nmicrobiol.2017.81.

Stams, A.J.M., 1994. Metabolic interactions between anaerobic bacteria in methanogenic environments. Antonie Leeuwenhoek 66, 271–294. https://doi.org/10.1007/BF00871644.

Stams, A.J.M., Plugge, C.M., 2009. Electron transfer in syntrophic communities of anaerobic bacteria and archaea. Nat. Rev. Microbiol. 7 (8), 568–577. https://doi.org/10.1038/nrmicro2166.

Stolyar, S., Van Dien, S., Hillesland, K.L., Pinel, N., Lie, T.J., Leigh, J.A., Stahl, D.A., 2007. Metabolic modeling of a mutualistic microbial community. Mol. Syst. Biol. 3, 1–14. https://doi.org/10.1038/msb4100131.

Stryer, L., 1995. Stryer Biochemistry, Biochemistry Textbook.

Thommes, M., Wang, T., Zhao, Q., Paschalidis, I.C., Segrè, D., 2019. Designing metabolic division of labor in microbial communities. mSystems 4. https://doi.org/10.1128/msystems.00263-18.

Treu, L., Campanaro, S., Kougias, P.G., Sartori, C., Bassani, I., Angelidaki, I., 2018. Hydrogen-fueled microbial pathways in biogas upgrading systems revealed by genome-centric metagenomics. Front. Microbiol. 9 https://doi.org/10.3389/fmicb.2018.01079.

Treu, L., Tsapekos, P., Peprah, M., Campanaro, S., Giacomini, A., Corich, V., Kougias, P. G., Angelidaki, I., 2019. Microbial profiling during anaerobic digestion of cheese whey in reactors operated at different conditions. Bioresour. Technol. 275, 375–385. https://doi.org/10.1016/j.biortech.2018.12.084.

Weinrich, S., Koch, S., Bonk, F., Popp, D., Benndorf, D., Klamt, S., Centler, F., 2019. Augmenting biogas process modeling by resolving intracellular metabolic activity. Front. Microbiol. 10 https://doi.org/10.3389/fmicb.2019.01095.

Westerholm, M., Dolfing, J., Schnürer, A., 2019. Growth characteristics and thermodynamics of syntrophic acetate oxidizers. Environ. Sci. Technol. 53, 5512–5520. https://doi.org/10.1021/acs.est.9b00288.

Yentekakis, I.V., Goula, G., 2017. Biogas management: advanced utilization for production of renewable energy and added-value chemicals. Front. Environ. Sci. 5 (FEB) https://doi.org/10.3389/fenvs.2017.00007.

Zacher, B., Lidschreiber, M., Cramer, P., Gagneur, J., Tresch, A., 2014. Annotation of genomics data using bidirectional hidden Markov models unveils variations in Pol II transcription cycle. Mol. Syst. Biol. 10, 768. https://doi.org/10.15252/msb.20145654.

Zhu, X., Campanaro, S., Treu, L., Kougias, P.G., Angelidaki, I., 2019. Novel ecological insights and functional roles during anaerobic digestion of saccharides unveiled by genome-centric metagenomics. Water Res. 151, 271–279. https://doi.org/10.1016/j.watres.2018.12.041.

Zhu, X., Campanaro, S., Treu, L., Seshadri, R., Ivanova, N., Kougias, P.G., Kyrpides, N., Angelidaki, I., 2020. Metabolic dependencies govern microbial syntrophies during methanogenesis in an anaerobic digestion ecosystem. Microbiome 8. https://doi.org/10.1186/s40168-019-0780-9.

Zomorrodi, A.R., Maranas, C.D., 2012. OptCom: a multi-level optimization framework for the metabolic modeling and analysis of microbial communities. PLoS Comput. Biol. 8 https://doi.org/10.1371/journal.pcbi.1002363.

Chapter 2

Insights into Ammonia Adaptation and Methanogenic Precursor Oxidation by Genome-Centric Analysis

Miao Yan[1], Laura Treu[2,*], Xinyu Zhu[1], Hailin Tian[1,3], **Arianna Basile**[2], Ioannis A. Fotidis[1], Stefano Campanaro[2,4,ψ], and Irini Angelidaki[1,ψ]

Environmental Science and Technology, Volume 54, August 2020, Pages 12568–12582
https://doi.org/10.1021/acs.est.0c01945

[1]Department of Environmental Engineering, Technical University of Denmark, Bygningstorvet Bygning 115, DK-2800 Kongens Lyngby, Denmark
[2]Department of Biology, University of Padova, Via U. Bassi 58/b, 35121 Padova, Italy
[3]NUS Environmental Research Institute, National University of Singapore, 1 Create Way, 138602, Singapore
[4]CRIBI Biotechnology Center, University of Padua, 35131 Padua, Italy

* Corresponding author
ψ Equal contribution

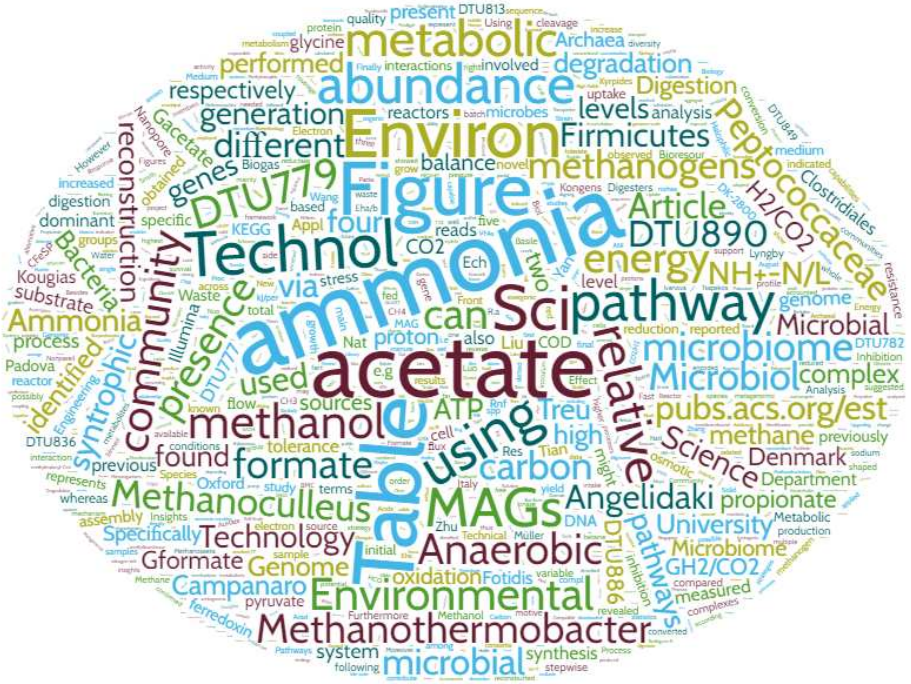

Environmental Science & Technology

pubs.acs.org/est

Article

Insights into Ammonia Adaptation and Methanogenic Precursor Oxidation by Genome-Centric Analysis

Miao Yan, Laura Treu,* Xinyu Zhu, Hailin Tian, Arianna Basile, Ioannis A. Fotidis, Stefano Campanaro,# and Irini Angelidaki#

Cite This: *Environ. Sci. Technol.* 2020, 54, 12568−12582

Read Online

ACCESS | Metrics & More | Article Recommendations | Supporting Information

ABSTRACT: Ammonia released from the degradation of protein and/or urea usually leads to suboptimal anaerobic digestion (AD) when N-rich organic waste is used. However, the insights behind the differential ammonia tolerance of anaerobic microbiomes remain an enigma. In this study, the cultivation in synthetic medium with different carbon sources (acetate, methanol, formate, and H_2/CO_2) shaped a common initial inoculum into four unique ammonia-tolerant syntrophic populations. Specifically, various levels of ammonia tolerance were observed: consortia fed with methanol and H_2/CO_2 could grow at ammonia levels up to 7.25 g NH^+-N/L, whereas the other two groups (formate and acetate) only thrived at 5.25 and 4.25 g NH^+-N/L, respectively. Metabolic reconstruction highlighted that this divergent microbiome might be achieved by complementary metabolisms to maximize biomethane recovery from carbon sources, thus indicating the importance of the syntrophic community in the AD of N-rich substrates. Besides, sodium/proton antiporter operon, osmoprotectant/K^+ regulator, and osmoprotectant synthesis operon may function as the main drivers of adaptation to the ammonia stress. Moreover, energy from the substrate-level phosphorylation and multiple energy-converting hydrogenases (*e.g.*, Ech and Eha) could aid methanogens to balance the energy request for anabolic activities and contribute to thriving when exposed to high ammonia levels.

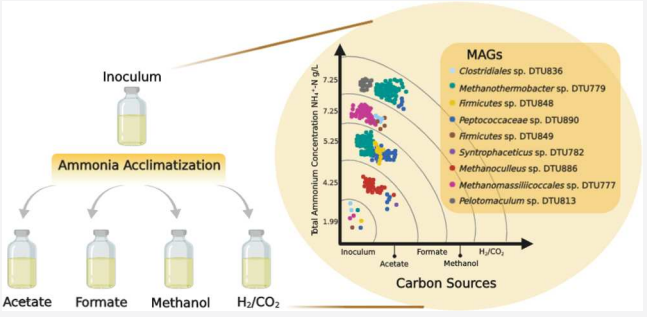

1. INTRODUCTION

The amount of nitrogen-rich organic waste generated worldwide is increasing significantly because of urbanization and population growth, which is becoming a major issue for the environment.[1] The application of anaerobic digestion (AD) can convert nitrogen-rich organic waste into a sustainable fuel.[2,3] However, free ammonia nitrogen (FAN) released from the degradation of protein or urea, once exceeding the threshold concentration, is a key parameter leading to low methane yield and process instability in AD.[4] Moreover, methanogens are more vulnerable to ammonia compared to the other AD microbes because of their weak cell wall structure lacking peptidoglycan.[5] FAN that permeates into cells can be converted to ammonium by protonation,[6] resulting in temporary proton imbalance, potassium deficiency, and strong osmotic stress.[7,8] Therefore, K^+ uptake is important for the microbial cells to overcome ammonia inhibition.[9,10] Meanwhile, the synthesis or transport of osmoprotectants such as glutamate, glutamine, phosphate, N^{ε}-acetyl-L-lysine, and glycine betaine has been reported to achieve osmotic balance and counteract ammonia inhibition.[10−12] These compatible solutes allow the survival at high osmolarity and the colonization of ecological niches in environmental conditions.[13,14] Therefore, more energy is needed for regulating the proton balance or potassium/osmoprotectant uptake during biosynthesis maintenance.[6,7] The electron-bifurcating flavoprotein complexes in *Bacteria* contribute to energy conservation through the energy-converting reductase complex (Rnf) or the energy-converting ferredoxin-dependent hydrogenase complex (Ech).[15] Specifically, Rnf catalyzes the reduction of NAD^+ with ferredoxin, thereby conserving the free-energy change in an electrochemical proton potential.[16] Likewise, HdrABC or Nuo present in methanogens is indicative of flavin-based electron bifurcation,[15] which contributes to obtaining energy from methanogenesis.[17] Additionally, Eha/b and Ech hydrogenases show high sequence similarity to the subunits of complex I, a protein pump, where they deposited NADH and reduced ferredoxin for the buildup of the proton motive force, suggesting an important role in adenosine triphosphate (ATP) synthesis.[18,19] Finally, the energy compensation to maintain the cation- and

Received: March 28, 2020
Revised: August 22, 2020
Accepted: August 27, 2020
Published: August 27, 2020

https://dx.doi.org/10.1021/acs.est.0c01945
Environ. Sci. Technol. 2020, 54, 12568−12582

Table 1. Standard Gibbs Free Energy of Relevant Reactions in the AD Process

reactions	$\Delta G^{\circ\prime}$ (kJ/reaction)	reference
4 methanol → $3CH_4 + CO_2 + 2H_2O$	−315	20
acetate → $CH_4 + HCO^- + H^+$	−36	21
4 formate + $H^+ + H_2O \rightarrow CH_4 + 3HCO^-$	−130.4	22
$4H_2 + HCO^- + H^+ \rightarrow CH + 3HO$	−135.6	22
acetate + $HCO^- + H^+ + 3H \rightarrow$ propionate + 3HO	−76.1	23
4 methanol + $2CO_2 \rightarrow$ 3 acetate + $3H^+ + 2H_2O$	−71	24

osmobalance against ammonia stress can be obtained from substrate-level phosphorylation (Table 1). The more exergonic the reaction is, the higher ammonia level they can possibly tolerate.

Different tolerance levels to the ammonia of AD microbiome have been previously observed; for example, anaerobic glucose degradation in batch reactors was inhibited by about 70% at 3.5 g NH^+-N/L concentration and at a pH of 8.0.[25] Yan *et al.* found that *Methanosaeta concilii* and *Methanosarcina soligelidi* were the dominant methanogens at low (less than 3 g NH^+-N/L) and high ammonia levels (5−9 g NH^+-N/L), respectively, when degrading municipal solid waste.[26] Further, high ammonia levels suppressed acetoclastic methanogenesis and enhanced the hydrogenotrophic pathway, as evidenced by the increase of the relative abundance of *Methanoculleus* spp. co-digesting cattle slurry and microalgae.[4] Westerholm *et al.* also discovered the strong impact of ammonia on the occurrence of syntrophic acetate-oxidizing bacteria and the increased abundance of hydrogenotrophic methanogens.[27] The last was generally proved to be more resistant to ammonia than acetoclastic methanogens in many cases.[28]

However, all methanogens mentioned above mainly grow on acetate and/or CO_2/H_2, whereas the capability of ammonia tolerance of other methanogens dependent on methanol and formate (two other important precursors of methanogenesis) was infrequently reported.[29] Obviously, the substrate, together with the concentrations of ammonia, could drive different complete and balanced microbiome formation, leading to variable capabilities of microbes to tolerate ammonia. Deciphering the metabolic pathway of ammonia-tolerant microbiome would improve our understanding of the dynamics and the molecular mechanisms determining stress resistance, which is necessary to unravel the black box of AD microbial ecology.

Until now, only part of the AD microbiome and its interactions have been uncovered because of the difficulty in exploring such complexity with traditional cultivation-based approaches and techniques (*e.g.*, 16S rRNA sequencing) because of the limited taxonomic assignment and the presence of unknown metabolisms. Metagenomics have been recently applied to analyze the known and novel physiological, metabolic, and genetic features.[16,30] So far, most AD metagenomic studies focus on communities shaped by real feedstocks such as manure, wastewater, industrial by-products, and municipal solid waste containing various carbon sources.[31,32] Accordingly, extremely diverse communities composed of thousands of metagenome-assembled genomes (MAGs) and complex metabolic activities adapted to mixed substrate degradation were found.[30,33,34] These findings raise the possibility that specific interactions of ammonia-tolerant microbial members fed with single and simple carbon sources (the common precursors, *i.e.*, acetate, formate, H_2-CO_2, and methanol) and their functionalities await discovery.

This study provides novel insights into ammonia-tolerant methanogenic communities grown using four different carbon sources in a synthetic basal anaerobic (BA) medium. Specifically, a common initial microbiome was simplified with a stepwise increase of ammonia levels and meanwhile by providing single chemically defined substrates as an energy source: acetate, formate, H_2-CO_2, and methanol, individually. Genome-centric metagenomics was applied to unravel the methanogenesis pathways occurring in the four trophic groups. Moreover, the first look into the metabolism of the four microbiomes shaped by specific carbon sources showed how metabolic interactions occur among microbes at high ammonia levels.

2. MATERIALS AND METHODS

2.1. Experimental Setup. The samples for microbial analysis were collected from four lab-scale methanogenic batch reactors with a 1.15 L total volume. The four reactors were initially inoculated with the same digestate obtained from a lab-scale continuous-stirring tank reactor fed with cattle manure at 55 °C. The total solids and volatile solids of the digestate were 30.51 ± 0.20 and 19.76 ± 1.30 g/kg, respectively. The feedstock used in each period was a BA medium[35] ($NaHCO_3$ was used as the buffer solution) supplemented with ammonia chloride and one of the four different carbon sources (acetate, methanol, formate, and H_2/CO_2), and thus the same buffering capacity was achieved (Table S1). Furthermore, the pH was maintained at the level of 8.00 ± 0.10 by NaOH solution (4 mol/L) adjustment throughout the whole acclimatization process (Table S1).

Several successive cultivations were performed under thermophilic conditions (55 ± 1 °C) in order to adapt the microbial community to the specific substrate and the increased ammonia levels. Specifically, once methane production reached 80% of its maximal theoretical yield during each generation, inocula samples were harvested to an increased ammonia level. The process was repeated in the four groups, and the ammonia level was increased stepwise by 1 g NH^+-N/L in each increment until the microbial community could not grow anymore. The specific experimental conditions for consortia cultivation and acclimatization are listed in Table S1.

Methane yields, volatile fatty acid (VFA) concentrations, and pH values in the reactor were recorded in order to evaluate the acclimatization process. The biogas production was analyzed by a gas chromatograph (Mikrolab, Aarhus A/S, Denmark), equipped with a thermal conductivity detector. VFA concentrations derived from the intermediate steps of degradation of the carbon source were measured using a gas chromatograph (Shimadzu GC-2010 AF, Kyoto, Japan), equipped with a flame ionization detector. Finally, the pH was measured by a PHM99 LAB pH meter (RadiometerTM).

2.2. DNA Extraction and Sequencing. According to the specific carbon source used, the metagenomic DNA was

https://dx.doi.org/10.1021/acs.est.0c01945
Environ. Sci. Technol. 2020, 54, 12568−12582

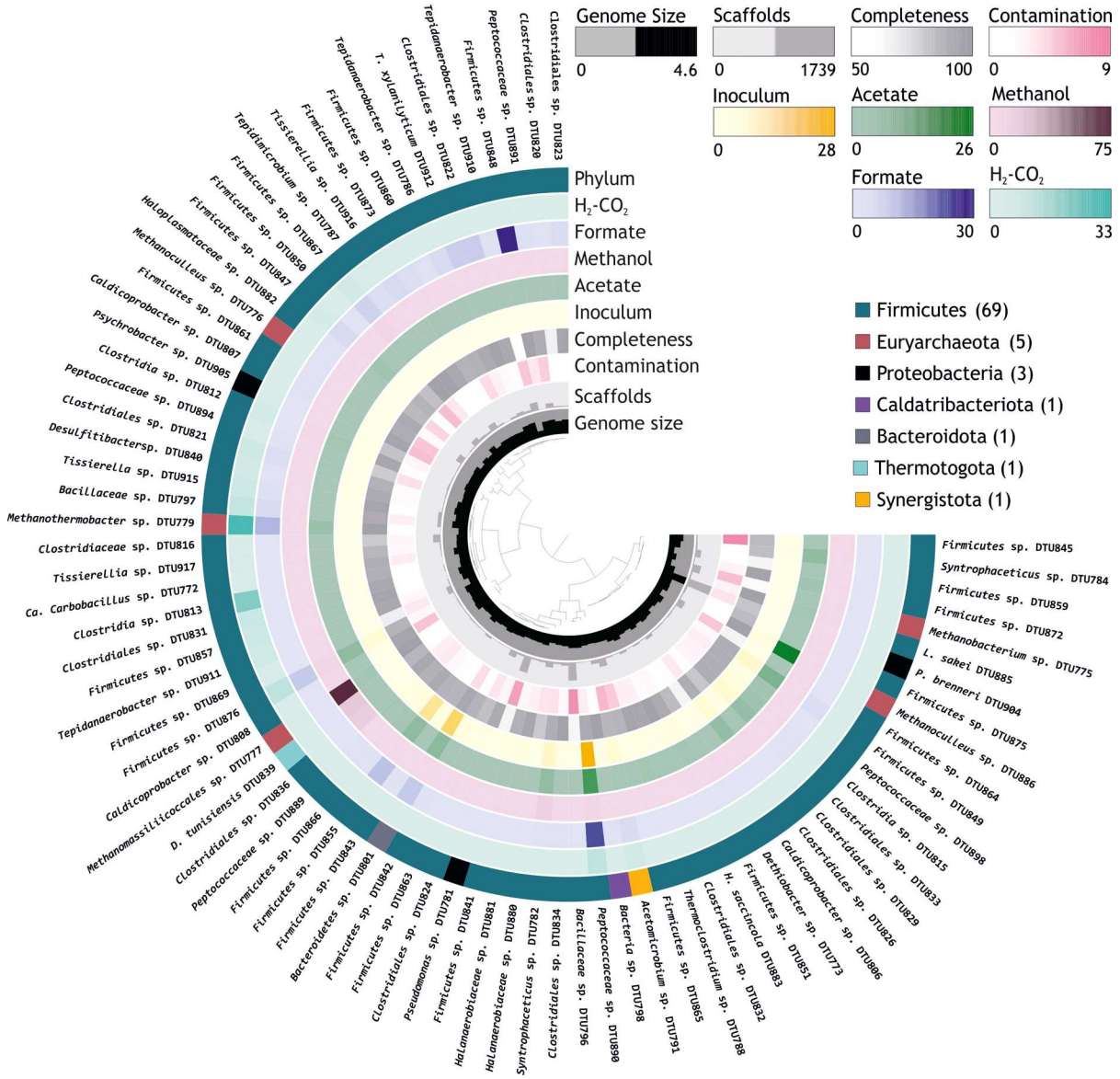

Figure 1. Microbial samples collected from five points of the batch reactors: $G_{methanol}$, $G_{formate}$, $G_{inoculum}$, $G_{acetate}$, and G_{H_2/CO_2}. The characteristics (coverage, quality, and taxonomic assignment) of 81 MAGs comprising the microbiome are reported. The outer layer represents the taxonomy at the phylum level. The five middle layers report the relative abundance of each MAG in the different microbiomes (% of relative abundance). The completeness (%), contamination (%), number of scaffolds, and genome size (Mbp) are colored in green, red, gray, and black, respectively. The middle phylogenetic tree represents the Pearson clustering of MAGs based on the relative abundances.

collected from five sampling points: $G_{inocula}$, an initial microbial community without additional ammonia and fed with cow manure (2.25 g NH^+-N/L); G, a methanol-degrading community (7.25 g NH^+-N/L); G, an acetate-degrading community (4.25 g NH^+-N/L); $G_{formate}$, a formate-degrading community (5.25 g NH^+-N/L); and G, a H/CO-degrading community (7.25 g NH^+-N/L) (Table S1). PowerSoil DNA Isolation Kit (QIAGEN, Germany) was used for genomic DNA extraction, and an additional phenol-cleaning step was performed in order to increase DNA purification.[36] Nanodrop 2000 (ThermoFisher Scientific, Waltham, MA) was used to evaluate the quality of the extracted DNA.

2.3. Genome-Centric Metagenomics and Statistics. A sequencing strategy including both Illumina and Oxford Nanopore MinION single-molecule sequencers was chosen. Library preparation was performed using the Nextera DNA Flex Library Prep Kit (Illumina Inc., San Diego CA) and the SQK rapid sequencing kit (Oxford Nanopore Technologies, Oxford, UK); libraries were sequenced with the Illumina NextSeq 500 platform (Illumina Inc., San Diego CA) with a paired-end and FLO-MIN106 R9 flow cell on a MinION device (Oxford Nanopore Technologies, Oxford, UK) at the CRIBI Biotechnology Center sequencing facility (University of Padova, Italy). Raw sequences were uploaded to the Sequence Read Archive (NCBI) under the project PRJNA613371. Oxford Nanopore Technologies base-calling for translating raw electrical signals to nucleotide sequences was performed using Guppy (v2.3.7 + e041753).[37] The total raw data provided 426,815,859 bases of sequence. Illumina reads with low-quality or ambiguous bases were filtered with Trimmomatic (v0.39). High-quality reads were independently assembled with three software, namely Spades (v3.13.0),[38]

https://dx.doi.org/10.1021/acs.est.0c01945
Environ. Sci. Technol. 2020, 54, 12568−12582

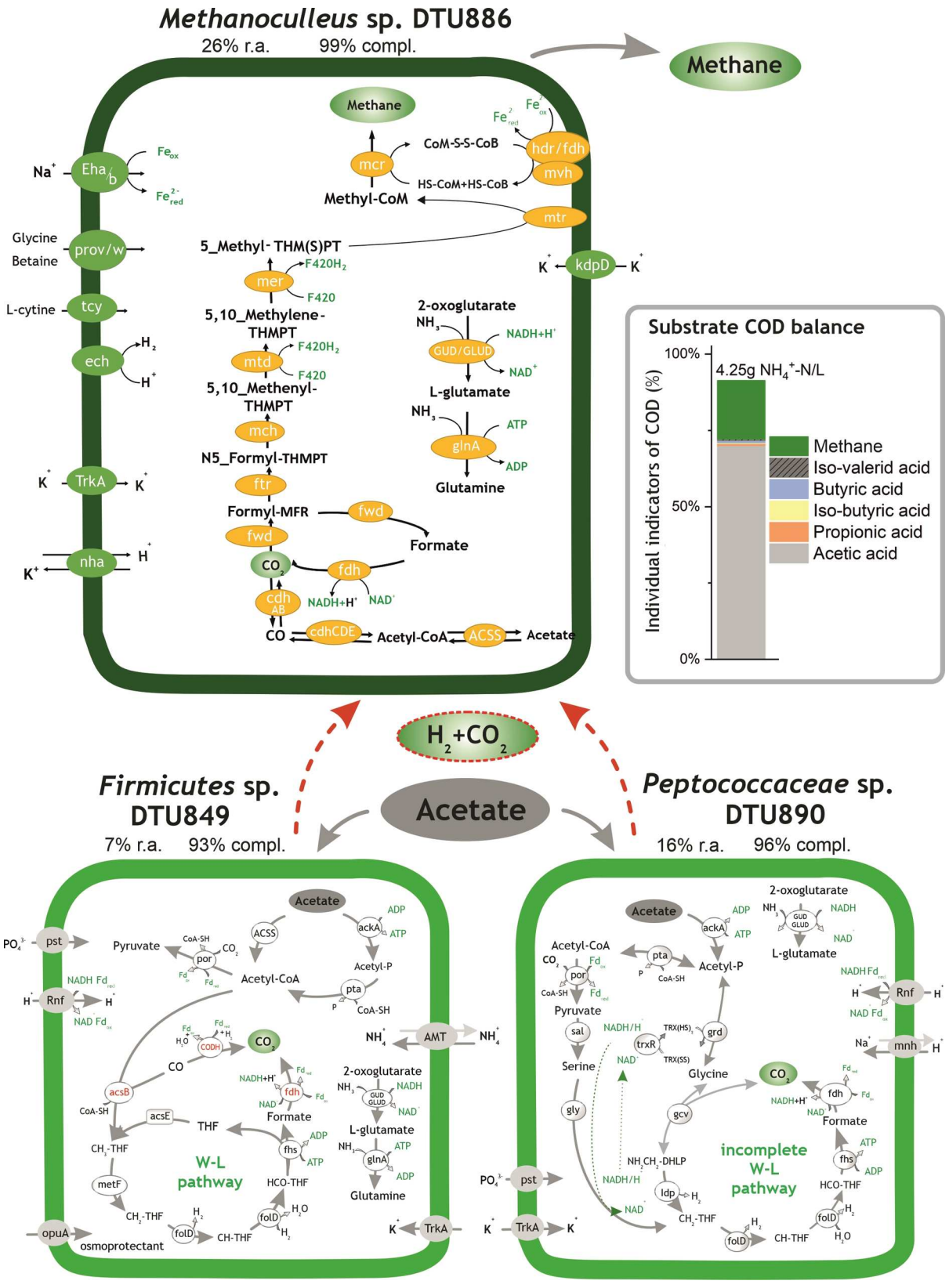

Figure 2. Histogram on the right side represents the substrate digestion profile (COD flow) measured in $G_{acetate}$. Obligate syntrophic acetate degradation pathway proposed in *Methanoculleus* sp. DTU886, *Firmicutes* sp. DTU849, and *Peptococcaceae* sp. DTU890. "R.a." and "compl." are abbreviations of the terms "relative abundance" and "completeness", respectively. The red dotted arrows represent the syntrophic intake of H_2/CO_2 by methanogens. All the relevant genes used for metabolic reconstruction can be found in Table S6.

OPERA-MS,[39] and Unicycler (v0.4.8-beta).[37] The assembly process was applied to Illumina reads alone and also to Illumina reads combined with Nanopore data using MEGAHIT (V1.2.4beta) software.[40] After the assembly, all the

https://dx.doi.org/10.1021/acs.est.0c01945
Environ. Sci. Technol. 2020, 54, 12568−12582

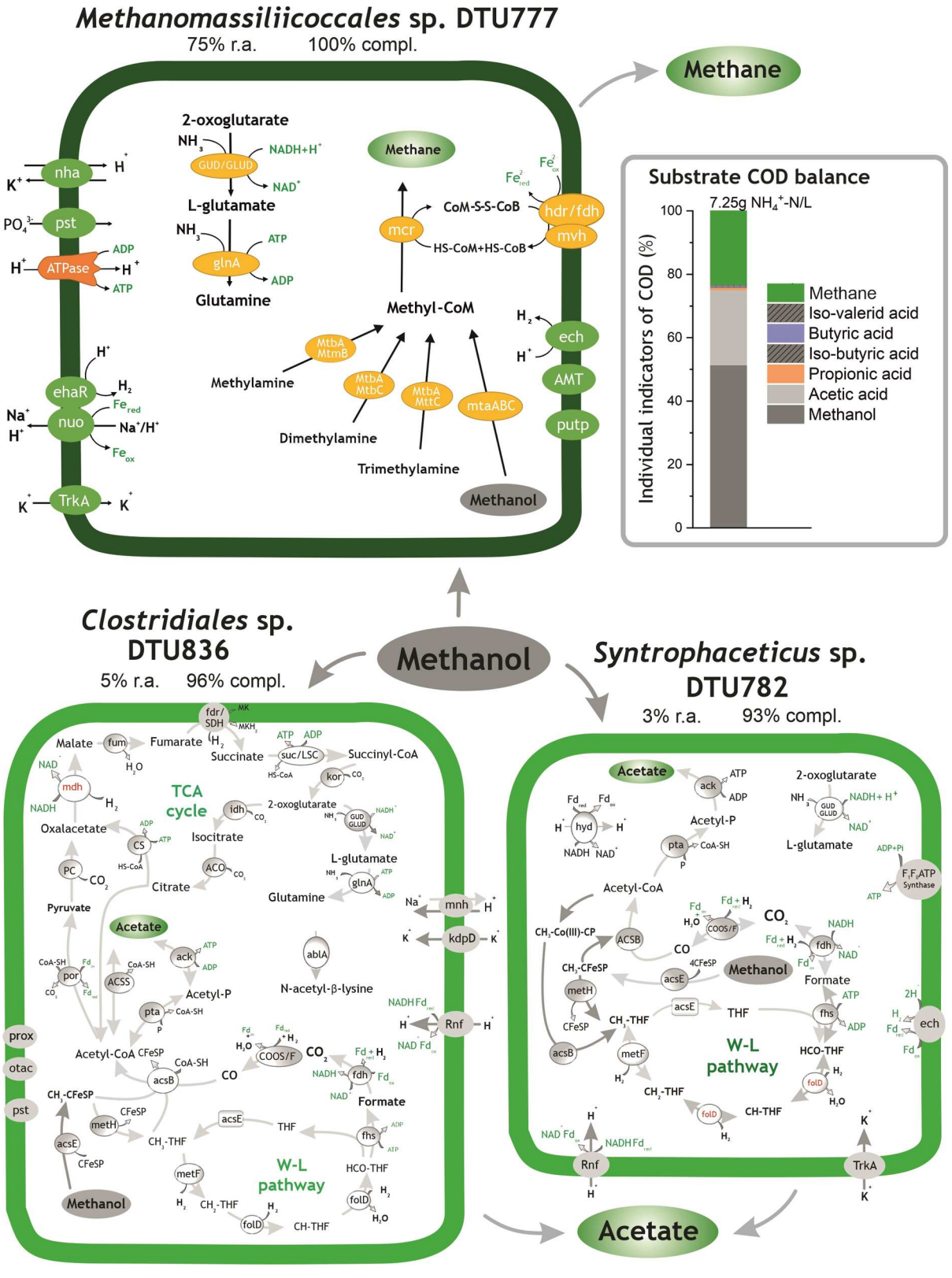

Figure 3. Histogram on the right side represents the substrate digestion profile (COD flow) measured in $G_{methanol}$. Methanol degradation pathways identified in *Methanomassiliicoccales* sp. DTU777, *Syntrophaceticus* sp. DTU782, and *Clostridiales* sp. DTU836. "R.a." and "compl." are abbreviations of the terms "relative abundance" and "completeness", respectively. All the relevant genes used for metabolic reconstruction can be found in Table S6.

scaffolds shorter than 1 kb were removed, and the statistics of the assemblies were determined using Quality Assessment Tool for Genome Assemblies (QUAST, V4.1).[41] The scaffolds' coverage was determined by aligning the reads of each sample back to the assembly with Bowtie 2 (v2.2.4)[42] and converting the output SAM files to BAM format using SAMtools (v1.9).[43]

https://dx.doi.org/10.1021/acs.est.0c01945
Environ. Sci. Technol. 2020, 54, 12568−12582

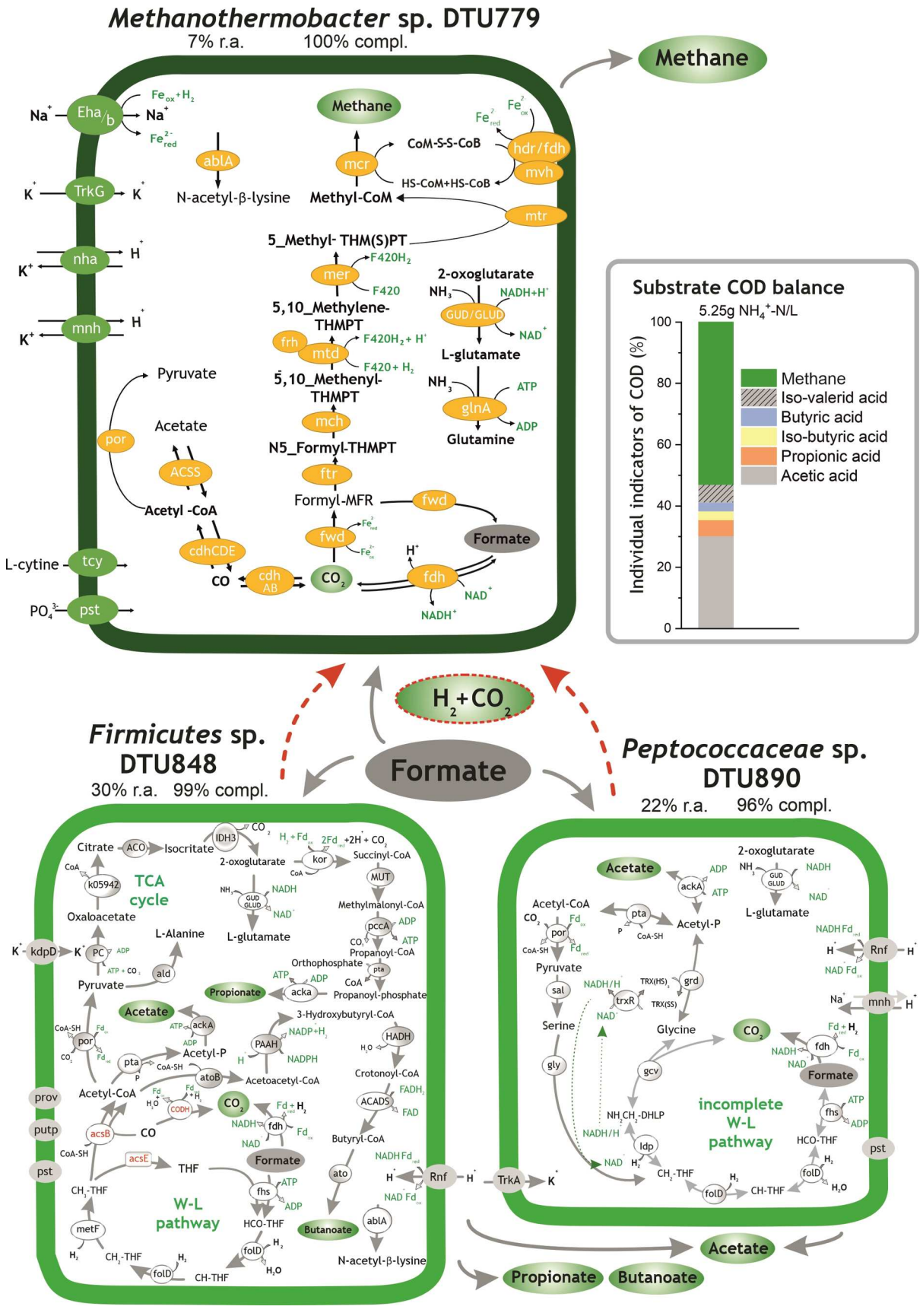

Figure 4. Histogram on the right side represents the substrate digestion profile (COD flow) measured in $G_{formate}$. Formate degradation pathways identified in *Methanothermobacter* sp. DTU779, *Peptococcaceae* sp. DTU890, and *Firmicutes* sp. DTU848. "R.a." and "compl." are the abbreviations of the terms "relative abundance" and "completeness", respectively. The red dotted arrows represent the syntrophic intake of H_2/CO_2 by *Bacteria*. All the relevant genes used for metabolic reconstruction can be found in Table S6.

https://dx.doi.org/10.1021/acs.est.0c01945
Environ. Sci. Technol. 2020, 54, 12568−12582

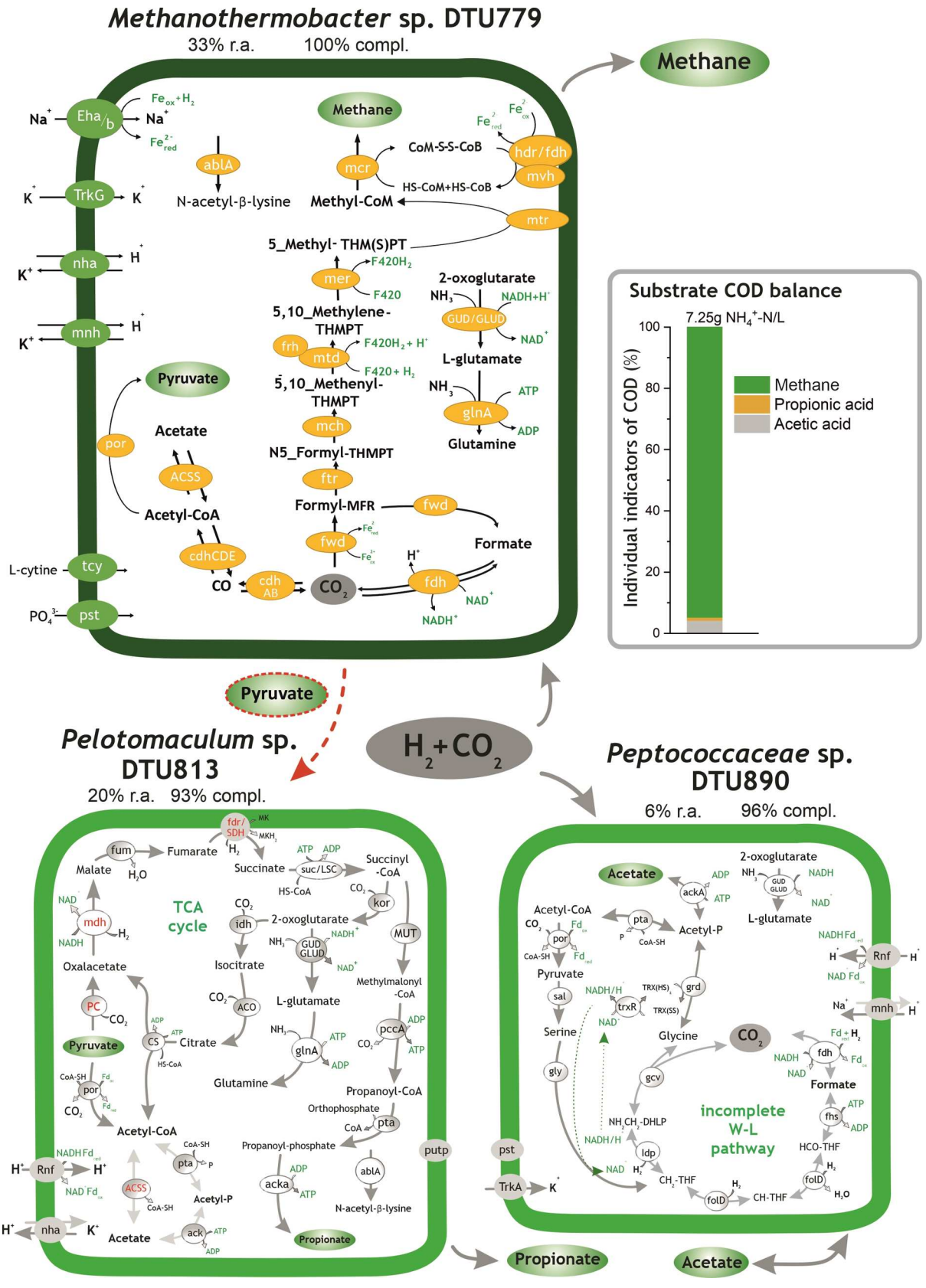

Figure 5. Histogram on the right side represents the substrate digestion profile (COD flow) measured in G_{H_2/CO_2}. H_2/CO_2 degradation pathways identified in *Methanothermobacter* sp. DTU779, *Peptococcaceae* sp. DTU890, and *Pelotomaculum* sp. DTU813. "R.a." and "compl." are the abbreviations of the terms "relative abundance" and "completeness", respectively. The red dotted arrows represent the syntrophic intake of pyruvate by methanogens. All the relevant genes used for metabolic reconstruction can be found in Table S6.

https://dx.doi.org/10.1021/acs.est.0c01945
Environ. Sci. Technol. 2020, 54, 12568−12582

Metagenomic binning was performed using MetaWRAP software[45] which implements Metabat2 (v2.12.1) and MaxBin2 (v2.2.6).[44] Among the recovered MAGs, 143 were obtained from metaspades, 136 were from OPERA-MS, and 105 were from unicycler; the final selection was obtained by removing the redundancy and keeping the highest quality MAGs.

The completeness, contamination, and genome properties of the final MAGs were determined using CheckM (v1.0.3), and details can be found in Table S2. The relative abundance of microbes on each sample was obtained by aligning the reads to the assembly and subsequently using "BAM" files to calculate the final values using CheckM coverage (v1.0.3).The diversity index for each sample was measured from the unassembled Illumina reads using Nonpareil v3.303 with default parameters.[45]

Similarity with publicly available genomes was calculated by means of average nucleotide identity (ANI),[46] and the results are reported in Table S3. Taxonomical assignment and functional analysis were performed using GTDB-Tk[47] and CAT.[48] Protein-encoding genes were predicted using Prodigal (v2.6.2)[49] run in normal mode and associated with KEGG IDs using Diamond (v0.9.22.123).[50] The KEGG IDs were associated with modules to determine completeness using the KEGG mapper-reconstruct pathway tool, as previously described.[51] The functional visualization of MAG metabolism was performed using GhostKOALA.[52] Hierarchical clustering of the binned MAGs across five samples was constructed using the MultiExperiment viewer (v4.9.0) with the Pearson distance metric and visualized by Anvi'o.[53]

Simultaneously, MAGs were used for genome-scale metabolic reconstruction and the subsequent analysis of interactions within a flux balance analysis framework, adopting CarveMe (v. 1.2.1)[54] for the genome-scale metabolic reconstruction and a revised version of MMinte software (v.1.0.3)[55] for the inspection of interactions, following the pipeline developed by Basile and colleagues (https://github.com/arianccbasile/ADinteractions). Literature-guided metabolic reconstruction was manually performed based on the genes and pathways present in the most abundant MAGs for each microbiome.

Four genomes of ammonia-sensitive *Methanosaeta* spp. were downloaded from public databases of NCBI to compare the energy-converting mechanism. The GenBank assembly accession numbers of these four genomes were GCA_012729025.1; GCA_012798255.1; GCA_012798025.1; and GCA_012516895.1.

3. RESULTS AND DISCUSSION

3.1. Ammonia-Tolerant Reactor Performance Using Different Carbon Sources. The microbial consortia were cultivated in batch reactors fed with specific carbon sources, namely acetate, methanol, formate, and H_2/CO_2. After five to six consecutive generations of cultivation under stepwise ammonia increase, the microbial species present in each group showed different capabilities of resistance to ammonia (Figures 1−5). Specifically, in comparison to other groups, the community in $G_{methanol}$ and G_{H_2/CO_2} showed higher resistance to ammonia inhibition and were able to grow up to 7.25 g NH^+-N/L. Additionally, the highest methane yield (up to 91%) could be observed in G_{H_2/CO_2} at 7.25 g NH^+-N/L (Figure 5). On the contrary, the lowest methane yield (19%) was found in $G_{acetate}$ at 4.25 g NH^+-N/L (Figure 2). VFAs (*i.e.* acetate, propionate, iso-butyrate, butyrate, and iso-valerate) were detected as an important indicator of chemical oxygen demand (COD) flow from the substrate during the metabolic degradation driven by the microbial community. Trace amounts of VFAs were present in $G_{acetate}$ and G_{H_2/CO_2} (Figures 2 and 5); more than 20% of acetate (COD ratio of acetate to the added carbon source) was found in $G_{methanol}$ and $G_{formate}$, suggesting that acetate is a key intermediate during carbon degradation at high ammonia levels. To clearly decipher the main metabolic pathways that occurred during the different substrate degradations, the methane production and the intermediate accumulation (*e.g.*, VFAs) were expressed as the percentage (%) of the overall COD content to highlight the transformation processes and directly couple them with the metagenomic data. Besides, the methane yield is reported in Figure S1.

3.2. Microbial Community Composition and Activities. The assembly and binning process resulted in a total of 81 MAGs based on sequence mapping, and these microbial species accounted for 62.5−91.8% of the entire community, depending on the sample (Table S2 and Table S4). These MAGs represented the most abundant members of the microbiome; 52 out of 81 MAGs were of high quality (more than 90% completeness and lower than 5% contamination), whereas the remaining 29 MAGs were of medium quality (completeness from 50 to 90% and contamination from 5 to 10%) according to the minimum information about the metagenome-assembled genome (MIMAG)[56] (Figure 1 and Table S4). The 81 MAGs were taxonomically assigned into seven phyla, namely *Firmicutes*, *Proteobacteria*, *Thermotogae*, *Actinobacteria*, *Chloroflexi*, *Bacteroidetes*, and *Euryarchaeota* (Figure 1).

The different carbon sources (methanol, formate, acetate, and H_2/CO_2) used in this study, as well as the stepwise increased ammonia levels, worked as selecting pressure that shaped the microbial communities inducing considerable distinction in terms of diversity. In particular, attention was focused on the dominant members in each microbiome (Figures 1−5) and on the corresponding metabolic maps that were reconstructed using KEGG modules (Table S5), as well as individual gene's annotation and literature-based information. Hydrogenotrophic methanogenesis using H_2 or formate as electron donors was observed as the only methane-producing pathway in $G_{formate}$, G_{H_2/CO_2}, and $G_{acetate}$. Meanwhile, methylotrophic methanogenesis was solely observed in $G_{methanol}$, as revealed by the presence of methanol transferase and methyl-CoM reductase in *Methanomassiliicoccales* sp. DTU777.

The presence of acetate in each reactor was indicative of acetogenesis, performed *via* the conventional Wood−Ljungdahl (WL) pathway, methanol oxidation, and glycine cleavage system (Figure 3 and Table S6). The assumption is evidenced by the presence of these pathways in *Firmicutes* sp. DTU848, *Clostridiales* sp. DTU836, and *Peptococcaceae* sp. DTU890. In addition, a novel propionate synthesis pathway was reconstructed in *Firmicutes* sp. DTU848 based on the gene presence (*e.g.*, k05942, *kor*, and *acka*) using KEGG and the analysis of residual metabolites present in the medium (*e.g.*, acetate, propionate, and methane), growing in $G_{formate}$ (Figure 4 and Table S6). The following sections focus on how interspecies

https://dx.doi.org/10.1021/acs.est.0c01945
Environ. Sci. Technol. 2020, 54, 12568−12582

interactions were established in a syntrophic consortium and the resistance mechanism to high ammonia levels.

3.2.1. Microbiome in the Original Inoculum. In $G_{inocula}$, *Bacteria* dominated the microbial community with a relative abundance of 98% of the binned microbiome (this value refers to the percent of reads aligned on the binned scaffolds), which accounted for 63.1% of the entire community, whereas *Archaea* were quite rare. Specifically, sugar-converting microbes (identified by the presence of Embden−Meyerhof pathway) represented the dominant MAGs consisting of *Peptococcaceae* sp. DTU890, *Bacteroidetes* sp. DTU801, *Firmicutes* sp. DTU855, and *Firmicutes* sp. DTU849 with 27.8, 16.6 10.7, and 3.8% of relative abundance, respectively (Figure 1 and Table S5). Results from ANI evaluation indicated that *Peptococcaceae* sp. DTU890 was 99.8% similar to *Clostridiales* sp. DTU010 and to other MAGs previously identified in different AD systems (Table S3).[57] According to the pathways present in these *Bacteria*, they are capable of performing a complete fermentation, converting glucose to acetate *via* the Embden−Meyerhof pathway and pyruvate oxidation (Table S5). These results show consistency with previous findings which suggested the main driving forces expanding the complexity and stability of the AD microbiome.[58] Meanwhile, *Peptococcaceae* sp. DTU890 was also involved in acetogenesis using a novel glycine cleavage system and the phosphate acetyltransferase−acetate kinase pathway (Figure 3). The other two MAGs, namely, *Syntrophaceticus* sp. DTU782 (4.3%) and *Acetomicrobium* sp. DTU791 (2.9%), were predicted to show the acetate-oxidizing ability that may work in syntrophy with hydrogenotrophic methanogens for methane production. The five identified *Euryarchaeota* sp. represented only 1.28% of the whole microbial community; among these, the most dominant MAG was *Methanoculleus* sp. DTU886 with 1.2% of relative abundance, followed by *Methanothermobacter* sp. DTU779 and *Methanomassiliicoccales* sp. DTU777, with 0.05 and 0.03%, respectively. Methanogenesis was performed by these three archaeal MAGs, having different metabolic traits of performing hydrogenotrophic and methylotrophic methanogenesis. Interestingly, no acetoclastic methanogens have been identified in the initial inoculum. The possible explanation is that the total ammonia level in $G_{inocula}$ was 2.25 g NH^+-N/L, which possibly suppressed the abundance of acetoclastic methanogens. This result also agrees with the microbial community of inocula (collected not on the same day but under the same operating conditions with our initial inocula) analyzed by 16S sRNA gene amplicon sequencing in our previous research.[59]

3.2.2. Ammonia-Tolerant Microbiome in the Acetate-Based Medium. In $G_{acetate}$, the microbiome shifted markedly, as evidenced by the change in the relative abundance of dominant MAGs when compared with the initial inoculum. In fact, the population evolved into a more simplified and specialized community, as confirmed by the diversity indexes (Table S7). $G_{acetate}$ was dominated by *Methanoculleus* sp. DTU886, *Firmicutes* sp. DTU849, and *Peptococcaceae* sp. DTU890 (Figure 2), with a cumulative relative abundance of 48% (Table S4).

More specifically, *Methanoculleus* sp. DTU886 had 99.6% ANI when compared with Candidatus *Methanoculleus thermohydrogenotrophicum*.[60] The archaeon dominated the microbiome with 26% of relative abundance and was the only methanogen present in the community. It was previously reported that *Methanoculleus* sp. could perform methanogenesis from H_2/CO_2 or formate but not acetate.[61] Interestingly, *Methanoculleus* sp. DTU886 in this study was found to harbor a series of genes for the conversion of acetate to CH_4 as well as the genes for H_2/CO_2 oxidation to CH_4 (Figure 2). Furthermore, the genomes of *Firmicutes* sp. DTU849 (7%) and *Peptococcaceae* sp. DTU890 (16%) encoded proteins involved in H_2 and CO_2 generation, suggesting the presence of a syntrophic interaction occurring between these two species and the methanogen. The presence of such interplay was confirmed by flux balance analysis revealing that *Methanoculleus* sp. DTU886 is favored by the interaction within both couples (Table S8). Specifically, *Firmicutes* sp. DTU849 possesses an incomplete gene set involved in the conventional syntrophic acetate oxidation pathway for H_2/CO_2 generation through the reverse WL pathway, whereas *CODH*, *acsB*, and *fdh* were not identified. According to the reconstructed pathway, acetate was possibly converted to pyruvate through the inverse phosphotransacetylase−acetate kinase pathway and acyl-CoA synthetase pathway (ACS). The genes encoded in *Peptococcaceae* sp. DTU890 suggested the use of an alternative glycine cleavage system for acetate oxidation (Figure 2). Specifically, the glycine cleavage system was combined with a partial WL pathway to convert acetate to CO_2/H_2, supporting the syntrophic activity with hydrogenotrophic methanogens.[62] Both syntrophic *Bacteria* possess the Rnf complex, which is involved in proton motive force-driven reverse electron transport from NADH to Fd_{ox}, where Fd_{red} was produced as a high-energy-electron carrier to facilitate H_2 generation. Regarding energy metabolism, *Methanoculleus* sp. DTU886 encodes a set of energy-conserving hydrogenases (Eha/b, Ech, and Fdh) contributing to the proton motive force by coupling proton translocation across the membrane to Fe_{red}; the same set of proteins can also be used for CO_2 reduction (Figure 2). Furthermore, methyl-THMPT HS-COM methyltransferase (Mtr), the membrane-bound enzyme complex, extruded Na^+/H^+ out of the cell, creating a Na^+/H^+-based ion motive force used for both ATP generation and methanogenesis.

3.2.3. Ammonia-Tolerant Microbiome in the Methanol-Based Medium. In $G_{methanol}$, the dominant *Methanomassiliicoccales* sp. DTU777 (75% of relative abundance) was the main player that was responsible for methane generation from methanol (Figure 3). The complete methanogenic pathway from methanol and methylamine was found in the genome (Figure 3 and Table S6). Additionally, the presence of membrane-bound NADH-ubiquinone oxidoreductase (Nuo) suggested the formation of a Fpo-like complex, capable of reoxidizing the reduced ferredoxin, with the concomitant translocation of protons or sodium ions across the membrane (Figure 3 and Table S6). The proton gradient generated by the complex mentioned above facilitated the ATP synthesis, employing the energy-conserving hydrogenase (Ech) complex, thereby coupling methane generation with energy conservation and enabling internal hydrogen cycling.[12,63]

D. tunisiensis DTU839, *Syntrophaceticus* sp. DTU782, and *Clostridiales* sp. DTU836 accounted for 7.3, 3, and 5% of relative abundance, respectively, and *Syntrophaceticus* sp. DTU782 and *Clostridiales* sp. DTU836 were chosen as the representatives of the whole bacterial community because of their high genome completeness and relative abundance. The flux balance analysis revealed a parasitic interaction between these two microbes, with *Clostridiales* sp. DTU836 taking advantage of the coexistence with *Syntrophaceticus* sp. DTU782 (Table S8). The presence of acetate in $G_{methanol}$ suggested that

https://dx.doi.org/10.1021/acs.est.0c01945
Environ. Sci. Technol. 2020, 54, 12568−12582

acetogenic methanol degradation was performed as reported in the following description. According to the metabolic reconstruction, the methylic group was probably transferred to the methyl acceptor−−corrinoid Fe−S protein (CFeSP) into CH_3−CFeSP−−and followed two possible pathways of CH_3−CFeSP oxidation. First, a part of CH_3−CFeSP was converted into acetate *via* the acetate kinase pathway; second, the rest of CH_3−CFeSP was oxidized through the WL pathway, with a concomitant reduction of CO_2 into acetate. The reduction of ferredoxin and ATP for energy conservation for the above two pathways would occur following previously proposed mechanisms.[24,64] *Syntrophaceticus* sp. DTU782 had the potential to perform the first pathway using methyltransferase and acetyl synthase (ACSE and ACSB); these genes can activate and transfer the methyl group to a corrinoid Fe−S protein and oxidize it to acetyl-CoA *via* ACSB (Figure 3 and Table S6).

Meanwhile, *Clostridiales* sp. DTU836 harbored the two complete gene complexes related to acetate generation from methanol (Figure 3 and Table S6). The excess of ATP derived from the first pathway (the oxidation of one methanol to acetate) might be sacrificed to drive the endergonic oxidation of 2-methyltetrahydrofuran to 5,10-methylenetetrahydrofolate, which is in consistence with the previous study.[64]

3.2.4. Ammonia-Tolerant Microbiome in the Formate-Based Medium. The microbiome of $G_{formate}$ was mainly composed of two highly abundant *Bacteria*, *Peptococcaceae* sp. DTU890 and *Firmicutes* sp. DTU848, and one *Archaea*, *Methanothermobacter* sp. DTU779, with an aggregate relative abundance of 59% (Figure 5 and Table S4). The analyses of flux balance revealed that the growth rate of *Methanothermobacter* sp. DTU779 is positively influenced by the presence of *Firmicutes* sp. DTU848 (Table S8).

In *Methanothermobacter* sp. DTU779, the reduction of CO_2 to formyl-MFR using H_2 was driven by the electrochemical sodium ion potential (Nha and Mnh) (Figure 4 and Table S6). Furthermore, methyl-COM reduction to methane could proceed *via* the MvhADG/HdrABC complex and was coupled to ferredoxin (Fd) reduction.[65,66] Two sets of energy-conserving hydrogenases, Eha and Ehb, were found in the genome of *Methanothermobacter* sp. DTU779 (Table S6). These genes were shown to be critical for the refilling of methanogenesis intermediates (*e.g.*, H_2) and for CO_2 assimilation.[17] *Firmicutes* sp. DTU848 harbored the genes involved in the conversion of formate to acetate *via* the partial reverse WL pathway, which can explain the presence of acetate in $G_{formate}$. According to the metabolic reconstruction, propionate could be generated through a novel pathway, which involves the oxidation of acetyl-CoA into pyruvate *via* pyruvate ferredoxin oxidoreductase and the final step of amination to form citrate. Similarly, isocitrate could be transformed from citrate catalyzed into oxoglutarate, then oxidized into succinyl-CoA, and further into methylmalonyl-CoA (Figure 4 and Table S6). Finally, methylmalonyl-CoA can be converted into propionate *via* propionyl-CoA carboxylase and phosphate acetyltransferase, as previously described by Bar-Even *et al.*[67] Thereby, the sodium pumping pathway coupled with the decarboxylation of methylmalonyl-CoA derived from succinate-CoA to propionyl-CoA with the pumping of two Na^+ across the cell membrane, leading to a net energy gain.[68] Therefore, the clear carbon flow from formate conversion to propionate generation and the reductive citric acid (rTCA) cycle found in *Firmicutes* sp. DTU848 for energy conservation[69] confirmed that the bacterium could outcompete *Methanothermobacter* sp. DTU779 (30−7% of relative abundance) for formate utilization. As mentioned before, the absence of acetyl-CoA synthetase in the genome of *Peptococcaceae* sp. DTU890 indicated that an alternative glycine cleavage system was possibly employed for acetate oxidation. Additionally, both *Peptococcaceae* sp. DTU890 and *Firmicutes* sp. DTU848 encoded a sodium-ion pump (Rnf) that coupled the electron transfer for H_2 generation and ATP synthesis (Figure 4 and Table S6).

3.2.5. Ammonia-Tolerant Microbiome in the H_2/CO_2-Based Medium. In the G_{H_2/CO_2} microbiome adapted to 7.25 g NH^+-N/L, *Methanothermobacter* sp. DTU779 reached a remarkable relative abundance of 33% (5 times more than that in $G_{formate}$) (Figure 5). This finding indicated that, in the presence of formate, hydrogenotrophic methanogenesis was the main pathway. However, it can be assumed from these results that *Methanothermobacter* sp. DTU779 prefers H_2 as an electron donor for autotrophic growth, when compared to formate. Additionally, according to similarity results, DTU779 was found to have 99.8% of ANI with *Methanothermobacter wolfeii* and with other MAGs identified in previous studies[70,71] (Table S3). Interestingly, it is evidenced by Lins *et al.* that by replacing formate with H_2 in the feed, the doubling time of *M. wolfeii* can decrease to 7.65 h.[72]

The bacterial community in G_{H_2/CO_2} is mainly represented by *Pelotomaculum* sp. DTU813 and *Peptococcaceae* sp. DTU890 (26% of aggregate relative abundance). Although *Pelotomaculum* spp. are known syntrophic propionate-oxidizing *Bacteria*,[73] no propionate was provided in the feed of the H_2/CO_2-fed reactor. The metabolic reconstruction indicated that *Methanothermobacter* sp. DTU779 could produce pyruvate, suggesting a survival strategy of *Pelotomaculum* sp. DTU813, based on a parasitic relationship with *Archaea* in this specific condition. The flux balance analysis performed on this reactor actually revealed that the couple has a commensalistic behavior, with *Pelotomaculum* sp. DTU813 being favored by the coexistence. *Methanothermobacter* sp. DTU779 is not indeed negatively influenced by the coexistence, thus explaining its high abundance in the community (Table S8). This hypothesis, based on the gene content and metabolites presence, was also supported by previous literature. In fact, *Pelotomaculum thermopropionicum* is known for fermenting pyruvate into acetate and propionate (3:1 molar ratio)[73] and the same products were measured in the reactor (Figure 5). Finally, acetate, potentially produced by *Pelotomaculum* sp. DTU813, could be further utilized by *Peptococcaceae* sp. DTU890 for biomass production, with the consequent CO_2/H_2 generation. However, *Peptococcaceae* sp. DTU890 seems to have a versatile metabolism that can alternatively produce or consume different carbon sources (*i.e.*, acetate and CO_2/H_2) depending on the metabolites' concentrations in the medium.

3.3. Proposed Mechanisms for Ammonia Acclimatization. The adaptation of microbiome to ammonia through the strategy of single and simple carbon source cultivation under stepwise increased ammonia levels achieved the specialized and simplified microbiome discussed above. Most importantly, it also clarified some aspects of the mechanisms involved in ammonia resistance by identifying the metabolic pathways involved in the adaptation and unraveling the trophic niches occupied by each MAG. The variable capabilities of different microbiomes to tolerate ammonia seemed to be

https://dx.doi.org/10.1021/acs.est.0c01945
Environ. Sci. Technol. 2020, 54, 12568−12582

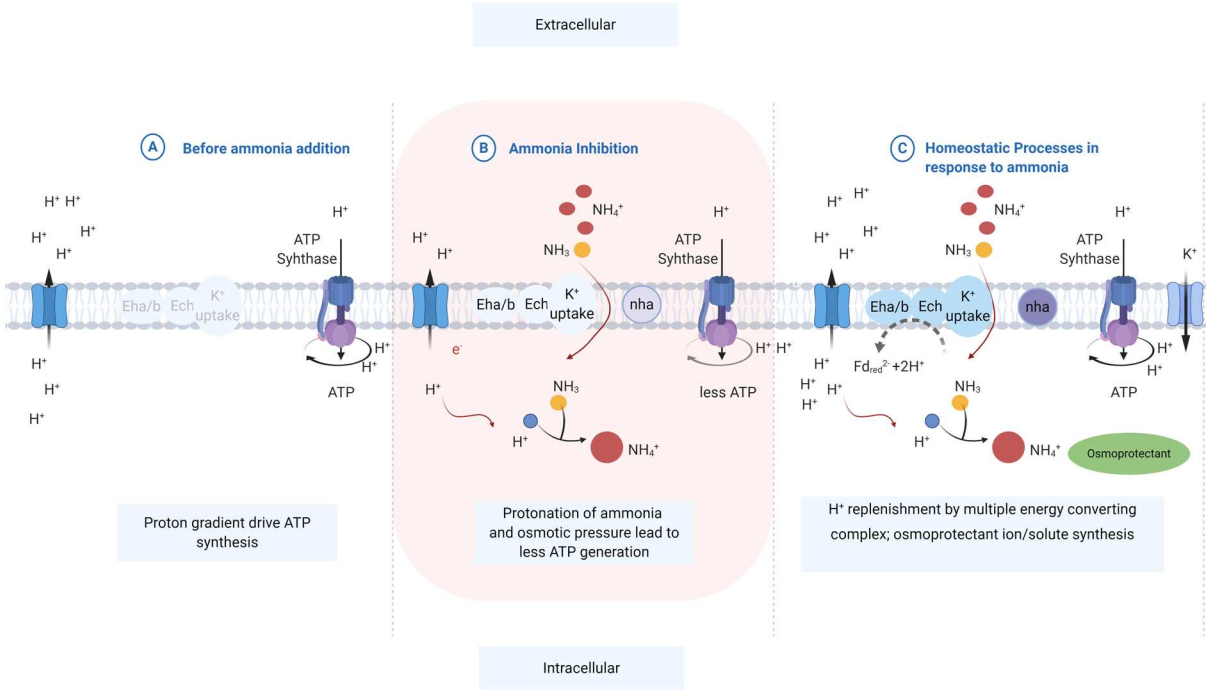

Figure 6. Proposed response of methanogen in different situations. (a) Before ammonia inhibition. (b) During ammonia inhibition, the protonation of ammonia and osmotic pressure lead to less ATP generation. (c) Homeostatic regulation in response to ammonia by following strategies: H^+ replenishment by multiple energy-converting complexes, osmoprotectant ion/solute synthesis, and H^+ binding by pumping K^+ into the cell for cation balance.

connected with the homeostatic system, energy conservation strategies, and different ATP generation *via* substrate-level phosphorylation (Table S6).

From the homeostatic perspective, the presence of the potassium or sodium/proton antiporter (nha) system and the K^+ uptake system (TrKA) had the potential to top-up intracellular protons and K^+ for homeostatic processes, including the regulation of the turgor pressure and maintenance of cytoplasmic pH in response to the protonation of ammonia (Figures 2−6 and Table S6). As a confirmation of this process, Kraegeloh *et al.* revealed a process in which the loss of TrKA abolished any K^+ uptake activity leading to osmotic sensitivity.[7] Considering the osmotic stress induced by ammonium, a possible resistance mechanism of the MAGs identified in the current study could be related to the activity of glutamate dehydrogenase, glutamine, glycine betaine, and N^{ε}-acetyl-L-lysine synthase. These enzymes can synthesize known osmoprotectants such as glutamate, glutamine, glycine betaine, and N^{ε}-acetyl-L-lysine, which contribute to the survival of the cells at high osmotic stress and allow the colonization of ecological niches in severe environmental conditions. It seemed that the co-occurrence of the two systems (*i.e.*, osmoprotectant generation and potassium uptake) was a necessity against ammonia stress. This finding was in agreement with previous studies, highlighting that the synthesis of glutamate requires a stable level of K^+.[74−76]

To regulate proton balance, potassium uptake, and biosynthesis maintenance, extra energy is needed. Thus, the raised question is how energy conservation can be achieved in order to survive during ammonia inhibition. The metabolic reconstruction provided novel insights regarding membrane-bound NADH-ubiquinone oxidoreductase (Nuo) in *Methanomassiliicoccales* sp. DTU777. In fact, the presence of a Fpo-like complex capable of reoxidizing the reduced ferredoxin, with simultaneous translocation of protons or sodium ions across the membrane, can generate the proton gradient needed for the ATP synthesis, as previously reported.[12,64] Similarly, Hdr, Fwd, and Fdh present in *Methanothermobacter* sp. DTU779 were described to support the assembly of a bifurcating multienzyme complex, and Mnh was employed as an electrochemical potential-driven transporter (Figure 5 and Table S6).

Additionally, the coexistence of Eha/b and Ech complexes, in the presence of optimized energy conservation in DTU779, could be a reason for its extraordinary adaption to ammonia-inhibiting conditions (Figure 5). This hypothesis may be supported by the ability of *Methanothermobacter* sp. to outcompete other methanogens for establishing a syntrophic relationship with fatty acid-oxidizing *Bacteria*.[16] Interestingly, the genome comparison of three identified *Archaea* in this study (*Methanoculleus* sp. DTU886, *Methanomassiliicoccales* sp. DTU777, and *Methanothermobacter* sp. DTU779) with the four ammonia-sensitive *Methanosaeta* spp. (downloaded from public databases) verified that the Eha/b and Ech energy-converting system was only present in the former three methanogens.

Obviously, when exposed to ammonia stress, methanogens with the multiple energy-converting hydrogenases mentioned above could become more energy-efficient and thereafter thrive easier than methanogens without these complexes (Figure 6). Additionally, the number of genes responsible for energy conservation in *Methanothermobacter* sp. DTU779 (n:25) was much higher than in *Methanomassiliicoccales* sp. DTU777 (n:18) and *Methanoculleus* sp. DTU886 (n:13), which is consistent with the variable capability of ammonia tolerance of each methanogen (Table S6).

Differential tolerance to ammonia might also be attributed to variable Gibbs free energies obtained by the different

https://dx.doi.org/10.1021/acs.est.0c01945
Environ. Sci. Technol. 2020, 54, 12568−12582

microbes from substrate-level phosphorylation. According to previous studies (listed in Table 1), the energy for cell maintenance could be obtained *via* methanogenesis from methanol (−315 kJ/per reaction),[20] H_2/CO_2 (−135.6 kJ/per reaction),[77] formate (−130.4 kJ/per reaction),[77] and acetate (−36 kJ/per reaction).[21] Obviously, methanogenesis from methanol and H_2/CO_2 is far more exergonic compared to the other methanogenic processes, which might lead to the higher ammonia tolerance of *Methanomassiliicoccales* sp. DTU777 in $G_{methanol}$ and *Methanothermobacter* sp. DTU779 in G_{H_2/CO_2} than *Methanoculleus* sp. DTU886 in $G_{acetate}$. In particular, it is known from the literature that the conversion of 1 mol methanol to acetate in *Clostridiales* sp. and *Syntrophaceticus* sp. could release 0.625 ATP (the highest ATP gain identified for acetogens so far), with efficient sustained cell growth at energy-limited situations.[24,64] Interestingly, in $G_{formate}$, *Methanothermobacter* sp. DTU779 could only grow at an ammonia level up to 5.25 $N-NH^+$ g/L, whereas it could stand up to 7.25 $N-NH^+$ g/L in H/CO feeding, aided by the cooperative interaction with *Pelotomaculum* sp. DTU813. Furthermore, the presence of other intermediate metabolites (*e.g.*, acetate and propionate) in the four reactors indicated that alternative exergonic pathways were occurring. Specifically, the energy released from the conversion of acetate to propionate (−76.1 kJ/mol)[23] and methanol to acetate (−71 kJ/mol)[24] might support the growth of the whole consortium. Thus, ATP derived from *Archaea* and *Bacteria via* substrate-level phosphorylation might play a crucial role in overcoming bioenergetic barriers induced by ammonia inhibition and in driving thermodynamically unfavorable reactions. Besides, the difference in net ATP gain among the four microbial groups ($G_{acetate}$, $G_{methanol}$, $G_{formate}$, and G_{H_2/CO_2}) might determine the variable capabilities of ammonia tolerance.

■ ASSOCIATED CONTENT

Supporting Information

The Supporting Information is available free of charge at https://pubs.acs.org/doi/10.1021/acs.est.0c01945.

BA medium composition, characteristics of the reactors, and methane yields in the four groups; details and statistics for the total MAGs; average nucleotide identity comparison with previous projects; statistics and relative abundances of the MAGs selected according to MIMAG quality; KO terms used in KEGG mapper to visualize the metabolic pathways per MAG; metabolic reconstruction of the dominant MAGs; diversity indexes calculated for each sample using Nonpareil; results of pairwise interactivity in the microbiome of the four reactors characterized by different carbon sources (XLSX)

■ AUTHOR INFORMATION

Corresponding Author

Laura Treu − *Department of Biology, University of Padova, 35121 Padova, Italy*; orcid.org/0000-0002-5053-4452; Phone: +390498276165; Email: laura.treu@unipd.it

Authors

Miao Yan − *Department of Environmental Engineering, Technical University of Denmark, DK-2800 Kongens Lyngby, Denmark*

Xinyu Zhu − *Department of Environmental Engineering, Technical University of Denmark, DK-2800 Kongens Lyngby, Denmark*

Hailin Tian − *Department of Environmental Engineering, Technical University of Denmark, DK-2800 Kongens Lyngby, Denmark; NUS Environmental Research Institute, National University of Singapore, 138602, Singapore*

Arianna Basile − *Department of Biology, University of Padova, 35121 Padova, Italy*

Ioannis A. Fotidis − *Department of Environmental Engineering, Technical University of Denmark, DK-2800 Kongens Lyngby, Denmark; School of Civil Engineering, Southeast University, 210096 Nanjing, China*; orcid.org/0000-0003-4587-3617

Stefano Campanaro − *Department of Biology, University of Padova, 35121 Padova, Italy; CRIBI Biotechnology Center, University of Padua, 35131 Padua, Italy*

Irini Angelidaki − *Department of Environmental Engineering, Technical University of Denmark, DK-2800 Kongens Lyngby, Denmark*; orcid.org/0000-0002-6357-578X

Complete contact information is available at: https://pubs.acs.org/10.1021/acs.est.0c01945

Author Contributions

#S.C. and I.A. equal contribution.

Notes

The authors declare no competing financial interest.

■ ACKNOWLEDGMENTS

This work was supported by Energinet.dk under the project framework ForskEL "MicrobStopNH3-Innovative bioaugmentation strategies to tackle ammonia inhibition in anaerobic digestion process" (program no. 2015-12327). The authors acknowledge the financial support from MUDP (Miljøstyrelsens) under the project framework VARGA (MST-141-01377). M.Y. appreciates the financial support from China Scholarship Council.

■ REFERENCES

(1) Korai, M. S.; Mahar, R. B.; Uqaili, M. A. The Feasibility of Municipal Solid Waste for Energy Generation and Its Existing Management Practices in Pakistan. *Renew. Sustain. Energy Rev.* **2017**, *72*, 338−353.

(2) Fotidis, I. A.; Wang, H.; Fiedel, N. R.; Luo, G.; Karakashev, D. B.; Angelidaki, I. Bioaugmentation as a Solution to Increase Methane Production from an Ammonia-Rich Substrate. *Environ. Sci. Technol.* **2014**, *48*, 7669−7676.

(3) Satchwell, A. J.; Scown, C. D.; Smith, S. J.; Amirebrahimi, J.; Jin, L.; Kirchstetter, T. W.; Brown, N. J.; Preble, C. V. Accelerating the Deployment of Anaerobic Digestion to Meet Zero Waste Goals. *Environ. Sci. Technol.* **2018**, *52*, 13663.

(4) Tian, H.; Fotidis, I. A.; Kissas, K.; Angelidaki, I. Effect of Different Ammonia Sources on Aceticlastic and Hydrogenotrophic Methanogens. *Bioresour. Technol.* **2018**, *250*, 390−397.

(5) Capson-Tojo, G.; Moscoviz, R.; Astals, S.; Robles, Á.; Steyer, J.-P. Unraveling the Literature Chaos around Free Ammonia Inhibition in Anaerobic Digestion. *Renew. Sustain. Energy Rev.* **2020**, *117*, 109487.

(6) Kayhanian, M. Ammonia Inhibition in High-Solids Biogasification: An Overview and Practical Solutions. *Environ. Technol.* **1999**, *20*, 355−365.

(7) Kraegeloh, A.; Amendt, B.; Kunte, H. J. Potassium Transport in a Halophilic Member of the Bacteria Domain: Identification and Characterization of the K+ Uptake Systems TrkH and TrkI from Halomonas Elongata DSM 2581T. *J. Bacteriol.* **2005**, *187*, 1036.

(8) Liu, Y.; Yuan, Y.; Wang, W.; Wachemo, A. C.; Zou, D. Effects of Adding Osmoprotectant on Anaerobic Digestion of Kitchen Waste with High Level of Salinity. *J. Biosci. Bioeng.* **2019**, *128*, 723−732.
(9) Martin, D. D.; Ciulla, R. A.; Roberts, M. F. Osmoadaptation in Archaea. *Appl. Environ. Microbiol.* **1999**, *65*, 1815−1825.
(10) Vyrides, I.; Santos, H.; Mingote, A.; Ray, M. J.; Stuckey, D. C. Are Compatible Solutes Compatible with Biological Treatment of Saline Wastewater? Batch and Continuous Studies Using Submerged Anaerobic Membrane Bioreactors (SAMBRs). *Environ. Sci. Technol.* **2010**, *44*, 7437−7442.
(11) Grammann, K.; Volke, A.; Kunte, H. J. New Type of Osmoregulated Solute Transporter Identified in Halophilic Members of the Bacteria Domain: TRAP Transporter TeaABC Mediates Uptake of Ectoine and Hydroxyectoine in Halomonas Elongata DSM 2581T. *J. Bacteriol.* **2002**, *184*, 3078−3085.
(12) Vanwonterghem, I.; Evans, P. N.; Parks, D. H.; Jensen, P. D.; Woodcroft, B. J.; Hugenholtz, P.; Tyson, G. W. Methylotrophic Methanogenesis Discovered in the Archaeal Phylum Verstraetearchaeota. *Nat. Microbiol.* **2016**, *1*, 16170.
(13) Müller, V.; Spanheimer, R.; Santos, H. Stress Response by Solute Accumulation in Archaea. *Curr. Opin. Microbiol.* **2005**, *8*, 729−736.
(14) Kadam, P. C.; Boone, D. R. Influence of PH on Ammonia Accumulation and Toxicity in Halophilic, Methylotrophic Methanogens. *Appl. Environ. Microbiol.* **1996**, *62*, 4486−4492.
(15) Buckel, W.; Thauer, R. K. Flavin-Based Electron Bifurcation, Ferredoxin, Flavodoxin, and Anaerobic Respiration With Protons (Ech) or NAD+ (Rnf) as Electron Acceptors: A Historical Review. *Front. Microbiol.* **2018**, *9*, 401.
(16) Liu, P.; Lu, Y. Concerted Metabolic Shifts Give New Insights into the Syntrophic Mechanism between Propionate-Fermenting Pelotomaculum Thermopropionicum and Hydrogenotrophic Methanocella Conradii. *Front. Microbiol.* **2018**, *9*, 1551.
(17) Megaw, J.; Gilmore, B. F. Archaeal Persisters: Persister Cell Formation as a Stress Response in Haloferax Volcanii. *Front. Microbiol.* **2017**, *8*, 1589.
(18) Nobu, M. K.; Narihiro, T.; Rinke, C.; Kamagata, Y.; Tringe, S. G.; Woyke, T.; Liu, W.-T. Microbial Dark Matter Ecogenomics Reveals Complex Synergistic Networks in a Methanogenic Bioreactor. *ISME J.* **2015**, *9*, 1710. —Supplementary Information—35
(19) Lie, T. J.; Costa, K. C.; Lupa, B.; Korpole, S.; Whitman, W. B.; Leigh, J. A. Essential Anaplerotic Role for the Energy-Converting Hydrogenase Eha in Hydrogenotrophic Methanogenesis. *Proc. Natl. Acad. Sci.* **2012**, *109*, 15473−15478.
(20) Lovley, D. R.; Klug, M. J. Methanogenesis from Methanol and Methylamines and Acetogenesis from Hydrogen and Carbon Dioxide in the Sediments of a Eutrophic Lake †. *Appl. Environ. Microbiol.* **1983**, *45*, 1310−1315.
(21) Smith, M. R.; Mah, R. A. Growth and Methanogenesis by Methanosarcina Strain 227 on Acetate and Methanol. *Appl. Environ. Microbiol.* **1978**, *36*, 870−879.
(22) Schauer-Gimenez, A. E.; Zitomer, D. H.; Maki, J. S.; Struble, C. A. Bioaugmentation for Improved Recovery of Anaerobic Digesters after Toxicant Exposure. *Water Res.* **2010**, *44*, 3555−3564.
(23) Van Lier, J. B.; Grolle, K. C.; Frijters, C. T.; Stams, A. J.; Lettinga, G. Effects of Acetate, Propionate, and Butyrate on the Thermophilic Anaerobic Degradation of Propionate by Methanogenic Sludge and Defined Cultures. *Appl. Environ. Microbiol.* **1993**, *59*, 1003−1011.
(24) Keller, A.; Schink, B.; Müller, N. Alternative Pathways of Acetogenic Ethanol and Methanol Degradation in the Thermophilic Anaerobe Thermacetogenium Phaeum. *Front. Microbiol.* **2019**, *10*, 423.
(25) Fujishima, S.; Miyahara, T.; Noike, T. Effect of Moisture Content on Anaerobic Digestion of Dewatered Sludge: Ammonia Inhibition to Carbohydrate Removal and Methane Production. *Water Sci. Technol.* **2000**, *41*, 119−127.
(26) Yan, M.; Fotidis, I. A.; Tian, H.; Khoshnevisan, B.; Treu, L.; Tsapekos, P.; Angelidaki, I. Acclimatization Contributes to Stable Anaerobic Digestion of Organic Fraction of Municipal Solid Waste under Extreme Ammonia Levels: Focusing on Microbial Community Dynamics. *Bioresour. Technol.* **2019**, *286*, 121376.
(27) Westerholm, M.; Levén, L.; Schnürer, A. Bioaugmentation of Syntrophic Acetate-Oxidizing Culture in Biogas Reactors Exposed to Increasing Levels of Ammonia. *Appl. Environ. Microbiol.* **2012**, *78*, 7619−7625.
(28) Yang, Z.; Wang, W.; Liu, C.; Zhang, R.; Liu, G. Mitigation of Ammonia Inhibition through Bioaugmentation with Different Microorganisms during Anaerobic Digestion: Selection of Strains and Reactor Performance Evaluation. *Water Res.* **2019**, *155*, 214−224.
(29) Sorokin, D. Y.; Makarova, K. S.; Abbas, B.; Ferrer, M.; Golyshin, P. N.; Galinski, E. A.; Ciordia, S.; Mena, M. C.; Merkel, A. Y.; Wolf, Y. I.; van Loosdrecht, M. C. M.; Koonin, E. V. Discovery of Extremely Halophilic, Methyl-Reducing Euryarchaea Provides Insights into the Evolutionary Origin of Methanogenesis. *Nat. Microbiol.* **2017**, *2*, 17081.
(30) Wang, T.; Zhang, D.; Dai, L.; Dong, B.; Dai, X. Magnetite Triggering Enhanced Direct Interspecies Electron Transfer: A Scavenger for the Blockage of Electron Transfer in Anaerobic Digestion of High-Solids Sewage Sludge. *Environ. Sci. Technol.* **2018**, *52*, 7160−7169.
(31) Ruiz-Sánchez, J.; Campanaro, S.; Guivernau, M.; Fernández, B.; Prenafeta-Boldú, F. X. Effect of Ammonia on the Active Microbiome and Metagenome from Stable Full-Scale Digesters. *Bioresour. Technol.* **2018**, *250*, 513−522.
(32) Xia, Y.; Wang, Y.; Fang, H. H.; Jin, T.; Zhong, H.; Zhang, T. Thermophilic Microbial Cellulose Decomposition and Methanogenesis Pathways Recharacterized by Metatranscriptomic and Metagenomic Analysis. *Sci. Rep.* **2014**, *4*, 6708.
(33) Campanaro, S.; Treu, L.; Rodriguez-R, L. M.; Kovalovszki, A.; Ziels, R. M.; Maus, I.; Zhu, X.; Kougias, P. G.; Basile, A.; Luo, G. New Insights from the Biogas Microbiome by Comprehensive Genome-Resolved Metagenomics of Nearly 1600 Species Originating from Multiple Anaerobic Digesters. *Biotechnol. Biofuels* **2020**, *13*, 1−18.
(34) Liu, H.; Chen, Y. Enhanced Methane Production from Food Waste Using Cysteine To Increase Biotransformation ofl-Monosaccharide, Volatile Fatty Acids, and Biohydrogen. *Environ. Sci. Technol.* **2018**, *52*, 3777−3785.
(35) Tian, H.; Karachalios, P.; Angelidaki, I.; Fotidis, I. A. A Proposed Mechanism for the Ammonia-LCFA Synergetic Co-Inhibition Effect on Anaerobic Digestion Process. *Chem. Eng. J.* **2018**, *349*, 574−580.
(36) Treu, L.; Kougias, P. G.; de Diego-Díaz, B.; Campanaro, S.; Bassani, I.; Fernández-Rodríguez, J.; Angelidaki, I. Two-Year Microbial Adaptation during Hydrogen-Mediated Biogas Upgrading Process in a Serial Reactor Configuration. *Bioresour. Technol.* **2018**, *264*, 140−147.
(37) Wick, R. R.; Judd, L. M.; Holt, K. E. Performance of Neural Network Basecalling Tools for Oxford Nanopore Sequencing. *Genome Biol.* **2019**, *20*, 129.
(38) Bankevich, A.; Nurk, S.; Antipov, D.; Gurevich, A. A.; Dvorkin, M.; Kulikov, A. S.; Lesin, V. M.; Nikolenko, S. I.; Pham, S.; Prjibelski, A. D.; Pyshkin, A. V.; Sirotkin, A. V.; Vyahhi, N.; Tesler, G.; Alekseyev, M. A.; Pevzner, P. A. SPAdes: A New Genome Assembly Algorithm and Its Applications to Single-Cell Sequencing. *J. Comput. Biol.* **2012**, *19*, 455−477.
(39) Bertrand, D.; Shaw, J.; Kalathiyappan, M.; Ng, A. H. Q.; Kumar, M. S.; Li, C.; Dvornicic, M.; Soldo, J. P.; Koh, J. Y.; Tong, C.; Ng, O. T.; Barkham, T.; Young, B.; Marimuthu, K.; Chng, K. R.; Sikic, M.; Nagarajan, N. Hybrid Metagenomic Assembly Enables High-Resolution Analysis of Resistance Determinants and Mobile Elements in Human Microbiomes. *Nat. Biotechnol.* **2019**, *37*, 937−944.
(40) Li, D.; Liu, C.-M.; Luo, R.; Sadakane, K.; Lam, T.-W. MEGAHIT: An Ultra-Fast Single-Node Solution for Large and Complex Metagenomics Assembly via Succinct de Bruijn Graph. *Bioinformatics* **2015**, *31*, 1674−1676.

https://dx.doi.org/10.1021/acs.est.0c01945
Environ. Sci. Technol. 2020, 54, 12568−12582

(41) Gurevich, A.; Saveliev, V.; Vyahhi, N.; Tesler, G. QUAST: Quality Assessment Tool for Genome Assemblies. *Bioinformatics* **2013**, *29*, 1072−1075.
(42) Langmead, B.; Salzberg, S. L. Fast Gapped-Read Alignment with Bowtie 2. *Nat. Methods* **2012**, *9*, 357.
(43) Li, H.; Handsaker, B.; Wysoker, A.; Fennell, T.; Ruan, J.; Homer, N.; Marth, G.; Abecasis, G.; Durbin, R. The Sequence Alignment/Map Format and SAMtools. *Bioinformatics* **2009**, *25*, 2078−2079.
(44) Tsuji, J. M.; Tran, N.; Schiff, S. L.; Venkiteswaran, J. J.; Molot, L. A.; Tank, M.; Hanada, S.; Neufeld, J. D. Genomic Potential for Photoferrotrophy in a Seasonally Anoxic Boreal Shield Lake. *bioRxiv* **2020**, 653014.
(45) Rodriguez-R, L. M.; Gunturu, S.; Tiedje, J. M.; Cole, J. R.; Konstantinidis, K. T. Nonpareil 3: Fast Estimation of Metagenomic Coverage and Sequence Diversity. *mSystems* **2018**, *3*, No. e00039.
(46) Varghese, N. J.; Mukherjee, S.; Ivanova, N.; Konstantinidis, K. T.; Mavrommatis, K.; Kyrpides, N. C.; Pati, A. Microbial Species Delineation Using Whole Genome Sequences. *Nucleic Acids Res.* **2015**, *43*, 6761−6771.
(47) Chaumeil, P.-A.; Mussig, A. J.; Hugenholtz, P.; Parks, D. H. GTDB-Tk: A Toolkit to Classify Genomes with the Genome Taxonomy Database. *Bioinformatics* **2020**, *36*, 1925−1927.
(48) von Meijenfeldt, F. A. B.; Arkhipova, K.; Cambuy, D. D.; Coutinho, F. H.; Dutilh, B. E. Robust Taxonomic Classification of Uncharted Microbial Sequences and Bins with CAT and BAT. *Genome Biol.* **2019**, *20*, 217.
(49) Hyatt, D.; Chen, G.-L.; LoCascio, P. F.; Land, M. L.; Larimer, F. W.; Hauser, L. J. Prodigal: Prokaryotic Gene Recognition and Translation Initiation Site Identification. *BMC Bioinf.* **2010**, *11*, 119.
(50) Buchfink, B.; Xie, C.; Huson, D. H. Fast and Sensitive Protein Alignment Using DIAMOND. *Nat. Methods* **2015**, *12*, 59−60.
(51) Treu, L.; Campanaro, S.; Kougias, P. G.; Sartori, C.; Bassani, I.; Angelidaki, I. Hydrogen-Fueled Microbial Pathways in Biogas Upgrading Systems Revealed by Genome-Centric Metagenomics. *Front. Microbiol.* **2018**, *9*, 1079.
(52) Kanehisa, M.; Sato, Y.; Morishima, K. BlastKOALA and GhostKOALA: KEGG Tools for Functional Characterization of Genome and Metagenome Sequences. *J. Mol. Biol.* **2016**, *428*, 726−731.
(53) Eren, A. M.; Esen, Ö. C.; Quince, C.; Vineis, J. H.; Morrison, H. G.; Sogin, M. L.; Delmont, T. O. Anvi'o: An Advanced Analysis and Visualization Platform for 'omics Data. *PeerJ* **2015**, *3*, No. e1319.
(54) Machado, D.; Andrejev, S.; Tramontano, M.; Patil, K. R. Fast Automated Reconstruction of Genome-Scale Metabolic Models for Microbial Species and Communities. *Nucleic Acids Res.* **2018**, *46*, 7542−7553.
(55) Mendes-Soares, H.; Mundy, M.; Soares, L. M.; Chia, N. MMinte: An Application for Predicting Metabolic Interactions among the Microbial Species in a Community. *BMC Bioinf.* **2016**, *17*, 343.
(56) Bowers, R. M.; Kyrpides, N. C.; Stepanauskas, R.; Harmon-Smith, M.; Doud, D.; Reddy, T. B. K.; Schulz, F.; Jarett, J.; Rivers, A. R.; Eloe-Fadrosh, E. A.; Tringe, S. G.; Ivanova, N. N.; Copeland, A.; Clum, A.; Becraft, E. D.; Malmstrom, R. R.; Birren, B.; Podar, M.; Bork, P.; Weinstock, G. M.; Garrity, G. M.; Dodsworth, J. A.; Yooseph, S.; Sutton, G.; Glöckner, F. O.; Gilbert, J. A.; Nelson, W. C.; Hallam, S. J.; Jungbluth, S. P.; Ettema, T. J. G.; Tighe, S.; Konstantinidis, K. T.; Liu, W.-T.; Baker, B. J.; Rattei, T.; Eisen, J. A.; Hedlund, B.; McMahon, K. D.; Fierer, N.; Knight, R.; Finn, R.; Cochrane, G.; Karsch-Mizrachi, I.; Tyson, G. W.; Rinke, C.; Lapidus, A.; Meyer, F.; Yilmaz, P.; Parks, D. H.; Murat Eren, A.; Schriml, L.; Banfield, J. F.; Hugenholtz, P.; Woyke, T. Minimum Information about a Single Amplified Genome (MISAG) and a Metagenome-Assembled Genome (MIMAG) of Bacteria and Archaea. *Nat. Biotechnol.* **2017**, *35*, 725−731.
(57) Campanaro, S.; Treu, L.; Kougias, P. G.; Luo, G.; Angelidaki, I. Metagenomic Binning Reveals the Functional Roles of Core Abundant Microorganisms in Twelve Full-Scale Biogas Plants. *Water Res.* **2018**, *140*, 123−134.
(58) Yan, M.; Treu, L.; Campanaro, S.; Tian, H.; Zhu, X.; Khoshnevisan, B.; Tsapekos, P.; Angelidaki, I.; Fotidis, I. A. Effect of Ammonia on Anaerobic Digestion of Municipal Solid Waste: Inhibitory Performance, Bioaugmentation and Microbiome Functional Reconstruction. *Chem. Eng. J.* **2020**, *401*, 126159.
(59) Tian, H.; Yan, M.; Treu, L.; Angelidaki, I.; Fotidis, I. A. Hydrogenotrophic Methanogens Are the Key for a Successful Bioaugmentation to Alleviate Ammonia Inhibition in Thermophilic Anaerobic Digesters. *Bioresour. Technol.* **2019**, *293*, 122070.
(60) Kougias, P. G.; Campanaro, S.; Treu, L.; Zhu, X.; Angelidaki, I. A Novel Archaeal Species Belonging to Methanoculleus Genus Identified via De-Novo Assembly and Metagenomic Binning Process in Biogas Reactors. *Anaerobe* **2017**, *46*, 23−32.
(61) Anderson, I. J.; Sieprawska-Lupa, M.; Lapidus, A.; Nolan, M.; Copeland, A.; Glavina Del Rio, T.; Tice, H.; Dalin, E.; Barry, K.; Saunders, E.; Han, C.; Brettin, T.; Detter, J. C.; Bruce, D.; Mikhailova, N.; Pitluck, S.; Hauser, L.; Land, M.; Lucas, S.; Richardson, P.; Whitman, W. B.; Kyrpides, N. C. Complete Genome Sequence of Methanoculleus Marisnigri Romesser et al. 1981 Type Strain JR1. *Stand. Genomic Sci.* **2009**, *1*, 189−196.
(62) Zhu, X.; Campanaro, S.; Treu, L.; Seshadri, R.; Ivanova, N.; Kougias, P. G.; Kyrpides, N.; Angelidaki, I. Metabolic Dependencies Govern Microbial Syntrophies during Methanogenesis in an Anaerobic Digestion Ecosystem. *Microbiome* **2020**, *8*, 22.
(63) Oehler, D.; Poehlein, A.; Leimbach, A.; Müller, N.; Daniel, R.; Gottschalk, G.; Schink, B. Genome-Guided Analysis of Physiological and Morphological Traits of the Fermentative Acetate Oxidizer Thermacetogenium Phaeum. *BMC Genom.* **2012**, *13*, 723.
(64) Kremp, F.; Poehlein, A.; Daniel, R.; Müller, V. Methanol Metabolism in the Acetogenic Bacterium Acetobacterium Woodii. *Environ. Microbiol.* **2018**, *20*, 4369−4384.
(65) Smith, S. G.; Rouvière, P. E. Purification and characterization of the reduced-nicotinamide-dependent 2,2′-dithiodiethanesulfonate reductase from Methanobacterium thermoautotrophicum delta H. *J. Bacteriol.* **1990**, *172*, 6435−6441.
(66) Kaster, A.-K.; Moll, J.; Parey, K.; Thauer, R. K. Coupling of Ferredoxin and Heterodisulfide Reduction via Electron Bifurcation in Hydrogenotrophic Methanogenic Archaea. *Proc. Natl. Acad. Sci.* **2011**, *108*, 2981−2986.
(67) Bar-Even, A.; Noor, E.; Milo, R. A Survey of Carbon Fixation Pathways through a Quantitative Lens. *J. Exp. Bot.* **2012**, *63*, 2325−2342.
(68) Hilpert, W.; Dimroth, P. On the Mechanism of Sodium Ion Translocation by Methylmalonyl-CoA Decarboxylase from Veillonella Alcalescens. *Eur. J. Biochem.* **1991**, *195*, 79−86.
(69) Springsteen, G.; Yerabolu, J. R.; Nelson, J.; Rhea, C. J.; Krishnamurthy, R. Linked Cycles of Oxidative Decarboxylation of Glyoxylate as Protometabolic Analogs of the Citric Acid Cycle. *Nat. Commun.* **2018**, *9*, 91.
(70) Fontana, A.; Kougias, P. G.; Treu, L.; Kovalovszki, A.; Valle, G.; Cappa, F.; Morelli, L.; Angelidaki, I.; Campanaro, S. Microbial Activity Response to Hydrogen Injection in Thermophilic Anaerobic Digesters Revealed by Genome-Centric Metatranscriptomics. *Microbiome* **2018**, *6*, 194.
(71) Kougias, P. G.; Campanaro, S.; Treu, L.; Tsapekos, P.; Armani, A.; Angelidaki, I. Spatial Distribution and Diverse Metabolic Functions of Lignocellulose-Degrading Uncultured Bacteria as Revealed by Genome-Centric Metagenomics. *Appl. Environ. Microbiol.* **2018**, *84*, No. e01244.
(72) Lins, P.; Schwarzenauer, T.; Reitschuler, C.; Wagner, A. O.; Illmer, P. Methanogenic Potential of Formate in Thermophilic Anaerobic Digestion. *Waste Manag. Res.* **2012**, *30*, 1031.
(73) Imachi, H. Pelotomaculum Thermopropionicum Gen. Nov., Sp. Nov., an Anaerobic, Thermophilic, Syntrophic Propionate-Oxidizing Bacterium. *Int. J. Syst. Evol. Microbiol.* **2002**, *52*, 1729−1735.
(74) Maus, I.; Wibberg, D.; Stantscheff, R.; Stolze, Y.; Blom, J.; Eikmeyer, F.-G.; Fracowiak, J.; König, H.; Pühler, A.; Schlüter, A. Insights into the annotated genome sequence of Methanoculleus

bourgensis MS2T, related to dominant methanogens in biogas-producing plants. *J. Biotechnol.* **2015**, *201*, 43−53.
(75) Yan, D.; Ikeda, T. P.; Shauger, A. E.; Kustu, S. Glutamate Is Required to Maintain the Steady-State Potassium Pool in Salmonella Typhimurium. *Proc. Natl. Acad. Sci.* **1996**, *93*, 6527−6531.
(76) Manzoor, S.; Schnürer, A.; Bongcam-Rudloff, E.; Müller, B. Complete Genome Sequence of Methanoculleus Bourgensis Strain MAB1, the Syntrophic Partner of Mesophilic Acetate-Oxidising Bacteria (SAOB). *Stand. Genomic Sci.* **2016**, *11*, 80.
(77) Schauer, N. L.; Ferry, J. G. Metabolism of Formate in Methanobacterium Formicicum. *J. Bacteriol.* **1980**, *142*, 800−807.

https://dx.doi.org/10.1021/acs.est.0c01945
Environ. Sci. Technol. 2020, 54, 12568−12582

Chapter 3

Genome-Scale Metabolic Modeling of the Human Microbiome in the Era of Personalized Medicine

Almut Heinken[1], **Arianna Basile**[2], Johannes Hertel[1,3], Cyrille Thinnes[1], Ines Thiele[1,4,5,*]

Annual Review of Microbiology, Volume 75, September 2021
https://doi.org/10.1146/annurev-micro-060221-012134

[1]School of Medicine, National University of Ireland, Galway, H91 TK33, Ireland
[2]Department of Biology, University of Padua, Padua 35121, Italy
[3]Department of Psychiatry and Psychotherapy, University of Greifswald, 17489 Greifswald, Germany
[4]Division of Microbiology, National University of Ireland, Galway, H91 TK33, Ireland
[5]APC Microbiome Ireland, University College Cork, Cork, T12 K8AF, Ireland

* Corresponding author

Annual Review of Microbiology

Genome-Scale Metabolic Modeling of the Human Microbiome in the Era of Personalized Medicine

Almut Heinken,[1] Arianna Basile,[2] Johannes Hertel,[1,3] Cyrille Thinnes,[1] and Ines Thiele[1,4,5]

[1]School of Medicine, National University of Ireland, Galway, H91 TK33, Ireland; email: ines.thiele@nuigalway.ie

[2]Department of Biology, University of Padua, Padua 35121, Italy

[3]Department of Psychiatry and Psychotherapy, University of Greifswald, 17489 Greifswald, Germany

[4]Division of Microbiology, National University of Ireland, Galway, H91 TK33, Ireland

[5]APC Microbiome Ireland, University College Cork, Cork, T12 K8AF, Ireland

Annu. Rev. Microbiol. 2021. 75:10.1–10.24

The *Annual Review of Microbiology* is online at micro.annualreviews.org

https://doi.org/10.1146/annurev-micro-060221-012134

Keywords

personalized medicine, constraint-based reconstruction and analysis, metabolic modeling, gut microbiome, metabolomics

Abstract

The human microbiome plays an important role in human health and disease. Meta-omics analyses provide indispensable data for linking changes in microbiome composition and function to disease etiology. Yet, the lack of a mechanistic understanding of, e.g., microbiome-metabolome links hampers the translation of these findings into effective, novel therapeutics. Here, we propose metabolic modeling of microbial communities through constraint-based reconstruction and analysis (COBRA) as a complementary approach to meta-omics analyses. First, we highlight the importance of microbial metabolism in cardiometabolic diseases, inflammatory bowel disease, colorectal cancer, Alzheimer disease, and Parkinson disease. Next, we demonstrate that microbial community modeling can stratify patients and controls, mechanistically link microbes with fecal metabolites altered in disease, and identify host pathways affected by the microbiome. Finally, we outline our vision for COBRA modeling combined with

meta-omics analyses and multivariate statistical analyses to inform and guide clinical trials, yield testable hypotheses, and ultimately propose novel dietary and therapeutic interventions.

Contents

1. INTRODUCTION: THE HUMAN MICROBIOME

1.1. Overview of the Human Microbiome

The human gut microbiome performs essential functions for human health, such as maturation of the host immune system, host cell proliferation, maintenance of intestinal endocrine functions, protection against pathogens, and digestion of food (3, 84, 121). Changes in gut microbiome composition and activity have been linked to noncommunicable diseases, such as inflammatory bowel disease, obesity, type 2 diabetes, colorectal cancer (CRC), and cardiovascular disease (30, 83, 84, 131, 170), as well as to neurological and neurodegenerative diseases (27).

The human microbiome consists of bacteria, archaea, fungi, eukaryotes, and viruses (82, 128). Of the bacterial residents, the majority belong to the *Bacteroidetes* and *Firmicutes* phyla, with smaller constituencies of other phyla, such as *Actinobacteria*, *Fusobacteria*, *Proteobacteria*, and *Verrucomicrobia* (82, 128). The relative fractions of these phyla differ greatly even between healthy individuals, with species and even phyla varying in abundance by more than an order of magnitude (82). Other body sites carrying microbiomes include the mouth, skin, lung, and urogenital tract (82, 128). These microbiomes differ in composition from the gut microbiome and also between individuals (82, 128). Host factors that influence the composition of the microbiome include age; sex; location; ethnicity; and lifestyle, including diet, exercise, and medication (3, 76, 93, 155). In contrast, the functional capabilities of the microbiome are much more conserved (82, 128), and it is believed that there is a core healthy microbiome with a set of functions that promote stable interactions with the host and that are partially specific to body site (82). Accordingly, the study of the microbiome has moved beyond the question "Who is there?" to "What are they doing?"

In this review, we discuss how meta-omics, constraint-based metabolic modeling, and multivariate statistics can complement each other to elucidate functional host-microbiome interactions, with the ultimate aim to gain insight into the role of the human microbiome in health and disease.

1.2. Meta-Omics Methods to Study the Microbiome

Modern microbiome research became possible with the advent of culture-independent analysis techniques, namely, 16S rRNA sequencing and whole-genome shotgun metagenomic sequencing (39, 74, 120). In 16S rRNA sequencing, a specific microbial amplicon, namely, the bacterial 16S rRNA gene, is sequenced and then matched to reference taxa (39). In whole-genome shotgun sequencing, some or all reads are sequenced and used to determine the members of a microbiome and their species- or strain-level abundances (39, 120, 162). Both techniques are commonly grouped under metagenomic sequencing. Additionally, metagenomic analysis is used for functional profiling on the level of protein-coding sequences (16, 39). For an in-depth overview of metagenomic sequencing, refer to References 74 and 81.

One fundamental limitation of metagenomics is that, while one can elucidate the community composition of the microbiome, it is not possible to directly measure community activity (39). To functionally profile the microbiome and elucidate its activity ("What are they doing?"), techniques such as metatranscriptomics, metaproteomics, and metabolomics are used (39). In metatranscriptomics, the mRNAs present in a fecal sample are sequenced, yielding information on genes expressed by the microbiome community (12). In the metaproteomic analysis, the abundance of proteins expressed by the microbiome community is measured through mass spectrometry combined with taxonomic analyses (117).

The most immediate and direct view of the activity of a biological system, such as the gut microbiome, can be obtained through metabolomics. Metabolomics measures the metabolite concentrations in a biofluid, tissue, or cell and provides a direct readout of the current metabolic activity of a biological system (158). As such, metabolomics is well-suited for the development of biomarkers for drug-intervention strategies or for monitoring disease progression. Different strategies of metabolomic analysis can be used depending on the biological question: targeted analysis (97) or global (or untargeted) metabolomic profiling (44). In targeted analysis, only a defined group of metabolites is investigated. In contrast, global metabolomic profiling allows the detection of a broad range of metabolites, aiming to outline a comprehensive profile of the metabolome. According to the origin of the samples, two applications are possible: metabolomic fingerprinting (96) and metabolomic footprinting (28, 75). Both high-throughput fingerprinting and footprinting methods enable sample classification and screening. The main difference between the two is that in the latter, samples are drawn from the extracellular fluids and therefore represent the exometabolome or secretome (62). For an overview of metabolomic methods in human microbiome research and their advantages and drawbacks, please refer to References 25 and 132.

To improve our understanding of the human microbiome's structure and function, ideally, multiple omics techniques are combined into a multi-omics analysis (89, 154, 168). This integration enables the taxonomical and functional characterization of the microbiome and is a crucial step toward insight into the role of the microbiome in disease states and exploiting the microbiome for medical applications (89, 168). However, integrative analysis of multiple omics data types is not trivial, e.g., due to the difference in timescales and data sparsity (74). To facilitate multi-omics data integration, computational pipelines (e.g., 38); statistical methods, such as Procrustes analysis (45), partial least-squares (20), and canonical correlation analysis (159); and machine learning methods (95) are used (74, 168). More recently, network-based models have been proposed as a valuable complementary approach to gain mechanistic insight by integrating multi-omics microbiome data (78, 119, 168).

1.3. Microbiome-Metabolome Interactions

The human fecal metabolome consists of at least 1,800 unique metabolites, many of which are derived from the gut microbiome (69). The fecal metabolome can be viewed as a functional readout of the microbiome, as the variance in the fecal metabolome could be largely explained by the gut microbial composition (171). Metabolites of gut microbial origin have also been found in plasma (150), urine (150), and cerebrospinal fluid (152). Microbial metabolites, such as indole-3-propionate and hippurate, show much greater variation in the plasma metabolome than human-derived metabolites do, suggesting that they could be modulated by targeting the microbiome (150). Moreover, gut microbes impact the host metabolome in distant organs and cells, such as the liver (103), adipocytes (17), and brain (33, 99). Many of these human-microbial cometabolites have been implicated in diseases (**Figure 1**; **Supplemental Figures 1** and **2**, **Supplemental Table 1**).

Gut microbial metabolites vary between individuals both qualitatively and quantitatively (150), yet it remains challenging to link these variations to specific taxa. In a small but growing number of studies, e.g., gnotobiotic animal studies, metabolites have been mechanistically linked to specific microbes. For instance, the production of indole-3-propionate depended solely on the presence of *Clostridium sporogenes* in an animal study (156).The anti-inflammatory metabolite indoleacrylate is produced by the commensal *Peptostreptococcus russellii* (160). However, due to the ease of application, most studies employ only statistical methods to link abundances of microbial taxa with metabolite concentrations. For instance, trimethylamine-*N*-oxide (TMAO), a metabolite implicated in cardiovascular disease, correlated positively with *Prevotella* sp. and negatively with *Faecalibacterium prausnitzii* (110), but the mechanisms behind such microbe-metabolite correlations remain unknown. Identification of potential mechanisms can be facilitated through network-based models approaches, such as constraint-based modeling (78, 168).

2. THE CONSTRAINT-BASED MODELING APPROACH IN A NUTSHELL

Constraint-based reconstruction and analysis (COBRA) is a mechanistic metabolic modeling approach that relies on biochemically detailed genome-scale reconstructions of the target organism's metabolism (109). These genome-scale reconstructions are traditionally built through manual curation efforts from the organisms' annotated genome as well as its known biochemical and physiological traits (144). Genome-scale reconstructions are available for over 7,000 organisms from all three domains of life (48, 52) and can be converted into mathematical models that take the form of a stoichiometric matrix with metabolites as the rows and reactions as the columns (**Figure 2*a***). Constraint-based modeling applies physicochemical constraints, such as mass conservation; operates under the steady-state assumption such that the change in metabolite concentration over time is zero; and consequently allows for computational exploration of the resulting feasible steady-state solution space (111). Further constraints are imposed on the model through the use of condition-specific data, such as meta-omics data and allowed uptake of nutrients (**Figure 2*a***) (109).

Recent advances in constraint-based modeling have led to the development of multiscale modeling frameworks that allow for the simulation of metabolic interactions between microbe-microbe pairs and within small-scale communities (122, 133, 149, 173) and, more recently, the metabolic properties of the microbiome communities with hundreds of members (53). The large-scale microbiome models can be generated by mapping metagenomic sequencing data onto a reference set of sequenced strains with available genome-scale reconstructions and then integrating the corresponding reconstructions (133). To further facilitate the application of constraint-based

modeling to human microbiome research (e.g., investigation of host-microbiome cometabolism), a resource of 773 manually curated genome-scale reconstructions of human gut microbes, AGORA (assembly of gut organisms through reconstruction and analysis), has been developed (86) and subsequently been expanded (52). Ultimately, modeling the human microbiome could improve our understanding of the roles of individual species and microbial communities in human health and disease (133, 149).

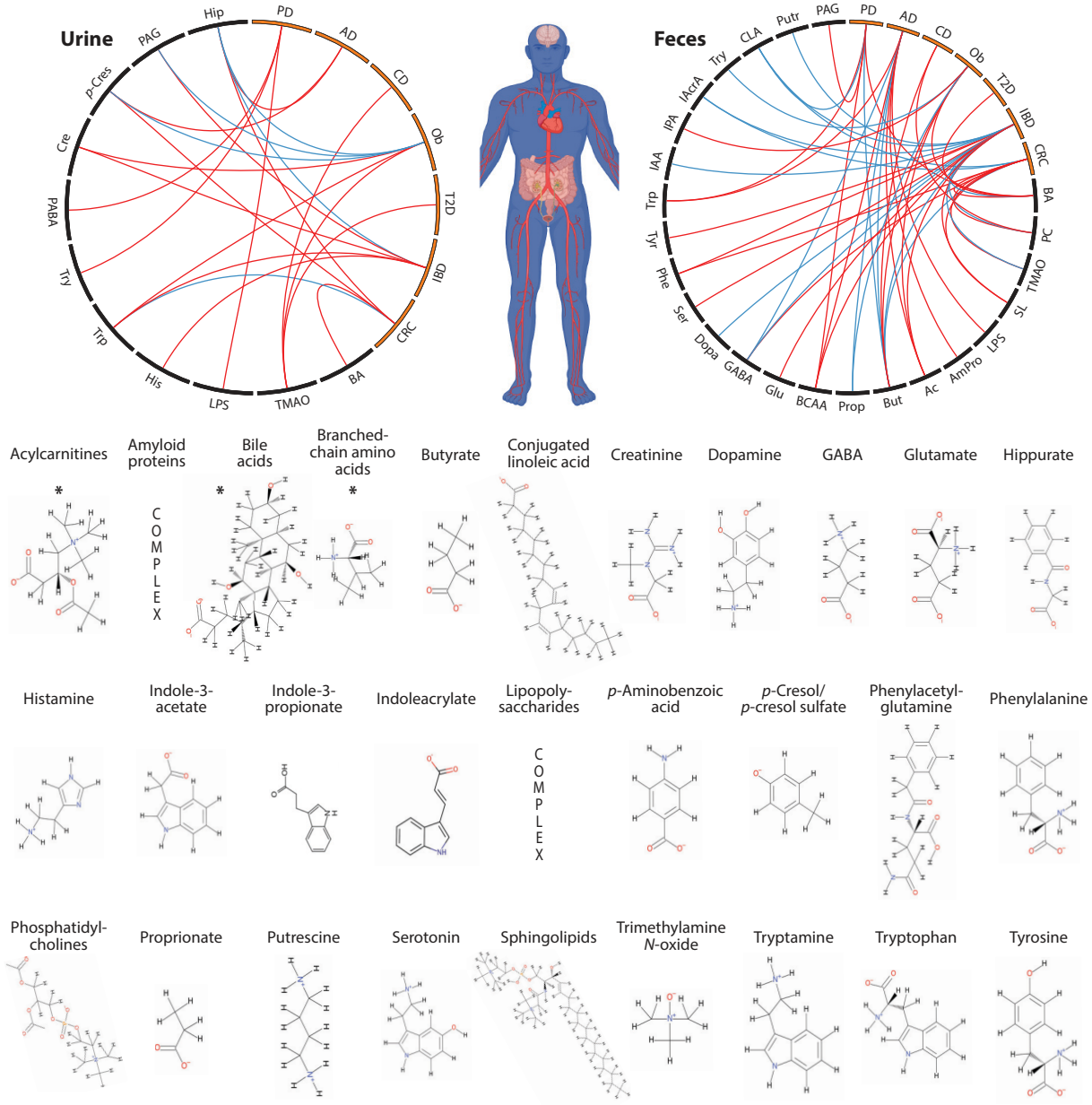

(*Caption appears on following page*)

Figure 1 (*Figure appears on preceding page*)

Human-microbial cometabolites (*black*) implicated in diseases (*orange*). Shown are the main metabolite variations reported for (*left*) urinary and (*right*) fecal samples in the diseases discussed in this review. The links are blue if the metabolite was decreased in patients compared to healthy controls, and red otherwise. If available, the structures of the metabolites are provided. The asterisk indicates metabolite groups that encompass multiple individual metabolites (see **Supplemental Table 1**). Metabolite variations reported for plasma and cerebrospinal fluid samples can be found in **Supplemental Figures 1** and **2**, respectively. Abbreviations: Ac, acylcarnitine; AD, Alzheimer disease; AmPro, amyloid protein; BA, bile acid; BCAA, branched-chain fatty acid; But, butyrate; CD, Crohn disease; CLA, conjugated linoleic acid; CRC, colorectal cancer; Cre, creatinine; Dopa, dopamine; GABA, γ-aminobutyric acid; Glu, glutamate; Hip, hippurate; His, histamine; IAA, indole-3-acetate; IAcrA, indoleacrylate; IBD, inflammatory bowel disease; IPA, indole-3-propionate; LPS, lipopolysaccharide; Ob, obesity; PABA, *p*-aminobenzoic acid; PAG, phenylacetylglutamine; PC, phosphatidylcholine; *p*-cres, *p*-cresol/*p*-cresol sulfate; PD, Parkinson disease; Prop, propionate; Putr, putrescine; Ser, serotonin; SL, sphingolipid; TMAO, trimethylamine-*N*-oxide; Try, tryptamine; T2D, type 2 diabetes. Figure adapted from images of the human body created with BioRender.com.

3. MODELING HOST-MICROBIOME-DIET INTERACTIONS IN METABOLIC AND NEURODEGENERATIVE DISEASES

3.1. Cardiometabolic Diseases

Lifestyle factors, such as a Westernized diet, which is high in sugar and low in fiber, and a lack of exercise, are main causes for the development of cardiometabolic diseases (137). There is increasing evidence that the gut microbiome and its metabolites are important in the development of associated diseases, e.g., obesity (30, 123), type 2 diabetes (57, 170), non-alcoholic fatty liver disease (NAFLD) (63), nonalcoholic steatohepatitis (21), and cardiovascular disease (22). Notably, short-chain fatty acids (SCFAs), mainly produced by gut microbe fermentation of fiber, can influence host metabolism through multiple routes that protect the host from obesity and glucose intolerance, including serving as carbon sources for colonocytes, promoting gluconeogenesis, acting as histone deacetylase inhibitors, and functioning as signaling molecules (137). Trimethylamine, a microbial metabolite of choline and carnitine that is converted to TMAO in the liver, plays a causal role in cardiovascular disease (22) and may also be implicated in type 2 diabetes (170) and NAFLD (63). Increased levels of branched-chain amino acids are biomarkers for insulin resistance and risk of type 2 diabetes (123). Other host-microbial cometabolites, such as secondary bile acids, have also been implicated in obesity, type 2 diabetes, NAFLD, and nonalcoholic steatohepatitis (21, 30, 79, 170) (**Figure 1**; **Supplemental Figures 1** and **2**, **Supplemental Table 1**).

As cardiometabolic diseases are strongly linked to changes in metabolic pathways, COBRA modeling is an attractive approach to interrogate how underlying genetic, dietary, and gut microbial factors intersect and to propose personalized therapies (104). For instance, Mardinoglu et al. (90) used a tissue-specific genome-scale reconstruction of the hepatocyte to create personalized models of liver metabolism for 86 NAFLD patients. The modeling combined with animal experiments revealed disturbed redox balance in NAFLD and suggested supplementation with NAD^+ and glutathione precursors as a treatment (90). Similar personalized modeling efforts can also readily integrate condition-specific host models with models of the microbiome. In one study, the abundances of five common gut microbial species in 45 obese and overweight subjects after a dietary intervention were determined and the metabolic interactions between the five species were simulated in silico (136). Microbial amino acid biosynthesis by the five species has been predicted and found to differ between individuals with low and high microbial gene richness, as previously determined based on metagenomic sequencing (136). In another study, genome-scale reconstructions were used to systematically interrogate the metabolic capabilities of four gut bacterial strains that increased in abundance in type 2 diabetes patients after metformin treatment (127). Ultimately, the aim is to formulate personalized dietary interventions that take the microbiome into account so as to prevent metabolic diseases (76).

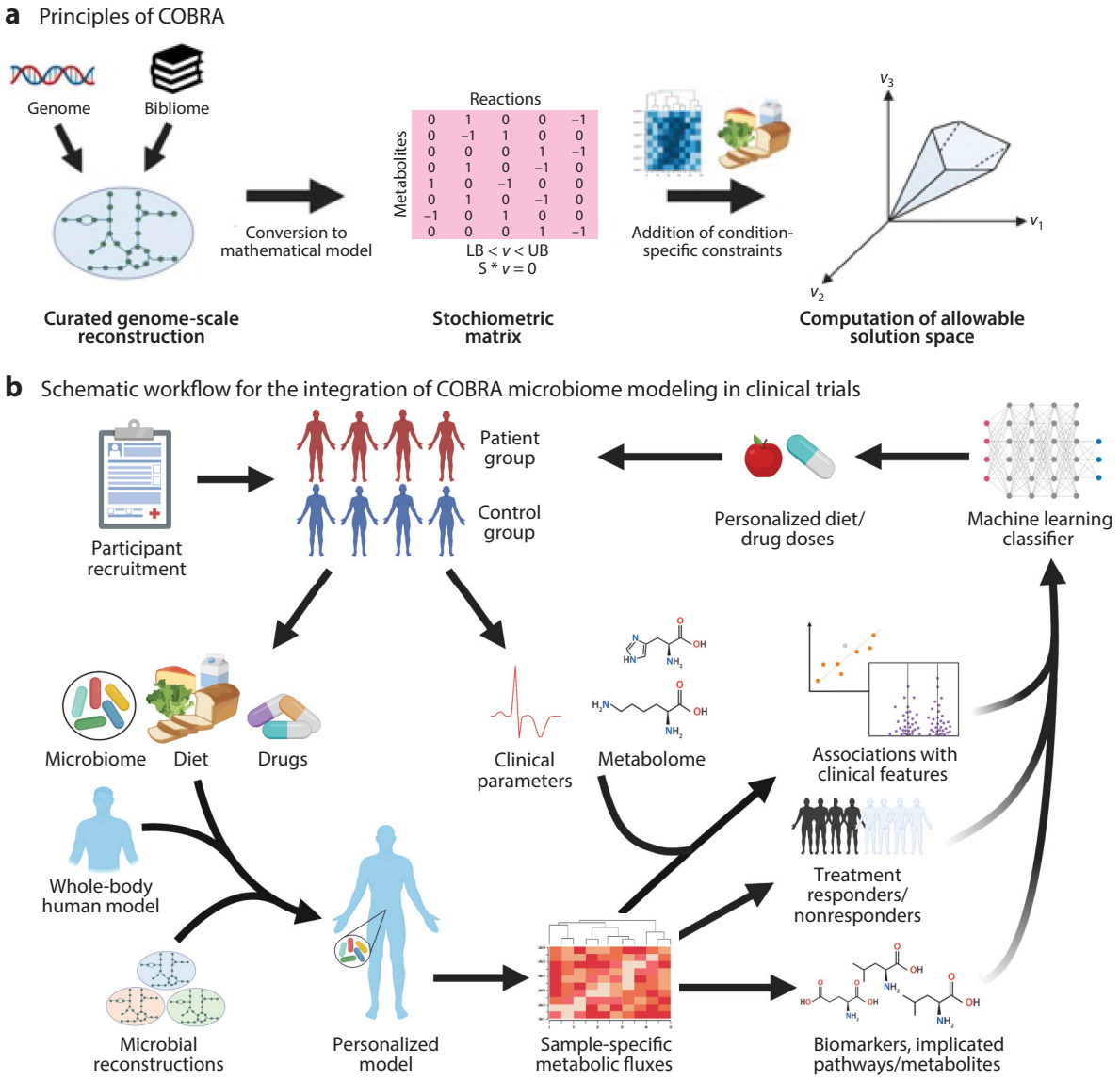

Figure 2

The COBRA approach and its application to personalized medicine. (*a*) Overview of the COBRA approach, consisting of manual curation of a genome-scale metabolic reconstruction, conversion of the reconstruction to a condition-specific mathematical model through the contextualization of the reconstruction with condition-specific data, and computation of allowed steady-state flux states. (*b*) Schematic workflow for the integration of COBRA microbiome modeling to inform and guide clinical trials. Here, participants are first comprehensively characterized, including with regard to the metagenome, the metabolome, and clinical parameters. Next, personalized microbiome community models are created from a collection of microbial reconstructions, AGORA (52, 86), combined with a human organ-resolved whole-body metabolic reconstruction (145) and contextualized with metabolome data, clinical parameters, dietary information, and drug use. Computed sample-specific metabolic fluxes are stratified and associated with clinical features through multivariate statistics. Finally, through machine learning methods, classifiers may be constructed that can be used to propose personalized treatment. Abbreviations: AGORA, assembly of gut organisms through reconstruction and analysis; COBRA, constraint-based reconstruction and analysis. Figure adapted from images created with BioRender.com.

3.2. Inflammatory Bowel Disease

Inflammatory bowel disease (IBD) describes a group of diseases characterized by chronic inflammation of the gastrointestinal tract that have a prevalence of about 0.3% since 2019 in the Western world and increasing incidence in developing countries (100, 131). Based on the location and extent of the inflammation, two main subtypes can be distinguished, Crohn disease (CD) and ulcerative colitis (131). IBD has been linked to host genetics and environmental factors, such as antibiotic exposure in childhood (131). The gut microbiome also plays an important role in IBD, where, for example, host signaling to the microbiome is disrupted (131). IBD patients generally have a dysbiotic microbiota characterized by decreases in abundances of beneficial butyrate-producing microbes, such as *Roseburia* spp. and *Faecalibacterium prausnitzii*, and increases in abundances of potentially proinflammatory microbes, such as *Escherichia coli* and *Ruminococcus gnavus* (64, 131). Broad changes in the fecal metabolome have been observed in IBD patients (40), reflecting altered microbial activity (130) (**Figure 1**). As a result of the reduction in butyrate-producing clostridia, fecal butyrate, which is protective against inflammation, is decreased in IBD patients (64, 80). Increased concentrations of fecal amino acids have also been observed in IBD patients (102). In contrast, tryptophan levels in serum were decreased due to increased microbial degradation (105). Moreover, conversion of primary into secondary bile acids was reduced in IBD (40, 105).

Computational modeling has been recognized as a promising approach for mechanistically linking host-microbiome-environment interactions to IBD-related changes (29). For instance, constraint-based modeling has been used to test the oxygen hypothesis, which states that increased oxygen levels in the gut cause a shift toward facultative anaerobes, such as *E. coli*, in IBD (56). It has been found that in a community of *E. coli*, *Bacteroides thetaiotaomicron*, and *F. prausnitzii*, *E. coli* can outcompete the beneficial *F. prausnitzii* with increasing oxygen availability, as *E. coli* can achieve a much higher growth increase in the presence of oxygen than *F. prausnitzii* (56). In another study, a pangenome and pan-reactome analysis of 110 *E. coli* strains, including IBD-associated and non-IBD-associated strains, has been performed (36). Strains of the B2 phylogroup, which is associated with IBD, were enriched in capabilities enabling them to colonize the intestinal mucosa (36). Pangenome and pan-reactome analysis has also been performed for *E. coli* strains identified through metagenomic sequencing in a time series of stool samples from a CD patient (37). The strain that bloomed during peak inflammation was highly similar to known pathogenic *E. coli* strains (37).

Several studies have modeled the microbiome in IBD by mapping available 16S rRNA or metagenomic sequencing data onto the AGORA resource of gut microbial genome-scale reconstructions. In one study using publicly available metagenomic data, personalized microbiome models have been built for a cohort of pediatric CD patients, age-matched controls, and a cohort of healthy human adults (55). For each sample, the microbiome's combined potential to deconjugate primary bile acids and convert them to secondary bile acids has been predicted. Microbiomes of CD patients had significantly lower conversion potential for the secondary bile acid 12-dehydrocholate and a trend toward less primary bile acid deconjugation (55). Accordingly, increased fecal primary bile acid levels had been observed in CD patients, which also suggested reduced secondary bile acid conversion (40). Taking advantage of the model's ability to predict fluxes in a strain-resolved manner, the strain-level contributions to overall bile acid metabolism have been computed and found to be distinct in CD patient microbiomes (55). In a follow-up study using the same cohort of CD patients and controls, the complete metabolome and the strains contributing to each metabolite were systematically explored (54). The simulations predicted that the secretion potential across multiple metabolic subsystems was significantly different in dysbiotic microbiomes of CD patients compared to those of controls

and nondysbiotic microbiomes of subjects with IBD (54).The analysis of strain contributions to metabolites revealed that the predicted increased potential for microbial amino acid biosynthesis in dysbiotic microbiomes of CD patients was due to contributions of *Proteobacteria* (54). These predictions agreed with metabolomic findings of increased fecal amino acid concentrations in the same cohort, which correlated with *Proteobacteria* abundance (102). These examples illustrate how metabolic modeling can provide valuable, novel insight into microbe-metabolite relationships and help overcome the difficulty of disentangling human and microbial contributions to fecal metabolites (102). Importantly, neither transcriptomic nor metabolomic data were used as input data for the modeling; hence, the predicted amino acid–*Proteobacteria* relationships emerged in an unbiased manner from the capabilities present in the metabolic networks.

Another study used a similar personalized modeling approach to characterize the altered metabolic capabilities of microbiomes in subjects with IBD (163). Sample-specific microbiome metabolic networks were constructed from biopsies of subjects with multiple IBD subtypes and healthy controls (163). The abundances of several vitamin and lipid metabolism pathways differed between CD and ulcerative colitis and between IBD subtypes and controls, revealing subtype-specific disturbances in the gut microbial network (163). Furthermore, the gut microbiomes of controls and IBD patients and rheumatic disease patients treated with anti–tumor necrosis factor (anti-TNF) therapy were modeled (2). By mapping 16S rRNA data onto AGORA, Aden et al. (2) predicted microbe-microbe interactions and the potential for metabolic cross feeding in patients and controls. Antagonistic interactions and the potential for metabolic cross feeding decreased in IBD patients, with the latter being alleviated in patients achieving remission after anti-TNF therapy (2). Furthermore, the efficacy of treatment in IBD was similarly evaluated through metabolic modeling (34). 16S rRNA sequencing was performed for IBD patients treated with either anti-TNF or azathioprine at three time points. With the use of microbiome community modeling, microbial butyrate production potential was found to be higher in patients achieving remission, especially those treated with azathioprine, demonstrating the efficacy of this drug (34). In another effort to predict the outcome of treatment in silico, individual-specific dietary supplementation to improve SCFA production in IBD patients with dysbiosis has been predicted (13).

Taken together, these studies showcase how constraint-based microbial community modeling can elucidate host-microbiome-metabolome links in IBD. Moreover, modeling has been shown to be predictive for treatment success. Building on these efforts, personalized microbial community modeling could ultimately be used to propose personalized microbiome-targeted dietary or drug interventions or to predict patients' responses to treatment.

3.3. Colorectal Cancer

CRC is the second-most common cause of cancer death in the world, and its incidence is increasing (66). Most CRC cases have been associated with diet and lifestyle factors; heritability plays only a minor role (83). Environmental factors have been estimated to contribute 70–90% to CRC etiology, most important among them being a diet low in fiber and high in red meat (66). A role for the microbiome in CRC pathology has long been recognized. However, unlike stomach cancer, CRC has not been linked to a specific pathogen. Rather, an oncogenic, dysbiotic microbiome is thought to promote genotoxicity and inflammation (66). Several organisms have been consistently found to be increased in the gut in CRC patients, including *Fusobacterium nucleatum*, *Peptostreptococcus* spp., *Porphyromonas* spp., *Parvimonas micra*, and *Gemella morbillorum* (66, 142). A microbial signature consisting of 29 species, including the aforementioned, has been found to be specific for CRC (157). Moreover, species such as *E.coli* and *F. nucleatum* have been shown to increase tumor load in animal models (66).

Host-microbial cometabolism plays an important role in CRC (**Figure 1**; **Supplemental Table 1**). Microbes produce genotoxic metabolites, such as hydrogen sulfide, amino acid breakdown products, and the secondary bile acid deoxycholic acid, whereas the SCFA butyrate appears to have both pro- and antitumorigenic effects (66, 83, 142). Other microbial metabolites also accumulate in CRC (142). To improve our understanding of the role of the microbiome in tumorigenesis (142), tissue-specific, constraint-based models have been used to gain insight into metabolic differences in cancer cells (7, 19, 31, 164), with some studies focusing on metabolic reprogramming in CRC cells (8, 153, 167). Several constraint-based modeling works have also included the microbiome to elucidate metabolic host-microbe interactions in CRC. For instance, an integrated in silico and in vitro modeling framework to investigate host-microbe-diet interactions in CRC has been developed (47). In the HuMiX gut-on-a-chip model (135), colon adenocarcinoma cells have been grown together with probiotic *Lactobacillus rhamnosus* GG (LGG) on two dietary regimes, one rich in prebiotic fiber and one rich in simple sugars. An in silico model has been constructed by joining a cell type–specific model of colon adenocarcinoma cells with the AGORA reconstruction of LGG and using parameters mimicking the in vitro model. The combined modeling revealed that the symbiotic regime of LGG and the high-fiber diet downregulated carcinogenic and proinflammatory pathways in cancer cells (47). Moreover, diet-dependent cross feeding has been observed between the cancer cells and LGG. Both in vitro and in silico, LGG produced less lactate, which can serve as fuel for cancer cells (142), on the high-fiber diet (47). In a different study, species and metabolites that are abundant in CRC have been identified (42). The capabilities of 1,544 reconstructed strains to grow on 26 metabolites that are abundant in CRC have been computed. Species that are abundant in CRC showed significantly increased ability to exploit metabolites that are abundant in CRC as carbon and energy sources, suggesting that the tumor environment favors growth of these bacteria (42).

Sample-specific differences in microbiome-cancer interactions have also been modeled. The microbiomes of paired tumor tissue, adjacent colonic tissue and mucosa samples, and normal tissue from CRC patients have been sequenced, and microbiome models for each sample have been constructed (50). The simulated production of hydrogen sulfide has been predicted to be higher in tumor samples compared to controls (50). Overall hydrogen sulfide fluxes did not correlate with amino acid concentrations in colonic tissue; however, hydrogen sulfide production by *Fusobacterium* significantly correlated with amino acid concentrations (50). These results indicate that flux-concentration relationships are complex and individual species contributions matter. Moreover, they suggest a role for fusobacterial metabolism of amino acids in CRC. Follow-up work confirmed the relationship between microbial hydrogen sulfide production and increased amino acid concentrations (49). In another effort aiming at stratifying CRC microbiomes from healthy microbiomes, gut microbiome models have been constructed for a cohort of CRC patients and controls (161), and the SCFA potential has been predicted (60). The simulations were then validated against fecal metabolomic data from the same individuals (60). The integrated statistical analysis of model-derived fluxes and fecal metabolomics revealed that the higher the abundance of *Fusobacterium* spp., the higher the potential of the microbiome to convert lysine to glutarate and the lower the butyrate production potential (60). The lysine-to-glutarate pathway is present in *Fusobacterium* (60), suggesting again a role for amino acid metabolism by this genus in CRC. Intriguingly, species-butyrate associations predicted by the models agreed very well with fecal metabolomic measurements for the same cohort even though the metabolomic data had not been used as input for the modeling (60).

Taken together, these studies demonstrate that metabolic modeling can guide the interpretation of metabolomic measurements in an unbiased manner and suggest a role for microbial amino acid metabolism, especially by *Fusobacterium* spp., with a corresponding decrease in carbohydrate

degradation to butyrate, in CRC. In agreement with this, an increase in microbial genes for amino acid metabolism and a reduction in carbohydrate metabolism genes in the metagenomes of CRC patients had been previously observed (157).

3.4. Neurodegenerative Diseases

Neurodegenerative diseases are becoming a major cause of mortality and disease burden due to aging of populations (35). In addition to genetic and lifestyle factors, the gut microbiome has also been implicated in the etiology of these multifactorial diseases (27).

3.4.1. The microbiota-gut-brain axis. The gastrointestinal tract influences brain function through bidirectional communication, including the function of the vagus nerve, the enteric nervous system, and the immune system and signaling to enteroendocrine cells (27). The gut microbiome plays an important role in this bidirectional communication, leading to the concept of the gut-brain axis (27). The microbiome synthesizes bio- and neuroactive metabolites that signal to the host. It can thus be considered an additional endocrine organ (26). Microbial metabolites implicated in the microbiota-gut-brain axis include SCFAs, branched-chain amino acids, secondary bile acids, neurotransmitters, tryptophan, and indoles (27). For instance, the gut microbiome regulates the bioavailability of tryptophan, which affects both the biosynthesis of serotonin and the kynurenine pathway (71). Gut microbes also directly synthesize neurotransmitters, such as γ-aminobutyric acid (GABA), serotonin, and histamine (26, 27). Consequently, the gut microbiome has been implicated in behavior, cognition, and mood, including psychological (e.g., depression), psychiatric (e.g., schizophrenia), neurodevelopmental (e.g., autism spectrum disorder), and neurodegenerative diseases (27).

In conclusion, there is strong evidence for a link between the gut microbiome and brain health via the gut-brain axis (77, 85). Here, we discuss these gut microbiome-disease links, and opportunities for metabolic modeling, for the most common neurodegenerative diseases, Alzheimer disease (AD) and Parkinson disease (PD).

3.4.2. Alzheimer Disease. AD is characterized by the accumulation of β-amyloid plaques and of an abnormal form of tau protein in the brain (4). Besides the most prominent syndrome of mild to severe dementia and cognitive impairment, AD patients can experience various symptomatologies, ranging from aphasia and disturbed sleep to hallucinations and dysphagia (141). Furthermore, AD has a high rate of comorbidity with diabetes and is associated with a wide range of metabolic perturbations occurring especially in the first phases of the disease (101, 146). Several studies have highlighted a role for the gut microbiome in AD (18, 46). For instance, detrimental metabolites produced by the gut microbiota have been linked to increased permeability of the intestinal barrier (leaky gut) and of the blood-brain barrier (124) and inflammation in the gut, the enteric nervous system, and the central nervous system (169). Due to aging and vascular deficits, neurotoxic microbial metabolites can leak into the systemic circulation and reach the brain. Gut microbes, such as *E. coli*, synthesize amyloids and therefore play a causal role in amyloid plaque formation in the brain (41). AD has come to be viewed as, at least partially, a metabolic disease (**Figure 1**; **Supplemental Figures 1** and **2**, **Supplemental Table 1**), with brain aging associated with inflammation, mitochondrial dysfunction, and dysregulated energy metabolism (92).

Metabolic modeling has been used to explore mechanistic links between changes in brain metabolism and cognitive symptoms. For example, transcriptomic data from AD patients have been integrated with a genome-scale reconstruction of the brain to identify metabolic signatures (134). In other studies, gene regulatory networks were constructed for brains in AD (115, 165). In a recent effort to gain insight into changes in brain metabolism associated with AD, personalized

genome-scale models for seven brain regions have been constructed from 2,114 postmortem brain samples. There were significant differences in flux through bile acid and cholesterol metabolic pathways in the brain between AD and control samples (11). A link between cognitive decline and changes in ratios between primary and secondary bile acids in individuals with mild cognitive impairment and individuals with AD has been highlighted previously (87; **Supplemental Table 1**).

3.4.3. Parkinson disease. PD is a complex, progressive neurological disorder that is increasingly prevalent with age, affecting an estimated seven to ten million people worldwide (6). The disease is caused by progressing degeneration of dopaminergic neurons in the substantia nigra (68). While the core syndrome of PD is characterized by a complex of motor symptoms, such as tremor and rigidity (140), PD also manifests in the periphery, with patients displaying systemic inflammation (1) and prominent gastrointestinal problems, especially constipation (139). Although treatments to partially alleviate symptoms of motor dysfunction are available (5), no neuroprotective treatment has been established to slow progression of PD, which inevitably renders patients incapable of living independently.

Interestingly, the gastrointestinal component often presents itself decades before the onset of the neurological syndrome (129), leading to the controversial hypothesis that PD starts in the gut and may be triggered by the gut microbiome (43, 94). Noteworthy, a wealth of studies have shown that in PD the microbiome is substantially altered in composition and function (108). Despite the heterogeneity of the results, a certain pattern emerged, with increases in some genera, such as *Bifidobacterium*, *Lactobacillus*, *Akkermansia*, and *Bilophila*, and decreases in others, such as *Lachnospira* and *Faecalibacterium* (10, 94, 108). These changes also translate into possible differences in microbiome function. For instance, evidence from fecal metabolomics integrated with microbiome measurements points toward decreased SCFA production in PD (148). Based on pathway enrichment, Bedarf et al. (14) found alterations in β-glucuronate and tryptophan metabolism. The microbial abundance pattern, however, depended on age, sex, medication, and constipation (10, 61), highlighting that the changes of the microbiome in PD must be considered in the context of the individual's treatment and physiological attributes. Importantly, it is unclear from these human observational studies whether the PD-associated changes are a consequence of PD-associated gastrointestinal problems or a causative factor. Experiments with rodent models (94), however, suggest a microbial contribution to disease etiology and severity.

Few studies have used constraint-based modeling to elucidate changes in metabolic function in PD. In one study, simulations of metabolic states in PD were conducted using a central-metabolic model of the dopaminergic nerve cell (24). Utilizing microbial community modeling together with longitudinal blood metabolome data, Hertel et al. (59) showed that the longitudinal patterns of sulfur-containing metabolites, such as methionine, cystathionine, and taurine, are altered in blood in PD, while PD-related microbiomes were predicted to have higher secretion potentials for products of microbial sulfur metabolism, such as sulfate and hydrogen sulfide. Microbial community models revealed in this context a special role for the known proinflammatory microbe *Bilophila wadsworthia* (98), which has been demonstrated to be increased in PD (10, 59). In accordance, given that *B. wadsworthia* is associated with stage of disease after statistical adjustment for age and disease duration, it may be a marker of rapid progression of PD (10). Interestingly, *B. wadsworthia* can utilize taurine for ATP production, generating sulfate and hydrogen sulfide, which is a rare capability among gut microbes (116). Accordingly, taurine overflow in the gut leads to overgrowth of *B. wadsworthia* (98). Taurine, being an inhibitory neurotransmitter, is known to be secreted by neurons under oxidative stress (106, 118), and there is evidence of it accumulating in the blood of PD patients over time (59). Thus, microbial community modeling in conjunction with longitudinal data points toward a microbiome-host interaction in the domain

of sulfur metabolism with potential clinical implications. However, experimental data are needed to validate these hypotheses, which are derived from human observational data.

4. METHODS FOR MICROBIOME MODELING IN SYSTEMS MEDICINE

The paradigm of systems medicine, or data-driven medical care, that is tailored to each patient has been proposed (15, 70). The microbiome especially has been emphasized as a potential therapeutic target, e.g., through tailored probiotics or dietary interventions (70). Designing such targeted interventions would require mechanistic systems biology models that can integrate meta-omics data (15). In this section, we describe how microbiome modeling could be integrated with the host and diet, expanded to include drug metabolism, and ultimately applied in systems medicine approaches in the clinic.

4.1. Statistical Analysis of Large-Scale Metabolic Models

The emergence of COBRA-based microbial community modeling (9, 32, 149) in conjunction with the widespread availability of 16S and metagenomic data has led to the possibility of analyzing microbiome community models at the human population level (2, 10, 55, 59, 163). In this paradigm, metagenomic samples are taken from individuals to measure the composition of the microbiome at a specific body site and are analyzed by combining microbiome COBRA community modeling with population statistics approaches, such as regression modeling or machine learning. Instead of investigating a single microbial community model assigned to an individual and the relationships between microbes and predicted metabolic capabilities, the statistical patterns across a population of microbial community models are analyzed. Consequently, a myriad of statistical approaches can be used to better understand the interplay between characteristics of the host, microbial abundances, and community functions. The need for statistical approaches is underlined by the fact that microbes share metabolic pathways across phyla (86), meaning that two communities different in their microbial composition may be functionally largely equivalent. An advantage of analyzing a population of microbial community models over other omics analysis techniques is that microbial community models already incorporate a wealth of biological context, making statistical associations easier to interpret (107).

A main output of a microbial community model is the predicted metabolic flux profile, which consists of, for example, computed net uptake and secretion fluxes for each metabolite that can be transported by at least one microbial community member (9). Higher-level attributes of biological relevance can be defined based on these metabolic flux profiles, for example, metrics of metabolic diversity (i.e., the number of metabolites a microbial community can produce) or patterns of metabolic equivalence (i.e., whether two microbial communities are equivalent with respect to their functions in a metabolic domain) (60). The attributes of in silico metabolic fluxes can be utilized in statistical screening, similarly to how they are used in omics-wide association studies (10) or in multivariate analyses, such as principal component analyses, or integrated with other omics data, such as metabolome data (59). A further application, yet to be explored, is the utilization of in silico secretion profiles in machine learning approaches on the level of the human population, which may enable patient stratification and treatment individualization (58).

Importantly, statistical analyses of microbial community models share the challenges common to statistical analyses of observational data (51, 114); thus, they also require careful analysis design. As with other omics data, spurious correlations due to confounding factors can occur. As metabolic fluxes are direct consequences of abundance patterns, they will be influenced by the same factors as the microbiome composition, e.g., age, sex, body mass index, medication, and other physiological and behavioral attributes of the host (10). Hence, statistical analyses need to be adjusted for basic

covariates, either by matching or by including relevant factors as covariates in the statistical modeling (151). Important in this context, it has been shown that neither linearity (59) nor additivity can be expected (10). For example, Baldini et al. (10) found that certain secretion fluxes showed a covariate-dependent association with PD, with constipation, sex, and age influencing the relationship between metabolic functions and PD. This dependency highlights the context specificity of microbe-host interactions. Neglecting the complex interplay between the host's attributes and microbial functions in the specification of statistical modeling will lead to false positives and lower statistical power to detect real associations.

In conclusion, population statistics analyses applied to microbial community models promise deeper insight into host-microbiome interactions in terms of metabolic functions if carefully designed and executed. Importantly, while they can be analyzed statistically as metagenomic or metabolomic data can, they have the additional advantage of having molecule- and organism-resolved biochemical networks in the background, meaning that the mechanisms behind statistical associations can be directly retrieved. Although this analysis paradigm has only recently been developed and many methodological innovations can be expected, the metabolic modeling studies that utilized population statistics (10, 59, 60) prove the feasibility and translational potential for the clinical sciences.

4.2. Integration of Microbiome Models with the Human Host

Microbiome metabolism is dynamically affected by host influences. Microbes metabolize and chemically modify components of the human diet, e.g., polyphenols (112); xenobiotics, such as drugs (138); and host-derived metabolites, such as mucin glycans (91), catechols (88), cholesterol (72), and bile acids (125). Conversely, microbiome-derived metabolites are consumed by the host and have systemic effects in health and disease states, as detailed above. Hence, metabolic modeling of these complex host-microbiome-diet interactions requires integrative computational frameworks.

Various generic genome-scale reconstructions of human metabolism as well as cell- and tissue-specific reconstructions are available (23, 126). In addition, sex-specific, organ-resolved, whole-body reconstructions of human metabolism (WBM) have accounted for over 30 organs and blood cells, resolved at the molecular level, anatomic correctness of organ connectivity through blood circulation, and human physiology (145). The whole-body metabolism (WBM) reconstructions can be personalized using physiological and dietary data as well as omics data, such as metabolomics data, resulting into personalized WBM models (145). Crucially, the WBM reconstructions also account for the stomach, small intestine, and large intestine, allowing for the anatomically correct integration of personalized gut microbiome community models with WBM models (145). This feature has been demonstrated by contextualizing male and female WBM models with sex, weight, height, and fecal microbiome composition of 149 healthy adults. In addition, corresponding personalized germ-free WBM models have been created (145). The enzymatic fluxes predicted in the human brain, colon, and liver demonstrated that microbiome presence has the potential to drastically impact host metabolism, with interindividual differences (145). Therefore, such WBM models open up attractive opportunities for the prediction of personalized, organ-resolved, and microbiome-dependent responses to dietary and therapeutic interventions as well as individual biomarkers (**Figure 2*b***).

4.3. Modeling Microbe-Drug Interactions

The gut microbiome also impacts the activity, efficacy, and safety of prescription drugs (138, 155). Microbial enzymes may, for example, activate prodrugs and metabolize drugs into inactive or even

toxic drug metabolites (138). Recent studies have shown that two-thirds of 271 tested drugs were subject to gut microbial metabolism (172) and that the drug conversion capabilities of 20 healthy donor microbiomes were distinct (67). These results highlight the importance of considering the microbiome when planning treatments to minimize adverse effects and increase the desired drug response. For instance, the cancer drug irinotecan causes diarrhea in up to 80% of patients due to microbial β-glucuronidase activity, impeding treatment, and in certain patients, up to 50% of the cardiac drug digoxin is inactivated by microbial cardiac glycoside reductase (138). Therefore, predicting who will be a nonresponder may enable personalized drug treatment strategies. Precision microbiome modeling may be useful for predicting the microbiome's potential to metabolize a given drug, but it is dependent on the reconstruction of microbial drug-metabolizing reactions resolved by strain and drug metabolite. In this respect, for a subset of microbial enzymes and about 50 drugs, direct or indirect drug-affecting activities have been experimentally demonstrated and the encoding genes are known (73, 138, 147). Consequently, an expanded AGORA resource, named AGORA2, has been created accounting for over 7,000 strains (52). For AGORA2, comparative genomic analyses have been performed for 15 microbial enzymes directly or indirectly involved in drug metabolism for over 5,000 strains, and drug-metabolizing reactions for 98 drugs were manually formulated and added to the appropriate genome-scale reconstructions (52). With AGORA2, microbial community models enable the personalized prediction of microbial drug conversion and allow for the stratification of individuals according to their predicted drug metabolism profiles.

4.4. Application of Personalized Modeling in Clinical Trials

COBRA microbiome modeling has enabled the interrogation of personalized models and the stratification of patients and controls for IBD, CRC, and PD. With the recent development of integrated microbiome-diet-WBM models (145), and human microbial genome-scale reconstructions accounting for microbial drug metabolism (52), the tools are in place to inform clinical trials by personalizing predictions of drug metabolism and disease biomarkers in a data-driven manner (143) (**Figure 2*b***).

One could imagine a clinical trial roadmap with microbial communities integrated into the WBM models at its core that is aimed at stratifying participants, proposing personalized treatment, and ultimately gaining insights into the underlying mechanism of disease etiology (**Figure 2*b***). In such a scenario, each individual is profiled, including with respect to the metagenome, the metabolome, clinical parameters, prescribed drug doses, and food frequency (74). Second, using available bioinformatics pipelines (reviewed in, e.g., 81, 162), the taxonomic compositions of each individual's gut microbiome would be determined to map organism abundances onto the expanded resource of human microbial genome-scale reconstructions (52) and to construct personalized models (9). Finally, the microbiome models would be integrated with WBM models tailored to the individual's physiology, diet, and drug use (145) to predict the corresponding metabolic profiles (145). Machine learning methods could be used to uncover informative flux patterns (166) and to develop classifiers for individually tailored drug doses and dietary regimens (**Figure 2*b***). Finally, multivariate statistics would be used to correlate the computed fluxes with clinical parameters to identify metabolites and pathways that are increased or depleted in different disease states (**Figure 2*b***). Overall, this process outlines how personalized, data-driven, multi-scale modeling using genome-scale reconstructions may lead to novel dietary, therapeutic, and microbiome-targeted interventions to digitally augment clinical trials. Equally, this constraint-based modeling framework could become part of in silico clinical trials, i.e., trials with virtual study groups based on individual-specific computational models (113).

5. OUTLOOK

In this review, we have described recent advances in genome-scale reconstruction and analysis of microbiome interactions. We have discussed advances in reconstruction building and method development that now enable the generation and interrogation of sample-specific microbial community models (**Figure 2*b***), which demonstrates the value of the COBRA approach to generate testable hypotheses and support fundamental research. Future applications will catalyze elucidation of dynamic and context-dependent physiological processes at an individual level toward the conceptualization of virtual humans and digital twins, i.e., digital mirror images of ourselves, to catalyze technologies enabling preclinical in silico testing for mechanism-based hypothesis generation, and in silico clinical trials. One might also envision the development of decision-support systems involving COBRA host-microbiome modeling, e.g., software as a medical device (SaMD).

In a preclinical environment, mechanism-based hypothesis generation may complement, guide, or even replace some of the traditional benchtop testing to catalyze fundamental science and drug discovery. In particular, modeling holistic systems—e.g., host-microbiome interactions, lifestyle factors, and environmental contributions—in addition to the inherent host biochemistry and physiology will enhance our understanding of human health on an individual level so as to address unmet needs for therapeutics. For instance, microbial community modeling enabled mechanistic linking of PD etiology and altered host-microbe cometabolites in the trans-sulfuration pathway (59), which can be tested and could open up the opportunity for therapeutic intervention, e.g., through diet or probiotics. Similar studies could be performed for other diseases for which effective therapies are urgently needed, such as cardiometabolic diseases and AD.

Digital clinical trial approaches already alleviate administrative burden by streamlining study management [including, for example, enrolling and informing subjects and obtaining their consent (65)] and may augment study design through virtual interaction with personal devices, continuous monitoring using sensor data (for example, from wearables), and fostering protocol adherence by means of personalized coaching. Beyond the digitization of traditional approaches, as outlined in Section 4.4, future in silico trials may involve study cohorts entirely composed of virtual humans to complement traditional physical clinical studies (113). These in silico clinical trials may rely, at least in part, on the constraint-based modeling framework, as delineated in **Figure 2*b***.

From an SaMD perspective, the integration of multifactorial health variables of subject-specific data, including, for example, molecular, microbial, clinical, and lifestyle data, may enable a holistic precision approach toward decision-support systems in the future. Variables such as nutrition, probiotics, and drug regimens may be optimized for an individual for a desired outcome. Continuous monitoring in conjunction with real-time analyses will enable individuals to quickly decide what adjustments to make based on their particular needs. Ultimately, individuals will be empowered to make health care decisions in collaboration with their treating physician based on SaMD-driven iterative holistic adjustments as opposed to relying on outcomes of singular medical assessments.

DISCLOSURE STATEMENT

The authors are not aware of any affiliations, memberships, funding, or financial holdings that might be perceived as affecting the objectivity of this review.

ACKNOWLEDGMENTS

This study was funded by grants from the European Research Council (ERC) under the European Union's Horizon 2020 research and innovation program (grant agreement number 757922) to I.T., by grants from the National Institute on Aging (1RF1AG058942-01 and 1U19AG063744-01) to I.T., and by the EMBO short-term fellowship 8720 to A.B.

LITERATURE CITED

1. Adams B, Nunes JM, Page MJ, Roberts T, Carr J, et al. 2019. Parkinson's disease: a systemic inflammatory disease accompanied by bacterial inflammagens. *Front. Aging Neurosci.* 11:210
2. Aden K, Rehman A, Waschina S, Pan WH, Walker A, et al. 2019. Metabolic functions of gut microbes associate with efficacy of tumor necrosis factor antagonists in patients with inflammatory bowel diseases. *Gastroenterology* 157:1279–92.e11
3. Alexander M, Turnbaugh PJ. 2020. Deconstructing mechanisms of diet-microbiome-immune interactions. *Immunity* 53:264–76
4. Alzheimer's Assoc. 2020. 2020 Alzheimer's disease facts and figures. *Alzheimers Dement*. 16:391–460
5. Armstrong MJ, Okun MS. 2020. Diagnosis and treatment of Parkinson disease: a review. *JAMA* 323:548–60
6. Ascherio A, Schwarzschild MA. 2016. The epidemiology of Parkinson's disease: risk factors and prevention. *Lancet Neurol.* 15:1257–72
7. Aurich MK, Fleming RMT, Thiele I. 2017. A systems approach reveals distinct metabolic strategies among the NCI-60 cancer cell lines. *PLOS Comput. Biol.* 13:e1005698
8. Auslander N, Cunningham CE, Toosi BM, McEwen EJ, Yizhak K, et al. 2017. An integrated computational and experimental study uncovers FUT9 as a metabolic driver of colorectal cancer. *Mol. Syst. Biol.* 13:956
9. Baldini F, Heinken A, Heirendt L, Magnusdottir S, Fleming RMT, Thiele I. 2018. The Microbiome Modeling Toolbox: from microbial interactions to personalized microbial communities. *Bioinformatics* 35:2332–34
10. Baldini F, Hertel J, Sandt E, Thinnes CC, Neuberger-Castillo L, et al. 2020. Parkinson's disease-associated alterations of the gut microbiome predict disease-relevant changes in metabolic functions. *BMC Biol.* 18:62
11. Baloni P, Funk CC, Yan J, Yurkovich JT, Kueider-Paisley A, et al. 2019. Identifying differences in bile acid pathways for cholesterol clearance in Alzheimer's disease using metabolic networks of human brain regions. bioRxiv 782987. **https://doi.org/10.1101/782987**
12. Bashiardes S, Zilberman-Schapira G, Elinav E. 2016. Use of metatranscriptomics in microbiome research. *Bioinform. Biol. Insights* 10:19–25
13. Bauer E, Thiele I. 2018. From metagenomic data to personalized in silico microbiotas: predicting dietary supplements for Crohn's disease. *NPJ Syst. Biol. Appl.* 4:27
14. Bedarf JR, Hildebrand F, Coelho LP, Sunagawa S, Bahram M, et al. 2017. Functional implications of microbial and viral gut metagenome changes in early stage L-DOPA-naïve Parkinson's disease patients. *Genome Med.* 9:39. Erratum. 2017. *Genome Med.* 9:61
15. Beger RD, Dunn W, Schmidt MA, Gross SS, Kirwan JA, et al. 2016. Metabolomics enables precision medicine: "A White Paper, Community Perspective". *Metabolomics* 12:149
16. Bharti R, Grimm DG. 2019. Current challenges and best-practice protocols for microbiome analysis. *Brief Bioinform.* 22:178–93
17. Bohan R, Tianyu X, Tiantian Z, Ruonan F, Hongtao H, et al. 2019. Gut microbiota: a potential manipulator for host adipose tissue and energy metabolism. *J. Nutr. Biochem.* 64:206–17
18. Bonfili L, Cecarini V, Gogoi O, Gong C, Cuccioloni M, et al. 2021. Microbiota modulation as preventative and therapeutic approach in Alzheimer's disease. *FEBS J.* 288:2836–55
19. Bordel S. 2018. Constraint based modeling of metabolism allows finding metabolic cancer hallmarks and identifying personalized therapeutic windows. *Oncotarget* 9:19716–29
20. Boulesteix AL, Strimmer K. 2007. Partial least squares: a versatile tool for the analysis of high-dimensional genomic data. *Brief Bioinform.* 8:32–44
21. Brandl K, Schnabl B. 2017. Intestinal microbiota and nonalcoholic steatohepatitis. *Curr. Opin. Gastroenterol.* 33:128–33
22. Brown JM, Hazen SL. 2018. Microbial modulation of cardiovascular disease. *Nat. Rev. Microbiol.* 16:171–81
23. Brunk E, Sahoo S, Zielinski DC, Altunkaya A, Drager A, et al. 2018. Recon3D enables a three-dimensional view of gene variation in human metabolism. *Nat. Biotechnol.* 36:272–81

24. Buchel F, Saliger S, Drager A, Hoffmann S, Wrzodek C, et al. 2013. Parkinson's disease: dopaminergic nerve cell model is consistent with experimental finding of increased extracellular transport of alpha-synuclein. *BMC Neurosci*. 14:136
25. Chen MX, Wang SY, Kuo CH, Tsai IL. 2019. Metabolome analysis for investigating host-gut microbiota interactions. *J. Formos. Med. Assoc.* 118(Suppl. 1):S10–22
26. Clarke G, Stilling RM, Kennedy PJ, Stanton C, Cryan JF, Dinan TG. 2014. Minireview: Gut microbiota; the neglected endocrine organ. *Mol. Endocrinol.* 28:1221–38
27. Cryan JF, O'Riordan KJ, Cowan CSM, Sandhu KV, Bastiaanssen TFS, et al. 2019. The microbiota-gut-brain axis. *Physiol. Rev.* 99:1877–2013
28. de Maistre S, Gaillard S, Martin JC, Richard S, Boussuges A, et al. 2020. Cecal metabolome fingerprint in a rat model of decompression sickness with neurological disorders. *Sci. Rep.* 10:15996
29. de Souza HSP, Fiocchi C. 2018. Network medicine: a mandatory next step for inflammatory bowel disease. *Inflamm. Bowel Dis.* 24:671–79
30. Delzenne NM, Rodriguez J, Olivares M, Neyrinck AM. 2020. Microbiome response to diet: focus on obesity and related diseases. *Rev. Endocr. Metab. Disord.* 21:369–80
31. Di Filippo M, Colombo R, Damiani C, Pescini D, Gaglio D, et al. 2016. Zooming-in on cancer metabolic rewiring with tissue specific constraint-based models. *Comput. Biol. Chem.* 62:60–69
32. Diener C, Gibbons SM, Resendis-Antonio O. 2020. MICOM: metagenome-scale modeling to infer metabolic interactions in the gut microbiota. *mSystems* 5:e00606-19
33. Dinan TG, Cryan JF. 2017. The microbiome-gut-brain axis in health and disease. *Gastroenterol. Clin. N. Am.* 46:77–89
34. Effenberger M, Reider S, Waschina S, Bronowski C, Enrich B, et al. 2021. Microbial butyrate synthesis indicates therapeutic efficacy of azathioprine in IBD patients. *J. Crohn's Colitis* 15:88–98
35. Erkkinen MG, Kim M, Geschwind MD. 2018. Clinical neurology and epidemiology of the major neurodegenerative diseases. *Cold Spring Harb. Perspect. Biol.* 10(4):a033118
36. Fang X, Monk JM, Mih N, Du B, Sastry AV, et al. 2018. *Escherichia coli* B2 strains prevalent in inflammatory bowel disease patients have distinct metabolic capabilities that enable colonization of intestinal mucosa. *BMC Syst. Biol.* 12:66
37. Fang X, Monk JM, Nurk S, Akseshina M, Zhu Q, et al. 2018. Metagenomics-based, strain-level analysis of *Escherichia coli* from a time-series of microbiome samples from a Crohn's disease patient. *Front. Microbiol.* 9:2559
38. Forsberg EM, Huan T, Rinehart D, Benton HP, Warth B, et al. 2018. Data processing, multi-omic pathway mapping, and metabolite activity analysis using XCMS Online. *Nat. Protoc.* 13:633–51
39. Franzosa EA, Hsu T, Sirota-Madi A, Shafquat A, Abu-Ali G, et al. 2015. Sequencing and beyond: integrating molecular 'omics' for microbial community profiling. *Nat. Rev. Microbiol.* 13:360–72
40. Franzosa EA, Sirota-Madi A, Avila-Pacheco J, Fornelos N, Haiser HJ, et al. 2019. Gut microbiome structure and metabolic activity in inflammatory bowel disease. *Nat. Microbiol.* 4:293–305
41. Friedland RP, Chapman MR. 2017. The role of microbial amyloid in neurodegeneration. *PLOS Pathog.* 13:e1006654
42. Garza DR, Taddese R, Wirbel J, Zeller G, Boleij A, et al. 2020. Metabolic models predict bacterial passengers in colorectal cancer. *Cancer Metab.* 8:3
43. Gershanik OS. 2018. Does Parkinson's disease start in the gut? *Arq. Neuropsiquiatr.* 76:67–70
44. Gika HG, Theodoridis GA, Plumb RS, Wilson ID. 2014. Current practice of liquid chromatography-mass spectrometry in metabolomics and metabonomics. *J. Pharm. Biomed. Anal.* 87:12–25
45. Gower JC. 1975. Generalized Procrustes analysis. *Psychometrika* 40:33–51
46. Goyal D, Ali SA, Singh RK. 2021. Emerging role of gut microbiota in modulation of neuroinflammation and neurodegeneration with emphasis on Alzheimer's disease. *Prog. Neuropsychopharmacol. Biol. Psychiatry* 106:110112
47. Greenhalgh K, Ramiro-Garcia J, Heinken A, Ullmann P, Bintener T, et al. 2019. Integrated in vitro and in silico modeling delineates the molecular effects of a synbiotic regimen on colorectal-cancer-derived cells. *Cell Rep.* 27:1621–32.e9
48. Gu C, Kim GB, Kim WJ, Kim HU, Lee SY. 2019. Current status and applications of genome-scale metabolic models. *Genome Biol.* 20:121

49. Hale VL, Jeraldo P, Chen J, Mundy M, Yao J, et al. 2018. Distinct microbes, metabolites, and ecologies define the microbiome in deficient and proficient mismatch repair colorectal cancers. *Genome Med.* 10:78
50. Hale VL, Jeraldo P, Mundy M, Yao J, Keeney G, et al. 2018. Synthesis of multi-omic data and community metabolic models reveals insights into the role of hydrogen sulfide in colon cancer. *Methods* 149:59–68
51. Hammer GP, du Prel JB, Blettner M. 2009. Avoiding bias in observational studies: part 8 in a series of articles on evaluation of scientific publications. *Dtsch. Arztebl. Int.* 106:664–68
52. Heinken A, Acharya G, Ravcheev DA, Hertel J, Nyga M, et al. 2020. AGORA2: Large scale reconstruction of the microbiome highlights wide-spread drug-metabolising capacities. bioRxiv 2020.11.09.375451. **https://doi.org/10.1101/2020.11.09.375451**
53. Heinken A, Basile A, Thiele I. 2021. Advances in constraint-based modelling of microbial communities. *Curr. Opin. Syst. Biol.* In press. **https://doi.org/10.1016/j.coisb.2021.05.007**
54. Heinken A, Hertel J, Thiele I. 2021. Metabolic modelling reveals broad changes in gut microbial metabolism in inflammatory bowel disease patients with dysbiosis. *npj Syst. Biol. Appl.* 7(1):19
55. Heinken A, Ravcheev DA, Baldini F, Heirendt L, Fleming RMT, Thiele I. 2019. Systematic assessment of secondary bile acid metabolism in gut microbes reveals distinct metabolic capabilities in inflammatory bowel disease. *Microbiome* 7:75
56. Henson MA, Phalak P. 2017. Microbiota dysbiosis in inflammatory bowel diseases: in silico investigation of the oxygen hypothesis. *BMC Syst. Biol.* 11:145
57. Herrema H, Niess JH. 2020. Intestinal microbial metabolites in human metabolism and type 2 diabetes. *Diabetologia* 63:2533–47
58. Hertel J, Frenzel S, Konig J, Wittfeld K, Fuellen G, et al. 2019. The informative error: a framework for the construction of individualized phenotypes. *Stat. Methods Med. Res.* 28:1427–38
59. Hertel J, Harms AC, Heinken A, Baldini F, Thinnes CC, et al. 2019. Integrated analyses of microbiome and longitudinal metabolome data reveal microbial-host interactions on sulfur metabolism in Parkinson's disease. *Cell Rep.* 29:1767–77.e8
60. Hertel J, Heinken A, Martinelli F, Thiele I. 2021. Integration of constraint-based modelling with faecal metabolomics reveals large deleterious effects of*Fusobacterium* spp. on community butyrate production. *Gut Microbes* 13(1):1–23
61. Hill-Burns EM, Debelius JW, Morton JT, Wissemann WT, Lewis MR, et al. 2017. Parkinson's disease and Parkinson's disease medications have distinct signatures of the gut microbiome. *Mov. Disord.* 32:739–49
62. Hollywood K, Brison DR, Goodacre R. 2006. Metabolomics: current technologies and future trends. *Proteomics* 6:4716–23
63. Houttu V, Boulund U, Grefhorst A, Soeters MR, Pinto-Sietsma SJ, et al. 2020. The role of the gut microbiome and exercise in non-alcoholic fatty liver disease. *Therap. Adv. Gastroenterol.* 13:1756284820941745
64. Imhann F, Vich Vila A, Bonder MJ, Fu J, Gevers D, et al. 2018. Interplay of host genetics and gut microbiota underlying the onset and clinical presentation of inflammatory bowel disease. *Gut* 67:108–19
65. Inan OT, Tenaerts P, Prindiville SA, Reynolds HR, Dizon DS, et al. 2020. Digitizing clinical trials. *NPJ Digit. Med.* 3:101
66. Janney A, Powrie F, Mann EH. 2020. Host-microbiota maladaptation in colorectal cancer. *Nature* 585:509–17
67. Javdan B, Lopez JG, Chankhamjon P, Lee YJ, Hull R, et al. 2020. Personalized mapping of drug metabolism by the human gut microbiome. *Cell* 181:1661–79.e22
68. Kalia LV, Lang AE. 2015. Parkinson's disease. *Lancet* 386:896–912
69. Karu N, Deng L, Slae M, Guo AC, Sajed T, et al. 2018. A review on human fecal metabolomics: methods, applications and the human fecal metabolome database. *Anal. Chim. Acta* 1030:1–24
70. Kashyap PC, Chia N, Nelson H, Segal E, Elinav E. 2017. Microbiome at the frontier of personalized medicine. *Mayo Clin. Proc.* 92:1855–64
71. Kennedy PJ, Cryan JF, Dinan TG, Clarke G. 2017. Kynurenine pathway metabolism and the microbiota-gut-brain axis. *Neuropharmacology* 112:399–412

72. Kenny DJ, Plichta DR, Shungin D, Koppel N, Hall AB, et al. 2020. Cholesterol metabolism by uncultured human gut bacteria influences host cholesterol level. *Cell Host Microbe* 28:245–57.e6
73. Klaassen CD, Cui JY. 2015. Review: mechanisms of how the intestinal microbiota alters the effects of drugs and bile acids. *Drug Metab. Dispos.* 43:1505–21
74. Knight R, Vrbanac A, Taylor BC, Aksenov A, Callewaert C, et al. 2018. Best practices for analysing microbiomes. *Nat. Rev. Microbiol.* 16:410–22
75. Knott ME, Manzi M, Zabalegui N, Salazar MO, Puricelli LI, Monge ME. 2018. Metabolic footprinting of a clear cell renal cell carcinoma in vitro model for human kidney cancer detection. *J. Proteome Res.* 17:3877–88
76. Kolodziejczyk AA, Zheng D, Elinav E. 2019. Diet-microbiota interactions and personalized nutrition. *Nat. Rev. Microbiol.* 17:742–53
77. Kowalski K, Mulak A. 2019. Brain-gut-microbiota axis in Alzheimer's disease. *J. Neurogastroenterol. Motil.* 25:48–60
78. Lamichhane S, Sen P, Dickens AM, Oresic M, Bertram HC. 2018. Gut metabolome meets microbiome: a methodological perspective to understand the relationship between host and microbe. *Methods* 149:3–12
79. Lang S, Schnabl B. 2020. Microbiota and fatty liver disease—the known, the unknown, and the future. *Cell Host Microbe* 28:233–44
80. Lavelle A, Sokol H. 2020. Gut microbiota-derived metabolites as key actors in inflammatory bowel disease. *Nat. Rev. Gastroenterol. Hepatol.* 17:223–37
81. Liu Y-X, Qin Y, Chen T, Lu M, Qian X, et al. 2021. A practical guide to amplicon and metagenomic analysis of microbiome data. *Protein Cell* 12:315–30
82. Lloyd-Price J, Abu-Ali G, Huttenhower C. 2016. The healthy human microbiome. *Genome Med.* 8:51
83. Louis P, Hold GL, Flint HJ. 2014. The gut microbiota, bacterial metabolites and colorectal cancer. *Nat. Rev. Microbiol.* 12:661–72
84. Lynch SV, Pedersen O. 2016. The human intestinal microbiome in health and disease. *N. Engl. J. Med.* 375:2369–79
85. Ma Q, Xing C, Long W, Wang HY, Liu Q, Wang RF. 2019. Impact of microbiota on central nervous system and neurological diseases: the gut-brain axis. *J. Neuroinflamm.* 16:53
86. Magnusdottir S, Heinken A, Kutt L, Ravcheev DA, Bauer E, et al. 2017. Generation of genome-scale metabolic reconstructions for 773 members of the human gut microbiota. *Nat. Biotechnol.* 35:81–89
87. MahmoudianDehkordi S, Arnold M, Nho K, Ahmad S, Jia W, et al. 2019. Altered bile acid profile associates with cognitive impairment in Alzheimer's disease—an emerging role for gut microbiome. *Alzheimer's Dement.* 15:76–92. Erratum. 2019. *Alzheimer's Dement.* 15:604
88. Maini Rekdal V, Nol Bernadino P, Luescher MU, Kiamehr S, Le C, et al. 2020. A widely distributed metalloenzyme class enables gut microbial metabolism of host- and diet-derived catechols. *eLife* 9:e50845
89. Mallick H, Ma S, Franzosa EA, Vatanen T, Morgan XC, Huttenhower C. 2017. Experimental design and quantitative analysis of microbial community multiomics. *Genome Biol.* 18:228
90. Mardinoglu A, Bjornson E, Zhang C, Klevstig M, Soderlund S, et al. 2017. Personal model-assisted identification of NAD^+ and glutathione metabolism as intervention target in NAFLD. *Mol. Syst. Biol.* 13:916
91. Martens EC, Neumann M, Desai MS. 2018. Interactions of commensal and pathogenic microorganisms with the intestinal mucosal barrier. *Nat. Rev. Microbiol.* 16:457–70
92. Mattson MP, Arumugam TV. 2018. Hallmarks of brain aging: adaptive and pathological modification by metabolic states. *Cell Metab.* 27:1176–99
93. McBurney MI, Davis C, Fraser CM, Schneeman BO, Huttenhower C, et al. 2019. Establishing what constitutes a healthy human gut microbiome: state of the science, regulatory considerations, and future directions. *J. Nutr.* 149:1882–95
94. Miraglia F, Colla E. 2019. Microbiome, Parkinson's disease and molecular mimicry. *Cells* 8:222
95. Mirza B, Wang W, Wang J, Choi H, Chung NC, Ping P. 2019. Machine learning and integrative analysis of biomedical big data. *Genes* 10:87

96. Murgia F, Atzori L, Carboni E, Santoru ML, Hendren A, et al. 2020. Metabolomics fingerprint induced by the intranigral inoculation of exogenous human alpha-synuclein oligomers in a rat model of Parkinson's disease. *Int. J. Mol. Sci.* 21:6745
97. Myint KT, Aoshima K, Tanaka S, Nakamura T, Oda Y. 2009. Quantitative profiling of polar cationic metabolites in human cerebrospinal fluid by reversed-phase nanoliquid chromatography/mass spectrometry. *Anal. Chem.* 81:1121–29
98. Natividad JM, Lamas B, Pham HP, Michel ML, Rainteau D, et al. 2018. *Bilophila wadsworthia* aggravates high fat diet induced metabolic dysfunctions in mice. *Nat. Commun.* 9:2802
99. Needham BD, Kaddurah-Daouk R, Mazmanian SK. 2020. Gut microbial molecules in behavioural and neurodegenerative conditions. *Nat. Rev. Neurosci.* 21:717–31
100. Ng SC, Shi HY, Hamidi N, Underwood FE, Tang W, et al. 2017. Worldwide incidence and prevalence of inflammatory bowel disease in the 21st century: a systematic review of population-based studies. *Lancet* 390(10114):2769–78
101. Nguyen TT, Ta QTH, Nguyen TTD, Le TT, Vo VG. 2020. Role of insulin resistance in the Alzheimer's disease progression. *Neurochem. Res.* 45:1481–91
102. Ni J, Shen TD, Chen EZ, Bittinger K, Bailey A, et al. 2017. A role for bacterial urease in gut dysbiosis and Crohn's disease. *Sci. Transl. Med.* 9:eaah6888
103. Nicholson JK, Holmes E, Kinross J, Burcelin R, Gibson G, et al. 2012. Host-gut microbiota metabolic interactions. *Science* 336:1262–67
104. Nielsen J. 2017. Systems biology of metabolism: a driver for developing personalized and precision medicine. *Cell Metab.* 25:572–79
105. Nikolaus S, Schulte B, Al-Massad N, Thieme F, Schulte DM, et al. 2017. Increased tryptophan metabolism is associated with activity of inflammatory bowel diseases. *Gastroenterology* 153:1504–16.e2
106. Niu X, Zheng S, Liu H, Li S. 2018. Protective effects of taurine against inflammation, apoptosis, and oxidative stress in brain injury. *Mol. Med. Rep.* 18:4516–22
107. Noecker C, Chiu HC, McNally CP, Borenstein E. 2019. Defining and evaluating microbial contributions to metabolite variation in microbiome-metabolome association studies. *mSystems* 4:e00579-19
108. Nuzum ND, Loughman A, Szymlek-Gay EA, Hendy A, Teo WP, Macpherson H. 2020. Gut microbiota differences between healthy older adults and individuals with Parkinson's disease: a systematic review. *Neurosci. Biobehav. Rev.* 112:227–41
109. O'Brien EJ, Monk JM, Palsson BO. 2015. Using genome-scale models to predict biological capabilities. *Cell* 161:971–87
110. Org E, Blum Y, Kasela S, Mehrabian M, Kuusisto J, et al. 2017. Relationships between gut microbiota, plasma metabolites, and metabolic syndrome traits in the METSIM cohort. *Genome Biol.* 18:70
111. Orth JD, Thiele I, Palsson BO. 2010. What is flux balance analysis? *Nat. Biotechnol.* 28:245–48
112. Ozdal T, Sela DA, Xiao J, Boyacioglu D, Chen F, Capanoglu E. 2016. The reciprocal interactions between polyphenols and gut microbiota and effects on bioaccessibility. *Nutrients* 8:78
113. Pappalardo F, Russo G, Tshinanu FM, Viceconti M. 2019. In silico clinical trials: concepts and early adoptions. *Brief Bioinform.* 20:1699–708
114. Pearl J. 2009. Causal inference in statistics: an overview. *Statist. Surv.* 3:96–146
115. Pearl JR, Colantuoni C, Bergey DE, Funk CC, Shannon P, et al. 2019. Genome-scale transcriptional regulatory network models of psychiatric and neurodegenerative disorders. *Cell Syst.* 8:122–35.e7
116. Peck SC, Denger K, Burrichter A, Irwin SM, Balskus EP, Schleheck D. 2019. A glycyl radical enzyme enables hydrogen sulfide production by the human intestinal bacterium *Bilophila wadsworthia*. *PNAS* 116:3171–76
117. Peters DL, Wang W, Zhang X, Ning Z, Mayne J, Figeys D. 2019. Metaproteomic and metabolomic approaches for characterizing the gut microbiome. *Proteomics* 19:e1800363
118. Prentice H, Pan C, Gharibani PM, Ma Z, Price AL, et al. 2017. Analysis of neuroprotection by taurine and taurine combinations in primary neuronal cultures and in neuronal cell lines exposed to glutamate excitotoxicity and to hypoxia/re-oxygenation. *Adv. Exp. Med. Biol.* 975(Part 1):207–16
119. Qian G, Ho JWK. 2020. Challenges and emerging systems biology approaches to discover how the human gut microbiome impact host physiology. *Biophys. Rev.* 12:851–63

120. Quince C, Walker AW, Simpson JT, Loman NJ, Segata N. 2017. Shotgun metagenomics, from sampling to analysis. *Nat. Biotechnol.* 35:833–44
121. Rastelli M, Cani PD, Knauf C. 2019. The gut microbiome influences host endocrine functions. *Endocr. Rev.* 40:1271–84
122. Reed JL. 2017. Genome-scale metabolic modeling and its application to microbial communities. In *The Chemistry of Microbiomes: Proceedings of a Seminar Series*, pp. 85–92. Washington, DC: Natl. Acad. Press
123. Regan JA, Shah SH. 2020. Obesity genomics and metabolomics: a nexus of cardiometabolic risk. *Curr. Cardiol. Rep.* 22:174
124. Riccio P, Rossano R. 2019. Undigested food and gut microbiota may cooperate in the pathogenesis of neuroinflammatory diseases: a matter of barriers and a proposal on the origin of organ specificity. *Nutrients* 11:2714
125. Ridlon JM, Harris SC, Bhowmik S, Kang DJ, Hylemon PB. 2016. Consequences of bile salt biotransformations by intestinal bacteria. *Gut Microbes* 7:22–39
126. Robinson JL, Kocabas P, Wang H, Cholley PE, Cook D, et al. 2020. An atlas of human metabolism. *Sci. Signal.* 13:eaaz1482
127. Rosario D, Benfeitas R, Bidkhori G, Zhang C, Uhlen M, et al. 2018. Understanding the representative gut microbiota dysbiosis in metformin-treated type 2 diabetes patients using genome-scale metabolic modeling. *Front. Physiol.* 9:775
128. Ruan W, Engevik MA, Spinler JK, Versalovic J. 2020. Healthy human gastrointestinal microbiome: composition and function after a decade of exploration. *Dig. Dis. Sci.* 65:695–705
129. Schapira AHV, Chaudhuri KR, Jenner P. 2017. Non-motor features of Parkinson disease. *Nat. Rev. Neurosci.* 18:435–50
130. Schirmer M, Franzosa EA, Lloyd-Price J, McIver LJ, Schwager R, et al. 2018. Dynamics of metatranscription in the inflammatory bowel disease gut microbiome. *Nat. Microbiol.* 3:337–46
131. Schirmer M, Garner A, Vlamakis H, Xavier RJ. 2019. Microbial genes and pathways in inflammatory bowel disease. *Nat. Rev. Microbiol.* 17:497–511
132. Segers K, Declerck S, Mangelings D, Heyden YV, Eeckhaut AV. 2019. Analytical techniques for metabolomic studies: a review. *Bioanalysis* 11:2297–318
133. Sen P, Oresic M. 2019. Metabolic modeling of human gut microbiota on a genome scale: an overview. *Metabolites* 9:22
134. Sertbas M, Ulgen K, Cakir T. 2014. Systematic analysis of transcription-level effects of neurodegenerative diseases on human brain metabolism by a newly reconstructed brain-specific metabolic network. *FEBS Open Bio* 4:542–53
135. Shah P, Fritz JV, Glaab E, Desai MS, Greenhalgh K, et al. 2016. A microfluidics-based in vitro model of the gastrointestinal human-microbe interface. *Nat. Commun.* 7:11535
136. Shoaie S, Ghaffari P, Kovatcheva-Datchary P, Mardinoglu A, Sen P, et al. 2015. Quantifying diet-induced metabolic changes of the human gut microbiome. *Cell Metab.* 22:320–31
137. Sonnenburg JL, Backhed F. 2016. Diet-microbiota interactions as moderators of human metabolism. *Nature* 535:56–64
138. Spanogiannopoulos P, Bess EN, Carmody RN, Turnbaugh PJ. 2016. The microbial pharmacists within us: a metagenomic view of xenobiotic metabolism. *Nat. Rev. Microbiol.* 14:273–87
139. Stocchi F, Torti M. 2017. Constipation in Parkinson's disease. *Int. Rev. Neurobiol.* 134:811–26
140. Sveinbjornsdottir S. 2016. The clinical symptoms of Parkinson's disease. *J. Neurochem.* 139(Suppl. 1):318–24
141. Tarawneh R, Holtzman DM. 2012. The clinical problem of symptomatic Alzheimer disease and mild cognitive impairment. *Cold Spring Harb. Perspect. Med.* 2:a006148
142. Ternes D, Karta J, Tsenkova M, Wilmes P, Haan S, Letellier E. 2020. Microbiome in colorectal cancer: how to get from meta-omics to mechanism? *Trends Microbiol.* 28:401–23
143. Thiele I, Clancy CM, Heinken A, Fleming RMT. 2017. Quantitative systems pharmacology and the personalized drug-microbiota-diet axis. *Curr. Opin. Syst. Biol.* 4:43–52
144. Thiele I, Palsson BO. 2010. A protocol for generating a high-quality genome-scale metabolic reconstruction. *Nat. Protoc.* 5:93–121

145. Thiele I, Sahoo S, Heinken A, Hertel J, Heirendt L, et al. 2020. Personalized whole-body models integrate metabolism, physiology, and the gut microbiome. *Mol. Syst. Biol.* 16:e8982
146. Toledo JB, Arnold M, Kastenmuller G, Chang R, Baillie RA, et al. 2017. Metabolic network failures in Alzheimer's disease: a biochemical road map. *Alzheimer's Dement*. 13:965–84
147. Tralau T, Sowada J, Luch A. 2015. Insights on the human microbiome and its xenobiotic metabolism: What is known about its effects on human physiology? *Expert Opin. Drug Metab. Toxicol.* 11:411–25
148. Unger MM, Spiegel J, Dillmann KU, Grundmann D, Philippeit H, et al. 2016. Short chain fatty acids and gut microbiota differ between patients with Parkinson's disease and age-matched controls. *Parkinsonism Relat. Disord.* 32:66–72
149. van der Ark KCH, van Heck RGA, Martins Dos Santos VAP, Belzer C, de Vos WM. 2017. More than just a gut feeling: constraint-based genome-scale metabolic models for predicting functions of human intestinal microbes. *Microbiome* 5:78
150. Van Treuren W, Dodd D. 2020. Microbial contribution to the human metabolome: implications for health and disease. *Annu. Rev. Pathol.* 15:345–69
151. VanderWeele TJ. 2019. Principles of confounder selection. *Eur. J. Epidemiol.* 34:211–19
152. Vogt NM, Romano KA, Darst BF, Engelman CD, Johnson SC, et al. 2018. The gut microbiota-derived metabolite trimethylamine N-oxide is elevated in Alzheimer's disease. *Alzheimer's. Res. Ther.* 10:124
153. Wang FS, Wu WH, Hsiu WS, Liu YJ, Chuang KW. 2019. Genome-scale metabolic modeling with protein expressions of normal and cancerous colorectal tissues for oncogene inference. *Metabolites* 10:16
154. Wang Y, Zhou Y, Xiao X, Zheng J, Zhou H. 2020. Metaproteomics: a strategy to study the taxonomy and functionality of the gut microbiota. *J. Proteom.* 219:103737
155. Weersma RK, Zhernakova A, Fu J. 2020. Interaction between drugs and the gut microbiome. *Gut* 69:1510–19
156. Wikoff WR, Anfora AT, Liu J, Schultz PG, Lesley SA, et al. 2009. Metabolomics analysis reveals large effects of gut microflora on mammalian blood metabolites. *PNAS* 106:3698–703
157. Wirbel J, Pyl PT, Kartal E, Zych K, Kashani A, et al. 2019. Meta-analysis of fecal metagenomes reveals global microbial signatures that are specific for colorectal cancer. *Nat. Med.* 25:679–89
158. Wishart DS. 2016. Emerging applications of metabolomics in drug discovery and precision medicine. *Nat. Rev. Drug Discov.* 15:473–84
159. Witten DM, Tibshirani RJ. 2009. Extensions of sparse canonical correlation analysis with applications to genomic data. *Stat. Appl. Genet. Mol. Biol.* 8:28
160. Wlodarska M, Luo C, Kolde R, d'Hennezel E, Annand JW, et al. 2017. Indoleacrylic acid produced by commensal *Peptostreptococcus* species suppresses inflammation. *Cell Host Microbe* 22:25–37.e6
161. Yachida S, Mizutani S, Shiroma H, Shiba S, Nakajima T, et al. 2019. Metagenomic and metabolomic analyses reveal distinct stage-specific phenotypes of the gut microbiota in colorectal cancer. *Nat. Med.* 25:968–76
162. Yan Y, Nguyen LH, Franzosa EA, Huttenhower C. 2020. Strain-level epidemiology of microbial communities and the human microbiome. *Genome Med.* 12:71
163. Yilmaz B, Juillerat P, Oyas O, Ramon C, Bravo FD, et al. 2019. Microbial network disturbances in relapsing refractory Crohn's disease. *Nat. Med.* 25:323–36
164. Yizhak K, Gaude E, Le Devedec S, Waldman YY, Stein GY, et al. 2014. Phenotype-based cell-specific metabolic modeling reveals metabolic liabilities of cancer. *eLife* 3:
165. Yu H, Blair RH. 2019. Integration of probabilistic regulatory networks into constraint-based models of metabolism with applications to Alzheimer's disease. *BMC Bioinform.* 20:386
166. Zampieri G, Vijayakumar S, Yaneske E, Angione C. 2019. Machine and deep learning meet genome-scale metabolic modeling. *PLOS Comput. Biol.* 15:e1007084
167. Zhang C, Aldrees M, Arif M, Li X, Mardinoglu A, Aziz MA. 2019. Elucidating the reprograming of colorectal cancer metabolism using genome-scale metabolic modeling. *Front. Oncol.* 9:681
168. Zhang X, Li L, Butcher J, Stintzi A, Figeys D. 2019. Advancing functional and translational microbiome research using meta-omics approaches. *Microbiome* 7:154
169. Zhu S, Jiang Y, Xu K, Cui M, Ye W, et al. 2020. The progress of gut microbiome research related to brain disorders. *J. Neuroinflamm.* 17:25

170. Zhu T, Goodarzi MO. 2020. Metabolites linking the gut microbiome with risk for type 2 diabetes. *Curr. Nutr. Rep.* 9:83–93
171. Zierer J, Jackson MA, Kastenmuller G, Mangino M, Long T, et al. 2018. The fecal metabolome as a functional readout of the gut microbiome. *Nat. Genet.* 50:790–95
172. Zimmermann M, Zimmermann-Kogadeeva M, Wegmann R, Goodman AL. 2019. Mapping human microbiome drug metabolism by gut bacteria and their genes. *Nature* 570:462–67
173. Zuniga C, Zaramela L, Zengler K. 2017. Elucidation of complexity and prediction of interactions in microbial communities. *Microb. Biotechnol.* 10:1500–22

Chapter 4

Longitudinal flux balance analyses of a patient with Crohn's disease

Arianna Basile[1], Almut Heinken[2], Johannes Hertel[3], Larry Smarr[4], Laura Treu[1]*, Giorgio Valle[1], Stefano Campanaro[1,5ψ], Ines Thiele[2,6,7]*ψ

Manuscript under preparation

[1]Department of Biology, University of Padova, Via U. Bassi 58/b, 35121 Padua, Italy.
[2]School of Medicine, National University of Galway, Galway, Ireland
[3]Department of Psychiatry and Psychotherapy, University Medicine Greifswald, Germany
[4]Center for Microbiome Innovation, University of California San Diego, La Jolla, California; Department of Computer Science and Engineering, University of California San Diego, La Jolla, California; California Institute of Telecommunications and Information Technology, University of California San Diego, La Jolla, California.
[5]CRIBI Biotechnology Center, University of Padova, 35131 Padua, Italy.
[6]Discipline of Microbiology, National University of Galway, Galway, Ireland
[7]APC Microbiome Ireland, University College Cork, Cork, Ireland

*corresponding authors: laura.treu@unipd.it, ines.thiele@nuigalway.ie
ψEqual contribution

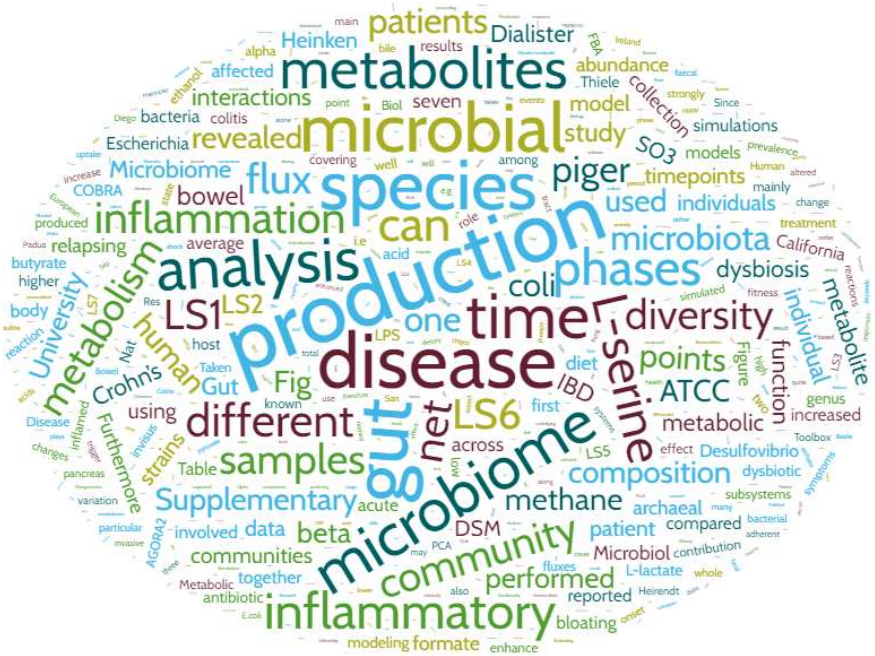

Longitudinal flux balance analyses of a patient with Crohn's disease

Arianna Basile[1], Almut Heinken[2], Johannes Hertel[3], Larry Smarr[4], Laura Treu[1]*, Giorgio Valle[1], Stefano Campanaro[1,5§], Ines Thiele[2,6,7*§]

[1]Department of Biology, University of Padova, Via U. Bassi 58/b, 35121 Padua, Italy.
[2]School of Medicine, National University of Galway, Galway, Ireland
[3]Department of Psychiatry and Psychotherapy, University Medicine Greifswald, Germany
[4]Center for Microbiome Innovation, University of California San Diego, La Jolla, California; Department of Computer Science and Engineering, University of California San Diego, La Jolla, California; California Institute of Telecommunications and Information Technology, University of California San Diego, La Jolla, California.
[5]CRIBI Biotechnology Center, University of Padova, 35131 Padua, Italy.
[6]Discipline of Microbiology, National University of Galway, Galway, Ireland
[7]APC Microbiome Ireland, University College Cork, Cork, Ireland

*corresponding authors: laura.treu@unipd.it, ines.thiele@nuigalway.ie
[§]equal contribution

Graphical abstract

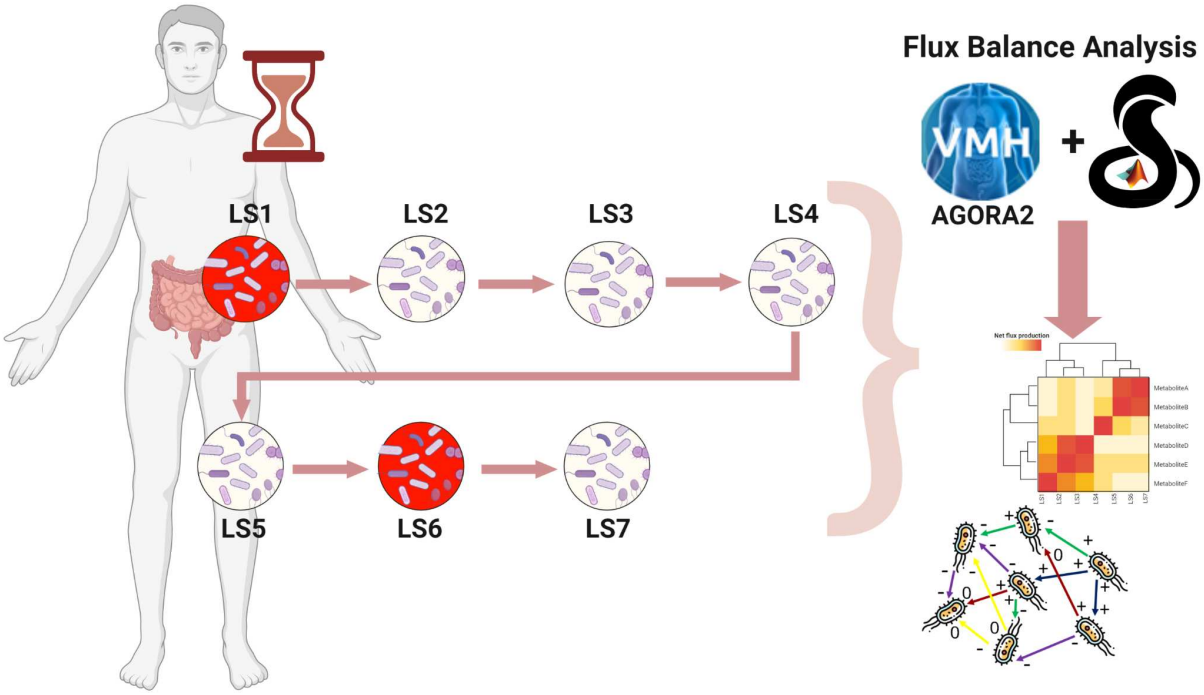

Abstract

Inflammatory bowel diseases are disorders characterised by an inflammation of the gastro-intestinal tract. Although still unidentified, the pathoetiology is characterised by dysbiosis in the gut microbiome. However, the microbial composition of an individual is not constant over time making the identification of the dysbiotic signature complex. The present work, using a constraint based modeling approach, aims for the first time to identify variations in one individual across multiple timepoints rather than between individuals. The seven time points cover inflamed and relapsing stages and 15 months. The analysis revealed that the microbial production of some metabolites is variable through time. During inflammation the production of methane and lipopolysaccharides is enhanced compared to the relapsing stages of the disease, thus contributing to the bloating effect and the inflammation. The microbe-metabolite contribution analysis revealed that the behaviour of some microbes belonging to the *Dialister* genus changes according to the disease phase. During the inflammation phases, they produce L-serine or formate. These compounds, through a cascade effect, mediated by the interaction with pathogenic *Escherichia coli* strains and *Desulfovibrio piger*, trigger the production of host-toxic compounds such as sulfur trioxide. The integration of the human whole body model was used to track the effect of the dysbiosis on different body sites, organs and tissues. The analysis evidenced an imbalance in the synthesis of the prostaglandin E2 at the level of the pancreas during the inflammatory stages. Taken together these results underline the importance of tracking the microbiome over time as a video rather than a screenshot and pave the way to new analyses for self-quantified medicine.

Introduction

The human gut microbiome performs essential functions in shaping the host immune system, the host cell proliferation, and is involved in the maintenance of the endocrine functions [1,2]. The human microbiome consists of a large number of archaeal and bacterial, but also of viral and fungal species [3]. The composition of the microbiome depends on host factors, such as age, sex, location, ethnicity, and lifestyle, including diet, exercise, and medication [4]. Between healthy individuals, the relative abundances of taxa are highly variable, while the functional capabilities are more stable in terms of composition and abundance [5]. Contrariwise, many multifactorial diseases are characterised by a dysbiotic microbiome. Accordingly, it is believed that there is a "core" healthy microbiome performing a set of functions which promotes stable interactions with the host [6].

Following this rule, the study of the microbiome has moved from "Who is there?" to "What are they doing?". With the implementation of flux balance analysis (FBA), the question further moved to "What do they produce?", "How do they interact?" [7,8]. FBA implemented in the Constraint-based reconstruction and analysis (COBRA) framework is a mechanistic modeling approach [9]. It relies on the genome-scale reconstructions of the target organism's metabolism [10]. The model can be constrained with the use of condition-specific data (e.g. meta-omics data and allowed uptake of nutrients). The basic assumption of the constraint-based modeling is the steady-state assumption and the change in metabolite concentration over time is zero [11]. In order to facilitate the application of constraint-based modeling to research on the human gut microbiome, the AGORA (assembly of gut organisms through reconstruction and analysis) collection was established [12] and expanded [13] to include in total over 7'000 manually curated genome-scale reconstructions.

Not only the gut microbiota has relevant differences among individuals, and variable composition in different parts of the digestive tract, but it can also undergo extensive modifications throughout life [14]. This aspect has been regarded as an obstacle to the gut microbiome-based medical applications for the additional difficulty of identifying a clear signature of the dysbiotic microbiota. The microbiome of an individual can change during the outbreak of a disease, and the symptomatology of the patient changes accordingly [15]. This is particularly true for patients affected by Inflammatory Bowel Disease (IBD), which is an umbrella term describing disorders characterised by chronic inflammation of the gastrointestinal tract [16]. It has a prevalence of 0.3% in the developed Western countries and its incidence is increasing in developing countries [16]. As an example, IBD incidence increased from 0.60 to 1.20 per 100'000 person-years from 1986 to 1998 in the Asian population [17]. The severity of the symptoms depends on the O_2 gut leakage and the *Enterobacteriaceae* invasion in the gut [18]. Two main subtypes can be defined according to the location and extent of the inflammation, namely Crohn's Disease (CD) and Ulcerative Colitis (UC) [19,20]. While the UC is confined to the large bowel and its major symptoms reflect an unbalance of the gastrointestinal (GI) system alone, CD can affect the entire GI tract from the mouth to the anus. Furthermore, it may also affect skin, eyes, joints, and liver [21].

Despite its systemic nature, the pathoetiology of IBD seems to have a clear microbial signature characterised by a dysbiotic microbiota [22], depauperated of beneficial butyrate-producing taxa, such as *Roseburia* spp. and *Faecalibacterium prausnitzii* [23]. As a result of the reduction in butyrate-producing clostridia, faecal butyrate, which has anti-inflammatory properties, is decreased in

IBD patients [24]. Furthermore, the abundance of potentially pro-inflammatory taxa, such as *Escherichia coli* and *Ruminococcus gnavus*, is increased [25].

The altered microbial activity is evidenced by broad changes in the faecal metabolome. COBRA modeling has been used to link mechanistically host-microbiome-environment interactions to IBD-related changes [26]. The potential of 818 microbial strains to deconjugate primary bile acids into secondary bile acids was investigated with a combined approach based on comparative genomics followed by FBA. It has been reported that microbial species can complement each other's bile acid pathway to achieve the broader bile acid production repertoire observed in faecal samples [27].

Despite the numerous studies performed on CD, the evolution of the gut microbiome during disease onset progress has not been inspected with FBA yet. Another unexplored aspect of the disease is the interaction existing between the host metabolism and the compounds produced by the normal and the dysbiotic gut microbiome. This specific aspect can be investigated using sex specific organ resolved whole-body metabolic models of human metabolism, which account for 28 organs, tissues, and cell types [28].

The present study tracked the modifications of the microbial community in an individual affected by Crohn disease across multiple seven timepoints covering a period of 15 months. The timepoints covered both stable and inflamed states of the disease. The metagenomic data were mapped onto the AGORA2 collection [13]. Therefore, the composition of the microbiome samples for each time point was analyzed and diversity indexes were computed. The contribution of each microbial species to the global profile of metabolites present in the gut was inspected. FBA was performed considering the microbiome composition and integrating the human metabolism as well. With this approach multiple personalised models of the patient covering different timepoints was obtained. To date this is the first COBRA study that shows the variation in one individual instead of between individuals. Taken together, our analysis revealed that numerous metabolite production fluxes are altered during the seven time points and follow the state of inflammation. In particular, methane, LPS, L-lactate and L-serine may be useful as potential biomarkers of the inflammatory phases. However, further validation in other patients would be required. Taken together, our results indicate that through the production of few metabolites, i.e., L-serine and formate, species of the *Dialister* genus cooperate with many pathological strains such as adherent invasive *Escherichia coli* strains, archaeal species and *Desulfovibrio piger*. The interactions trigger inflammatory responses and enhance methane production. Furthermore, *D. piger* ATCC2 plays an important role in the production of the host-toxic SO_3. The analysis on the whole body model revealed that there is an influence of the dysbiosis on the metabolism of the prostaglandins E2 in the pancreas.

Results and discussion

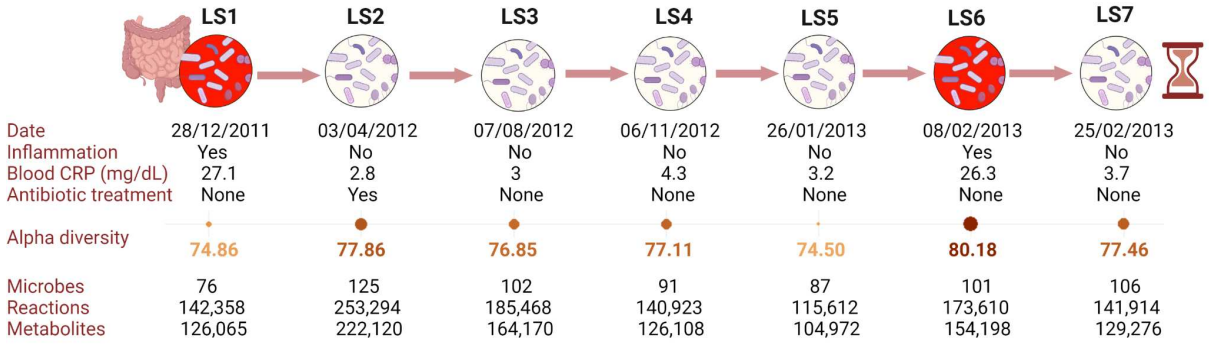

Figure 1: Timeline with metadata of the different samples. In the timeline, realized with BioRender, collection date, inflammation state, measured blood CRP, and presence of antibiotic treatment are reported. The antibiotic treatment consisted of ciprofloxacin, metronidazole and prednisone

The n=1 patient was a non-smoker male, named LS. A detailed description of his medical history is reported in Supplementary file 1. The analysis focused on seven time points, named from LS1 to LS7 according to the time of collection. Samples have been collected both during acute and relapsing phases as defined by the concentration of the blood Complex Reactive Protein (CRP) (Fig. 1, Supplementary Table 1). The antibiotic therapy faced during LS2 (Fig. 1) consisted of ciprofloxacin 500 mg administered twice on a daily basis and metronidazole 250 mg administered three times per day for one month starting from 31st of January 2012 [29]. During that period, the patient also underwent a treatment consisting of 40 mg Prednisone daily. Since LS1 and LS6 have been collected during the manifestation of the disease, their importance will be emphasised in the description and discussion of results.

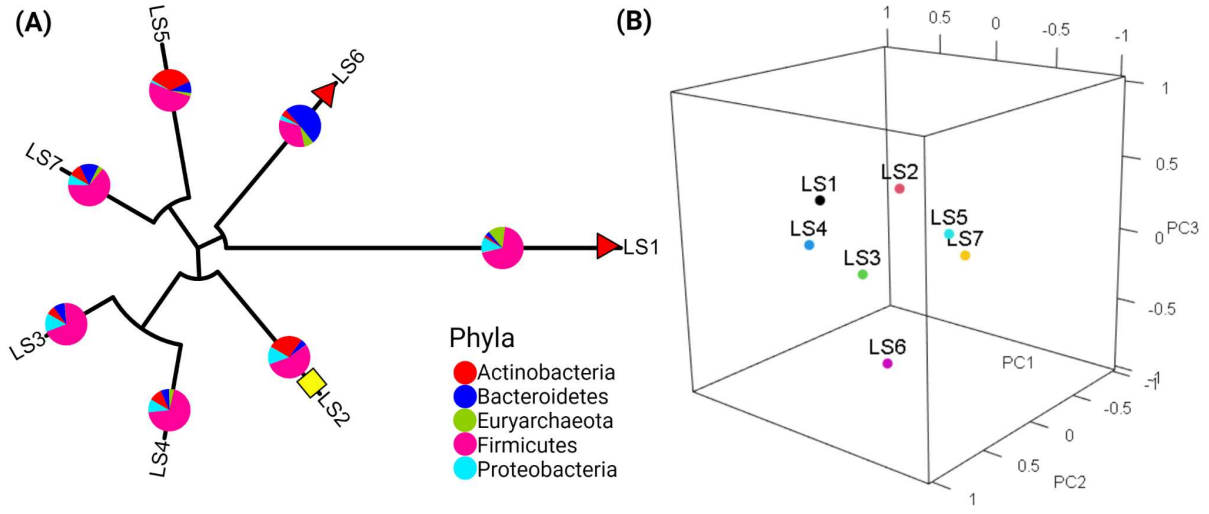

Figure 2: Graphical representation of the beta diversity between samples. (A) 3D Principal component analysis resumes the beta diversity. (B) phylogenetic tree of the samples. The red triangle close to the names of the phases indicates the presence of an inflammatory state. The yellow square indicates that the community is influenced by antibiotic usage. The pie-charts represent the relative abundance of the different phyla.

First, the metagenomic data were mapped onto the AGORA2 collection [13]. After the mapping, the composition of the microbiome samples for each time point was analyzed and alpha and beta diversity were computed. On total the seven microbial communities simulated account both for bacteria and archaea species and are composed by microbes from eight phylum: Actinobacteria, Bacteroidetes, Euryarchaeota, Firmicutes, Fusobacteria, Proteobacteria, Spirochaetes, and Synergistetes (Fig. 2A). Firmicutes covering the vast majority of all the communities (with the exception of LS6). In LS6 the Firmicutes cover 30.58% of the community, while Bacteroidetes 47.06% being the most abundant phylum of the community (Fig. 2B). The archaeal species are generally quite rare in the relapsing phases covering between 2.5% and 3.6% of the whole community in LS2, LS3, LS4, LS5, and LS7. In LS6 the archaeal community covers up to 6.7% of the community and in LS1 12.12%. The Bacteroides are typical of LS2 and LS5 covering 24.95% and 32.34% of the communities respectively. The number of simulated species in the microbiome ranged between 76 (in LS1) and 125 (in LS2) (Fig. 1, Supplementary Table 2). Although LS2 is the phase with the highest number of species, it is not the one with the highest alpha diversity with a value of 77.86. This is due to the fact that alpha diversity was calculated taking into account the taxonomic assignment and LS2 is mainly composed of Firmicutes and Actinobacteria, which cover more than 70% of the relative abundance, and accounting, therefore, for a relatively low alpha diversity (Supplementary Table 2). The cause of the low biodiversity in LS2 is probably the effect of antibiotic therapy which strongly reduces the biodiversity in the gut microbiome [30].

The average beta diversity between samples is 58.00%. The two most dissimilar samples are LS1 and LS2 (84.06%), again possibly reflecting the effect of the antibiotic therapy performed before LS2 collection against the dysbiotic microbiota. The two lowest beta diversity are between couples of relapsing phases. LS3 with LS4 has a beta diversity of 23.44%, and LS5 with LS7 of 35.76%. The beta diversity between the phases of acute inflammation is 79.53% (Supplementary file 2). In the Principal Component Analysis (PCA) performed on microbial composition and abundances (Fig. 2B, Supplementary Figure 1, Supplementary Figure 2), the first component accounts for 54.7% of the total variability, while both the second and the third components account for approximately 20% of the total variability. The different components are driven mainly by the differential abundance of two Archaea species, i.e, Methanobrevibacter *smithii* ATCC 35061 and *Methanosphaera stadtmanae* DSM 3091. Both Archaea are more abundant in LS1 and LS6 in comparison to LS2, LS3, LS4, LS5 and LS7. Another driving factor is played by butyrate producing bacteria such as *Collinsella aerofaciens* ATCC 25986 and *Eubacterium siraeum* DSM 15702 which are more abundant in the relapsing phases compared to the inflammatory ones. The impact of antibiotic usage on LS2 is evidenced by the relatively high distance occurring between this sample and the other time points in the PCA (Fig. 2A, Supplementary Figure 2).

Metabolic and subsystem signature of each phase

The metabolic modelling was performed mapping the metagenomic data on the AGORA2 collection and simulating the behavior of the seven communities through FBA. Microbe-metabolite contributions were computed as well. The differences in metabolite net flux production and the microbe-metabolite contribution will be discussed in parallel. The constraint-based modelling approach followed by statistical analysis revealed that the reaction subsystems strongly changed during the disease progress and this resulted in a modification of the metabolites produced (Supplementary Table 3). It has been reported that the prevalence or absence of reaction subsystems in microbial community models can reflect healthy or dysbiotic microbial communities [31]. Consistently with the beta diversity analysis, the simulated production of some metabolites reflects the proximity of LS3 with LS4 and LS5 with LS7 (Fig. 3A). The clustering analysis performed considering all the metabolites predicted with net flux production lower than ten revealed the existence of three main clusters (Fig. 3A). The threshold of ten was selected arbitrarily for graphical purposes. The first cluster, named low fluxes (LF), groups together all the metabolites with a very low net production; the second cluster the metabolites with intermediate net production (IF); the third includes the metabolites with high net production (HF). The three clusters are heterogeneous in subsystem composition. Some metabolites, whose fluxes rates are variable among the different phases of the disease, will be discussed more in detail underlying the roles of the microbial species mainly involved in their production. The prevalence of subsystems including reactions related to that metabolite will be discussed as well.

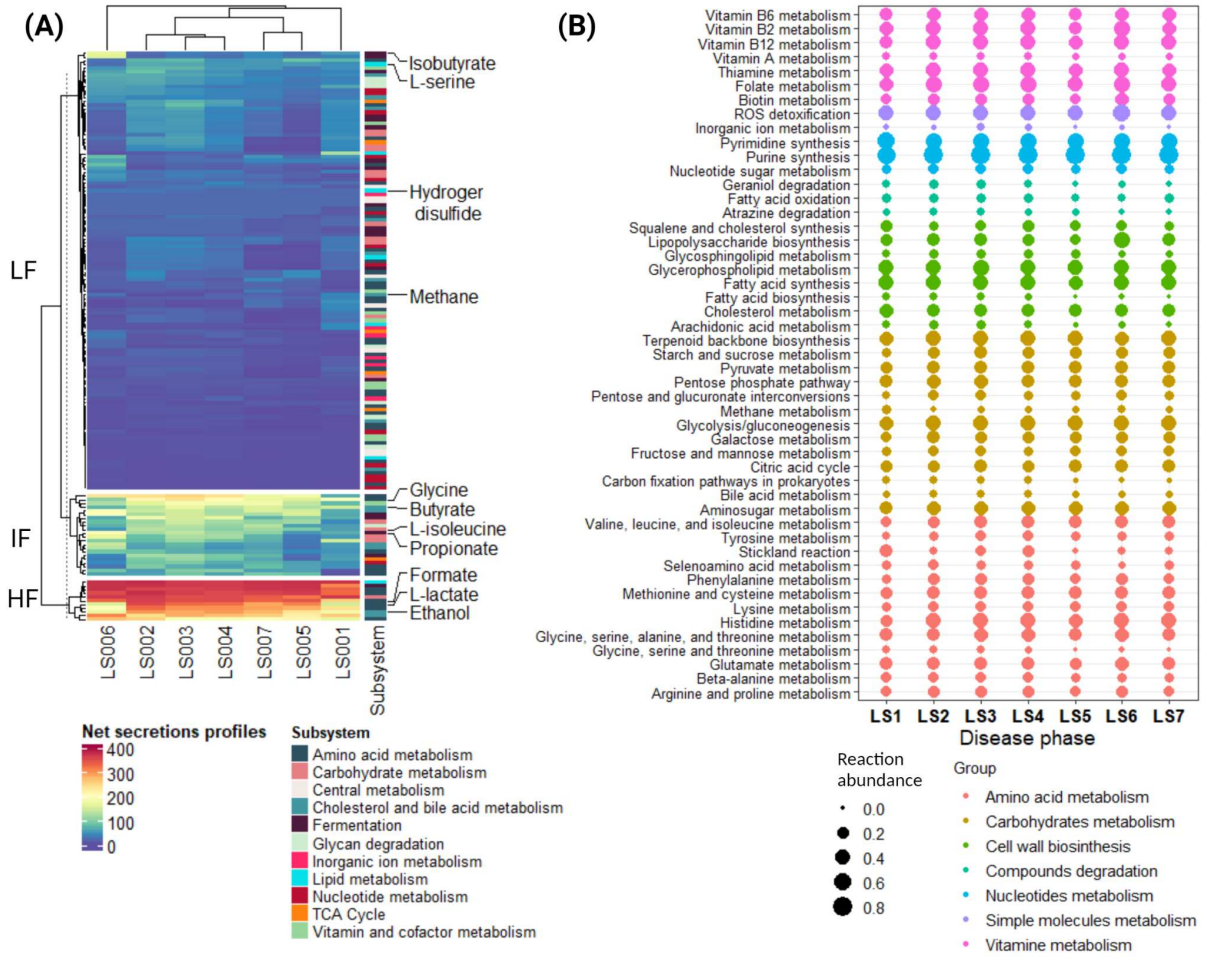

Figure 3: Overview of metabolites produced and reactions subsystems across the different timepoints. (A) heatmap of the net flux production of all metabolites with a summed net flux higher than 10. Key metabolites commented in the manuscript have been evidenced in the heatmap (B) geom plot of reaction subsystem prevalence across the different time points. The colours of the circles refer to the group of each subsystem, groups have been attributed manually. The diameter of the circles are proportional to the abundance of the reactions in the simulated communities.

As expected, “Methane metabolism” is strongly increased in LS1 and LS6 compared to the other phases. Since methane metabolism is related to methanogenesis, the increase of methane metabolism depends on the higher abundance of Archaea in LS1 and LS6 and it may be one co-determinant of abdominal bloating experienced by the individual at these time points. Accordingly, the production of methane is enhanced in LS1 and LS6 (Pearson residuals 7.39 and 2.99, respectively). In contrast, there are some subsystems that are peculiar to only one of the two acute phases of the disease onset (Supplementary Table 4). This is the case for the “Stickland reaction” which couples oxidation and reduction of amino acids to organic acids [32] and characterises LS1. In studies exploring the subproducts of common degradation pathways, 80% (8/10) of Stickland reaction products have been frequently detected in IBD patient stool [33]. Since all the time points received the same diet, the differences introduced above are a result of the differential composition. The diet used to constrain the

models, there is a 10% shortfall in Stickland acceptors, which results in hydrogen production. The increase in hydrogen production can be an additional cause of the bloating event experienced in LS1. Levitt and Olsson have already linked the hydrogen production to the adverse bloating event [34]. Phase LS6 is characterised by an increased abundance of E.coli strains, e.g., *E. coli* 042, *E. coli* B354, and *E. coli* FVEC1302, which encodes enzymes belonging to Lipopolysaccharide (LPS) biosynthesis subsystems. LPS are produced and secreted by Gram-negative bacteria, which can cause an immune response [REF]. LPS secreted are generally soluble as monomers but they can aggregate into fibrous and highly insoluble lipoproteins leading to inflammation [35]. In literature, it has been reported that the concentration of LPS is increased in the acute phases of the disease compared to relapsing [36].

Pearson residuals analysis revealed that butyrate net flux production drops significantly in LS6 (Pearson residual = -5.42), while the propionate rate is increased (Pearson residual = 8.42). Gut microbial butyrate production is generally reduced in IBD [37,38], the production of microbial butyrate can be a crucial discriminating factor between relapsing and acute phases. The microbe-metabolite computation underlined that in the other timepoints, the butyrate production is mediated mainly by members of the Lachnospiraceae (i.e., *Anaerostipes caccae* DSM 14662, *Coprococcus comes* ATCC 27758, *Butyrivibrio crossotus* DSM 2876, *Roseburia intestinalis* XB6B4, *Butyrivibrio proteoclasticus* B316, ND *Dorea formicigenerans* ATCC 27755). Butyrate production in the vicinity of epithelial cells has been suggested to be important in maintaining gut health [39].

L-lactate belongs to the HF cluster. Its distribution along the samples is particularly interesting because L-lactate fluxes are lower in LS1 and LS6 compared to the other phases. The other phases accounted for at least 30 different microbial species involved in the synthesis of L-lactate, while in LS1 and LS6 there are 19 and 24 respectively. Accordingly, lactic acid concentration has been shown to increase significantly in all the patients with colitis [40]. In particular a higher severity of the symptoms has been reported with higher lactate [40].

The production of L-serine is enhanced in LS6 compared to the other time points. L-serine is known to elicit the secretion of antimicrobial molecules, such as bacteriocins. *E.coli* pathogenic strains can use L-serine anabolism to enhance their fitness in the inflamed gut [41]. Contrariwise, this pathway has a minor role in pathogenic bacterial growth of healthy guts [42] suggesting that the signals or transduction pathways necessary for L-serine catabolism activation could be responsible for pathogen-specific adaptation to the inflammatory microenvironment. Intestinal inflammation can result in the generation of a microenvironment that is conducive to the growth of Enterobacteriaceae, allowing them to outcompete obligate anaerobes [43]. Therefore, enterobacterial blooms, such as those seen in CD, are a hallmark of inflammation-associated dysbiosis [44]. Accordingly, *E.coli* can catabolize L-serine converting it to pyruvate, a crucial substrate for gluconeogenesis and tricarboxylic acid cycle pathways [45]. L-serine also plays a role as a signalling molecule targeting the expression of stress response genes [46]. Furthermore, it can be used as a precursor in the synthesis of gene products involved in stress adaptation [47]. In this context, it is known that L-serine catabolism is increased in *E. coli* under heat shock conditions and L-serine is used for the generation of heat shock proteins [47]. L-serine uptake during inflammatory conditions is probably a conserved mechanism utilized by pathogenic bacteria for their competitive fitness [48].

Taken together, our analysis revealed that numerous metabolite production fluxes are altered during the seven time points and follow the state of inflammation. In particular, methane, LPS, L-lactate and

L-serine may be useful as potential biomarkers of the inflammatory phases. However, further validation in other patients would be required.

Insight into Dialister metabolism

The microbe-metabolite contribution was calculated using the cooperative tradeoff algorithm which implies that it favors individual growth still together with a community sup-optimal growth rate. Flux variability analysis (FVA) for each exchanged metabolite on the exchange reaction was not performed. The microbe-metabolite contribution showed that in LS6 the production of L-serine is mediated mainly by members of the *Dialister* genus, i.e. *Dialister succinatiphilus* YIT 11850 and *Dialister invisus* DSM 15470.

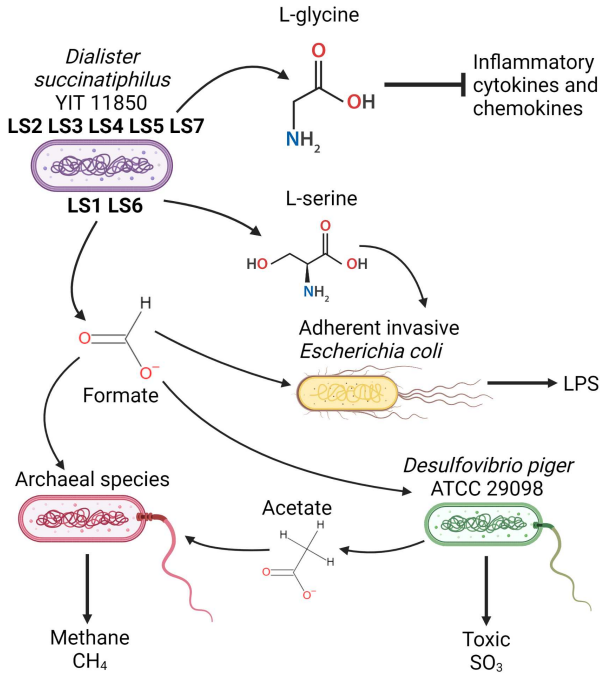

Figure 4: Map of interspecies interactions. The map represents how microbial species are interconnected in a network of dependencies aiming to enhance their fitness. It was realized with Biorender.

Dialister invisus DSM 15470 is involved in the establishment of the dysbiosis typical of the IBD microbiota [49]. Hence, metabolites produced by species of the same genus have been inspected in more detail. *Dialister invisus* DSM 15470 was identified in all the time points except LS5, but its activity is very different according to the time point analysed. In LS1, *D. invisus* produces 12 metabolites and takes up 52, while in the other time points it takes an average of 10 metabolites (Supplementary Table 5). Notably, *D. invisus* produces L-serine only in LS6 and formate only in LS1 (Supplementary Table 5). The other species of the *Dialister* genus, *D. succinatiphilus* YIT 11850 produces L-serine in the acute phases of inflammation (LS1 and LS6) and glycine in the remission phases (Fig. 4). In literature, dietary glycine is known to prevent chemical-induced colitis by inhibiting induction of inflammatory cytokines and chemokines [50].

Contrariwise, both L-serine and formate mediate proinflammatory mechanisms. In LS6, L-serine uptake is mediated mainly by members of the Enterobacteriaceae family (e.g. *E. coli* 042, B354, FVEC1302, H299). Formate production in LS1 has a key role too. Indeed, formate in LS1 is absorbed by *E. coli* F11, *Methanobrevibacter smithii* ATCC 35061 and *Desulfovibrio piger* ATCC 29098 (Fig. 4). *E. coli* F11 is an adherent invasive and pathogenic strain, which takes advantage of the leaking gut to replace strictly anaerobic bacteria [51]. *M. smithii* ATCC 35061 is a hydrogenotrophic archaea which can use either CO_2 and H_2 or formate alone for methane production. The increase of methane production, and, therefore, constipation and bloating events, is known to be partially caused by the increase of this archaeal species (Fig. 4) [52]. The prevalence of *D. piger* is significantly higher in patients hospitalized for IBD in comparison to healthy individuals or patients hospitalized for other pathologies [53]

The multifaceted role of *Desulfovibrio piger* ATTC2

It is known that in different individuals and conditions the taxonomic composition of the gut microbiome can be highly different [54], however, this is not necessarily reflected in a modification of the functional activities [5]. According to this concept, even if most of the species are absent in at least one time point, the vast majority of metabolic functions and reactions are conserved [5]. However, the production of some metabolites is mediated by a small core of microbial species, and therefore metabolic reconstructions, whose occurrence is sufficient and necessary to ensure the production of some metabolites [55]. Genome-scale reconstructions were inspected to evidence those whose presence is necessary and sufficient for the production of each metabolite in each community.

The analysis revealed that *D. piger* ATCC2 is the only microbial species involved in the production of sulfite (SO_3) in the communities. Patients affected by IBD, such as ulcerative colitis, are strongly discouraged to consume foods with high SO_3 levels as being harmful and favouring tightening of inflammation [56]. Furthermore, sodium sulfite, a common food additive, inhibits activity of commensal and anti-inflammatory bacteria, such as *Faecalibacterium prausnitzii* [57]. Large part of the SO_3 present in the gut derives from dietary intake, however, some microbial species are known to produce SO_3. *D. piger* ATTC2 was not able to synthesise SO_3 in single species simulations. The pairwise simulations revealed that this species interacts with the Archaea *Methanosphaera stadtmanae* DSM3091, which can stimulate SO_3 production. This dependency reflects a cooperative behaviour culminating in the production of the host-toxic SO_3.

The paired simulations revealed that *D. piger* ATCC 29098 absorbs ethanol, which is converted into acetate, which is imported by the acetoclastic archaea *Methanosphaera stadtmanae* DSM 3091. *D. piger* ATCC 2909 oxidises ethanol using two different anaerobic pathways: in one case, the ethanol is oxidised to acetate producing acetaldehyde as intermediate. In the second one other intermediates between acetaldehyde and acetate are generated, namely acetyl-CoA and Acetyl-P [58]. In the simulations, the conversion of ethanol to acetate has a yield of ~1 (0.93) as expected from experimental data [59]. The nearly 1:1 ethanol-to-acetate ratio reflects the release of an excess of reducing equivalents, such as methane, by the syntrophic partner [58]. It is possible that *D. piger* ATCC 29098 ability to synthesise and export SO_3 is recovered through the interaction with other archaeal partners as well.

Consistently, due to the commensalistic interplay, when *M. stadtmanae* DSM 3091 and *D. piger* ATCC 29098 are co-occurrent, the net flux production of methane is higher (Supplementary Table 3) co-causing the adverse bloating events experienced by LS during the inflammation (Supplementary File). The abundance of *D. piger* strains in IBD patients has already been reported [53]. *Desulfovibrio* and other bacterial genera (e.g., Bacteroides, Eikenella, and Streptococcus) use sulfate as a terminal electron acceptor for respiration and concomitantly produce hydrogen disulfide (H_2S_2), a toxic metabolic byproduct [60]. Consistently, in the simulations, H_2S_2 is produced by *Bacteroides vulgatus* PC510, *Eikenella corrodens* ATCC 23834, *Slackia exigua* ATCC 700122, *Streptococcus anginosus* F0211, and *Escherichia coli* S88 along with *D. piger* ATCC 2909. The production of H_2S_2 does not change significantly in the different time points.

Taken together our results indicate that through the production of few metabolites, i.e., L-serine and formate, species of the Dialister genus cooperate with many pathological strains such as adherent invasive E.coli strains, archaeal species and Desulfovibrio piger. The interactions trigger inflammatory responses and enhance methane production. Furthermore, Desulfovibrio piger ATCC2 plays an important role in the production of SO_3 which is host-toxic.

Metabolites fluctuations across the timepoints

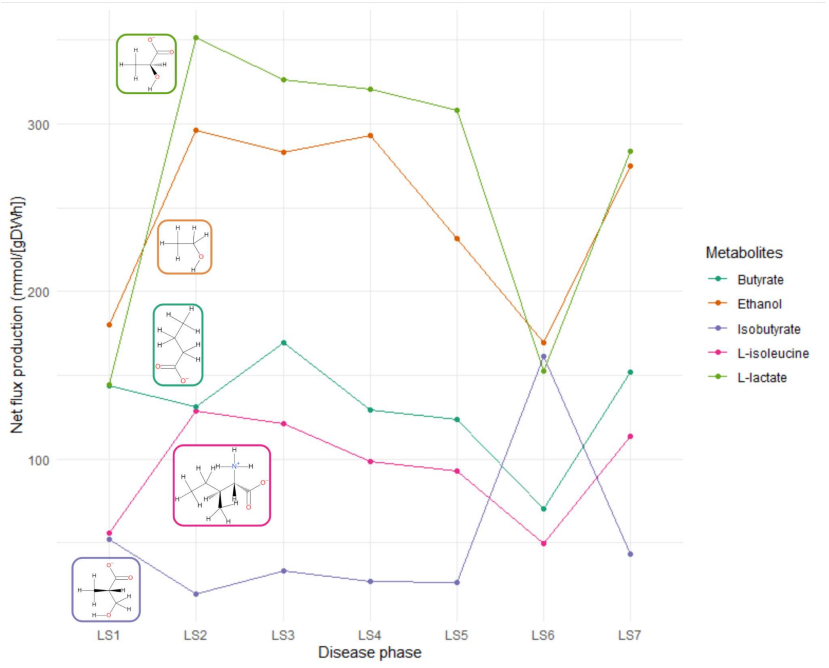

Figure 5: Metabolites net flux variation. Line plot of the net flux production (mmol/gDWh) of metabolites having a marked change over the different time points. For each metabolite the respective chemical structure is reported.

The net production of some metabolites increases or decreases constantly from LS3 to LS5 and culminates in LS6 in a very high or low value (Fig. 5). This behaviour suggests that monitoring the

fluctuations of these molecules could help to keep track of the species and biological processes carried out by them, which anticipate the acute phases of inflammation (Fig. 5). Since usually the net production rate of these metabolites is similar in the time points LS1-LS6, and in the group LS2-LS3-LS4-LS5-LS7, their variation is not significant at any time point. The net flux production of L-isoleucine, ethanol, and L-lactate, is very low in LS1 and LS6 (average net flux production 130.48), while it is increased in the remaining time points (average net flux production 234.93). Contrariwise, the production of isobutyrate follows an opposite trend and has a higher simulated accumulation in the acute phases of inflammation (average net flux production 106.87) compared to the relapsing phases (average net flux production 30.14).

Whole-body model integration

The time-point specific microbial community models were integrated with, a male-specific, organ-resolved, whole-body model (mWBM) of human metabolism was integrated in the simulations to determine the impact of the dysbiosis on the host metabolism. The dysbiosis seems to affect some body sites more than others. The PCA performed considering the data from the pancreas alone revealed an altered activity of the sodium-coupled monocarboxylate transporter 1 (SMCT1). This transporter is involved in the import and export of pyruvate [61]. Furthermore, transports of sugars, such as fructose and mannose, are highly influenced during the onset of the disease. Both fructose and mannose are less exported in LS2 and LS7 compared to the other phases. Fructose and mannose can be used as precursors of pyruvate. The metabolism of the prostaglandin E2 is strongly influenced in the pancreas by the disease onset, as well. Prostaglandins are one of the first triggering factors of the inflammatory cascade typical of the CD. Furthermore, many drugs, such as Mesalazine, are targeted to inhibit the release of prostaglandins and leukotrienes in different body sites [62].

Conclusions

The time course analysis performed on a patient affected by IBD enabled the analysis of how metabolites concentration intended as net flux production have been affected by the change of the microbial community. This is one of the first COBRA studies that shows the variation in one individual instead of between individuals. In particular the main focus was the research of the main causes of bloating events experienced by LS as one of the main symptoms. The study revealed that the cause of the symptom is to be found in a few microbes intercoursing in specific interactions which enhance the fitness of the archaeal species. As being interconnected in a net of exchanges, the same microbial species are the driving force behind other symptoms such as the abdominal pain caused by inflammatory events. The present study tracked the modifications of the microbial community in an individual affected by Crohn disease across multiple seven timepoints covering a period of 15 months. The timepoints covered both stable and inflamed states of the disease. This pioneeristic analysis is the first one charting the variation among samples in one individual rather than between individuals.

Taken together, our study underlined how different metabolite production fluxes are affected during the seven timepoints following the inflammation state. Accordingly, methane, LPS, L-lactate and L-serine can be identified as potential biomarkers of the inflammatory phases. Nevertheless, additional validations accounting for other patients would be required. Through the production of few metabolites, i.e., L-serine and formate, species of the *Dialister* genus become commensals with adherent invasive *Escherichia coli* strains, archaeal species and *Desulfovibrio piger*. The production of formate by *D. invisus* DSM 15470 is involved in inflammation worsening and in determining a negative outcome through three different mechanisms. The interactions trigger inflammatory responses and enhance methane production. Finally, the analysis on the whole body model revealed that there is an influence of dysbiosis on the metabolism of the prostaglandins E2 in the pancreas. To date, this is the first analysis inspecting the evolution of a patient affected by Crohn's disease with flux balance. Since the microbial composition is quite variable among individuals, to obtain a wide and general representation of the microbiome the time course inspection of a high number of patients is needed. However, despite the microbiome composition being different between individuals, the functions are quite conserved and the results obtained here can recapitulate the functional modification in other patients as well.

Methods

Ethics statement

The stool samples of the patient were collected by consent under two protocols: HRPP 141853 (American Gut Project) and HRPP 150275 (Evaluating the Human Microbiome). The protocols include written informed consent concerning dissemination and scientific publication of the results. Both protocols were approved by the Human Research Protection Program (HRPP) of the University of California, San Diego.

Longitudinal sample collection

The samples were collected from naturally passed feces and immediately stored without a buffer at −80°C. Seven samples were selected. A personal symptom log entry was generated at the time that each fecal sample was passed. Additionally, the weight and body mass index (BMI) of the patient were determined on the day associated with each sample. Other metadata were collected from previous publications [63].

Metagenomics data generation

The metagenomics sequence of the 7 samples have been submitted by Fang and colleagues [63] to EBI under study PRJEB24161.

Definition of the average European diet

The diet represents the nutrient intake of an average European individual. Its description, along with the corresponding flux values, was obtained from the nutrition resource in the Virtual Metabolic Human database [64]. The diet was supplemented with metabolites which had been previously [12] determined as necessary for the biomass production of at least one AGORA reconstruction. The dedicated function (adaptVMHDietToAGORA.m) of the Microbiome Modeling Toolbox [65] was used to constrain each microbiota community model. The lower bounds on all other dietary exchange reactions were set to zero in order to prevent uptake of other metabolites.

Simulations

Simulations were carried out using the COBRA Toolbox [9] and the Microbiome Modeling Toolbox [65] in MATLAB version 2018b (Mathworks, Inc.) as programming environments. Metagenomics reads were mapped over the AGORA2 collection in order to create the community for the simulation. For this purpose the function translateMetagenome2AGORA2 of the COBRA suite was used. For the simulations the function initMgPipe was used. It incorporates the function adaptVMHDietToAGORA which is used to apply the diet constraints to the community model. Microbe-metabolite contributions were performed following Basile et al [66]. In particular, the MICOM software [67] was used through the cooperative tradeoff algorithm. The optimization solver used was CPLEX. Subsystems were assigned following the procedure proposed by Laurent Heirendt et al. [9].
The integration of the whole body model was performed using the Harvey reconstruction [28]. To create the personalised gut model, the function combineHarveyMicrotiota was used and the simulations were performed with the minNorm algorithm.

Statistical analysis

Alpha diversity and beta diversity analysis were calculated with the “vegan” package [68] and using R software v.4.0.3. The taxonomic differences of the different samples were weighted with a hierarchical tree based on the taxonomies of AGORA2 [13] with the function taxa2dist. The alpha diversity was calculated with taxondive [69]. The score considered for the alpha diversity was Δ^*. For the beta diversity, the function vegdist was applied [70]. The values of beta diversity were converted to newick format and used to generate a tree representing the differences between samples with the function nj of the ape package. The PCA [71] was performed with the function princomp with the parameters “cor=TRUE, scores=TRUE”. The 3D plot of the PCA was realised with the function plot3d of the package “rgl”. The χ^2 test of Independence to characterise metabolites production across samples was accomplished with chisq.test in the package stats. Pearson’s residuals were obtained from the same function.

Data availability statement

The metagenomics sequence of the 7 samples have been submitted by Fang and colleagues [63] to EBI under study PRJEB24161. Note that these samples are only a subset of the metagenomics data under this study.

Acknowledgments

This work was financially supported by the “Budget Integrato della Ricerca Dipartimentale” (BIRD198423) PRID 2019 of the Department of Biology of the University of Padua, entitled “SyMMoBio: inspection of Syntrophies with Metabolic Modelling to optimize Biogas Production” to LT. Furthermore, this study was funded by grants from the European Research Council (ERC) under the European Union’s Horizon 2020 research and innovation programme (grant agreement No 757922) and by the National Institute on Aging grants (1RF1AG058942-01 and 1U19AG063744-01) to IT. The PhD fellowship of AB is supported by “Progetto di Eccellenza DiBio” of University of Padua. AB was recipient of the EMBO short-term fellowship 8720. A final acknowledgement to the Italian Consortium for Biotechnologies (CIB) for the support.

Cited Literature

1. I T, Cm C, A H, Rmt F. Quantitative systems pharmacology and the personalized drug-microbiota-diet axis. Current opinion in systems biology [Internet]. 2017 [cited 2021 Sep 6];4. Available from: https://pubmed.ncbi.nlm.nih.gov/32984662/
2. Heinken A, Hertel J, Thiele I. Metabolic modelling reveals broad changes in gut microbial metabolism in inflammatory bowel disease patients with dysbiosis. NPJ Syst Biol Appl. 2021;7:19.
3. Hoffmann C, Dollive S, Grunberg S, Chen J, Li H, Wu GD, et al. Archaea and fungi of the human gut microbiome: correlations with diet and bacterial residents. PLoS One. 2013;8:e66019.
4. Manor O, Dai CL, Kornilov SA, Smith B, Price ND, Lovejoy JC, et al. Health and disease markers correlate with gut microbiome composition across thousands of people. Nat Commun. 2020;11:5206.
5. Eng A, Borenstein E. Taxa-function robustness in microbial communities. Microbiome. 2018;6:45.
6. Lozupone CA, Stombaugh JI, Gordon JI, Jansson JK, Knight R. Diversity, stability and resilience of the human gut microbiota. Nature. 2012;489:220–30.
7. Jansma J, El Aidy S. Understanding the host-microbe interactions using metabolic modeling. Microbiome. 2021;9:16.
8. Mendes-Soares H, Mundy M, Soares LM, Chia N. MMinte: an application for predicting metabolic interactions among the microbial species in a community. BMC Bioinformatics. 2016;17:343.
9. Heirendt L, Arreckx S, Pfau T, Mendoza SN, Richelle A, Heinken A, et al. Creation and analysis of biochemical constraint-based models using the COBRA Toolbox v.3.0. Nat Protoc. 2019;14:639–702.
10. Gu C, Kim GB, Kim WJ, Kim HU, Lee SY. Current status and applications of genome-scale metabolic models. Genome Biol. 2019;20:121.
11. Reimers A-M, Reimers AC. The steady-state assumption in oscillating and growing systems. J Theor Biol. 2016;406:176–86.
12. Magnúsdóttir S, Heinken A, Kutt L, Ravcheev DA, Bauer E, Noronha A, et al. Generation of genome-scale metabolic reconstructions for 773 members of the human gut microbiota. Nat Biotechnol. 2017;35:81–9.
13. Heinken A, Acharya G, Ravcheev DA, Hertel J, Nyga M, Okpala OE, et al. AGORA2: Large scale reconstruction of the microbiome highlights wide-spread drug-metabolising capacities. bioRxiv.

2020;2020.11.09.375451.
14. Cheng M, Ning K. Stereotypes About Enterotype: the Old and New Ideas. Genomics Proteomics Bioinformatics. 2019;17:4–12.
15. Cho I, Blaser MJ. The human microbiome: at the interface of health and disease. Nat Rev Genet. 2012;13:260–70.
16. Xia B, Crusius JBA, Meuwissen SGM, Pe?a AS. Inflammatory bowel disease: definition, epidemiology, etiologic aspects, and immunogenetic studies. World J Gastroenterol. 1998;4:446–58.
17. Prideaux L, Kamm MA, De Cruz PP, Chan FKL, Ng SC. Inflammatory bowel disease in Asia: a systematic review. J Gastroenterol Hepatol. 2012;27:1266–80.
18. Yoo JY, Groer M, Dutra SVO, Sarkar A, McSkimming DI. Gut Microbiota and Immune System Interactions. Microorganisms. 2020;8:E1587.
19. British Society of Gastroenterology consensus guidelines on the management of inflammatory bowel disease in adults - PubMed [Internet]. [cited 2021 Sep 6]. Available from: https://pubmed.ncbi.nlm.nih.gov/31562236/
20. Sahu P, Kedia S, Ahuja V, Tandon RK. Diet and nutrition in the management of inflammatory bowel disease. Indian J Gastroenterol. 2021;40:253–64.
21. Sarikaya M, Ergül B, Doğan Z, Filik L, Can M, Arslan L. Intestinal fatty acid binding protein (I-FABP) as a promising test for Crohn's disease: a preliminary study. Clin Lab. 2015;61:87–91.
22. Miyoshi J, Chang EB. The gut microbiota and inflammatory bowel diseases. Transl Res. 2017;179:38–48.
23. Machiels K, Joossens M, Sabino J, De Preter V, Arijs I, Eeckhaut V, et al. A decrease of the butyrate-producing species Roseburia hominis and Faecalibacterium prausnitzii defines dysbiosis in patients with ulcerative colitis. Gut. 2014;63:1275–83.
24. Magnusson MK, Isaksson S, Öhman L. The Anti-inflammatory Immune Regulation Induced by Butyrate Is Impaired in Inflamed Intestinal Mucosa from Patients with Ulcerative Colitis. Inflammation. 2020;43:507–17.
25. Lobionda S, Sittipo P, Kwon HY, Lee YK. The Role of Gut Microbiota in Intestinal Inflammation with Respect to Diet and Extrinsic Stressors. Microorganisms. 2019;7:E271.
26. Heinken A, Basile A, Thiele I. Advances in constraint-based modelling of microbial communities. Current Opinion in Systems Biology. 2021;27:100346.
27. Heinken A, Ravcheev DA, Baldini F, Heirendt L, Fleming RMT, Thiele I. Systematic assessment of secondary bile acid metabolism in gut microbes reveals distinct metabolic capabilities in inflammatory bowel disease. Microbiome. 2019;7:75.
28. Thiele I, Sahoo S, Heinken A, Hertel J, Heirendt L, Aurich MK, et al. Personalized whole-body models integrate metabolism, physiology, and the gut microbiome. Mol Syst Biol. 2020;16:e8982.
29. Mills RH, Vázquez-Baeza Y, Zhu Q, Jiang L, Gaffney J, Humphrey G, et al. Evaluating Metagenomic Prediction of the Metaproteome in a 4.5-Year Study of a Patient with Crohn's Disease. mSystems. 2019;4:e00337-18.
30. Ianiro G, Tilg H, Gasbarrini A. Antibiotics as deep modulators of gut microbiota: between good and evil. Gut. 2016;65:1906–15.
31. Heinken A, Thiele I. Systems biology of host-microbe metabolomics. Wiley Interdiscip Rev Syst Biol Med. 2015;7:195–219.
32. de Vladar HP. Amino acid fermentation at the origin of the genetic code. Biol Direct. 2012;7:6.
33. Theriot CM, Fletcher JR. Human fecal metabolomic profiling could inform Clostridioides difficile infection diagnosis and treatment. J Clin Invest. 2019;129:3539–41.
34. Levitt MD, Furne J, Olsson S. The relation of passage of gas an abdominal bloating to colonic gas production. Ann Intern Med. 1996;124:422–4.
35. Deng Z, Liu S. Inflammation-responsive delivery systems for the treatment of chronic inflammatory diseases. Drug Deliv Transl Res. 2021;11:1475–97.
36. Magro DO, Kotze PG, Martinez CAR, Camargo MG, Guadagnini D, Calixto AR, et al. Changes in serum levels of lipopolysaccharides and CD26 in patients with Crohn's disease. Intest Res. 2017;15:352–7.
37. Marchesi JR, Holmes E, Khan F, Kochhar S, Scanlan P, Shanahan F, et al. Rapid and noninvasive metabonomic characterization of inflammatory bowel disease. J Proteome Res. 2007;6:546–51.
38. Imhann F, Vich Vila A, Bonder MJ, Fu J, Gevers D, Visschedijk MC, et al. Interplay of host genetics and gut microbiota underlying the onset and clinical presentation of inflammatory bowel disease. Gut. 2018;67:108–19.
39. Maynard CL, Elson CO, Hatton RD, Weaver CT. Reciprocal interactions of the intestinal microbiota and immune system. Nature. 2012;489:231–41.
40. Vernia P, Caprilli R, Latella G, Barbetti F, Magliocca FM, Cittadini M. Fecal lactate and ulcerative colitis. Gastroenterology. 1988;95:1564–8.
41. Faber F, Bäumler AJ. The impact of intestinal inflammation on the nutritional environment of the gut microbiota. Immunol Lett. 2014;162:48–53.

42. Kitamoto S, Alteri CJ, Rodrigues M, Nagao-Kitamoto H, Sugihara K, Himpsl SD, et al. Dietary L-serine confers a competitive fitness advantage to Enterobacteriaceae in the inflamed gut. Nat Microbiol. 2020;5:116–25.
43. Zeng MY, Inohara N, Nuñez G. Mechanisms of inflammation-driven bacterial dysbiosis in the gut. Mucosal Immunol. 2017;10:18–26.
44. Stecher B. The Roles of Inflammation, Nutrient Availability and the Commensal Microbiota in Enteric Pathogen Infection. Microbiol Spectr. 2015;3.
45. Sawers G. The anaerobic degradation of L-serine and L-threonine in enterobacteria: networks of pathways and regulatory signals. Arch Microbiol. 1998;171:1–5.
46. Sassone-Corsi M, Nuccio S-P, Liu H, Hernandez D, Vu CT, Takahashi AA, et al. Microcins mediate competition among Enterobacteriaceae in the inflamed gut. Nature. 2016;540:280–3.
47. Matthews RG, Neidhardt FC. Elevated serine catabolism is associated with the heat shock response in Escherichia coli. J Bacteriol. 1989;171:2619–25.
48. Connolly JPR, Gabrielsen M, Goldstone RJ, Grinter R, Wang D, Cogdell RJ, et al. A Highly Conserved Bacterial D-Serine Uptake System Links Host Metabolism and Virulence. PLoS Pathog. 2016;12:e1005359.
49. Joossens M, Huys G, Cnockaert M, De Preter V, Verbeke K, Rutgeerts P, et al. Dysbiosis of the faecal microbiota in patients with Crohn's disease and their unaffected relatives. Gut. 2011;60:631–7.
50. Tsune I, Ikejima K, Hirose M, Yoshikawa M, Enomoto N, Takei Y, et al. Dietary glycine prevents chemical-induced experimental colitis in the rat. Gastroenterology. 2003;125:775–85.
51. Mirsepasi-Lauridsen HC, Vallance BA, Krogfelt KA, Petersen AM. Escherichia coli Pathobionts Associated with Inflammatory Bowel Disease. Clin Microbiol Rev. 2019;32:e00060-18.
52. Ghoshal U, Shukla R, Srivastava D, Ghoshal UC. Irritable Bowel Syndrome, Particularly the Constipation-Predominant Form, Involves an Increase in Methanobrevibacter smithii, Which Is Associated with Higher Methane Production. Gut Liver. 2016;10:932–8.
53. Loubinoux J, Bronowicki J-P, Pereira IAC, Mougenel J-L, Faou AE. Sulfate-reducing bacteria in human feces and their association with inflammatory bowel diseases. FEMS Microbiol Ecol. 2002;40:107–12.
54. Greenhalgh K, Meyer KM, Aagaard KM, Wilmes P. The human gut microbiome in health: establishment and resilience of microbiota over a lifetime. Environ Microbiol. 2016;18:2103–16.
55. Hertel J, Heinken A, Martinelli F, Thiele I. Integration of constraint-based modeling with fecal metabolomics reveals large deleterious effects of Fusobacterium spp. on community butyrate production. Gut Microbes. 2021;13:1–23.
56. Magee EA, Edmond LM, Tasker SM, Kong SC, Curno R, Cummings JH. Associations between diet and disease activity in ulcerative colitis patients using a novel method of data analysis. Nutr J. 2005;4:7.
57. Jimenez Loayza JJ, Berendsen EM, Teh J-J, Hoedt EC, Zhang J, Liu Q, et al. P837 The common food additives sodium sulfite and polysorbate 80 have a profound inhibitory effect on the commensal, anti-inflammatory bacterium Faecalibacterium prausnitzii: the ENIGMA study. Journal of Crohn's and Colitis. 2019;13:S542–3.
58. Keller A, Schink B, Müller N. Alternative Pathways of Acetogenic Ethanol and Methanol Degradation in the Thermophilic Anaerobe Thermacetogenium phaeum. Front Microbiol. 2019;10:423.
59. Bertsch J, Siemund AL, Kremp F, Müller V. A novel route for ethanol oxidation in the acetogenic bacterium Acetobacterium woodii: the acetaldehyde/ethanol dehydrogenase pathway. Environ Microbiol. 2016;18:2913–22.
60. Metwaly A, Dunkel A, Waldschmitt N, Raj ACD, Lagkouvardos I, Corraliza AM, et al. Integrated microbiota and metabolite profiles link Crohn's disease to sulfur metabolism. Nat Commun. 2020;11:4322.
61. Melhem H, Kaya B, Ayata CK, Hruz P, Niess JH. Metabolite-Sensing G Protein-Coupled Receptors Connect the Diet-Microbiota-Metabolites Axis to Inflammatory Bowel Disease. Cells. 2019;8:E450.
62. Tromm A, Griga T, May B. Oral mesalazine for the treatment of Crohn's disease: clinical efficacy with respect to pharmacokinetic properties. Hepatogastroenterology. 1999;46:3124–35.
63. Fang X, Monk JM, Nurk S, Akseshina M, Zhu Q, Gemmell C, et al. Metagenomics-Based, Strain-Level Analysis of Escherichia coli From a Time-Series of Microbiome Samples From a Crohn's Disease Patient. Front Microbiol. 2018;9:2559.
64. Noronha A, Modamio J, Jarosz Y, Guerard E, Sompairac N, Preciat G, et al. The Virtual Metabolic Human database: integrating human and gut microbiome metabolism with nutrition and disease. Nucleic Acids Res. 2019;47:D614–24.
65. Baldini F, Heinken A, Heirendt L, Magnusdottir S, Fleming RMT, Thiele I. The Microbiome Modeling Toolbox: from microbial interactions to personalized microbial communities. Bioinformatics. 2019;35:2332–4.
66. Basile A, Campanaro S, Kovalovszki A, Zampieri G, Rossi A, Angelidaki I, et al. Revealing metabolic mechanisms of interaction in the anaerobic digestion microbiome by flux balance analysis. Metab Eng.

2020;62:138–49.
67. Diener C, Gibbons SM, Resendis-Antonio O. MICOM: Metagenome-Scale Modeling To Infer Metabolic Interactions in the Gut Microbiota. mSystems. 2020;5:e00606-19.
68. Callahan BJ, Sankaran K, Fukuyama JA, McMurdie PJ, Holmes SP. Bioconductor Workflow for Microbiome Data Analysis: from raw reads to community analyses. F1000Res. 2016;5:1492.
69. Alpha-, beta-, and gamma-diversity of bacteria varies across habitats - PubMed [Internet]. [cited 2021 Sep 16]. Available from: https://pubmed.ncbi.nlm.nih.gov/32966309/
70. Anderson MJ, Ellingsen KE, McArdle BH. Multivariate dispersion as a measure of beta diversity. Ecol Lett. 2006;9:683–93.
71. Ringnér M. What is principal component analysis? Nat Biotechnol. 2008;26:303–4.